Doctoral Program in Sustainable Management of Agricultural, Forestry and Food Resources, University of Florence (UNIFI)

CYCLE XXXVI

Doctoral Program in Engineering Sciences, Vrije Universiteit Brussel (VUB)

Exploring climate change impacts and adaptive capacity of agricultural systems:

Integration of risk assessment and agro-hydrological modelling

Settore Scientifico Disciplinare AGR/08

PhD candidate

Lorenzo Villani

Supervisors

Prof. Elena Bresci, UNIFI

Prof. Ann van Griensven, VUB

Prof. Daniele Penna, UNIFI

PhD Coordinator

Prof. Erminio Monteleone

Thesis submitted in fulfilment of the requirements for the Doctoral Program in Sustainable Management of Agricultural, Forestry and Food Resources, cycle n. XXXVI, Curriculum Agricultural and Forest Engineering (IAF) at the University of Florence and the Doctoral Program in Engineering Sciences at the Vrije Universiteit Brussel.

Jury members

Prof. Elena Bresci,

University of Florence, Department of Agriculture, Food, Environment and Forestry, Florence, Italy

Prof. Ann van Griensven,

Vrije Universiteit Brussel, Department of Water and Climate, Brussels, Belgium

IHE Delft Institute for Water Education, Department of Water Science and Engineering, Delft, the Netherlands

Prof. Abdellah Touhafi,

Vrije Universiteit Brussel, Department of Engineering Sciences and Technology, Brussels, Belgium

Vrije Universiteit Brussel, Department of Electronics and Informatics, Brussels, Belgium

Prof. Iris De Graeve,

Vrije Universiteit Brussel, Department of Materials and Chemistry, Brussels, Belgium

Prof. Marthe Wens,

Vrije Universiteit Amsterdam, Institute for Environmental Studies, Amsterdam, the Netherlands

Dr. Giovanni Francesco Ricci,

University of Bari Aldo Moro, Department of Agricultural and Environmental Sciences, Bari, Italy

Acknowledgement

Questo lavoro di tesi non sarebbe stato possibile senza il contributo di molte persone.

Ringrazio la Prof.ssa Elena Bresci, che per prima mi ha introdotto al mondo della ricerca e che non mi ha mai fatto mancare la fiducia e la libertà di sviluppare le mie idee, e il Prof. Daniele Penna, a cui sono grato per i molti preziosi consigli in questi anni. Un ringraziamento particolare a Giulio Castelli, che ho sempre considerato il mio supervisore "non ufficiale" e vero e proprio esempio di intraprendenza da seguire.

I wish to warmly thank Prof. Ann van Griensven for her supervision and for allowing me to develop my research in her group in Belgium: her positive attitude after reaching so many academic successes are truly inspiring to me.

Il mio percorso di dottorato non sarebbe stato lo stesso se non avessi potuto contare su tutti gli altri membri del Water Harvesting Lab, che ringrazio per tutto il tempo passato insieme e il mutuo sostegno: Luigi, Eleonora, Enrico, Niccolò, Francesco, Ismail.

I am also grateful to the researchers of the Surface Water team for making my research periods in Belgium so easy and pleasant. A particular thank to Estifanos, Albert, Katoria, James, Rahel, Abdennabi, Analy, Erasto and all the others.

A warm thank to Bert Van Schaeybroeck for the amazing support with climate models.

Un ringraziamento anche ai dipartimenti DAGRI a Firenze e HYDR a Bruxelles, con una menzione particolare a Lucia Castellucci che ha trasformato tutti i problemi burocratici in piacevoli conversazioni.

Ringrazio la mia famiglia ed i miei amici per avermi sempre supportato, aspettato e mai ostacolato in questo mio percorso fatto di tanti viaggi.

L'ultimo pensiero va a Carlotta, per avermi fatto sempre sentire a casa in tutte le case che abbiamo abitato in questi tre anni.

Abstract

Global agendas are converging to address the overlapping challenges related to climate change, disaster risk reduction and sustainable development. Thus, the respective research communities, that until a few years ago were working separately, should take the opportunity to further share and integrate knowledge and approaches. This would be particularly useful when dealing with water since its management involves multiple stakeholders, often with different opinions about its use. Indeed, water scarcity, which occurs when water supply fails to satisfy water demand, and water shortage, a lack of water supply of acceptable quality, caused either by climatic, infrastructural, or hydrological factors, are two of the main global challenges which will be likely worsened by climate change, hampering food security in many countries of the world.

This thesis revolves around four manuscripts that investigate the research topics in two study areas. I first apply the approaches of the disaster and climate research communities in Central and Southern Tuscany, Italy, starting with a drought risk assessment, in the first manuscript, and continuing with a climate change impact assessment, also evaluating the adaptive capacity of agricultural systems, in the second and third manuscripts, by applying the Soil and Water Assessment Tool + (SWAT+). In this study area, I also analyze the uncertainty in future climate aridity due to climate models and the vegetation responses to CO_2. Furthermore, I assess the impact of agricultural adaptation strategies on hydrological fluxes, an aspect which is often neglected.

As a second case study, I selected the Juba and Shabelle catchments in Somalia, an area which is highly exposed to extreme events and with a population mainly composed of small-holder agro-pastoral communities. In this fourth manuscript of the thesis, I integrate both approaches including indicators obtained after simulations of the SWAT+ agro-hydrological model in a climate risk assessment framework. In this way, the representation of climate change hazard and resilience, defined as the combination of coping, adaptive and transformative capacities, is improved.

Combining climate change impact and risk assessment, I provide useful information to be used by local decision-makers in Italy and Somalia to better tackle water-related, agricultural climate change challenges. Furthermore, in the four manuscripts of the thesis, I highlight specific issues and uncertainties of these methodologies and explore solutions to address them. Finally, I propose an example framework to combine the approaches to show how the integration is beneficial and helps to deliver a clear and robust message to achieve greater policy impact for a better water management.

List of symbols and abbreviations[1]

AGE Age
AGMIP Agricultural Model Intercomparison and Improvement Project
AGRIWATER Innovative and Sustainable Measures for Keeping Water in the Agricultural Landscape
AG-WaMED Advancing non-conventional water management for innovative climate-resilient water governance in the Mediterranean Area
AHP Analytical Hierarchical Process
AI Aridity Index
AM Arithmetic Mean
AR Assessment Report
ARTEA Azienda Regionale Toscana Per Le Erogazioni In Agricoltura
awc Available water capacity
bd Moist bulk density
bio Total biomass
bio_{agg} Above-ground biomass
biomix Biological mixing efficiency
bm_e Biomass-energy ratio
BSh Hot semi-arid climates
BSK Cold semi-arid climates
can_ht_max Maximum canopy height
canmx Maximum canopy storage
cbn Organic carbon content
CC Coping Capacity
CC Cover Crop
CDD Meteorological drought
CDO Climate Data Operators
CHIRPS Climate Hazards Group InfraRed Precipitation with Station data
Cim Composite Indicator Rank
CMCC Centro euro-Mediterraneo sui Cambiamenti Climatici
CMHyd Climate Change for Watershed Modeling
CMIP Coupled Model Intercomparison Project
CN Curve Number
CNR Consiglio Nazionale delle Ricerche
CNRM Centre National de Recherches Météorologiques
CO_2 carbon dioxide
CORDEX Coordinated Regional Downscaling Experiment
CROP Cropland
Csa Hot-summer Mediterranean climate
CYC25 1st quartile crop yield change
CYCavg Average crop yield change
d days
days_mat Days to maturity
DB Database
DEI Drought Exposure Index
DEM Digital Elevation Model
DHI Drought Hazard Index
DJF December-January-February
DRI Drought Risk Index
DS Drought Stress
DSSAT Decision Support System for Agrotechnology Transfer
DVI Drought Vulnerability Index
EDU Education
EM-DAT International Disaster Database
epco Plant evaporation Compensation factor
EPIC Environmental Policy Integrated Climate
ES Earlier Sowing
ES Ecological Susceptibility
esco Soil evaporation compensation factor
ESCWA United Nations Economic and Social Commission for Western Asia
EU European Union
EW Equal Weights
ext_co Light extinction coefficient
FAO Food and Agriculture Organization
FEWS NET Famine Early Warning Systems Network
flo_min Minimum aquifer storage to allow return flow
FLO20 Hydrological drought
frac_hu Fraction of the plant growing season corresponding to a point on the optimal leaf area development curve
GCM General Circulation Model
GDO Global Drought Observatory
GDP Gross Domestic Product
GERICS Climate Service Center Germany
GWP Global Water Partnership
harv_idx Harvest index
harv_idx_ws Lower limit of harvest index
HI Harvest Index
HRU Hydrological Response Unit
hu_lai_decl Fraction of growing season when leaf area begins to decline
hurs Relative humidity
ICHEC Irish Centre for High-End Computing
I_d Photosynthetically active radiation
IIASA International Institute for Applied Systems Analysis
InfoRM Index for Risk Management
IPCC Intergovernmental Panel on Climate Change

[1] Symbols in the text are specified every time they occur. Abbreviations are introduced again in each chapter.

IPSL Institut Pierre-Simon Laplace
ISIMIP Inter-Sectoral Impact Model Intercomparison Project
ISTAT Istituto nazionale di statistica
JJA June-July-August
k Saturated hydraulic conductivity
K_j Light interception
KNMI Royal Netherlands Meteorological Institute
LAI Leaf Area Index
lai_max Fraction of the maximum leaf area index corresponding to a point on the optimal leaf area development curve
lai_pot Maximum potential Leaf Area Index
LCAC Lack of Coping and Adaptive Capacity
LCC Longer Crop Cycle
LD Leaf area index development
LDS Longest Dry Spell
LS Later Sowing
LUH2 Land Use Harmonization 2
MedECC Mediterranean Experts on Climate and environmental Change
MODFLOW Modular finite-difference groundwater flow model
MP Mean Precipitation
MPI Max Planck Institute for Meteorology
MRI Meteorological Research Institute
MT Mean Temperature
N Number of municipalities
n Total number of observations
NCC Norwegian Climate Center
NDVI Normalized Difference Vegetation Index
NRSME Normalized Root Mean Square Error
NSE Nash-Sutcliffe Efficiency
nstrs Nitrogen stress
NUTS Nomenclature des unités territoriales statistiques
OECD Organisation for Economic Cooperation and Development
OP Model output with the input parameters set as base value
$O_{P+\Delta P}$, $O_{P-\Delta P}$ Model outputs with input parameters perturbed
OV_N Manning's "n" value for overland flow
P Base value of the input parameter.
Pbias Percent Bias
perco Percolation coefficient
PET Potential Evapotranspiration
PNACC Piano Adattamento ai Cambiamenti Climatici
POP Total population
ppm parts per million
pr Precipitation
PRIMA Partnership for Research and Innovation in the Mediterranean Area
pstrs Phosphorous stress
PW Proportional Weights
r Pearson correlation coefficient
r_1, r_2 Shape coefficients
R^2 Coefficient of Determination
R20 Extreme precipitation
r_c Stomatal resistance
$\bar{R}_S$ Average shift in municipalities' rankings
RCM Regional Climate Model
RCP Representative Concentration Pathway
RDrI-Agri Risk of Drought Impacts for Agriculture
revap_co Groundwater "revap" coefficient
revap_min Threshold depth of water in the shallow aquifer for “revap” or percolation to the deep aquifer to occur
r_l Minimum effective stomatal resistance of a single leaf
RMSE Root Mean Square Error
rsds Solar radiation
RSR RMSE-observations standard deviation ratio
rt_dp_max Maximum root depth
RUE Radiation Use Efficiency
sfcWind Wind speed
SI Supplemental Irrigation
SIR Regional Hydrological Service
SMHI Swedish Meteorological and Hydrological Institute
SPEI Standardized Precipitation Evapotranspiration Index
SPI Standardized Precipitation Index
S_r Relative sensitivity
SRTM Shuttle Radar Topography Mission
SS Social Susceptibility
SSP Shared Socioeconomic Pathways
$STDEV_{obs}$ Standard deviation of the observed values
SU40 Extreme temperature
surlag Surface runoff lag coefficient
SWALIM Somalia Water and Land Information Management
SWAT Soil and Water Assessment Tool
tasmax Maximum temperature
tasmin Minimum temperature
TCI Temperature Condition Index
TDS Total number of Dry Spells
TS Temperature Stress
tstrs Temperature stress
UN United Nations
UNEP UN Environmental Programme
UNISDR United Nations Office for Disaster Risk Reduction
URB Urbanization
USLE Universal Soil Loss Equation
VCI Vegetation Condition Index
VHI Vegetation Health Index
WF Water Footprint
WHO World Health Organization

WMO	World Meteorological Organization
wstrs	Water stress
WTRav	Water availability
WTRco	Water consumption
Y_i^{obs}	The ith observed value
Y_i^{sim}	The ith simulated value
yld	Crop yield
Y^{mean}	The average of the observed values
z	Depth from soil surface to bottom of layer
ZT	Zero Tillage
γr	Plant growth factor
Δ	Difference (expressed as percentage change)
Δbio_{act}	Daily biomass accumulation
ΔP	Absolute change in the value of the input parameter

List of tables

Table 2.1: Drought hazard indicators used for past and future drought. 15
Table 2.2: Drought exposure indicators used. 17
Table 2.3: Drought vulnerability indicators used. 17
Table 2.4: Characteristics of the seven clusters and suggested specific adaptation strategies. 25
Table 3.1: The five climate models used in the study with the General Circulation Model and the Regional Climate Model. 36
Table 3.2: Model performances for monthly streamflow during calibration and validation. 37
Table 3.3: Precipitation, average temperature and potential evapotranspiration in the historical, near and far future periods 41
Table 3.4: Water yield, percolation, evapotranspiration and irrigation in the historical and near future periods 43
Table 4.1: The adaptation strategies scenarios considered in the study, with the description and SWAT+ input files change. 57
Table 4.2: The parameters selected for calibration, the type of change, and the change in terms of percentage or new value. 58
Table 4.3: Model performances expressed as NRMSE (%) and Pbias (%) for calibration and validation for durum wheat, sunflower, and maize in the Siena and Grosseto provinces. 59
Table 4.4: Days to maturity for durum wheat, sunflower and maize used in the simulations. 59
Table 5.1: The five SSP narratives and their main characteristics 79
Table 5.2: Definitions used in the study. 80
Table 5.3: Indicators used in the risk assessment. 81
Table 5.4: Management schedule for the SWAT+ simulations considering the base, coping and adaptive scenarios. 85
Table 5.5: The main and 21 alternative options that we considered to evaluate the robustness of the assessment. 86
Table 5.6: Hazard, vulnerability, exposure and risk of the scenarios considered in this study 91

List of figures

Figure 1.1: The study catchments considered in the thesis. 6
Figure 1.2: The scheme of the thesis with the six chapters and their titles. 8
Figure 2.1: Tuscany region with the watersheds selected for the analysis. 15
Figure 2.2: Results of the uncertainty analysis reported according to the average shift in rankings 21
Figure 2.3: Maps of the DHI, DEI, DVI, and DRI. 22
Figure 2.4: Spatial visualization of the seven clusters individuated in the Tuscany region. 23
Figure 2.5: Boxplots of the normalized exposure indicators for the seven clusters individuated 23
Figure 2.6: Boxplots of the normalized vulnerability indicators for the seven clusters individuated 24
Figure 2.7: Boxplots of DHI, DEI, DVI, and DRI for the seven clusters 26
Figure 3.1: The Ombrone catchment with the three gauging stations, the subbasins, and the boundaries of the provinces of Siena and Grosseto. 33
Figure 3.2: Multi-site calibration and validation 38
Figure 3.3: Lineplot and boxplots of future temperature (°C).. 39
Figure 3.4: Lineplot and boxplots of future precipitation (mm). 40
Figure 3.5: Potential evapotranspiration and Aridity Index with constant or decreased stomatal conductance 42
Figure 3.6: Bar plots and tables with the water balance components 44
Figure 4.1: The Ombrone catchment with the provinces of Siena and Grosseto 55
Figure 4.2: Climate change impact on crop yield 60
Figure 4.3: Climate change impacts on water footprint 61
Figure 4.4: Effect of adaptation strategies on crop yield. 63
Figure 4.5: Effect of adaptation strategies on water footprint. 64
Figure 4.6: Effect of adaptation strategies on drought and temperature stress 65
Figure 4.7: Comparison of the effects of adaptation strategies on water balance components for the whole catchment and only for cropland where the adaptation strategies are implemented 66
Figure 4.8: Effect of adaptation strategies on evaporation, evapotranspiration, water yield, soil moisture and percolation, considering only cropland, and streamflow 67
Figure 4.9: Comparison of the management and climate change effects on the agricultural and hydrological variables considered in this study, under RCP 4.5. 71
Figure 4.10: The beneficial effects of adaptation strategies and of their combinations for wheat, sunflower and maize 72
Figure 5.1: Schematic representation of the conceptual and methodological risk framework 80
Figure 5.2: Elevation, precipitation and land cover maps of the Juba and Shabelle catchments. 84
Figure 5.3: Calibration and validation plots and tables with performance indicators 87
Figure 5.4: Irrigated maize and rainfed sorghum crop yields considering the coping and adaptive capacity simulations. 88
Figure 5.5: The relative percentage changes compared to the historical situation of individual indicators 90
Figure 5.6: Violin plot of risk scores considering the whole set of alternatives used in the uncertainty/sensitivity analysis and the main option. 92
Figure 5.7: The climate risk dimensions (hazard, vulnerability and exposure) for the six scenarios considered 93

Table of Contents

Acknowledgement ii

Abstract iii

List of symbols and abbreviations iv

List of tables vii

List of figures viii

Chapter 1 Introduction 1
1.1 General context 1
1.2 Key methodological concepts 3
1.2.1 Climate and drought risk assessments 3
1.2.2 Scenarios for the future: the SSP narratives and the climate models 4
1.2.3 Crop and hydrological models: the SWAT+ agro-hydrological model 5
1.2.4 The resilience concept 5
1.3 Study areas 6
1.4 Objectives, research questions and thesis structure 7

Chapter 2 Drought risk assessment 11
2.1 Abstract 11
2.2 Introduction 11
2.3 Methodology 13
2.3.1 Conceptual framework 13
2.3.2 Study area 14
2.3.3 Identification of indicators 15
2.3.4 Data acquisition and pre-processing 17
2.3.5 Assessment of multicollinearities 19
2.3.6 Normalization and weighted aggregation 19
2.3.7 Robustness evaluation 19
2.3.8 Archetype analysis 20
2.4 Results 20
2.4.1 Multicollinearity analysis 20
2.4.2 Robustness evaluation 21
2.4.3 Drought risk mapping and ranking 22
2.4.4 Archetype analysis 22
2.5 Discussion 26
2.5.1 Past and future drought hazard 26
2.5.2 Selection of indicators and limitations 26
2.5.3 Linking the results with adaptation strategies 27

2.6 Conclusion 29

Chapter 3 Climate change impact assessment 30
3.1 Abstract 30
3.2 Introduction 30
3.3 Methodology 32
3.3.1 Study area: the Ombrone catchment 32
3.3.2 The SWAT+ model 33
3.3.3 Multi-site calibration and validation 34
3.3.4 Climate change scenarios 35
3.4 Results 37
3.4.1 Multi-site calibration of SWAT+ 37
3.4.2 Projected temperature and precipitation changes over the Ombrone catchment 38
3.4.3 Impacts of climate change and vegetation responses to CO_2 on future potential evapotranspiration and future aridity 40
3.4.4 Impacts of climate change and vegetation responses to CO_2 on future water balance components 42
3.5 Discussion 45
3.5.1 Climate models' uncertainty in the Northern Mediterranean area 45
3.5.2 Impacts of vegetation responses to CO_2 46
3.6 Conclusion 48

Chapter 4 Management change impact assessment 50
4.1 Abstract 50
4.2 Introduction 50
4.3 Methodology 53
4.3.1 The SWAT+ model 53
4.3.2 The Ombrone catchment model 54
4.3.3 Calibration and validation 55
4.3.4 Climate projections and management 55
4.3.5 Simulation of adaptation strategies 56
4.4 Results 58
4.4.1 SWAT+ calibration and validation 58
4.4.2 Climate change impacts on crop yield and water footprint 59
4.4.3 The adaptive capacity of agricultural systems 61
4.4.4 Effects of adaptation strategies on water balance components 65
4.5 Discussion 66
4.5.1 Crop yield estimation with SWAT+ 66
4.5.2 Uncertain impacts of climate change on crops 68
4.5.3 The effectiveness of adaptation strategies 69
4.5.4 The impact of adaptation strategies on water balance components 71

4.6 Conclusion 74

Chapter 5 Integration of the approaches 75
5.1 Abstract 75
5.2 Introduction 75
5.3 Methods 78
5.3.1 Conceptual and methodological framework definition 78
5.3.2 Study area definition 82
5.3.3 Indicator analysis and selection 83
5.3.4 Normalization and weighted aggregation 85
5.3.5 Robustness evaluation 86
5.4 Results 86
5.4.1 SWAT+ calibration 86
5.4.2 Future climate and crop yield 87
5.4.3 Indicators' analysis 88
5.4.4 Future climate risk, hazard, vulnerability and exposure 89
5.4.5 Robustness evaluation 91
5.5 Discussion 94
5.5.1 Climate change impact assessment 94
5.5.2 Study limitations and further research 95
5.6 Conclusions 95

Chapter 6 Conclusions 97
6.1 Discussion 97
6.1.1 Future climate and risk in the study areas 97
6.1.2 The uncertainty in estimating future drought and aridity 98
6.1.3 The adaptive capacity of agricultural systems 99
6.1.4 Improving drought/climate risk assessments 100
6.1.5 Integrating climate impact and risk assessments 101
6.2 Limitations and future work 103
6.3 Key messages 105

Appendix 107
A2: Supplementary materials chapter 2 107
A3 : Supplementary materials chapter 3 109
A4 : Supplementary materials chapter 4 115
A5 : Supplementary materials chapter 5 128

Bibliography 143

List of publications 163

Chapter 1 Introduction

1.1 General context

Due to the potentially dramatic consequences and the uncertain cascading impacts on livelihoods, climate change is almost unanimously recognized as one of humanity's greatest challenges. Human activities have been responsible for climate change since the pre-industrial period and further global warming will affect the global water cycle, including the frequency and severity of extreme events (Arias et al., 2021). In general, warming induces evaporation and more water vapour in the atmosphere and increases the frequency and intensity of both droughts and heavy precipitation (Trenberth, 2011). While there is a large confidence that temperatures are increasing almost everywhere, past changes and future projections of precipitation show much more variability and uncertainty. An increase in globally-averaged precipitation has been observed in the last decades as is also expected in the future. Some regions, however, are experiencing a decrease in precipitation (Gutiérrez et al., 2021).

In recent years, after decades of steady decline, the number of people suffering from hunger has slightly increased, with Africa being the continent with the highest prevalence of undernourishment (FAO et al., 2019). Throughout the world, actual yields are far from their potential, also in some regions of the North (Schils et al., 2018). Nevertheless, high yield gaps are typically related to sub-Saharan Africa, where many recurrent limiting factors, such as water, climate, soil fertility and pests, affect the productivity, resilience and sustainability of agroecosystems (Tittonell and Giller, 2013; van Ittersum et al., 2013). Indeed, closing yield gaps and increasing resource efficiency are considered among the most effective strategies to achieve sustainable intensification (Mueller et al., 2012). Major efforts by the whole agriculture-related sectors will be needed to find effective solutions to feed the increasing world population, without further degrading natural resources (Foley et al., 2011).

Negative impacts of the changing climate on food security have already been observed, caused either by increased temperatures, changes in precipitation patterns, and a higher frequency of extreme events, such as droughts, floods and heat and cold waves (FAO, 2016; IPCC, 2018). Climate change will also produce unpredictable effects on pests, diseases and weeds that will likely harm future crop yields (Bindi and Olesen, 2011; Ciscar et al., 2018; Giannakopoulos et al., 2009; Spano et al., 2020). Conversely, CO_2 concentration increases will benefit crop yield through the CO_2 fertilization effect and stomatal conductance suppression, with the effects being greater for C3 crops (Ainsworth and Long, 2005; Webber et al., 2018). Nevertheless, climate change impacts will be highly variable according to the sector and location in the world and, in some cases, they will be mostly beneficial (Kang et al., 2009; Roudier et al., 2011). Regardless of the sign and magnitude of climate change effects, adaptation strategies will have a crucial role in limiting crop yield losses or enhancing the unlikely positive climate changes (Bindi and Olesen, 2011; Reidsma et al., 2015). This calls for the need to address the global climate change challenge with diverse, localized, context-specific adaptation strategies (Iglesias et al., 2010; Pasqui and Di Giuseppe, 2019).

When considering the water resources - and even more in the context of climate change - strong and urgent actions need to be implemented to address the two main water-related challenges, namely water shortage and water scarcity (FAO, 2020). Currently, 3.2 billion people live in agricultural areas with high levels of water scarcity or shortage, agriculture accounts for more than 70% of global water withdrawals, and almost half of irrigation occurs at the expense of environmental flow requirements (FAO, 2020; Mekonnen and Gerbens-Leenes, 2020). Improved water management strategies are crucial in drylands - which cover about 46.2% of the global land - where climate change will strongly exacerbate water stresses (Biazin et al., 2023; IPCC, 2018).

Water shortage refers to a shortage of water supply of acceptable quality, caused either by climatic, infrastructural, or hydrological factors, while water scarcity occurs when water supply fails to satisfy water demand (FAO, 2020; Ruane, 2012). Water shortage is mainly driven by biophysical factors which are expected to increase due to the warming climate and the greater frequency of extreme events (Rojas et al., 2019). Furthermore, several river basins are going to experience enhanced water scarcity caused by multiple drivers which will increase water demand and the changes in the hydrological cycle which will reduce water availability (Estrela et al., 2012; Garrote et al., 2015; Masia et al., 2018).

In agriculture, water shortage mainly threatens rainfed agriculture, while water scarcity issues refer mostly to irrigated agriculture (FAO, 2020). Having in mind that there is a continuum in technologies from fully irrigated to fully rainfed systems, different and integrated strategies need to be implemented to tackle these water-related challenges (FAO, 2020). In rainfed agriculture, water shortage is generally addressed by increasing plant uptake capacity, reducing evaporation and drainage losses, and harvesting more water (Rockström and Falkenmark, 2015; Piemontese et al., 2020), while for water scarcity in irrigated agriculture, the main solutions are to enhance the water productivity and to improve irrigation systems (Molden et al., 2010; Oweis and Hachum, 2006).

Adaptation strategies encompass a wide range of practices, tools and policies put in place by various stakeholders at different scales. Among them, farmers will have a crucial role in coping with climate change, by modifying their choices and management practices. Agricultural adaptation strategies can be categorized as planned (hard, institutional) and autonomous (soft, farmer-led). Planned adaptations refer to major structural changes at larger scales that generally require high investments and longer times, while autonomous adaptations consist of adjustments at smaller and shorter scales to optimize production (Bindi and Olesen, 2011). Autonomous adaptations, which generally are overlooked by decision-makers, might have a crucial role as they are highly accepted and will be easily implemented by farmers themselves (Bonzanigo et al., 2016; Varela-Ortega et al., 2016). Examples of such practices are changes in varieties, sowing date, input utilization, and management.

As a result of the increasing concerns about climate change impacts, new methods and approaches are now being applied to better understand how to address these impacts. Climate change adaptation and mitigation are the main focus of the United Nations Climate Change Conferences that led for example to the Paris Agreement (2015). Furthermore, it is also largely discussed in the other most important and recent global agendas. For example, “Climate Action” is included within the 17 Sustainable Development Goals to urgently tackle climate change impacts (UN, 2015). Moreover, experts from the disaster risk reduction community are always more actively involved in studying climate change impacts and dynamics (Marzi et al., 2021; Mysiak et al., 2018), following the Sendai Framework for Disaster Risk Reduction (UNISDR, 2015). Vogt et al. (2018) describe two different approaches for the assessment of risk. The disaster risk reduction community applies the contextual/factor approach, which generally relies on combined indicators, while the climate change adaptation community focuses on the outcome/impact approach, mainly based on quantitative measures of the relationship between stressor and response (Vogt et al., 2018). Notably, as a lesson learned from the previous Hyogo Framework for Action, adopted in 2005, it is reported:

> *“The intergovernmental negotiations on the post 2015 development agenda, financing for development, climate change and disaster risk reduction provide the international community with a unique opportunity to enhance coherence across policies, institutions, goals, indicators and measurement systems for implementation, while respecting the respective mandates. Ensuring*

credible links, as appropriate, between these processes will contribute to building resilience and achieving the global goal of eradicating poverty." (UNISDR, 2015).

The challenges related to climate change, disaster risk reduction and sustainable development are overlapping. From the global agendas also strongly emerges the opportunity for synergies that can be achieved. The academic community is advancing towards enhanced collaboration and knowledge-sharing among various fields, and the latest Intergovernmental Panel on Climate Change (IPCC) reports (AR5 and AR6) include all the challenges of the various agendas. Nevertheless, the integration between the approaches and methodologies of the disaster, climate change and development communities remains far from optimal (Challinor et al., 2010; Marzi et al., 2021; Mochizuki et al., 2018).

1.2 Key methodological concepts

Water scarcity and shortage are core challenges of the climate crisis, considering that water resource management is already facing several problems (FAO, 2020). Water resource management is a cutting-edge theme that involves multiple stakeholders and disciplines but, despite the efforts, solutions and policies are barely coordinated and effective (UN, 2020). The intrinsic nature of the water resource makes it difficult to account for. Furthermore, stakeholders might value water differently and might have opposite perspectives on its optimal use, especially when and where water is scarcer (UN, 2021). Another important challenge in water accounting is how to deal with the different scales at which water management is implemented (Chukalla et al., 2020; Gómez et al., 2020). To address these challenges, researchers developed frameworks, indicators, and methodologies to try to comprehensively analyze water uses to improve integrated water management (Biazin et al., 2023; Dalla Marta et al., 2018; Ruane, 2012), which is fundamental for addressing climate change impacts and risks. In this section, the key methodological concepts applied in this thesis are briefly introduced.

1.2.1 Climate and drought risk assessments

An established framework to evaluate climate risk, promoted also by the IPCC, is to conceptualize it as the combination of hazard, exposure and vulnerability (equation 1). According to the IPCC definitions, risk is "the potential for adverse consequences on lives, livelihoods, health, ecosystems and species, economic, social and cultural assets, services (including environmental services) and infrastructure", hazard is "the potential occurrence of a natural or human-induced physical event or trend or physical impact that may cause loss of life, injury, or other health impacts, as well as damage and loss to property, infrastructure, livelihoods, service provision, ecosystems and environmental resources", exposure is "the presence of people, livelihoods, species or ecosystems, environmental functions, services, and resources, infrastructure, or economic, social, or cultural assets in places and settings that could be adversely affected" and vulnerability is "the propensity or predisposition to be adversely affected and encompasses a variety of concepts and elements including sensitivity or susceptibility to harm and lack of capacity to cope and adapt" (IPCC, 2014).

$$Risk = Hazard \cdot Exposure \cdot Vulnerability \quad (1)$$

Many climate risk and vulnerability assessments have been performed considering drought or other hazards (Hagenlocher et al., 2019; Jurgilevich et al., 2017; Merz et al., 2014) from global to regional and local scales (Ahmadalipour et al., 2019; Carrão et al., 2016; Cotti et al., 2022; De Groeve et al. 2015; Mysiak et al. 2018). The Index for Risk Management (InfoRM) is one of the most interesting applications of composite indicators to improve the allocation of resources and the response to emergencies (De Groeve et al., 2015). The InfoRM index was recently updated to take into account climate change (Marzi et al., 2021), being probably the most

advanced coupling of disaster risk reduction and climate change adaptation communities' approaches. Other indexes exist and, interestingly, they show little agreement in hazard patterns, while there is a high correlation between socioeconomic vulnerability and lack of coping and adaptive capacities patterns (Garschagen et al., 2021). The choice of the hazard represented is one of the reasons for this discrepancy, but even when considering only one hazard its representation is not obvious. This is especially true for drought, which is extremely subtle and difficult to define and quantify (Hall and Leng, 2019; Satoh et al., 2021). Typically, four types of droughts are defined, namely meteorological, agricultural, hydrological and socio-economic droughts (Mishra and Singh, 2010). Another crucial problem in drought risk assessments is that only past and present drought hazards are generally considered (Hagenlocher et al., 2019). This calls for increased integration between disaster risk and climate change communities' approaches. Adaptation capacity is also poorly represented in climate change assessments (Andrijevic et al., 2023). Finally, estimating hazards is common practice, but the focus should indeed be on the actual impacts (Enenkel et al., 2020).

1.2.2 Scenarios for the future: the SSP narratives and the climate models

For the fifth IPCC assessment report (AR5), the scenarios were based on four Representative Concentration Pathways (RCPs) to represent alternative pathways of greenhouse gas emissions (Moss et al., 2010). The RCPs were used as the basis for the Coupled Model Intercomparison Project – phase 5 (CMIP5), providing four different radiative forcings. A parallel effort of the climate change research community established plausible global developments referred to as Shared Socioeconomic Pathways (SSPs, Riahi et al., 2017). In the newest framework, the SSPs were coupled with the RCPs and were used for CMIP6 (O'Neill et al., 2016). The five SSPs are based on different storylines/narratives and have low, intermediate or high adaptation and mitigation challenges (O'Neill et al., 2017). SSP1 – "Sustainability" and SSP3 – "Regional rivalry" are at the extreme with low and high mitigation and adaptation challenges, respectively. SSP2 – "Middle of the road" has intermediate challenges. SSP4 – "Inequality" has high adaptation challenges but low for mitigation, while the opposite is valid for SSP5 – "Conventional development". The SSP narratives facilitate integrated analysis of future climate impacts, vulnerabilities, and adaptation and mitigation strategies. SSP outputs are not meant to be directly analysed when advising for climate policy, but they can be used as a tool to produce effective and understandable assessments for policymakers (O'Neill et al., 2017).

Climate change modelling is the preliminary part of all impact, adaptation and risk research. Until their most recent report, the IPCC based the majority of their conclusions on climate-change projections from General Circulation Models (GCMs). These models simulate future climate at horizontal resolutions of 50-200 km, which is insufficient to realistically represent climatological conditions for regional studies. To obtain finer resolutions, Regional Climate Models (RCMs) are often used to dynamically downscale GCMs (Rummukainen, 2016; Doblas-Reyes et al., 2021) and results from the Coordinated Regional Downscaling Experiment (CORDEX, Giorgi and Gutowski, 2015) have been widely used in the latest IPCC report (Gutiérrez et al., 2021). Apart from better topographic maps and finer details, RCMs improve upon GCMs through a more realistic representation of atmospheric processes. Over Europe, for instance, more than 11 RCMs contribute to a large ensemble of climate projections at a resolution of 12.5 km within the EURO-CORDEX initiative (Jacob et al., 2014, 2020). These are nowadays commonly used as input for climate-impact studies for Europe and the Mediterranean region. GCMs and RCMs are forced considering multiple radiative forcings, expressed as RCPs. Despite their wide adoption, there are large uncertainties in future projections due to differences in the future scenarios, GCM and RCM errors, as well as substantial internal climate variability (Hawkins and Sutton, 2011).

1.2.3 Crop and hydrological models: the SWAT+ agro-hydrological model

When dealing with water management, distinct approaches can be observed in the study of climate change impacts and relative adaptation strategies. Most of the studies regard either the future water dynamics of the basins – with an emphasis on the water balance at the catchment scale – or the expected future crop water requirements – with an emphasis on crop productivity at the field scale - while rarely both aspects are combined (Garg et al., 2020; Gómez et al., 2020; Huai et al., 2020; Van Gaelen et al., 2017). Researchers select one of these perspectives based on their background, scale of analysis, data availability and target adaptation strategies to be investigated. Correspondingly, two different kinds of models are generally used: crop-growth and hydrological models (Gómez et al., 2020; Siad et al., 2019). The former are process-based models which simulate crop growth using soil, climate, plant, and management data as inputs; they are typically point-based, used for field-scale simulations, and mainly applied by agronomists and plant scientists (Holzworth et al., 2015; Rivington and Koo, 2010). Hydrological models are used to estimate, predict, and manage water distribution and fluxes; they are mainly applied at the catchment scale by hydrologists and, depending on the spatial discretization of the parameters, they are classified as lumped, semi-distributed, or distributed (Siad et al., 2019). When referring to agronomic adaptation strategies, crop-growth models are surely the most applied. The spatial application at different spatial scales of these point-based models to include the soil, climate, and management variability is nowadays common (Lorite et al., 2013; Tenreiro et al., 2020), even if horizontal processes related to water dynamics are neglected (van Noordwijk et al., 2022).

Hydrological models that include modules to simulate crop growth demonstrated to be an option to perform spatial analyses at wider scales (e.g. Bär et al., 2015; Schierhorn et al., 2014). Coupling crop-growth models and hydrological models, or directly using integrated agro-hydrological models, might be effective solutions to perform more comprehensive and meaningful analyses of agronomic adaptation strategies (Gómez et al., 2020; Siad et al., 2019). Among the many agro-hydrological models available, the Soil and Water Assessment Tool (SWAT) modelling suite (Arnold et al., 1998) is one of the most applied. SWAT is an integrated hydrological model which includes several modules that allow the simulation of the most important processes related to water and land resources, such as hydrological balance, erosion, water pollution, climate change and crop growth (Aloui et al., 2023). SWAT+ is an updated version of the model characterized by higher flexibility in the representation and connection of the spatial units (Bieger et al., 2017).

1.2.4 The resilience concept

The resilience concept was first introduced in ecology by Holling (1973) and assumes different interpretations according to the various disciplines. According to Folke et al. (2010), resilience thinking has three central aspects: resilience, which is “the capacity of a socio-ecological system to continually change and adapt yet remain within critical thresholds”, adaptability, which is “the capacity to adjust responses to changing external drivers and internal processes and thereby allow for development along the current trajectory” and transformability, which is “the capacity to cross thresholds into new development trajectories”. Most of the early work on resilience focused on the capacity of the systems to absorb shocks and maintain their functions (Folke, 2006). Comparing how the IPCC defined resilience in the third (AR3), fourth (AR4), and fifth (AR5) assessment reports, it is possible to observe how the concept evolved from the AR3, where resilience was the “amount of change a system can undergo without changing state” to a more complex definition that includes the coping, adaptive and transformative capacities (Jones, 2019). The definition given within the IPCC AR5 includes the most important aspects of resilience. Here, resilience is “the capacity of social, economic and environmental systems to cope with a hazardous event or trend or disturbance, responding or

re-organizing in ways that maintain their essential function, identity and structure, while also maintaining the capacity for adaptation, learning and transformation" (IPCC, 2014).

The resilience perspective is nowadays applied in multiple fields and it is at the core of sustainable development (Barrett and Constas, 2014; Barron et al., 2021; EU, 2016; Jeans et al., 2017; UN, 2015), risk management (Manyena, 2006; Marzi et al., 2019; Mochizuki et al., 2018) and climate change (IPCC, 2022) research. The resilience concept is also widely applied in water research, but mostly considering the engineering resilience of water supply infrastructure (Rodina, 2019). In disaster risk research, resilience is generally considered the opposite of vulnerability (Manyena, 2006; Mochizuki et al., 2018). Despite the great interest and the high number of papers published, there is still debate on how to practically apply the resilience concept in sustainable development (Barron et al., 2021), disaster risk (Mochizuki et al., 2018) and water research (Dewulf et al., 2019).

1.3 Study areas

The approaches and methodologies used in the thesis were applied in sensible case studies relevant to climate change impact, risk and adaptation studies (Fig. 1.1). Hence, the assessments alone provide useful and actionable information available to local decision-makers and practitioners. Further information about the study areas and the maps can be found in the respective chapters.

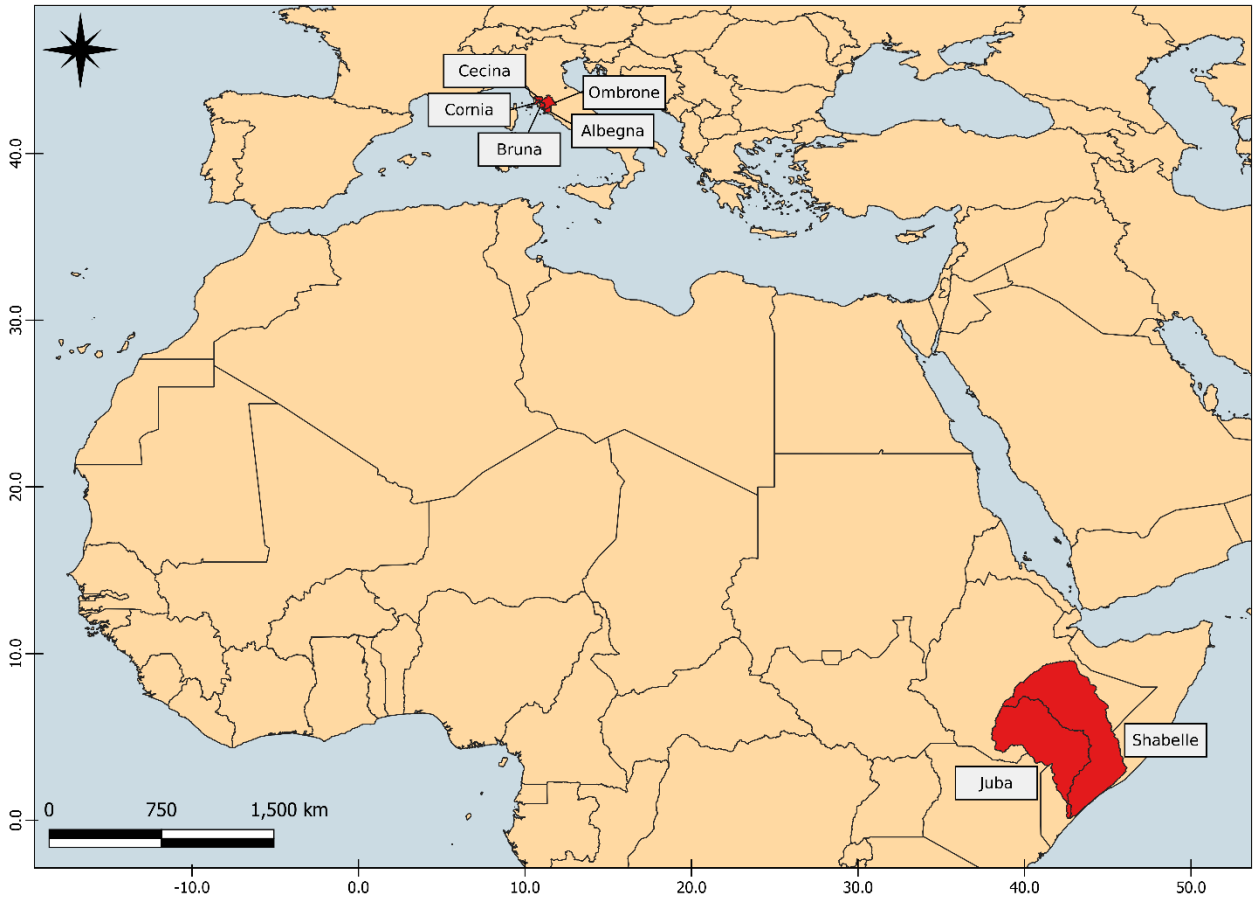

Figure 1.1: The study catchments considered in the thesis.

In the first study, corresponding to Chapter 2, the study area is represented by five coastal, agricultural catchments in Central and Southern Tuscany, namely the Cecina (925 km^2), Cornia (485 km^2), Bruna (745 km^2), Ombrone (3,565 km^2) and Albegna (832 km^2) catchments. Italy is in the middle of the Mediterranean region, which is a hotspot for climate change mainly due to precipitation (Lionello and Scarascia, 2018). A shared characteristic of the five catchments is that they are highly water-stressed especially in the lowland coastal plains during the summer season, due to the concomitant water demands for irrigation and domestic use for tourism.

In the second and third studies, corresponding to Chapters 3 and 4, the Ombrone is selected as the main study catchment for being the largest and most representative of the five considered. The choice was made considering the outcomes of the drought risk assessment, which showed that coastal municipalities within the Ombrone catchment had the highest risk and some internal municipalities had the highest exposure. Municipalities with high exposure were related mainly to the high-value wines' production, in areas like the Chianti hills and the Val d'Orcia. Furthermore, for the catchments others than the Ombrone, a lower amount of data was available, especially regarding river flow measurements.

In the Italian study area, the approaches and methodologies used in the thesis were applied in different studies, and therefore sequentially in time. As a final case study, corresponding to Chapter 5, to test a framework for the integration of the approaches, Somalia was selected, with a focus on the Juba and Shabelle catchments, 216,728 km^2 and 297,455 km^2 respectively. This is a very relevant area for the climate change, disaster and sustainable development research communities. The Juba and Shabelle are the only two permanent rivers in Somalia, and in their valleys is estimated that 90% of the food production in Somalia is produced (Basnyat, 2007). The population is mainly composed of agro-pastoral communities living in rural areas and agriculture and livestock contribute to more than 60% of the gross domestic product of Somalia (Mourad, 2022). Droughts and floods are frequent and often result in casualties, forced migrations and huge economic losses. Furthermore, Somalia is extremely vulnerable due to the weak governance and political instability, that also resulted in a civil war in the 1990s. Despite the relevance of the study area, very few studies were conducted in the Juba and Shabelle catchments.

1.4 Objectives, research questions and thesis structure

The scheme of the thesis is reported in Figure 1.2. One general research objective and two specific ones are the fundamental basis of the thesis. The four chapters of the thesis linked to manuscripts also have specific research questions. Each chapter has a research question more related to the assessments and one addressing specific methodological, theoretical or conceptual issues. Assessment research questions provide useful information for local decision-makers and practitioners to adapt their management strategies for the present and account for future climate change impacts. The other research questions are of interest to the larger community, as they focus on generalized and neglected issues and the integration of the different approaches used in this thesis. In Chapter 6, the discussion is organized to address the two specific objectives, including the answers to the research questions. Then, limitations and opportunities for further research are discussed, and some key messages are provided as conclusions.

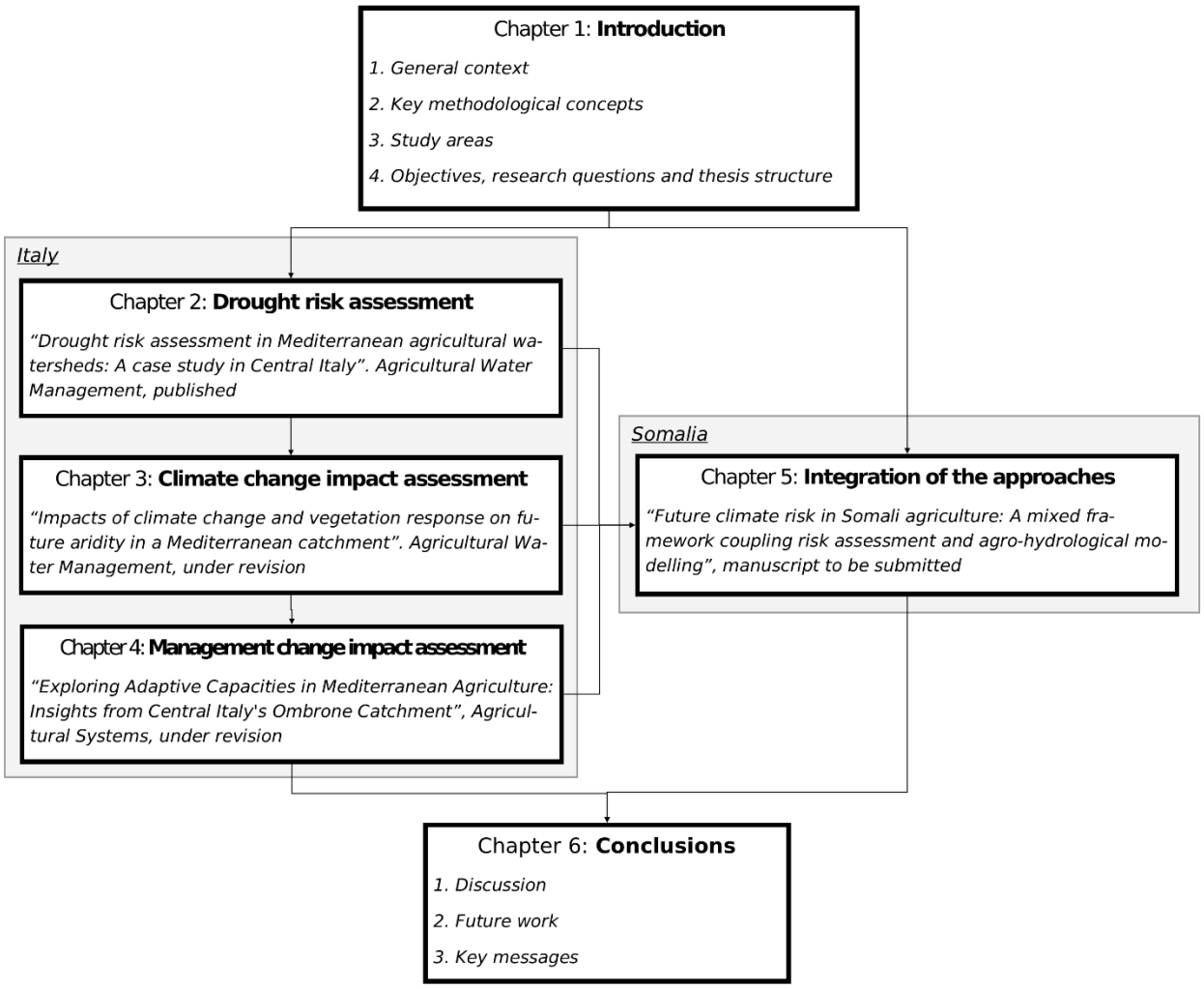

Chapter	2 (Italy)	3 (Italy)	4 (Italy)	5 (Somalia)
Objective 1	*Risk, hazard, exposure and vulnerability evaluation*	*Future climate and impact on water balance* *Effect of vegetation responses to CO_2 on future aridity*	*Climate change impacts on agriculture* *Adaptive capacity of agricultural systems* *Impacts of management changes on water balance* *Synergies and tradeoffs between adaptation strategies*	*Risk, hazard, exposure and vulnerability evaluation* *Climate change impacts on hydrology and agriculture* *Adaptive capacity of agricultural systems*
Objective 2	*Risk assessment methodology improvement*			*Agro-hydrological modelling and risk assessment frameworks integration*

Figure 1.2: The scheme of the thesis with the six chapters and their titles. For Chapters 2, 3, 4 and 5, the title of the corresponding manuscript is reported. In the table below are reported the part of the specific objectives addressed in each chapter.

The main, general objective of the thesis is to assess the expected impacts of climate change on crop production and hydrology and to evaluate the most promising agronomic adaptation strategies, integrating climate risk assessment and agro-hydrological modelling approaches, towards greater policy impact for better water management. Other objectives are related more specifically to the climate change impact and risk assessments of the selected study areas, as well as to the improvement and integration of the methodologies used:

O1. To evaluate the future climate impacts, risk and its components and to quantify the adaptive capacity of agricultural systems in the selected study areas, highlighting uncertainties and neglected issues.

O2. To improve the climate risk assessment methodology and integrate it with agro-hydrological modelling, to perform more relevant and comprehensive climate change risk/impact assessments.

As summarized in Figure 1.2, the first objective is addressed in the four chapters with manuscripts of the thesis, namely Chapters 2, 3, 4 and 5. Risk, hazard, vulnerability and exposure are assessed in Chapters 2 and 5. The climate change impacts on hydrological fluxes and agricultural outputs are assessed in Chapters 3, 4 and 5. The adaptive capacity of agricultural systems is evaluated in Chapters 4 and 5, and possible adaptation strategies are also discussed in Chapter 2. The uncertainties and neglected issues of the first objective are mainly analysed in the specific research questions of Chapters 2, 3 and 4. The second objective is more related to climate/drought risk assessments, and therefore mainly to Chapters 2 and 5. Nevertheless, since the second objective refers to the inclusion of agro-hydrological modelling within risk assessments, the analyses of Chapters 3 and 4 were crucial to achieving this objective.

In Chapter 2, I conducted a drought risk assessment of the main study area, five catchments in Central and Southern Tuscany, Italy. While assessing the patterns of risk, hazard, exposure and vulnerability of the municipalities within these five catchments, I also addressed some crucial limitations that characterize this kind of assessment, as reported by Hagenlocher et al. (2019), proposing an integrated and detailed methodological process to conduct drought risk assessments. This analysis was also fundamental to deciding the study catchment to be modelled in the following papers. The research questions specific to this chapter are:

- *What are the drought hazard, exposure, vulnerability and risk patterns in the coastal catchments of Southern and Central Tuscany?*

- *How can the reliability and actionability of (drought/climate) risk assessments be improved?*

In Chapter 3, I performed a climate change impact assessment of the Ombrone catchment, selected after the drought risk assessment as the most representative study catchment among the five analysed. I prepared, calibrated and validated a SWAT+ model and forced it with five EURO-CORDEX RCMs. Here, I analysed future climate patterns as predicted by the climate models used, focusing mainly on temperature and precipitation. Furthermore, I evaluated future aridity conditions, considering the uncertainty in precipitation and atmospheric water demand projections. In addition to the effects of altered climate variables due to climate change, I also evaluated the effects of increased CO_2 concentration. The research questions specific to this chapter are:

- *What is the expected future climate in the Ombrone catchment and how climate change will affect the water balance and aridity conditions?*

- *What is the uncertainty caused by climate models and vegetation responses to CO_2 when estimating future hydrological fluxes and aridity conditions?*

The study reported in Chapter 4 is an integration of the previous climate change impact assessment, with a focus on agricultural systems. Using the same climate models and re-calibrating the SWAT+ model of the

Ombrone catchment, I evaluated the impacts on crop yields and water footprint. Moreover, I assessed the adaptive capacity of the agricultural systems by simulating simple, autonomous, agronomic adaptation strategies, both individually and in combinations. Notably, I also evaluated the effects of these management changes on the water balance components of the catchment, an aspect which is often overlooked. The research questions specific to this chapter are:

- *What is the adaptive capacity of the agricultural systems of the Ombrone catchment and which strategies are the most important?*

- *Are the impacts of management changes on hydrological fluxes and agricultural outputs comparable in magnitude to those caused by climate change?*

Finally, in Chapter 5 I applied the main methodologies used in the other studies, trying to integrate them efficiently and making use of the lessons learned. As a case study, I selected Somalia with a focus on its two perennial rivers, the Juba and the Shabelle. I performed a climate risk assessment including indicators elaborated from outputs of the SWAT+ agro-hydrological model, to provide a more accurate representation of hazards and adaptive capacity. The research questions specific to this chapter are:

- *What will be the impacts of climate change on Somali agricultural systems and how will risk evolve under the five SSP narratives considered?*

- *How can agro-hydrological modelling be coherently included within climate risk assessment frameworks to improve the representation of future hazards and resilience?*

Chapter 2 Drought risk assessment

The manuscript reported as Chapter 2 was published in Agricultural Water Management (complete reference: Villani, L., Castelli, G., Piemontese, L., Penna, D., & Bresci, E. (2022). Drought risk assessment in Mediterranean agricultural watersheds: A case study in Central Italy. Agricultural Water Management, 271, 107748. https://doi.org/10.1016/j.agwat.2022.107748).

2.1 Abstract

Mediterranean watersheds are expected to face increased and more severe drought events due to climate change. Urgent actions are needed to shift from a reactive approach to a proactive one, for which drought risk assessment is fundamental. Nevertheless, the current methodology to calculate composite risk indicators is still debated, undermining the overall robustness and validity of drought risk assessment. Furthermore, different socio-ecological contexts, spatiotemporal scales, and data availability hamper the homogenization of the procedures. We present a complete drought risk assessment performed for the agricultural systems of five Italian coastal watersheds, introducing a simple robustness evaluation method to validate the assessment tool, combined with archetype analysis to link the outputs with adaptation strategies. Forty-two (42) indicators were finally included to represent hazard, exposure, and vulnerability. Past and future drought hazards were estimated considering multiple types of droughts with data from public observatories. Results showed that hazard was higher for the southern part of Tuscany, exposure was higher in the coastal and high-value wine producers' municipalities, while vulnerability patterns were less clear. Major adaptation efforts should target specific watersheds of the Grosseto province, which showed the highest drought risk. Archetype analysis was then used to suggest possible adaptation strategies for each cluster of municipalities individuated, allowing a context-specific generalization of the insights. In the pursue of shared and homogeneous guidelines to estimate drought risk, by introducing the robustness evaluation and the archetype analysis, this study proposes innovative methodologies to address major limitations of most drought risk assessments.

2.2 Introduction

The occurrence and severity of droughts - defined as "periods of abnormally dry weather long enough to cause a serious hydrological imbalance" (IPCC, 2012) – are expected to increase in the future due to climate change (Dai, 2011; IPCC, 2022). The Italian peninsula, being in the centre of the Mediterranean region, which is considered a hotspot for climate change (MedECC, 2020; Spano et al., 2020; Zollo et al., 2016), will likely face more frequent and intense drought events (Cammalleri et al., 2020; Caporali et al., 2021; Castellari et al., 2014; OECD, 2021). Typically, droughts have been considered a natural phenomenon triggered by a lack of precipitation, characterized in terms of frequency, severity, duration, and extent (Zargar et al., 2011). Many types of droughts have been identified, namely, the meteorological drought, "a lack of precipitation over a region for a period of time", the agricultural drought, "a period with declining soil moisture and consequent crop failure", the hydrological drought, "a period with inadequate surface and subsurface water resources for established water uses", and the socioeconomic drought, "a failure of water resources systems to meet water demands" (Mishra and Singh, 2010). In the past, these types of droughts were considered to propagate from meteorological to agricultural, hydrological and socioeconomic droughts; this approach has been recently questioned for its over-simplification since it fails to account for the feedback and the trade-offs between social and physical processes, the direct effect of human-induced climate change, and the long-term environmental impacts (AghaKouchak et al., 2021; Crausbay et al., 2017; Di Baldassarre et al., 2021; Van Loon

et al., 2016). As a result, the terms “ecological drought” and “human-induced hydrological drought” were recently introduced (Crausbay et al., 2017; Van Loon et al., 2016). A further step will need to be done to improve our understanding of “anthropogenic drought”, a multidimensional and multiscale phenomenon that should be intended as a “process” rather than a “product” (AghaKouchak et al., 2021).

Globally, it is estimated that drought damages account for a fifth of the total damages caused by natural hazards (WMO and GWP, 2017). In Europe, the annual economic losses caused by droughts are estimated to be around € 9 billion (€ 1.4 billion for Italy), mostly related to the agricultural sector (Cammalleri et al., 2020), with significant spatial variability between different regions (García-León et al., 2021). The entity of the losses, along with the expected increase due to climate change, boosted the interest of researchers and decision-makers towards this topic (Hagenlocher et al., 2019). To better deal with droughts, more and more studies call for a shift from the so-called “reactive” approach, taken in emergency situations and considered technically and economically inefficient, towards a “proactive” approach, including appropriate measures developed with the involvement of multiple stakeholders (Carrão et al., 2016; Murthy et al., 2015; Vogt et al., 2018). Specifically, it is claimed that the preparation and mitigation costs are by far lower compared to the relief costs, which significantly surge in case of inaction (Vogt et al., 2018; WMO and GWP, 2017). Drought vulnerability and risk assessments are considered of major importance to develop sound and effective strategies to tackle drought (WMO and GWP, 2014; World Bank, 2019).

Commonly, drought hazard is defined using drought indicators to quantify the severity, frequency, intensity, and duration of droughts. Many drought hazard indicators exist to describe meteorological, agricultural, and hydrological droughts (Kchouk et al., 2022; Mishra and Singh, 2010; Zargar et al., 2011), which might refer directly to physical variables such as precipitation, evapotranspiration, soil moisture or streamflow, or can infer drought from vegetation health. Despite the availability of multiple hazard indicators, drought risk assessments are generally carried out with the use of one or a few hazard indicators. To account for the complexity of the drought phenomenon, considering hazard indicators of meteorological, agricultural, and hydrological droughts, might improve the prediction of the drought hazard (Sun et al., 2012; World Bank, 2019). Furthermore, the most common approach to represent drought hazard is by using past data; nevertheless, many authors (e.g. Hagenlocher et al., 2019; Vogt et al., 2018) claim the importance of including predictions of future drought, but at the cost of higher uncertainty (Mysiak et al., 2018). Finally, many drought observatories exist around the world; they were mainly conceived to forecast drought and to support decision-makers with early warning systems. However, it is possible to obtain meaningful and easily accessible data about droughts from their monitoring activity, which is a service that is still probably underestimated. Hence, the utilization of data obtained from drought observatories is not only convenient but more meaningful as they can be used also by non-experts (Magno et al., 2018).

Two major limitations to the validity and practical use of drought risk assessments are commonly shared: only 11% of them conduct any form of validation and, generally, there is a missing link with possible adaptation strategies (Hagenlocher et al., 2019). The robustness of the methodology applied can be evaluated with uncertainty or sensitivity analyses (OECD, 2008), sometimes referred to as internal validation (Carrão et al., 2016; Fontaine and Steinemann, 2009), or by comparing results with external information, referred to also as external validation. Finding suitable data for external validation might be impossible in some cases, even more when dealing with small scales. Additionally, the validation with external datasets is complicated by the fact that composite indicators aim to represent complex past and future dynamics. Hence, the validity of composite indicators is generally evaluated by performing uncertainty and sensitivity analyses (OECD, 2008). Even if examples exist, a shared, simple but at the same time robust methodology for internal validation is still missing. Regarding the missing link with adaptation strategies, it is known that drought risk assessments

constitute the basis for decision-makers to take action, cope with drought, and start discussing drought management (Hagenlocher et al., 2019; OECD, 2008). However, the main outputs of drought risk assessments are usually detailed maps and rankings, that might be hard to understand, contextualize, and use. An emerging methodology to address this limitation is archetype analysis - an approach for identifying recurrent patterns within cases and supporting a context-specific generalization of insights (Eisenack et al., 2019; Oberlack et al., 2019) – that can be used to enhance the interpretation of drought risk assessments and simplify the operational implications for designing possible adaptation strategies.

The main objective of this study is to propose a detailed and integrated drought risk assessment of Mediterranean agricultural systems and present an application to the municipalities located in coastal watersheds of central and southern Tuscany (Central Italy). These areas are susceptible to drought especially during summer months, due to the concurrent high water demands for domestic and agricultural uses. Key innovations introduced with this paper are (1) a complete robustness evaluation of the assessment by applying alternative methodologies in crucial steps of the drought risk assessment; (2) the analysis of the results not only with maps and rankings but also by applying an archetype analysis, to streamline the identification of exposure and vulnerability patterns for planning possible adaptation strategies.

2.3 Methodology

The methodology of the present study draws on the approach introduced by OECD (2008) and by the drought risk assessments of Hagenlocher et al. (2018) and Meza et al. (2020), to propose a more integrated assessment including a robustness evaluation and archetype analysis in eight operational steps:

1. Conceptual framework;
2. Study area;
3. Identification of indicators;
4. Data acquisition and pre-processing;
5. Multicollinearity analysis;
6. Normalization and weighted aggregation;
7. Robustness evaluation;
8. Archetype analysis.

2.3.1 Conceptual framework

A drought risk assessment needs to be clearly framed starting from its funding components of risk, hazard, exposure, and vulnerability (Hagenlocher et al., 2019). Risk can be defined as “the potential for adverse consequences for human or ecological systems” (IPCC, 2022); hazard is “the possible, future occurrence of natural or human-induced physical events that may have adverse effects on vulnerable and exposed elements”; exposure considers “the inventory of elements in an area in which hazard events may occur”; vulnerability refers to “the propensity of exposed elements […] to suffer adverse effects when impacted by hazard events”, determined by physical, social, economic, and environmental factors (Cardona et al., 2012).

A Drought Hazard Index (DHI) and a Drought Exposure Index (DEI) were calculated as the arithmetic mean of the selected indicators. For the Drought Vulnerability Index (DVI), the components proposed by Meza et al. (2020, 2019) with some minor modifications were considered. Hence, DVI was calculated with the formula:

$$DVI = \frac{SS+ES+LCAC}{3} \quad (1)$$

where SS, ES, and LCAC are Social and Ecological Susceptibilities and Lack of Coping and Adaptive Capacity, respectively.

Similarly to Prabnakorn et al. (2019), the indexes were then aggregated to calculate the Drought Risk Index (DRI) with the formula:

$$DRI = DHI \cdot DEI \cdot DVI \cdot 100 \quad (2)$$

To assess drought hazard including different types of droughts, data of river discharge, groundwater levels, and precipitation from the Regional Hydrological Service (SIR) of the Tuscany region were considered; however, they were not homogeneously distributed in the study area considered and long series were available only for few locations. Therefore, the assessment was finally based on drought hazard indicators derived from remote sensing data. Still, a higher number of indicators compared to other assessments to represent more types of droughts, referring both to past and future conditions, was included. Since the assessment was conducted for agriculture, the indicators selected to estimate exposure represented infrastructural, social, and economic features of agricultural systems. The vulnerability was calculated through a composite indicator combining SS, ES, and LCAC (Meza et al., 2020). Generally, susceptibility is defined using only socioeconomic indicators; including environmental or ecological indicators is fundamental since agriculture has a strong impact on these components and agroecosystems are, by definition, social-ecological systems (Hagenlocher et al., 2019). For this assessment, indicators of the current lack of coping and the future lack of adaptative capacities were included to partially consider future vulnerability.

2.3.2 Study area

The assessment was performed for five coastal watersheds of central and southern Tuscany: the Cecina, Cornia, Bruna, Ombrone, and Albegna watersheds (Fig. 2.1). To allow for a sufficient discretization of the watersheds and to provide more accurate information that can be used when planning adaptation and mitigation strategies, municipalities (Local Administrative Units) were considered as units of analysis. A municipality was considered in the assessment if at least 10% of its area fell within any of the five watersheds. Finally, 58 municipalities were selected in four provinces (NUTS3): Pisa, Livorno, Siena, and Grosseto.

Coastal areas of Tuscany are particularly prone to drought as they currently receive the lowest amount of precipitation in the region (Caporali et al., 2021; Magno et al., 2018) and, in the future, they will likely increase their susceptibility to drought. Additionally, the main coastal streams show very reduced discharges in late spring and summer (Rossetto et al., 2013). The coastal watersheds are typically characterized upland by forests and rainfed agricultural areas, mainly grains and extensive rangeland (Märker et al., 2008; Orlandini et al., 2011). Olive trees are widespread as well as vineyards, with the latter being abundant in the Chianti hills, the famous high-value wine production area of central Tuscany. On the other hand, irrigated crops are prevalent in the coastal plains, with an important part of the irrigation supply pumped from the coastal aquifers (Rossetto et al., 2013). Additionally, tourism and other activities further stress the water resource uses during the summer months, with seawater intrusion and pollution of the aquifers that affect the sustainability of water extraction (Barazzuoli et al., 2008, 1999; Bianchi et al., 2011; Grassi et al., 2007). Past studies reported that some irrigated areas of the coastal plains suffered water deficit for six months per year and, despite the adoption of more efficient irrigation systems, farmers had to switch to less water-demanding, less profitable, and salinity-tolerant crops, or leave their lands uncultivated (Bianchi et al., 2011; Rossetto et al., 2013). Particularly vulnerable is the situation of the Cornia watershed since the groundwater of the aquifer also contributes to the water needs of Elba Island (Rossetto et al., 2018).

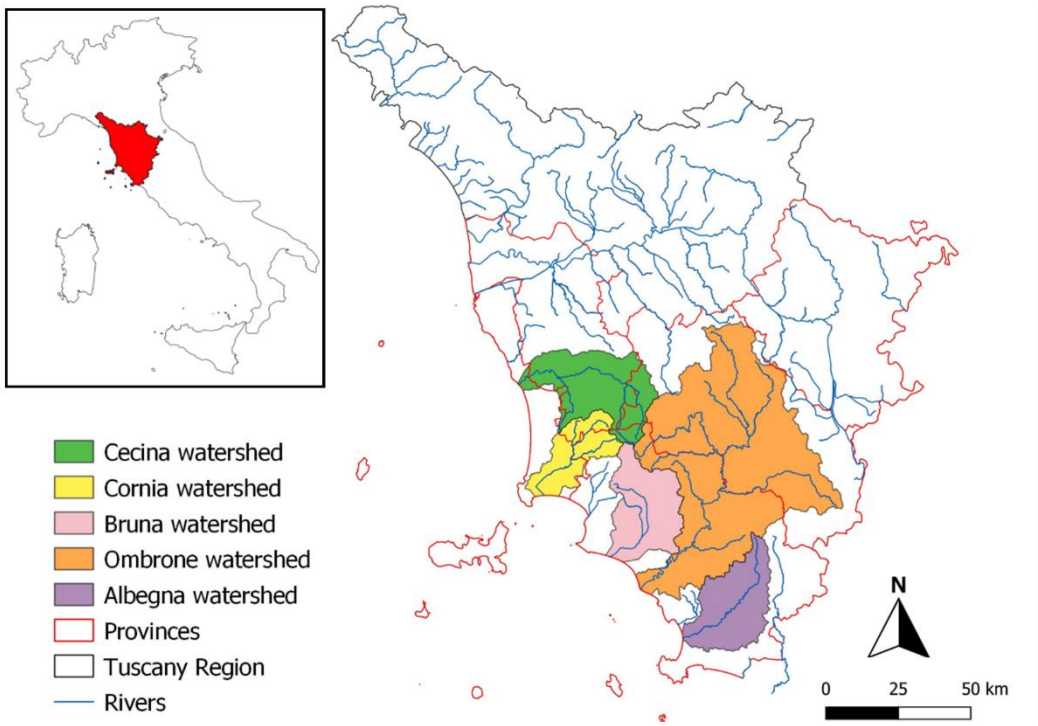

Figure 2.1: Tuscany region with the watersheds selected for the analysis.

2.3.3 Identification of indicators

All the data used to calculate the indicators were extracted from public databases at regional, national, or European levels. After a detailed literature review and after checking the availability and validity of the data, 46 indicators were included in the analysis. Tables 2.1, 2.2, and 2.3 report the lists of indicators of drought hazard, exposure, and vulnerability, respectively.

Past hazard indicators (Table 2.1), namely the Standardized Precipitation Index (SPI) (McKee et al., 1993) and the Vegetation Health Index (VHI) (Kogan, 1995), were obtained from the drought observatory of the Tuscany Region (Magno et al., 2018). Similarly, to express the future drought hazard, the ready-to-use Climate Impact Indicators (SMHI, 2021) available in the Copernicus Climate Data Store were used, representing Mean Temperature (MT) in °C, Mean Precipitation (MP) in mm/day, Longest Dry Spell (LDS) in number of days, and Total number of Dry Spells (TDS) of more than five days for 30-years periods.

SPI is the most used drought hazard indicator (Kchouk et al., 2022); it proved to be reliable and convenient since it can be easily calculated at multiple time scales by using only precipitation data. Furthermore, it allows comparisons between different locations due to its standardization. The main drawback of this index is that it considers only precipitation and does not include temperature, which is fundamental in drought analyses and even more in the context of climate warming (Di Lena et al., 2014). The drought observatory of the Tuscany region calculates the SPI with accumulation periods of 3, 6, and 12 months using validated daily CHIRPS data from 1981 (Magno et al., 2018), which were included to consider different drought types and impacts (Di Lena et al., 2014; Stagge et al., 2015). The definitions of duration, severity and frequency provided by Vogt et al. (2018) were used to calculate the hazard indicators. Duration is the total number of months below the threshold, the severity is the algebraic sum of the SPI values below the threshold level (as in Di Lena et al., 2014), and the frequency is the number of drought events of one or more months duration individuated when SPI dropped below the selected threshold. Drought onset was considered when the SPI

value was below -1.0, the threshold of "moderate drought". VHI is one of the most common agricultural drought hazard indicators, widely used to study drought from vegetation status, and the drought observatory of the Tuscany Region provides VHI values starting from 2010 (Magno et al., 2018). The VHI is a combination of the Temperature Condition Index (TCI), calculated with land surface temperature data, and the Vegetation Condition Index (VCI), calculated with NDVI data. Similar definitions of duration, severity and frequency used for the SPI were also applied to the VHI; the threshold value below which vegetation is considered stressed is 40 (Kogan, 2001).

Table 2.1: Drought hazard indicators used for past and future drought, with the data source, data availability, spatial and temporal resolutions, and a brief description.

Indicator	Data source	Data availability	Spatial resolution	Temporal resolution	Data description
Past drought – Severity, Duration, Frequency					
Standardized Precipitation Index (3, 6, 12)	CNR Drought Observatory	1981-onwards	5 km	Monthly	Average value at the municipality level
Vegetation Health Index	CNR Drought Observatory	2010-onwards	250 m	16 days	Average value at the municipality level
Future drought – short, medium and long term					
Temperature at 2 m above the ground	EURO-CORDEX – Copernicus Climate Data Store	1971-2000; 2011-2040; 2041-2070; 2071-2100.	5 km	30 year-time periods	Absolute mean value over 30 years
Precipitation	EURO-CORDEX – Copernicus Climate Data Store	1971-2000; 2011-2040; 2041-2070; 2071-2100.	5 km	30 year-time periods	Absolute mean value over 30 years
Number of dry spells	EURO-CORDEX – Copernicus Climate Data Store	1971-2000; 2011-2040; 2041-2070; 2071-2100.	5 km	30 year-time periods	Total number over 30 years
Longest dry spell	EURO-CORDEX – Copernicus Climate Data Store	1971-2000; 2011-2040; 2041-2070; 2071-2100.	5 km	30 year-time periods	Longest value over 30 years

The Climate Impact Indicators derived from EURO-CORDEX bias-corrected projections (SMHI, 2021). MT, MP, LDS, and TDS were used as future drought hazard indicators for the short (2011-2040), medium (2041-2070) and long (2071-2100) projection periods. These indicators were extracted from four Regional Climate Models (CCLM4-8-17, RACMO22E, RCA4, REMO2009), considering the Representative Concentration Pathway 4.5 and the different realizations available (SMHI, 2021). In total, the simulations considered in the ensemble were eight. Considering the duration, frequency, and severity of SPI3, SPI6, SPI12, and VHI, and MT, MP, LDS, and TDS in the short, medium, and long future periods, a total number of 24 indicators were finally considered to assess drought hazard (Table 2.1).

Five exposure indicators, which represent infrastructural, social, and economic features of agriculture in the coastal watersheds of Tuscany, were selected (Table 2.2). "Share of agricultural area" and "Volume of water used for irrigation" were included to consider both rainfed and irrigated agriculture. In many assessments, irrigation is considered as a measure to cope with drought (Carrão et al., 2016; Murthy et al., 2015), while others considered it as an asset exposed to drought (Meza et al., 2020). Indeed, irrigated agriculture might not suffer negative impacts during flash droughts of a few months' duration; nevertheless, it is highly impacted when prolonged droughts force authorities to restrict irrigation supplies (Gómez Gómez and Pérez Blanco, 2012; Masia et al., 2018; World Bank, 2019). For the economic dimension, the "Value of agricultural

products" was included, while for the social dimension the "Share of workers occupied in agriculture". Additionally, "Share of horticulture and fruticulture" was considered as an exposure indicator since these crops are highly valuable, irrigated, and with high water requirements.

Table 2.2: Drought exposure indicators used, with the data source, the method of relativization or standardization, and corresponding references.

Indicator	Data source	Calculation	Reference
Share of agricultural area	Tuscany region (2019)	$\frac{Agricultural\ area\ (ha)}{Total\ area\ (ha)}\%$	Carrão et al. (2016), Hagenlocher et al. (2019)
Volume of water used for irrigation	ISTAT – 2010	$\frac{Irrigation\ water\ (m^3)}{Agricultural\ area\ (ha)}$	Meza et al. (2020)*
Value of agricultural products	ISTAT – 2010	$\frac{Value\ of\ products\ (euro)}{Agricultural\ area\ (ha)}$	Ortega-Gaucin et al. (2021)
Share of workers occupied in agriculture	ISTAT – 2011	$\frac{Workers\ in\ agriculture}{Number\ of\ workers}\%$	Hagenlocher et al. (2019), Ortega-Gaucin et al. (2021)
Share of horticulture and fruticulture	ISTAT – 2010	$\frac{Horticulture\ +\ Fruitculture\ (ha)}{Agricultural\ area\ (ha)}\%$	/

** The indicator used in this study is very similar to the one considered in the "reference" column*

A total of 17 drought vulnerability indicators were selected, representing SS, ES, and LCAC (Table 2.3). Indicators of SS ("Education of farmers", "Age of farmers" and "Unemployment") are typically included in drought risk assessments. For ES, soil quality indicators considering data extracted from the Pedological Database of the Tuscany region, which provides detailed soil information, were considered, as well as the "Share of protected areas" calculated from the network Natura 2000. Selected indicators of LCAC refer to farm agricultural practices. Despite controversial results and opinions about organic agriculture (e.g. Clark and Tilman, 2017), the "Share of organic agriculture" was included as a vulnerability indicator, as it is commonly assumed that organic farms are less dependent on external inputs, apply good practices such as crop rotation, and are more diversified, and, therefore, have also an increased resilience to adverse events, such as drought (Märker et al., 2008; Sharafi et al., 2020); in addition, financial incentives to sustain organic agriculture also decrease the vulnerability of organic farms. Soil conservation practices are also considered to improve the capacity to cope with drought (Hagenlocher et al., 2019; Sharafi et al., 2020); hence, the "Share of land with minimum or no-tillage", available for cereal crops, was included. Other good practices linked to the informatization of farming were included with the indicators "Share of crops managed with the help of software" and "Share of land irrigated with decision support systems". The other indicators were related to irrigation, namely "Irrigation System", "Irrigation Source", and "Share of irrigable land". By including the latter, which was used as a proxy for the possibility to perform supplemental irrigation, might seem a contradiction with the decision to consider irrigated land as an exposed element; however, at the same time, irrigable land (or supplemental irrigation) is a fundamental adaptation strategy.

2.3.4 Data acquisition and pre-processing

The selected indicators were transformed from absolute to relative values or standardized, as indicated in Tables 2.2 and 2.3 to allow meaningful comparisons between municipalities of different size. For this procedure, the use of data from the same datasets was preferred. The indicators in which data were divided into categories, namely "Age of farmers", "Education of farmers", "Irrigation System", and "Irrigation Source", were ranked according to their vulnerability and assigned the lowest value "0" to the less vulnerable category and the highest value "1" to the most vulnerable one. Young and educated farmers were considered less vulnerable; regarding the "Irrigation System", drip irrigation was considered the less vulnerable, followed by sprinkler, furrow, and flood irrigation; for the "Irrigation Source", groundwater within the farm was considered

the less vulnerable, followed by private reservoirs within the farm, irrigation water from irrigation consortia, and surface water outside of the farm. For both "Irrigation System" and "Irrigation Source", to the category "Other" was assigned the value "0.5". The same procedure was applied to the indicators obtained from the Pedological Database of the Tuscany Region, which were divided according to their quality into 8 or 4 classes; for these indicators, only the agricultural soils were considered.

Few missing values were present for the exposure and vulnerability indicators. Although methods exist to replace missing data (OECD, 2008), we decided to keep them to not include further uncertainty in the model by estimating missing values. Hence, for the three municipalities with missing data, namely Monteroni d'Arbia, Gaiole in Chianti, and Radda in Chianti, results had to be evaluated even more cautiously.

Table 2.3: Drought vulnerability indicators used, grouped for Social Susceptibility, Ecological Susceptibility, and Lack of Coping and Adaptive Capacity, with the data source, the method of relativization or standardization, and corresponding references.

Indicator	Data source	Calculation	Reference
Social Susceptibility			
Education of farmers	ISTAT – 2010	Categorical*	Hagenlocher et al. (2019), Meza et al. (2019)
Age of farmers	ISTAT – 2010	Categorical*	Hagenlocher et al. (2019), Meza et al. (2019)
Unemployment	ISTAT - 2011	$\frac{Workers}{Active\ Population}$ %	Hagenlocher et al. (2019), Meza et al. (2019)
Ecological Susceptibility			
Share of protected areas	Natura 2000	$\frac{Protected\ areas}{Total\ area}$ %	Hagenlocher et al. (2019), Meza et al. (2019)
Soil erosion	Pedological DB (Tuscany region)	Categorical*	Hagenlocher et al. (2019), Ortega-Gaucin et al. (2021)
Soil fertility	Pedological DB (Tuscany region)	Categorical*	Hagenlocher et al. (2019)**, Meza et al. (2019)**
Soil salinity	Pedological DB (Tuscany region)	Categorical*	Ortega-Gaucin et al. (2021)**
Soil depth	Pedological DB (Tuscany region)	Categorical*	Hagenlocher et al. (2019), Hoque et al. (2021), Meza et al. (2019)
Climate interference	Pedological DB (Tuscany region)	Categorical*	Hoque et al. (2021)
Water Deficit	Pedological DB (Tuscany region)	Categorical*	Hoque et al. (2021), Murthy et al (2015)
Lack of coping and adaptive capacity			
Irrigation system	ISTAT – 2010	Categorical*	Hagenlocher et al. (2019)** Sharafi et al., (2020)**
Irrigation source	ISTAT – 2010	Categorical*	Hagenlocher et al. (2019)** Sharafi et al., (2020)**
Share of organic agriculture	Tuscany region (2019)	$\frac{Organic\ agriculture\ land\ (ha)}{Agricultural\ area\ (ha)}$ %	Sharafi et al., (2020)**
Share of irrigable land	ISTAT – 2010	$\frac{Irrigable\ land\ (ha)}{Agricultural\ area\ (ha)}$ %	Hagenlocher et al. (2019)
Share of land with minimum or no-tillage	ISTAT – 2010	$\frac{Minimum\ Tillage\ (ha)}{Cereal\ crops\ (ha)}$ %	Hagenlocher et al. (2019)**, Sharafi et al., (2020)**
Share of crops managed with the help of software	ISTAT – 2010	$\frac{Land\ with\ softwares\ (ha)}{Cereal\ crops\ (ha)}$ %	Hagenlocher et al. (2019)**
Share of land irrigated with decision support systems	ISTAT – 2010	$\frac{Land\ with\ DSS\ (ha)}{Agricultural\ area\ (ha)}$ %	Hagenlocher et al. (2019)** Sharafi et al., (2020)**

**Categorical indicators' methodology is described in the text*

*** The indicator used in this study is very similar to the one considered in the "reference" column*

2.3.5 Assessment of multicollinearities

Collinearity – or multicollinearity – occurs when two or more predictor variables are linearly related (Dormann et al., 2013). Generally, a multicollinearity analysis is performed to avoid the overrepresentation of the processes represented by the selected indicators (Ortega-Gaucin et al., 2021). Multicollinearity was assessed by applying the Spearman correlation matrix for the relativized and standardized exposure and vulnerability indicators in line with Meza et al. (2020). Compared to other similar studies, a very restrictive threshold ($|r|>0.4$) was considered to decide which indicators to further evaluate. The rationale for deciding whether to exclude an indicator was to assess if it expressed the same process as another one.

2.3.6 Normalization and weighted aggregation

The normalization was performed with the max-min method, which is convenient since it can be used with all the weighting methods (OECD, 2008). Due to the lack of justification for assuming that one indicator is more important than others, there is no consensus in the literature about the best weighting method. Hence, in our assessment, equal weights were considered, which is the most common weighting method in composite indicators (OECD, 2008) and has already been applied in other drought risk assessments (Brooks et al., 2005; Nauditt et al., 2022; Naumann et al., 2014; Prabnakorn et al., 2019). The normalized values of the indicators were directly used in the calculation of DHI, DEI, and DVI. However, it is important to notice that DHI, DEI, and DVI had different numbers of indicators; therefore, for example, exposure indicators contributed more compared to vulnerability indicators. Similarly, DVI was calculated as the mean of SS, ES, and LCAC, which are represented by 3, 5, and 6 indicators, respectively; hence, SS indicators contributed more to the final DRI compared to ES and LCAC indicators.

2.3.7 Robustness evaluation

Even though it is generally neglected, the robustness of the procedure should always be evaluated, considering that many of the steps of drought risk assessments have significant uncertainties (Hagenlocher et al., 2019). Ideally, uncertainty and sensitivity analyses should evaluate all the potential sources of uncertainty, including selection of indicators, normalization, weighting and aggregation methods, etc. (OECD, 2008). In drought risk assessments, the most uncertain parts of the methodology are the selection of individual indicators and weights (Murthy et al., 2015; Naumann et al., 2014), which are generally evaluated by including and excluding single indicators and applying different weighting methods. Instead, external validation has been performed in drought risk assessments using impact data (crop yield losses, population affected) (Hagenlocher et al., 2019; Meza et al., 2020), soil moisture data (Hoque et al., 2021), consulting experts (Brooks et al., 2005; Fontaine and Steinemann, 2009), or comparing results with external datasets (Ortega-Gaucin et al., 2021).

To verify the robustness of our model, both internal and external validations were considered. However, a good dataset could not be found for the selected study area at the municipality scale. Therefore, a specific uncertainty analysis to account for the most sensible choices to develop the DRI was performed:

1. Excluding individual exposure and vulnerability indicators.
2. Including excluded indicators with the multicollinearity analysis.
3. Using different weighting schemes for the calculation of the DEI and DVI.
4. Aggregating the DHI, DEI, and DVI with arithmetic mean instead of using formula (2).

The different weighting methods considered were the use of proportional weights (PW) (Naumann et al., 2014) – in our case by calculating the DVI without using ES, SS, and LCAC and formula (1), hence assigning proportional weights – and by applying an Analytical Hierarchical Process (AHP) (Cantini et al., 2019), by creating the pair comparison matrix and calculating the weights through geometric mean for both exposure and vulnerability indicators. Finally, the output of the uncertainty analysis – i.e. the rank of the municipality assigned by the composite indicator Rank (CIm), and the average shift in municipalities' rankings ($\bar{R}_s$) - were compared to evaluate the effect of these different methodologies (Naumann et al., 2014; OECD, 2008). The average shift was calculated as the average of the absolute differences in municipalities' ranks to a reference ranking – which in our case is the rank calculated with equal weights – in the N municipalities, with the equation:

$$\bar{R}_s = \frac{1}{N}\sum_{m=1}^{N}\left|Rank_{ref}(CI_m) - Rank(CI_m)\right| \quad (3)$$

2.3.8 Archetype analysis

Given the high number and diversity of indicators used in our drought risk assessment, the interpretation of the results might be complicated, affecting the potential usability of the insights provided in the assessment. To address this problem, archetype analysis, which is an emerging methodology to find recurrent patterns within cases and provide a simplified, but contextual, interpretation of results, was used (Eisenack et al., 2019; Oberlack et al., 2019). Akin to the approach used in other spatial archetypes research (Piemontese et al., 2021), a hierarchical cluster analysis was applied to understand the recurrent patterns of drought indicators within the selected municipalities. The municipalities were clustered through the Ward method (Ward, 1963) considering the whole set of normalized exposure and vulnerability indicators, also including the missing data, without further preprocessing; then, clusters were compared with boxplots and other basic statistics. Finally, considering that the ultimate objective of drought risk assessments is to provide the basis for developing drought management strategies (Hagenlocher et al., 2019; Hayes et al., 2004), the archetypes were used to discuss specific adaptation measures in municipalities with similar drought risk profiles.

2.4 Results

2.4.1 Multicollinearity analysis

Several significant (p-value<0.05) multicollinearities were detected. As a result, the indicator "Share of horticulture and fruticulture" was excluded from exposure indicators since it was highly correlated with "Value of Agricultural Products" and "Volume of water used for irrigation". For the vulnerability indicators, "Climate interference" and "Water deficit" were excluded since their variability was explained by other indicators, namely "Soil erosion" and "Soil fertility". Similarly, "Share of land irrigated with decision support systems" was excluded because of its high correlation with "Irrigable land"; in this case, the decision was also based on the data quality, which was lower for the excluded indicator. On the other hand, the indicator "Soil depth" showed a relatively high and significant correlation with "Soil erosion", but we decided to keep them both since they represent different processes. Finally, after the multicollinearity analysis, one exposure and three vulnerability indicators were excluded; hence, the number of indicators used to calculate the DRI was 42.

2.4.2 Robustness evaluation

Results in terms of $\bar{R}_s$ (Fig. 2.2) showed that DRI was more affected when individual exposure indicators were excluded, with an average $\bar{R}_s$ of 5.19. The indicator that was most impacting when excluded was the "Share of agricultural land" with an $\bar{R}_s$ of 6.45; this value was largely influenced by the extremely high difference in rankings of the municipality Monteroni d'Arbia, which was 43. As expected, excluding individual vulnerability indicators had a lower effect on DRI, since they were 14 in total (while the exposure indicators were only 4). A significant effect was also found by applying the AHP weighting method; assigning weights based on personal opinions, and giving more importance to indicators related to the irrigation practice, resulted in a $\bar{R}_s$ of 4.62, with a maximum shift of 16 for the municipality Gaiole in Chianti. Finally, the use of PW, the inclusion of the indicators excluded after the multicollinearity analysis, and the aggregation of DHI, DEI, and DVI with arithmetic mean, did not have a remarkable effect on $\bar{R}_s$. Summing up, our study confirms the findings of other drought risk assessments (Murthy et al., 2015; Naumann et al., 2014), that individuated as major sources of uncertainty the selection of indicators and the weighting method.

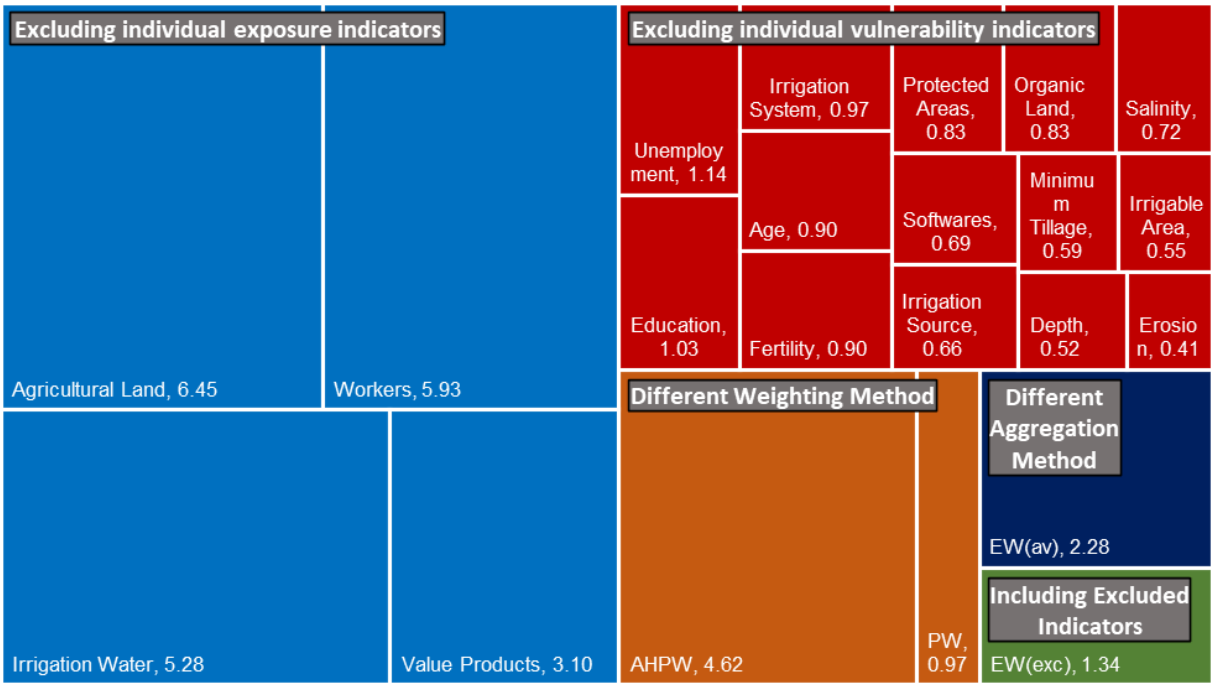

Figure 2.2: Results of the uncertainty analysis reported according to the average shift in rankings ($\bar{R}_s$) grouped as: excluding individual exposure indicators; excluding individual vulnerability indicators; different weighting method; different aggregation method; including excluded indicators.

Analysing the shifts in rankings of the single municipalities with the alternative methods, it is possible to affirm that, with some exceptions, the rankings were confirmed and the variations were minimal (Fig. A2.4), validating the assessment and confirming the robustness of the methodology. The municipalities that showed the highest $\bar{R}_s$ were also those with missing data, namely Radda in Chianti, ranked 23rd, and Monteroni d'Arbia, ranked 14th. The other municipality with missing data was Gaiole in Chianti, which was ranked 5th; probably this explains why the $\bar{R}_s$ was not as high as the others, since shifts upwards in the ranking had a minimal effect.

2.4.3 Drought risk mapping and ranking

Maps of DHI, DEI, DVI, and DRI are reported in Figure 2.3, while the rankings of the municipalities are reported in the appendix. Maps and rankings are briefly discussed in this section, while further analysis and discussion are performed when presenting the results of the cluster analysis.

Results of the DHI clearly showed that the Southern and Western (the coastal) municipalities will likely experience the highest drought hazard. In particular, the province of Grosseto, which includes the Albegna, Bruna, and lower Ombrone watersheds, will be the most affected. The most exposed municipalities were found in the coast - emblematic is the case of Campiglia Marittima with a very large share of land cultivated with industrial tomatoes, requiring high amounts of irrigation water - and where high-value wines are produced, such as Gaiole in Chianti and Montalcino. When analysing the drought vulnerability, it is necessary to consider that the indicators used to calculate DVI were 14; hence, results were more diversified without clear patterns. In general, it is possible to affirm that inland municipalities, located mostly in the provinces of Pisa and Siena, farthest from the coast and the main urban centres, were the most vulnerable. By combining the indexes, DRI provided an overall estimation of the risk; as expected, the coastal municipalities of the province of Grosseto were found to be the most at risk.

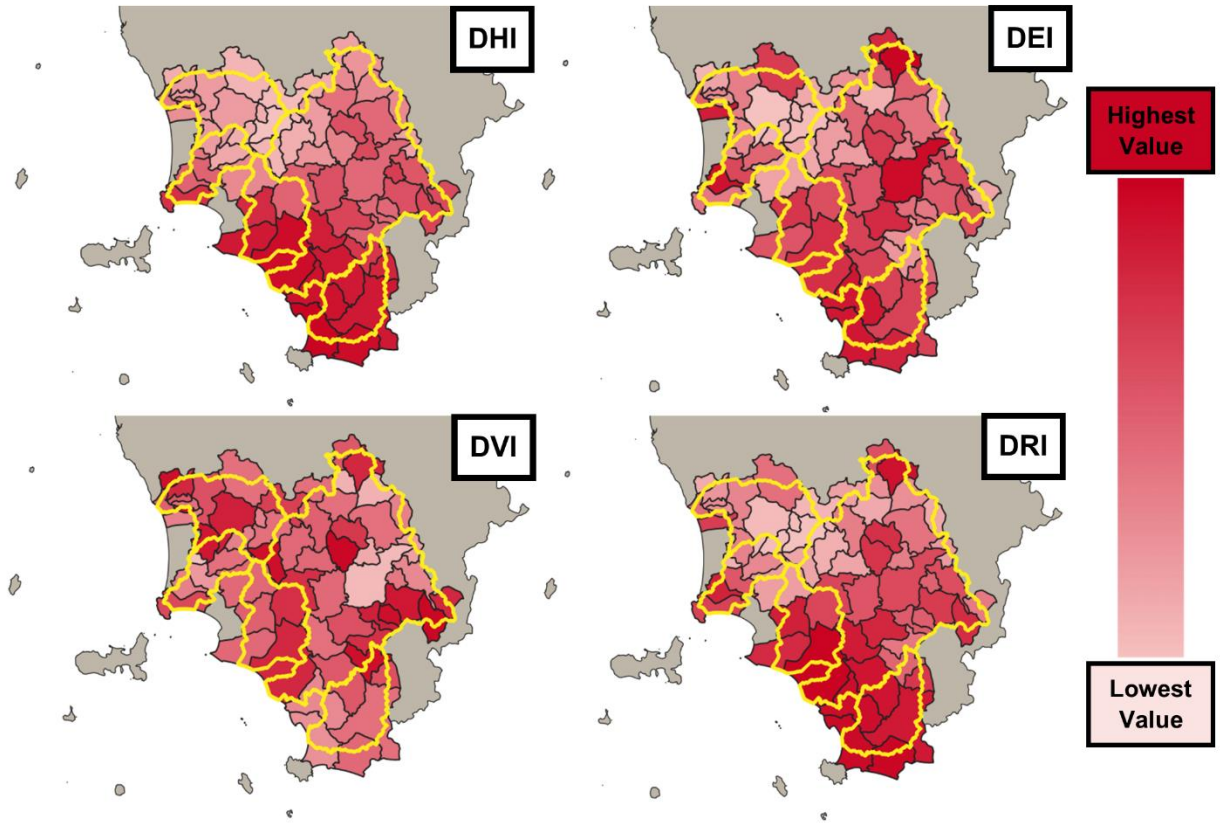

Figure 2.3: Maps of the DHI, DEI, DVI, and DRI; in light red the municipalities with the lowest values, and in dark red those with the highest. Watershed boundaries are depicted in yellow.

2.4.4 Archetype analysis

The hierarchical cluster analysis yielded seven clusters (Fig. 2.4). The characteristics of exposure and vulnerability of the clusters are reported as boxplots in Figures 2.5 and 2.6, while the main characteristics and the possible adaptation strategies are listed in Table 2.4. The clusters individuated were named according to

the most distinctive characteristics of the municipalities included. Cluster 1 – “high coastal irrigation” – comprised coastal municipalities spread among the five watersheds considered; cluster 2 – “high-value products” – comprised the wine producers’ municipalities of the Chianti hills in the upper Ombrone watershed, except Sassetta; cluster 3 – “high inland irrigation” – and 4 – “prevalence of agricultural land” – were mainly composed by inland municipalities of the provinces of Siena and Pisa; the municipalities of cluster 5 – “erosion-prone and vulnerable irrigation sources” – and 7 – “erosion-prone and vulnerable irrigation systems” – were spread among the provinces without an evident spatial pattern; cluster 6 – “prevalence of agricultural workers” – consisted in municipalities of the hills closest to the coast, mainly in the Grosseto province.

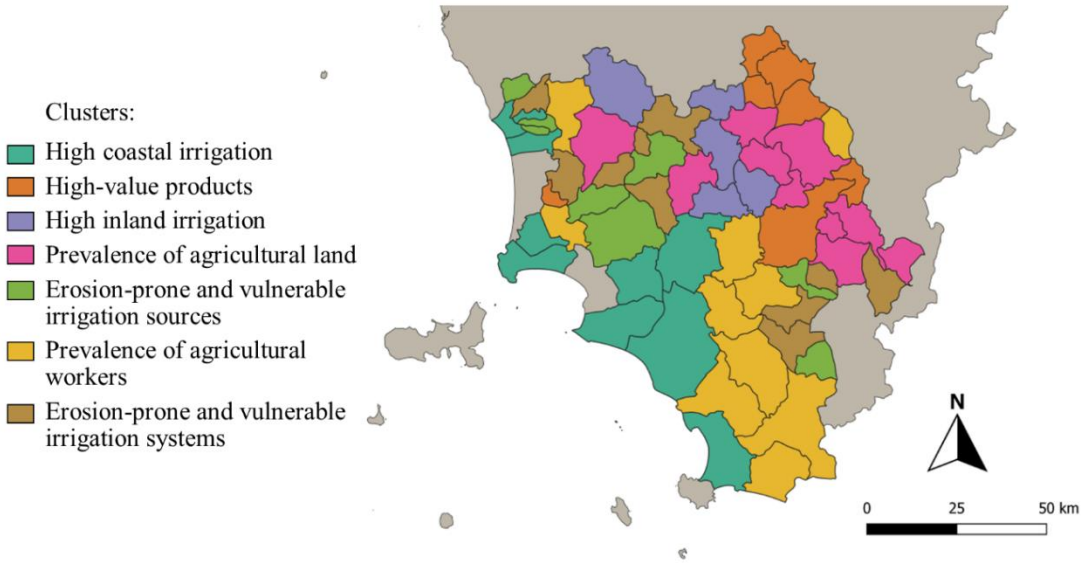

Figure 2.4: Spatial visualization of the seven clusters individuated in the Tuscany region.

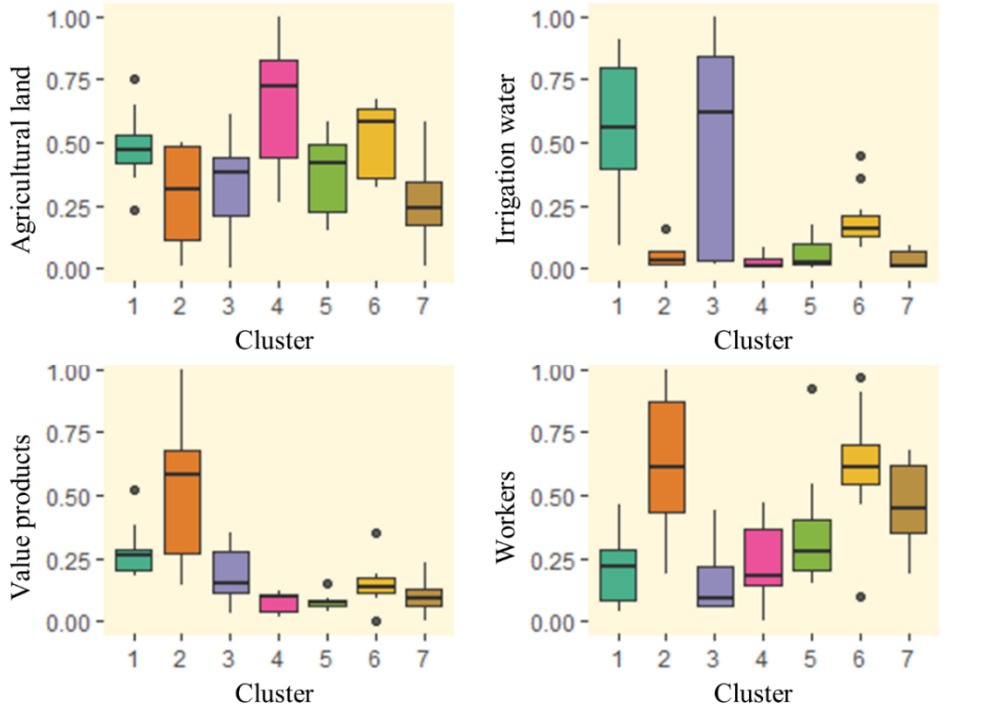

Figure 2.5: Boxplots of the normalized exposure indicators for the seven clusters individuated. The line represents the median, the box the upper and lower quartiles, the whiskers the highest and lowest values excluding outliers, and dots potential outliers.

By analyzing the main characteristics of exposure and vulnerability of the seven clusters (Fig. 2.5 and 2.6), possible adaptation strategies targeted to the specific characteristics of those clusters of municipalities can be suggested (Table 2.4). Certainly, further information needs to be considered when planning interventions, but these indications can be considered as a starting point. Being the most prone to drought hazard and risk, major efforts will have to be directed at the municipalities of cluster 1, and in particular the province of Grosseto and the Albegna, Bruna, and lower Ombrone watersheds.

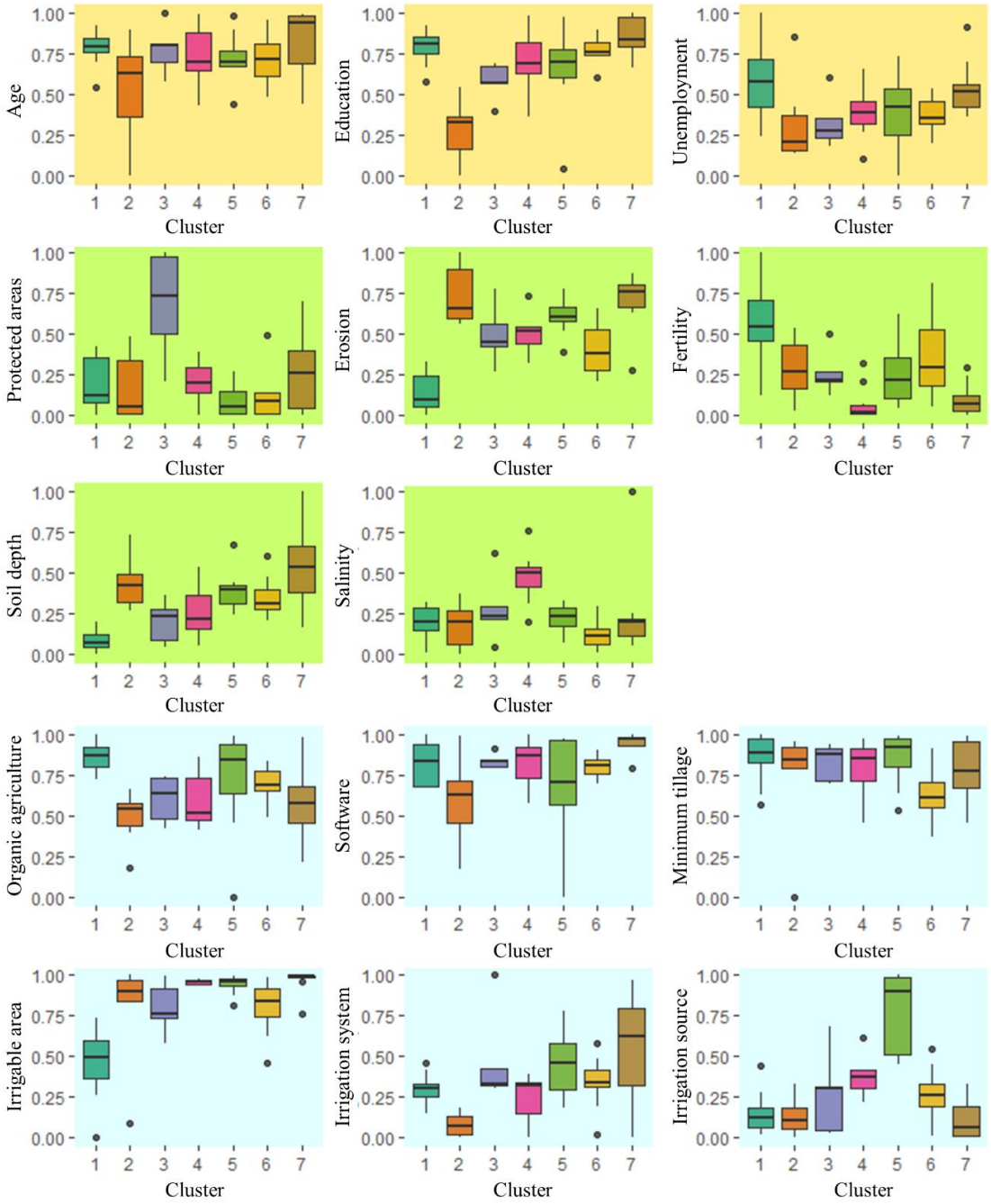

Figure 2.6: Boxplots of the normalized vulnerability indicators for the seven clusters individuated. The line represents the median, the box the upper and lower quartiles, the whiskers the highest and lowest values excluding outliers, and dots potential outliers. Light orange, light green, and light blue backgrounds represent indicators of Social Susceptibility, Ecological Susceptibility, and Lack of Coping and Adaptive Capacity, respectively.

Table 2.4: Characteristics of the seven clusters and suggested specific adaptation strategies.

Cluster	Characteristics	Specific adaptation strategies
1: High coastal irrigation	- High volumes of irrigation water - High irrigable areas - High unemployment - Low organic agriculture - Deep soils - Negligible erosion - Low soil fertility	- Increase water productivity - Improve irrigation efficiency - Managed aquifer recharge - Reduce water use (domestic and industrial) - Increase water supply (e.g. desalination, wastewater treatment) - New reservoirs
2: High-value products	- High-value products - High share of agricultural workers - High susceptibility to erosion - Youngest and most educated farmers - Diffused use of software to aid in crop management - Low vulnerability of irrigation systems	- Supplementary irrigation - Farm ponds
3: High inland irrigation	- High volumes of irrigation water - High share of protected areas	- New reservoirs - Improve irrigation efficiency
4: Prevalence of agricultural land	- High share of agricultural land - Good soil fertility - High salinity	
5: Erosion-prone and vulnerable irrigation sources	- High erosion rates - Low organic agriculture - Vulnerable irrigation sources - Vulnerable irrigation systems	- Shift from surface irrigation methods to pressurized systems - Soil conservation measures (e.g. contour trenches, terraces) - Conservation agriculture (no tillage, cover crops)
6: Prevalence of agricultural workers	- High share of agricultural workers - Good share of land with minimum tillage	
7: Erosion-prone and vulnerable irrigation systems	- Quite-high share of agricultural workers - High erosion rates - Shallow soils - Very fertile soils - The most vulnerable irrigation systems	- Shift from surface irrigation methods to pressurized systems - Soil conservation measures (e.g. contour trenches, terraces) - Conservation agriculture (no tillage, cover crops)

Some patterns can also be described by observing the DHI, DEI, DVI, and DRI for each cluster (Fig. 2.7) and the rankings of the municipalities belonging to different clusters (in the appendix). Even though drought hazard indicators were not included in the cluster analysis, the municipalities of clusters 1 and 6 ranked highest since they mostly represent the Grosseto province. Considering the DEI, the highest-ranked are municipalities of clusters 1 and 6, but also those of cluster 2 such as Gaiole in Chianti and Montalcino. The values of the DVI were less stretched; however, there is a prevalence of the municipalities of clusters 3, 4, 5, and 7 in the highest ranks. Being DRI the aggregation of DHI, DEI, and DVI, the highest rankings of the municipalities of the clusters 1 and 6 – except the municipality Gaiole in Chianti of cluster 2 – can be easily explained.

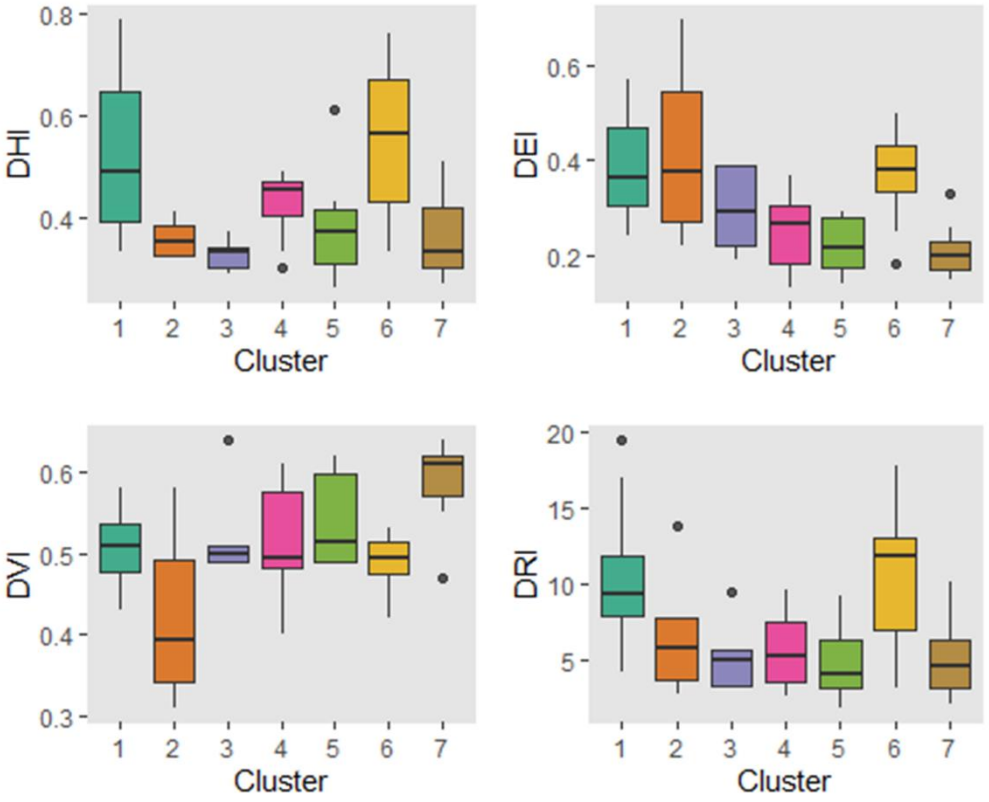

Figure 2.7: Boxplots of DHI, DEI, DVI, and DRI for the seven clusters. The line represents the median, the box the upper and lower quartiles, and the whiskers the highest and lowest values excluding outliers.

2.5 Discussion

2.5.1 Past and future drought hazard

Interesting results were found in the estimation of drought hazard. Correlations between the total severity, duration, and frequency calculated with SPI3, SPI6, SPI12, and VHI in the 58 municipalities were poor, meaning that if we selected only one of them a different pattern of drought hazard would have been found. The non-standardized indicators of future hazard showed very high correlations when considering the same indicator in the short-, medium-, and long-term future, while much worse correlations between different indicators; however, this was expected since these indicators do not directly estimate drought. Although many studies have been conducted on drought hazard indicators, these results confirm the need for further research to individuate the best indicators – both used individually and in an ensemble – to more accurately account for drought. Interestingly, the correlation between the DHI calculated with past and future hazard indicators showed a coefficient of determination of 0.42; hence, past drought hazard dynamics are expected to be confirmed in the future. In our opinion, the use of multiple drought hazard indicators to represent different drought types added value to the assessment and was theoretically sound, since the impacts on agriculture are represented by different accumulation periods for SPI (Stagge et al., 2015; Vergni and Todisco, 2011), even more so when including irrigated areas (Bachmair et al., 2018; Huang et al., 2018).

2.5.2 Selection of indicators and limitations

The choice of vulnerability and exposure indicators is also critical and needs to be justified properly in the conceptual framework. Even though some authors consider that a fundamental characteristic of drought risk

assessment is their objectivity and simplicity (Naumann et al., 2014), a relatively high number of indicators to include more information was used. As a result, we did not find clear vulnerability patterns both in the mapping and in the cluster analysis. However, vulnerability is influenced by many processes, thus over-simplifications might lead to unrealistic estimates. To sum up, a good balance should be found in the number of indicators, with multicollinearity analysis that proved to be useful for this scope. Additionally, we used some specific indicators in addition to the generic ones, which is commonly advised against, since specific vulnerability indicators should be linked to specific exposure indicators (Carrão et al., 2016). For example, irrigation indicators should be weighted more where volumes of irrigation water are higher, but to account for these complex processes would further complicate the procedure. Again, we argue that the benefits of the inclusion of a higher number of indicators outweigh these negative aspects. Certainly, data limitation is a recurrent problem in many regions of the world and the indicators selection is a crucial step that needs to be carefully performed according to data availability, objectives, spatial scale, unit of analysis etc. Hazard indicators can be calculated with remote sensing-based products; hence, the problem is restricted to exposure and vulnerability indicators. Given that at least one representative indicator is available for the risk components of equations (1) and (2), the approach can be replicated, using either a sub-set of the indicators we proposed or inferring them from other studies (e.g. Hagenlocher et al., 2019; Meza et al., 2019).

The inclusion of irrigated areas as an exposure indicator is highly recommended when dealing with developed countries. In some global (Carrão et al., 2016), continental (Naumann et al., 2014), and regional (Murthy et al., 2015; Prabnakorn et al., 2019) assessments it is considered a measure of coping capacity that reduces vulnerability, but this can be considered true only in some developing countries where irrigation is not largely practiced. Possibly, the use of different irrigated- and rainfed-specific indicators to represent vulnerability as in Meza et al. (2020) is a more appropriate approach, but in many cases rainfed and irrigated agriculture coexist, making it difficult to perform separated analyses.

A recurrent problem in drought studies is that to predict drought risk we consider drought hazards rather than impacts which, in the end, are what really matters (Enenkel et al., 2020). Furthermore, the role of local stakeholders is crucial for developing sound and effective strategies to cope with extreme events and climate change (Hayes et al., 2004; Nguyen et al., 2016; Vogt et al., 2018; World Bank, 2019), but the integration of local and expert knowledge in drought monitoring and adaptation is challenging due to the reciprocal scepticism (Giordano et al., 2013). Also, farmers' perceptions of drought do not always correspond to the commonly used drought indicators (Giordano et al., 2013; Stagge et al., 2015; Urquijo and De Stefano, 2016). Including hard and soft data, quantitative and qualitative data, and local and expert knowledge might allow performing a more detailed and meaningful drought risk assessment and should be considered in further research.

2.5.3 Linking the results with adaptation strategies

Comparing risk assessment outputs with similar assessments is difficult due to the context-specific meaning of the results. Also, no similar drought risk assessment has been performed for central and southern Tuscany. Hence, results were compared with more general climate risk analysis (for multiple natural hazards) performed at the national level with the provinces (NUTS3) as the units of analysis. Consistent with the results of our assessment, Mysiak et al. (2018) found that the Grosseto province has higher potential climate change impacts and lower adaptive capacity compared with the other provinces. Similarly, Spano et al. (2020) reported a lower adaptive capacity to climate change for the same area. Furthermore, the PNACC (2018) confirms our results in terms of risk patterns and the highest risk for the province of Grosseto, which has a medium-high adaptive capacity and high potential impacts; instead, the province of Livorno has a medium-

high adaptive capacity and medium-low potential impacts, while the provinces of Pisa and Siena have a high adaptive capacity, with the first one with expected medium potential impacts and the latter with high potential impacts. Projected climate change impacts on yields of durum and common wheat and maize reported in Spano et al. (2020) do not show clear differences within the areas considered in our assessment; overall, negative impacts for maize and slight increases in yield for wheat are expected.

Because of the high number of indicators used in the comprehensive risk assessment, we used archetype analysis to link the results of the risk assessment with possible adaptation strategies. Archetype analysis, by identifying municipalities with overall similar characteristics and risk profiles, can help decision-makers to better target the most relevant adaptation strategies. To show the potentiality of the approach proposed in this research, the suggested adaptation strategies for clusters 1 ("high coastal irrigation") and 2 ("high-value products"), which are the most representative, are discussed in detail. Municipalities of cluster 1 have a high drought risk (Fig. 2.7) driven by intense irrigation. Potential adaptation strategies include increasing water productivity and improving irrigation efficiency (e.g. Mantino et al., 2017), as well as increasing storage with new reservoirs. At the same time, seawater intrusion and groundwater pollution and depletion need to be considered (Barazzuoli et al., 2008, 1999; Grassi et al., 2007). Therefore, the use of nature-based solutions such as the managed aquifer recharge, already tested in a pilot project in the Cornia watershed, represents a very promising solution that could significantly reduce the vulnerability of groundwater-based irrigation areas (Rossetto et al., 2019, 2018). Additionally, these municipalities have the highest water demand in summer, in which the highest crop irrigation requirements coincide with the touristic season and with the lowest precipitation and highest evapotranspiration. Hence, further interventions to reduce other water uses (domestic and industrial) and increase water supply (e.g. desalination, wastewater treatment) could be beneficial (Mantino et al., 2017). On the other hand, municipalities of the second cluster show high exposure and low vulnerability to drought (Fig. 2.7). In addition to the highest income related to agriculture, this cluster has the youngest and most educated farmers; thus, the most likely to adopt innovative adaptation strategies. One crucial intervention is supplemental (or emergency) irrigation (Matese et al., 2018), which is still underdeveloped in the vineyards of Tuscany because of the limited availability of irrigation water (D. Bianchi et al., 2021). A possible solution is represented by runoff harvesting structures, such as farm ponds, which have been already suggested for the hilly areas of central Tuscany to overcome summer water shortage (Napoli et al., 2014).

In addition to the cluster-specific adaptation strategies proposed in Table 2.4, cross-cutting strategies such as improved agronomic management, drought-resistant varieties, cropping patterns' change and diversification, and crop insurance could be also considered to tackle drought. Win-win solutions with negligible side effects can be achieved by upgrading surface irrigation systems in erosion-prone areas (suggested in particular for clusters 5 and 7) and using alternative water sources such as desalinization and wastewater treatment (especially in cluster 1). Recent initiatives of the Italian government and other associations (ANBI and Coldiretti) strongly reintroduced the debate about the implementation of new reservoirs to cope with drought. If properly designed, respecting the ecosystems and ensuring sufficient environmental flows, this strategy can significantly reduce drought vulnerability in the context of climate change (Masia et al., 2018; Sordo-Ward et al., 2019). However, many examples of negative feedback exist linked to water infrastructures, such as increased water consumption and the sense of over-reliance that increases vulnerability (Di Baldassarre et al., 2021, 2018). Similar unintended negative consequences might also be promoted by crop insurance (Deryugina and Konar, 2017; OECD, 2021). Furthermore, the well-known efficiency paradox shows how water savings at the field scale with improved irrigation efficiencies might lead to increased water consumption at the watershed scale (Dumont et al., 2013; Grafton et al., 2018). These and other

counterintuitive dynamics further complicate the planning of some drought adaptation strategies. To deal with such complexity and uncertainty, the involvement of multiple stakeholders is crucial.

2.6 Conclusion

A complete drought risk assessment was conducted for 58 municipalities belonging to five coastal watersheds of Central and Southern Tuscany (Central Italy). The proposed approach allowed to produce a policy-relevant drought risk assessment, even though adjustments could further improve the methodology. The use of data from public drought observatories proved to be reliable and useful; furthermore, the inclusion of multiple drought hazard indicators provided a more comprehensive analysis of drought risk. The use of future projections to account for climate change impacts also confirmed the patterns of past hazards; however, future patterns of vulnerability and exposure should also be considered. Moreover, the inclusion of social and environmental indicators improved the comprehensiveness of the assessment. Robustness evaluation is necessary to validate the methodology used; in our case, we performed it with an internal validation, but comparing results with an external dataset is equally important. The robustness evaluation confirmed that the most uncertain parts of the methodology to calculate composite indicators are the choice of indicators and the weighting method. Finally, archetype analysis was successfully used to link the results of the assessment with possible adaptation strategies.

Composite indicators are debated and sometimes controversial, with multiple pros and cons; they need to be constructed and used carefully, so as not to foster policies with unintended negative impacts (OECD, 2008). Suggested adaptation strategies were proposed based on a literature review and our knowledge but, of course, caution and further analyses are needed when planning and investing economic resources. Southernmost municipalities of Tuscany showed to be the most at risk, in particular those belonging to the Albegna, Bruna and lower Ombrone watersheds. Also, major efforts should be devoted to the coastal municipalities since multiple sectors use the water resource, and the demand is particularly concentrated in the summer months. The results of this assessment are meant to be used by local decision-makers and experts to plan and promote more tailored and proof-based adaptation strategies. Ideally, the results of this drought risk assessment will be the base to fuel the discussion about drought management to involve farmers and other interested stakeholders.

Chapter 3 Climate change impact assessment

The manuscript reported as Chapter 3 was published in Agricultural Water Management (complete reference: Villani, L., Castelli, G., Yimer, E. A., Chawanda, C. J., Nkwasa, A., Van Schaeybroeck, B., van Griensven., A., Penna, D. & Bresci, E. (2024). Impacts of climate change and vegetation response on future aridity in a Mediterranean catchment. Agricultural Water Management, 299, 108878, https://doi.org/10.1016/j.agwat.2024.108878).

3.1 Abstract

The Mediterranean region's climate is projected to become warmer and drier but future projections of precipitation are uncertain, especially in the Northern part. Additionally, the difficulty in determining the plant physiological responses caused by CO_2 rising complicates the estimation of future evaporative demand, increasing the uncertainty of future aridity assessments. The main objective of this study is to estimate the effect of climate change and stomatal conductance reduction on projected water balance components and the resulting impact on aridity in a medium-sized catchment of Central Italy. We validate and couple a hydrological model with climate projections from five regional climate models and perform simulations considering or not the vegetation responses. Results show that their inclusion significantly affects potential evapotranspiration. The other water balance components, namely actual evapotranspiration, water yield, percolation and irrigation, are also influenced but with less significant changes. Considering or not the CO_2 suppression effect on stomatal conductance, coupled with the uncertainty related to precipitation, highly influences the estimation of future aridity as the future climate classification ranges from "humid" to "semi-arid" depending on the simulation and climate model, even if model outputs need to be evaluated cautiously with CO_2 concentration higher than 660 ppm.

3.2 Introduction

The Mediterranean area is considered a hotspot for climate change since, compared to other regions, temperatures will rise 20% faster and precipitation will decrease 4% faster per degree of warming than the global average (Lionello and Scarascia, 2018). Moreover, it will face increased extreme heat, heavy precipitation, and hydrological and agricultural droughts (Arias et al., 2021). Focusing on future precipitation in the Mediterranean region, many studies highlighted a clear North-South gradient, with the Southern areas facing the most severe impacts of climate change. Despite the great uncertainty, the zero-change line in precipitation is usually estimated to cross Northern and Central Italy (e.g., Coppola et al., 2021; Mariotti et al., 2015; Spano et al., 2020).

Understanding future precipitation trends and their spatial patterns in Italy is crucial given their large socio-economic and environmental impact (WHO, 2018). Indeed, according to the Organisation for Economic Co-operation and Development classification, Italy is currently considered a medium-high water-stressed country since more than 30% of renewable water resources are used, with a large share dedicated to agriculture (PNACC, 2018). Furthermore, water availability and demand are very inhomogeneously distributed throughout the country. Past studies on precipitation variability, reviewed and analysed by Caporali et al. (2021), showed that there is a negative trend in total annual precipitation for the whole Italian territory, which is most pronounced in the winter season. Interestingly, these past trends oppose future precipitation projections that simulate a reduction in summer precipitation and a slight increase in winter (Spano et al., 2020). More specifically, over Central Italy, no significant past trends were obtained for yearly precipitation, while significant positive trends in autumn and winter were identified. At the same time, meteorological

drought analyses showed an increasing trend in both severity and frequency for two other regions in Central Italy, Abruzzo and Umbria (Di Lena et al., 2014; Vergni and Todisco, 2011).

Past and future warming over land has a strong impact on the atmospheric evaporative demand (here referred to as potential evapotranspiration, PET), leading to a reduction in soil moisture and increased agricultural and ecological droughts (Douville et al., 2021; Seneviratne et al., 2021). Vicente-Serrano et al. (2022a) stressed the importance of PET changes in the observed increase in agricultural and ecological droughts. Temperature and humidity are strongly linked and the change in relative humidity is tightly related to the soil-moisture availability (Drobinski et al., 2020). The surface-drying effect due to increased temperatures will be reduced in the Northern Mediterranean due to the availability of sufficient soil moisture (Tramblay et al., 2020). Mariotti et al. (2015) inferred that in Europe future evapotranspiration changes over land were mainly linked to changes in projected precipitation. Surface insolation is projected to increase over the whole Mediterranean, mainly because of reduced cloudiness (Coppola et al., 2021). On the other hand, soil moisture is projected to decrease in many areas of the Mediterranean, but again with high uncertainties; for example, no significant changes are projected over large parts of Italy (Mariotti et al., 2015).

When trying to assess the future aridity conditions, another major source of uncertainty is the direct effect of CO_2 concentration increase through changes in plant transpiration and growth (Manzoni et al., 2022; Vicente-Serrano et al., 2022b). CO_2 rising boosts crop growth through the CO_2 fertilization effect and reduces plant transpiration and PET through the CO_2 suppression effect on stomatal conductance (Zhang et al., 2022). Overall, the decrease in transpiration caused by the stomatal conductance reduction is compensated by the increase in transpiration caused by the CO_2 fertilization effect (Manzoni et al., 2022), especially in dry and semi-arid climates (Fatichi et al., 2016). Increasing CO_2, therefore, has an indirect effect on runoff which is the main factor explaining the discrepancy between a projected increased future runoff as predicted by climate models and a drying trend that is projected from future drought and aridity estimations (Yang et al., 2019). Globally, the greening effect of CO_2 rising and climate change was demonstrated with evidence from the last ice age and the historical era (Scheff, 2018; Zhu et al., 2016). Assessing future aridity conditions using temperature-based indices without accounting for the CO_2 fertilization and stomatal suppression effects may result in an incomplete assessment (Scheff, 2018; Swann et al., 2016). Nevertheless, the current increase in CO_2 concentration is occurring at an unprecedented rate at which ecosystems might not be able to take advantage; also, nutrient availability might limit the positive effect of CO_2 fertilization (Scheff, 2018). Climate models already take into account the CO_2 fertilization mechanism, but this effect might be overestimated, and caution is suggested when directly using the outputs of climate models in the estimation of future drought (Vicente-Serrano et al., 2022a).

While the uncertainty related to projected precipitation is vastly explored in literature, the one related to PET, linked mainly to the CO_2 suppression effect on stomatal conductance, is rarely estimated. The objective of this study is to demonstrate the importance of considering the plant physiological responses to CO_2, mainly stomatal conductance reduction, when calculating projected PET, quantifying the difference in simulated water balance components and aridity when considering or not the vegetation responses. The impacts of climate change on water resources such as the water balance components and river flows are frequently assessed by coupling climate and hydrological models (Tramblay et al., 2020). Among the various hydrological models, the Soil and Water Assessment Tool (SWAT) has been frequently used in the Mediterranean region, including for climate change analyses in Italy (Aloui et al., 2023). Here, we use as meteorological data five bias-corrected EURO-CORDEX Regional Climate Models (RCMs) and evaluate their projected trends for precipitation and temperature in the Ombrone catchment in Central Italy. These are then used to force the SWAT+ model (Arnold et al., 2018; Bieger et al., 2017) to simulate future water balance. We evaluate the

model performance in predicting monthly streamflow using a multi-site calibration and validation process. We then simulate PET with constant and decreasing stomatal conductance and assess the effect of the plant physiological responses to CO_2 on aridity and other water balance components. In this study, we also focus on the SWAT+ approach to estimate PET upon exceedance of the 660 ppm threshold, which is considered the maximum value at which the equations used by the model are valid. Understanding the mechanisms behind and improving the quantification of the CO_2 suppression effect on stomatal conductance and CO_2 fertilization will allow the development of more robust aridity projections which, in turn, are required to optimally plan potential adaptation measures.

3.3 Methodology

3.3.1 Study area: the Ombrone catchment

Coastal, small-to-medium-sized, intermittent and ephemeral rivers prevail in the Mediterranean region, accounting for more than half of the total area (Ducrocq et al., 2016). The Ombrone catchment, located in Central and Southern Tuscany, is a typical example of a Mediterranean catchment, with an area of 3552 km^2, a maximum elevation of 1738 m.a.s.l., and the river outlet in the Tyrrhenian Sea (Fig. 3.1). The Ombrone river is the second longest river of Tuscany with a length of 161 km and has several tributaries, including the Arbia, Merse, Farma and Orcia (Diodato et al., 2023). The Ombrone catchment is almost entirely included in the provinces of Siena and Grosseto. As emerged from Chapter 2, this part of Tuscany is considered significantly water-stressed due to the high concomitant water demand for agriculture and tourism, especially in the coastal areas. Southern Tuscany is also the area of the region that receives less precipitation and is experiencing the most pronounced increases in dry spell occurrence (Bartolini et al., 2022). Furthermore, the analysis conducted by Diodato and Bellocchi (2008) classified this area as prone to agricultural drought. According to the Köppen classification, the prevalent climate can be described as a hot-summer Mediterranean (Csa) climate (Beck et al., 2018), characterized by hot, dry summers and cool, humid winters, with an annual precipitation of 600-1100 mm according to the data used in this study. The climate of the internal areas of the Ombrone catchment is more continental compared to the coastal areas, with slightly higher precipitation and shorter summers (Diodato et al., 2023). Future projections indicate that this might shift towards hot and cold semi-arid (BSh and BSK) climates (Beck et al., 2018). The Ombrone catchment is characterized by hilly and mountainous areas with slopes of over 20% and torrential streams (Diodato et al., 2023). According to the Corine Land Cover of 2018 used in this study, the main land covers of the catchment are forest (39%) and herbaceous annual crops (46.87%), and the other types of vegetation are permanent pastures (4.28%), vineyards (3.84%), and olive groves (1.89%). The remaining parts of the catchment are covered with artificial surfaces, shrubland and bare land.

In the last sixty years, Tuscany has experienced significant economic growth that led to a reduction in the number of farms and the abandonment of cultivated land, especially in the less productive areas (Napoli et al., 2017). The upland areas of the Ombrone catchment in the Siena province are mainly cultivated with non-irrigated crops such as cereals, olives, and grapevine. Vineyards and olive groves are widespread in the whole of Tuscany and are prevalent in rugged and sloped areas prone to erosion (Napoli et al., 2014; Napoli and Orlandini, 2015). In the coastal areas of the Grosseto province, irrigation is more widely used and orchards and horticultural crops are common. Water is thereby pumped mainly from the coastal aquifer of the Grosseto plain, which suffers from overexploitation, seawater intrusion, and pollution (Aldinucci et al., 2012; Zucaro and Tudini, 2008).

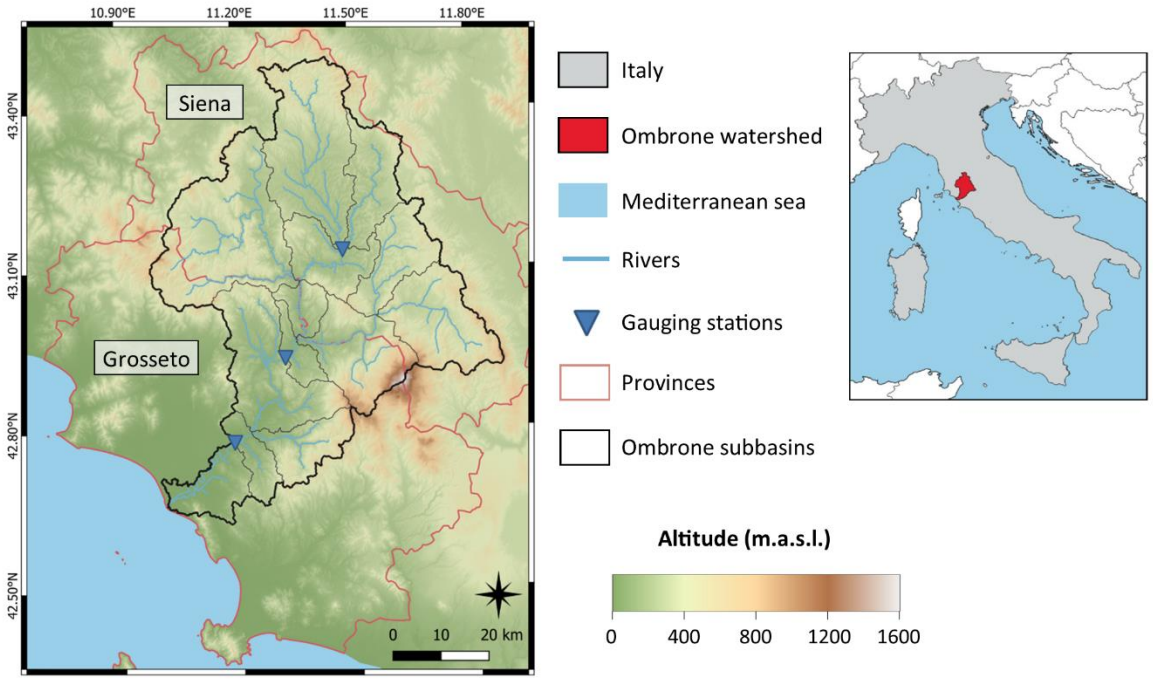

Figure 3.1: The Ombrone catchment with the three gauging stations, the subbasins, and the boundaries of the provinces of Siena and Grosseto.

3.3.2 The SWAT+ model

The SWAT+ model is a restructured version of SWAT that offers better spatial discretization of the catchment, improved code maintenance and more flexibility in representing management practices compared to the original version (Arnold et al., 2018; Bieger et al., 2017). This dynamical model uses a daily time step, and represents the catchment with a semi-distributed approach, by dividing it into subbasins, landscape units, and Hydrological Response Units (HRUs). The HRUs each have homogeneous characteristics of soil, slope, and land use. The different modules included in the model have been used for many applications, including hydrological, water quality, erosion, and climate change assessments (Aloui et al., 2023). Also, the SWAT+ model can simulate plant growth with the module based on a simplified version of the Environmental Policy Integrated Climate (EPIC) model (Neitsch et al., 2011). Plant growth is simulated here using daily-accumulated heat units and inhibited by water, temperature, and nutrient stress. The management schedule, including fertilization, irrigation, tillage, and rotations, can be specified at the HRU level, and crop parameters are available but can also be modified by the user. A key improvement in SWAT+ upon SWAT is the inclusion of decision tables, which allow for an improved representation and modelling of complex rules related to water and agricultural management (Arnold et al., 2018).

The SWAT/SWAT+ modelling suite can be conveniently used to evaluate the impacts of the plant physiological responses to CO_2, namely the CO_2 suppression effect on stomatal conductance and the CO_2 fertilization, on streamflow and water balance components (Wang et al. 2017, Wu et al., 2012). The modification of the Penman-Monteith approach to simulate the suppression effect on stomatal conductance included in SWAT is commonly applied (e.g., Lemaitre-Basset et al., 2022). In the traditional Penman-Monteith equation, stomatal resistance, which is the inverse of stomatal conductance, is assumed to remain constant and is therefore unrealistic (Lemaitre-Basset et al., 2022). Only when the Penman-Monteith method is used, SWAT+ has been adjusted to account for the stomatal suppression effect (Neitsch et al., 2011; Nkwasa et al., 2023). More specifically, in SWAT+ the stomatal resistance (r_c) is allowed to change with equation 1 (Easterling et al., 1992)

based on an experiment that reached a CO_2 concentration of 660 ppm (Morison, 1987), which is much lower than the projected increase by the end of the century under Representative Concentration Pathway (RCP) 8.5. Moreover, the CO_2 fertilization effect is accounted for in SWAT+ by simulating increased radiation use efficiency (RUE) with equation 2, which affects daily biomass accumulation (Neitsch et al., 2011).

$$r_c = \frac{r_l}{(0.5 \cdot LAI) \cdot (1.4 - 0.4 \cdot \frac{CO_2}{330})} \quad (1)$$

$$RUE = \frac{100 \cdot CO_2}{CO_2 + \exp(r_1 - r_2 \cdot CO_2)} \quad (2)$$

where r_l is the minimum effective stomatal resistance of a single leaf (s m^{-1}), LAI is the Leaf Area Index of the canopy, r_1 and r_2 are the shape coefficients calculated by the model for each crop.

For the SWAT+ model setup, we used the EU-DEM (version 1.0) at 25 m resolution and the 2018 Corine Land Cover and Land Use map from the Copernicus Land Monitoring Service. Default thresholds were used for channel and stream creation (17 and 171 km^2, respectively). As soil map, we used the Pedological Database of the Tuscany Region. In this database, soil texture and organic matter content are available as average in the whole soil profile, while hydraulic conductivity is reported for two layers. Other information, such as soil depth and salinity, are reported as categorical variables. To estimate soil properties, pedotransfer functions are typically used (Abbaspour et al., 2019). We estimated available water capacity with the widely used pedotransfer function of Saxton and Rawls (2006) as in Napoli et al. (2017), bulk density with the equation proposed by Manrique and Jones (1991) that performs well in Italy (Pellegrini et al., 2007), the soil erodibility factor with the method of Williams (1995), and the soil albedo with the equation introduced in Sugathan et al. (2014). Climate data were obtained from the Regional Hydrological Service (SIR) of the Tuscany Region. In SWAT+, weather stations are created based on climate input data and assigned to the HRUs. More details on climate input data are available in Table A3.1. A 10 ha area threshold was applied to filter the HRUs.

We defined a simplified representation of cropland using the four main herbaceous crops of the catchment. For this, we used the land covers provided by the Tuscany region through the ARTEA agency, which are published yearly and contain detailed field-specific characteristics of crop type, crop variety, and crop management. Hence, in the model, we split the herbaceous cropland use into four classes: durum wheat as the rainfed winter crop (30%), sunflower as the rainfed spring crop (15%), maize as the irrigated spring crop (15%), and alfalfa as the forage crop (40%). We checked and slightly modified the default decision tables already available in the model for sowing and harvesting crops to match the typical sowing and harvesting dates. We included in the management schedule mouldboard and harrow tillage and representative fertilization schemes. We prepared a decision table for automatic sprinkler irrigation of 20 mm per event triggered by a water stress threshold of 0.241. By using these values, we obtained volumes of irrigation of the same order of magnitude as compared to the most updated data retrieved from the National Institute of Statistics (ISTAT, 2010). In SWAT+, the water stress is calculated by comparing actual and potential plant transpiration (Neitsch et al., 2011). To confirm the consistency of the crop-management schedule, we compared it with reported crop schedules in the Tuscany region (Dalla Marta et al., 2010; Orlando et al., 2015; Giannini and Bagnoni, 2000; Tuscany Region, 2010).

3.3.3 Multi-site calibration and validation

We set up the SWAT+ model (revision 60.5.4) in QGIS for a period from 2010 until 2021. Then, we used the SWAT+ Toolbox to perform automatic sensitivity analysis, calibration and validation for monthly streamflow. The parameters considered for the automatic sensitivity analysis were selected from the literature, but we

also included other parameters related to the soil map (Table A3.2). We considered two years of warm-up for calibrations, validations and simulations.

Monthly streamflow data for three flow gauging stations were retrieved from SIR (Fig. 3.1). After the automatic sensitivity analysis performed with the SWAT+ Toolbox, we started calibrating the selected parameters in the upstream flow station of Buonconvento, using five years of monthly flow (2017-2021). Then, for Sasso d'Ombrone we calibrated the parameters using the same time window and validated with monthly flows from 2012 to 2016, maintaining the calibrated parameters for the subbasins of Buonconvento. We finally repeated the same procedure for Istia, where we considered three years of data for both calibration (2019-2021) and validation (2013-2015). The periods for calibration and validation were selected according to the data availability. Hence, the calibration was performed for all three gauging stations, while the validation was only in two of them.

In the automatic calibration for monthly streamflow, we used the Nash Sutcliffe Efficiency (NSE) as the objective function. The per cent bias (Pbias) and the RMSE-observations standard deviation ratio (RSR) were calculated as additional statistics to evaluate the performance of the model. The NSE quantifies how well the plot of observed and simulated data agree and NSE is equal to 1 for a perfect match and smaller otherwise; the Pbias expresses how much the modelled values differ from the observed values, with an optimal value of 0%; the RSR is retrieved by normalizing one of the most common error index – the Root Mean Square Error (RMSE) – with the standard deviation of the measured data (Moriasi et al. 2007). We evaluated the model performances following the criteria of Moriasi et al. (2015) for NSE and Pbias, while those of Moriasi et al. (2007) for RSR (Table A3.3). The equations to calculate NSE, Pbias and RSR are:

$$NSE = 1 - \frac{\sum_{i=1}^{n} \left(Y_i{}^{obs} - Y_i{}^{sim}\right)^2}{\sum_{i=1}^{n} \left(Y_i{}^{obs} - Y^{mean}\right)^2} \quad (3)$$

$$Pbias = \frac{\sum_{i=1}^{n} \left(Y_i{}^{obs} - Y_i{}^{sim}\right)}{\sum_{i=1}^{n} Y_i{}^{obs}} \cdot 100 \quad (4)$$

$$RSR = \frac{RMSE}{STDEV_{obs}} = \frac{\sqrt{\sum_{i=1}^{n} \left(Y_i{}^{obs} - Y_i{}^{sim}\right)^2}}{\sqrt{\sum_{i=1}^{n} \left(Y_i{}^{obs} - Y^{mean}\right)^2}} \quad (5)$$

where Y_i^{sim} is the *i*th simulated value, Y_i^{obs} is the *i*th observed value, *n* is the total number of observations, and Y^{mean} is the average of the observed values.

3.3.4 Climate change scenarios

To estimate future climate changes, we used five EURO-CORDEX climate models (Jacob et al., 2014) (Table 3.1) and RCPs 4.5 and 8.5 (Moss et al., 2010). We considered two periods of 30 years, 2041-2070 and 2071-2100, to evaluate medium- and long-term climate change impacts, comparing the projected values with those of the historical simulations (from 1976 to 2005) of each climate model. The criteria for selecting the climate models were (1) the availability of both RCPs, (2) the availability at daily frequency of precipitation and the climate variables needed to calculate evapotranspiration with the Penman-Monteith method (maximum and minimum temperatures, relative humidity, solar radiation, and wind speed), (3) the use of a complete (Gregorian) calendar, (4) a horizontal RCM resolution of 0.11° over the EURO-CORDEX domain. A bias correction of the climate-projection data is necessary as systematic biases are present in the meteorological

data (Maraun and Widmann, 2018). Among the different methodologies that exist for bias correction of climate models, we adopted distribution mapping which is commonly used for climate and hydrological studies (Teutschbein and Siebert, 2012; Themeßl et al. 2011).

We used the CMHyd software to bias correct temperature and precipitation (Rathjens et al., 2016). The software reprojects the data and applies the selected bias-correction method using the station data provided by the user. The CMHyd outputs can be directly used in the SWAT+ model without further preprocessing. Since bias correction is performed by comparing the historical simulation of the climate models with observed values before 2005, we used a lower number of stations compared to the calibration and validation period. The stations used for bias correction were included in the Ombrone catchment or very close and had more than 10 years of data as indicated in Fung (2018). More details about the climate data used for bias correction can be found in Table A3.1. To process the other climate variables, solar radiation, relative humidity and wind speed, we used the Climate Data Operators (CDO) software, version 2.0.5 (Schulzweida, 2021). These bias-corrected climate data were then used to run historical and future simulations. In the result section, we detected the changes by comparing future and historical simulations for each climate model and RCP.

In SWAT+, the crop cycle is defined with the number of days required to reach maturity, differently from the older version which used the number of heat units (Nkwasa et al., 2023). To account for the shortening of the crop cycles, we retrieved the heat units starting from the days to maturity used during the calibration and validation period. Then, we calculated the new crop cycle length considering the different temperatures in the historical and future periods.

Table 3.1: The five climate models used in the study with the General Circulation Model (GCM) and the Regional Climate Model.

	GCM institute	GCM model	RCM institute	RCM model
1	CNRM-CERFACS	CNRM-CM5	CNRM-CERFACS	ALADIN63
2	CNRM-CERFACS	CNRM-CM5	KNMI	RACMO22E
3	ICHEC	EC-EARTH	KNMI	RACMO22E
4	MPI-M	MPI-ESM-LR	SMHI	RCA4
5	NCC	NorESM1-M	GERICS	REMO2015

After the calibration and validation of the SWAT+ model, we performed simulations to assess the impacts of climate change considering the different climate models, RCPs, and periods. At first, we evaluated the magnitude and sign of the climate change signal for future precipitation and average temperature in the Ombrone catchment, considering the basin scale outputs of the SWAT+ model. To quantify the impacts of the plant physiological responses to CO_2 on PET and other water balance components, we performed simulations with constant CO_2 at 400 ppm, as in the calibration and validation, and others considering the values as reported by Büchner and Reyer (2022), for RCPs 4.5 and 8.5, for the historical, near and far future periods. We used the 30-year-average CO_2 concentration since it is a fixed input parameter in the SWAT+ model. The average CO_2 concentration for RCP 4.5 (522 and 589 ppm for the near and far futures, respectively) and the near future for RCP 8.5 (611 ppm) fall between the limit of the Morison experiment (330-660 ppm), while the average CO_2 concentration for the far future of RCP 8.5 is much higher (939 ppm).

We evaluated the impacts of climate change and vegetation responses to CO_2 on future PET and estimated future dryness conditions with the Aridity Index (AI). AI is calculated as the ratio between precipitation and PET (Middleton and Thomas, 1997) and is useful for classifying the climate following the UNEP climate classification. Despite the intrinsic simplifications of this method, AI is used for climate classification (Massari

et al., 2022) and as a benchmark for aridity conditions at the regional scale (He et al., 2022). Hence, AI estimation is useful to evaluate the uncertainty related to RCPs and the inclusion of the stomatal conductance reduction caused by CO_2 concentration rising. Finally, we performed a similar analysis for the water balance components and other variables simulated with the SWAT+ model, namely actual evapotranspiration, water yield (a direct output of the model defined as the sum of surface runoff, lateral soil flow, and tile flow), percolation, and irrigation.

We applied the Wilcoxon rank-sum non-parametric test to detect significant differences between historical and future periods and between simulations including and excluding the vegetation responses to CO_2. We considered the yearly values of the variables considered in the analysis. The two samples used to test the significant differences were always selected from the same climate model.

3.4 Results

3.4.1 Multi-site calibration of SWAT+

Out of the 15 parameters pre-selected for the sensitivity analysis, we considered only the most sensitive, specifically *cn2*, *esco*, *epco*, *bd*, and *revap_co*. More details about the calibrated parameters are available in the supplementary materials (Table A3.2, A3.3, A3.4). Despite overestimation of peak flows, we obtained more than satisfactory performances according to the criteria considered in this study (Table 3.2, Fig. 3.2). More in detail, the model achieved very good performances in Buonconvento during the calibration period for the three statistics considered, while in Sasso d'Ombrone we obtained very good performances considering NSE and RSR and good for Pbias. For the Istia gauging station, we obtained very good performances for NSE and RSR during validation and good for Pbias, while during the calibration period satisfactory performances for NSE and Pbias and good for RSR. The reduced performance for Istia during calibration can be mainly attributed to a discharge peak in February 2019 (see Fig. 3.2) which might be an error in the observed streamflow data since it is not present in the other sites.

Table 3.2: Model performances for monthly streamflow during calibration and validation for the three gauging stations considered. For Buonconvento only the calibration was carried out.

Monthly streamflow	**Calibration**			**Validation**		
Station	**NSE**	**Pbias**	**RSR**	**NSE**	**Pbias**	**RSR**
Buonconvento	0.86 [1]	3.2% [1]	0.38 [1]	-	-	
Sasso d'Ombrone	0.87 [1]	-6.3% [2]	0.36 [1]	0.80 [1]	9.2% [2]	0.45 [1]
Istia	0.66 [3]	13.0% [3]	0.58 [2]	0.80 [1]	8.9% [2]	0.44 [1]

[1] Very good; [2] Good; [3] Satisfactory.

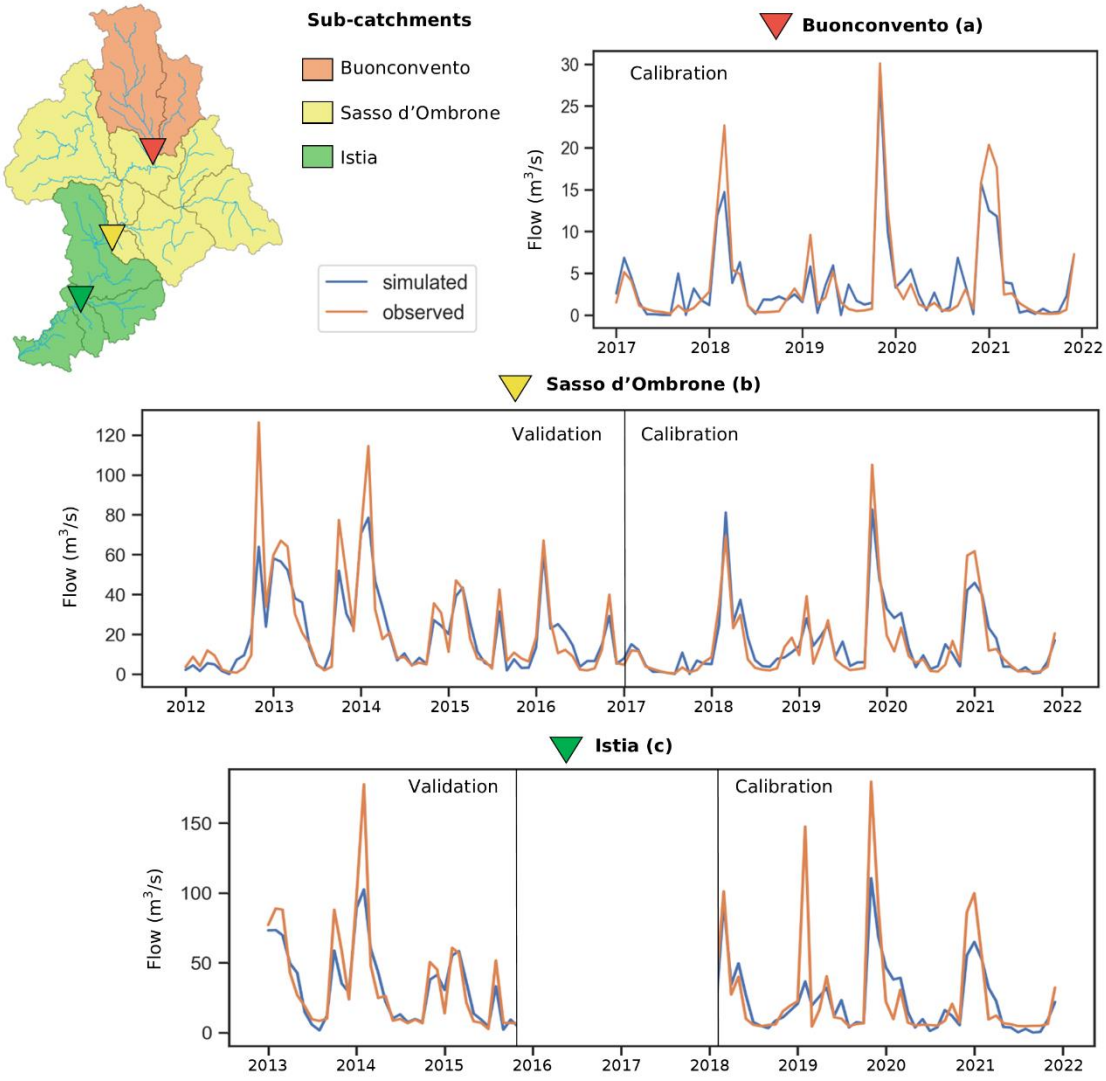

Figure 3.2: Multi-site calibration and validation, with the location of the gauging stations of Buonconvento (a), Sasso d'Ombrone (b), and Istia (c), and the respective hydrographs with simulated and observed monthly average flows.

3.4.2 Projected temperature and precipitation changes over the Ombrone catchment

A positive, significant climate change signal over the Ombrone catchment was obtained for annual average temperatures, for all future periods and RCPs considered (Fig. 3.3, Table 3.3, A3.5). While the increase in temperature under RCP 4.5 was of similar magnitudes in the near and far futures, under RCP 8.5 it continued to rise in the far future. In the far future, the highest increases of 18% and 32% were found for NorESM1-M – REMO2015, under RCPs 4.5 and 8.5 respectively. The ensemble-mean temperature increase at the end of the century was 2.1 °C and 4 °C for RCPs 4.5 and 8.5, respectively (Table A3.5). Temperature increases were largest for the summer season and daily minimum temperature. For average, maximum, and minimum temperatures, the increases in summer were higher than those in winter, particularly for RCP 8.5. The ensemble-mean increases were 1.9 °C and 3.5 °C for winter average temperature, for RCPs 4.5 and 8.5, respectively, while for summer these were 2.3 °C and 4.8 °C (Table A3.5).

For annual precipitation, climate change projections were much more uncertain (Fig. 3.4, Table 3.3, A3.5). The RCMs disagreed on the sign of change, with four RCMs predicting negligibly-small changes or increases

and one (NorESM1-M – REMO2015) a decrease (Table 3.3, Fig. A3.1). The ensemble-mean average annual precipitation increased at the end of the century by 70 and 32 mm for RCPs 4.5 and 8.5, respectively (Table A3.5). This difference is mainly caused by the significant decrease in precipitation by NorESM1-M – REMO2015 for RCP 8.5 (-21%) (Table 3.3). In RCP 4.5 the slight increase occurred by the end of the century, in contrast to RCP 8.5 in which the increase was found in the near future. The increases in precipitation were found mainly in winter, while the models indicated reduced increases or even decreases in spring and summer. More specifically, the ensemble-mean increases in winter average precipitation were 34 and 22 mm for RCPs 4.5 and 8.5 respectively, while the ensemble-mean changes for summer were 5 and -7 mm for RCPs 4.5 and 8.5 respectively (Table A3.5). In the far future, 3 out of 5 models projected significant increases in precipitation under RCP 4.5. Under RCP 8.5, two predicted significant increases while NorESM1-M – REMO2015 significant decreases (Table 3.3). Under RCP 4.5 in the near future, CNRM-CM5-RACMO22E behaved differently as compared to the other climate models and was the only one showing significant increases of 27% in precipitation (Table 3.3).

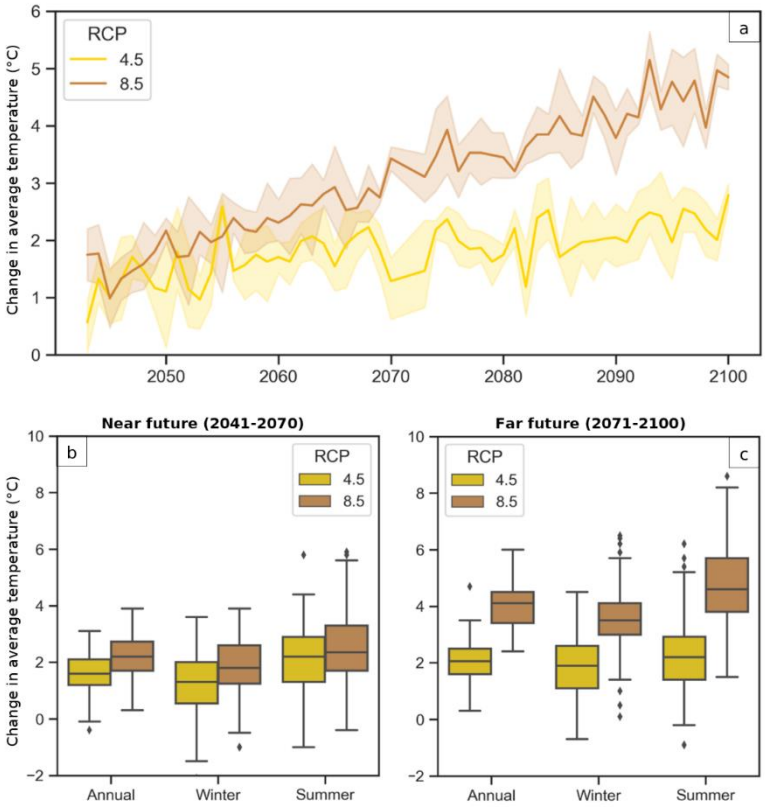

Figure 3.3: Lineplot and boxplots of future temperature (°C). Lineplot (a) reports the absolute difference between the future years (2041-2100) and the yearly average of the historical period (1976-2005), for RCPs 4.5 and 8.5. The line represents the average of the five climate models, while the band is the confidence interval. The values of average temperature calculated with the same procedure considering annual, winter and summer values, for the near (b, 2041-2070) and far futures (c, 2071-2100), are used in the boxplots.

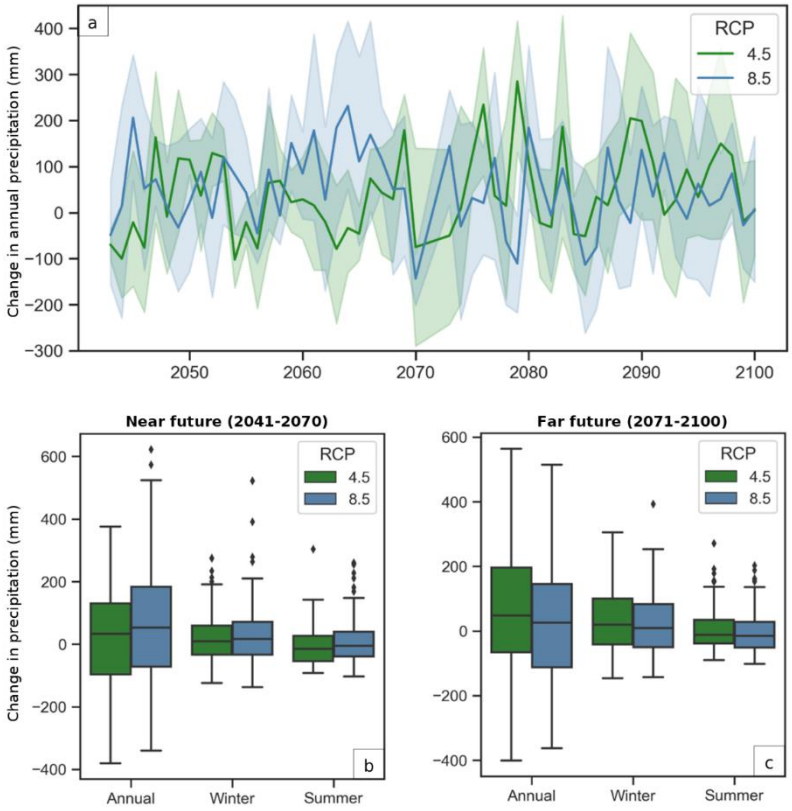

Figure 3.4: Lineplot and boxplots of future precipitation (mm). Lineplot (a) reports the absolute difference between the future years (2041-2100) and the yearly average of the historical period (1976-2005), for RCPs 4.5 and 8.5. The line represents the average of the five climate models, while the band is the confidence interval. The same values considering annual, winter and summer values, for the near (b, 2041-2070) and far futures (c, 2071-2100), are used in the boxplots.

3.4.3 Impacts of climate change and vegetation responses to CO_2 on future potential evapotranspiration and future aridity

Projected PET drastically changed, both in terms of magnitude and sign, considering RCPs 4.5 and 8.5 and due to the inclusion of the stomatal conductance reduction effect (Fig. 3.5a, Table 3.3). Consequently, the other components of the water balance such as actual evapotranspiration, water yield, percolation, and irrigation were similarly influenced (Fig. 3.6, Table 3.4). As expected, the changes in PET in the far future were particularly high for RCP 8.5. When not including the suppression effect, PET increased in line with temperature. In that case, under RCP 4.5, the average PET increased up to 110 mm (Table A3.6) mainly in the near future, while in the far future, the increases remained of a similar magnitude. This reflects the increase in temperature that occurred early in the near future and slowed down by the end of the century (Fig. 3.3). Under RCP 8.5, on the contrary, PET continued to increase until the end of the century, reaching an average increase of 225 mm (Table A3.7). The CO_2 suppression effect balanced the temperature-induced change in PET, quenching its increase under RCP 4.5 to 16 mm (Table A3.6). The CO_2 concentration used in the long-term future period under RCP 8.5, on the other hand, was 939 ppm, far above the upper limit of 660 ppm of the Morison experiment. This explains the drop in PET in the period 2071-2100, with an ensemble-mean decrease of -211 mm (Table A3.7).

Table 3.3: Precipitation, average temperature and potential evapotranspiration in the historical, near and far future periods for the five climate models considered in this study. For potential evapotranspiration, the values for both cases, constant and reduced stomatal conductance, are reported. Significance levels of the Wilcoxon test between future and historical periods and between the two cases considered are also included in the table.

Climate model	Precipitation (mm)		Average temperature (°C)		Potential evapotranspiration (mm)			
					Constant stomatal conductance		Stomatal conductance suppression	
Historical								
1	711		13.8		1008		1020	
2	648		13.9		930		942	
3	716		13.7		990		1003	
4	693		13.9		1193		1211	
5	667		13.6		1203		1220	
Near Future								
	RCP 4.5	**RCP 8.5**	**RCP 4.5**	**RCP 8.5**	**RCP 4.5**	**RCP 8.5**	**RCP 4.5**	**RCP 8.5**
1	714 (0%)	790 (11%)	15.7 (14%)**	16.1 (17%)**	1160 (15%)**	1158 (15%)**	1118 (10%)**, ††	1076 (6%)**, ††
2	700 (8%)	820 (27%)**	15.2 (10%)**	16.0 (15%)**	998 (7%)**	1013 (9%)**	958 (2%)††	936 (-1%)††
3	712 (-1%)	801 (12%)	14.9 (9%)**	15.5 (13%)**	1066 (8%)**	1083 (9%)**	1024 (2%)†	1002 (0%)††
4	762 (10%)	752 (9%)	15.3 (10%)**	16.2 (17%)**	1275 (7%)**	1321 (11%)**	1216 (0%)††	1206 (0%)††
5	632 (-5%)	607 (-9%)	15.6 (14%)**	16.1 (18%)**	1303 (8%)**	1331 (11%)**	1250 (2%)††	1228 (1%)††
Far future								
	RCP 4.5	**RCP 8.5**	**RCP 4.5**	**RCP 8.5**	**RCP 4.5**	**RCP 8.5**	**RCP 4.5**	**RCP 8.5**
1	840 (18%)*	749 (5%)	16.1 (17%)**	18.0 (30%)**	1163 (15%)**	1290 (28%)**	1090 (7%)**, ††	891 (-13%)**, ††
2	784 (21%)**	766 (18%)*	15.8 (14%)**	17.4 (26%)**	1009 (9%)**	1085 (17%)**	941 (0%)††	733 (-22%)**, ††
3	817 (14%)*	851 (19%)**	15.5 (13%)**	17.5 (28%)**	1055 (7%)**	1183 (19%)**	987 (-2%)††	809 (-19%)**, ††
4	704 (2%)	706 (2%)	15.9 (14%)**	18.1 (30%)**	1318 (10%)**	1441 (21%)**	1218 (1%)††	924 (-24%)**, ††
5	639 (-4%)	524 (-21%)**	16.0 (18%)**	17.9 (32%)**	1331 (11%)**	1456 (21%)**	1240 (2%)††	976 (-20%)**, ††

* p-value < 0.05 for the Wilcoxon rank-sum test with variables from simulations with historical and future
** p-value < 0.01 for the Wilcoxon rank-sum test with variables from simulations with historical and future
† p-value < 0.05 for the Wilcoxon rank-sum test with variables from simulations with constant and reduced stomatal conductance
†† p-value < 0.01 for the Wilcoxon rank-sum test with variables from simulations with constant and reduced stomatal conductance

The uncertainty in future precipitation as predicted by the five climate models considered (Fig. 3.4, S1, Table 3.3) and the one in future PET as predicted by the SWAT+ model forced with the climate projections (Fig. 3.5a) escalated when considering AI. While AI was simulated to be around 0.65 in the historical simulations, that is the threshold that divides the "dry sub-humid" and "humid" climates, AI drastically disperses depending on the RCPs, climate models, and whether or not the CO_2 suppression effect on stomatal conductance is included (Fig. 3.5b). By the end of the century, under RCP 4.5, the deviation between the different models will be higher as compared to the historical simulations. When considering stomatal conductance reduction, the AI values ranged between 0.83 and 0.52, while they were slightly lower with constant stomatal conductance, between 0.78 and 0.48. Following the more uncertain predictions under RCP 8.5, the projected AI ranged between 0.72 and 0.36 when considering constant stomatal conductance and between 1.05 and 0.54 when analysing the simulations with stomatal conductance reduction. Therefore, according to the UNEP classification (Middleton and Thomas, 1997), the current humid/dry sub-humid climate is predicted to shift towards a much more humid climate for RCP 8.5 when considering the vegetation responses to CO_2, while it shifts towards a much more arid climate when considering the same RCP but calculated with constant stomatal conductance. With the driest climate projections of the NorESM1-M – REMO2015 climate model,

under RCP 8.5 and constant stomatal conductance, AI was predicted to be below 0.5, the threshold that divides “dry sub-humid” and “semi-arid” climates.

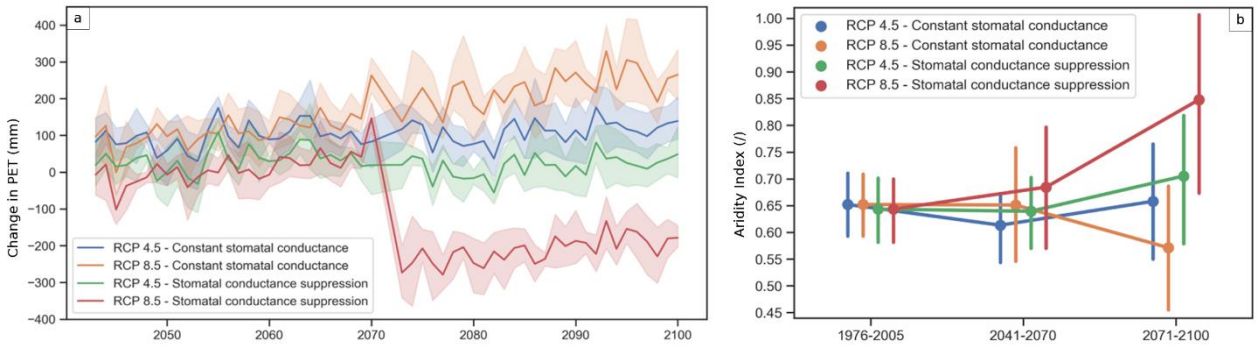

Figure 3.5: Potential evapotranspiration and Aridity Index (AI) with constant or decreased stomatal conductance. (a) Lineplot of projected potential evapotranspiration (mm), reported as the absolute difference between the future years (2041-2100) and the yearly average of the historical period (1976-2005), for RCPs 4.5 and 8.5, considering constant and decreasing stomatal conductance. The line represents the average of the five climate models, while the band is the confidence interval. The abrupt change occurring in 2070 is due to the fact that the CO_2 concentration value was averaged and considered constant for the two future periods (2041-2070 and 2071-2100). (b) The AI, calculated as the ratio between precipitation and potential evapotranspiration for the historical (1976-2005), medium-term (2041-2070) and long-term (2071-2100) future periods considering RCPs 4.5 and 8.5, and constant and increasing CO_2 concentration values. The dots represent the average values and the uncertainty is reported considering the five climate models.

3.4.4 Impacts of climate change and vegetation responses to CO_2 on future water balance components

Since equation 1 used in the SWAT+ model was tested only until 660 ppm, we opted to analyze future impacts of climate change and vegetation responses to CO_2 on water balance components only in the near future (2041-2070), with CO_2 concentrations lower than the threshold.

Changes in water yield and percolation were strictly linked to precipitation. In the near future, the climate models which predicted precipitation increases were CNRM-CM5-RACMO22E and MPI-ESM-LR-RCA4 under RCP 4.5 and all except NorESM1-M-REMO2015 under RCP 8.5 (Table 3.3). If the precipitation increases were mostly not significant, for water yield and percolation the Wilcoxon test always resulted in p-values lower than 5% (Table 3.4). The percentage changes were much higher for water yield and percolation as compared to precipitation increases, reaching up to 105% and 73% increases for CNRM-CM5-RACMO22E under RCP 8.5 and with stomatal conductance suppression for water yield and percolation, respectively (Table 3.4).

For evapotranspiration and constant stomatal conductance, we observed significant changes (-8%) only for NorESM1-M-REMO2015 under RCP 8.5. Instead, we found more significant differences when including the stomatal conductance suppression. For example, under both RCPs, evapotranspiration in MPI-ESM-LR-RCA4 and NorESM1-M-REMO2015 significantly decreased by up to -11%. Irrigation amounts in the future will mostly decrease (Table 3.4). With constant stomatal conductance, significant decreases (-12% under both RCPs) were found only in MPI-ESM-LR-RCA4. Including stomatal conductance suppression, CNRM-CM5-ALADIN63 and CNRM-CM5-RACMO22E showed significant decreases under RCP 8.5, while the decreases for MPI-ESM-LR-RCA4 were up to -23% under RCP 8.5.

The variables related to temperature – PET and actual evapotranspiration – were reduced when considering the plant physiological responses to CO_2, while those related to precipitation – water yield and percolation – showed an increase when the vegetation responses were included. If the changes caused by the inclusion/exclusion of the stomatal conductance suppression were significant for PET (Table 3.3), the changes

found for the other balance components were not significant in most cases. We obtained significant changes only under RCP 8.5 for evapotranspiration (3 models out of 5) and irrigation (2 models out of 5). Figure 3.6 reports the absolute values of the ensemble water balances for the two cases considered in this study and their relative percentage difference. Differences in the historical period were minimal (1-2%) and they increased as the CO_2 concentration was higher. Under RCP 8.5, irrigation changed the most with a difference of 10.1%, followed by percolation (-8%), soil evaporation (7.1%), water yield (-5.5%) and transpiration (3.2%). Canopy evaporation was barely affected by the change in potential evapotranspiration driven by different CO_2 concentrations. The magnitude of percentage changes caused by the vegetation responses to CO_2 ranged between -4.8% and 4.1% for RCP 4.5, while between -8% and 10.1% for RCP 8.5.

Table 3.4: Water yield, percolation, evapotranspiration and irrigation in the historical and near future periods for the five climate models and for both cases, constant and reduced stomatal conductance, considered in this study. Significance levels of the Wilcoxon test between future and historical periods and between the two cases considered are also included in the table.

Climate model	Water yield (mm)		Percolation (mm)		Evapotranspiration (mm)		Irrigation (mm)	
Historical (Constant stomatal conductance)								
1	98		127		499		11	
2	93		112		453		11	
3	106		134		483		11	
4	91		108		513		14	
5	84		78		519		16	
Near Future (Constant stomatal conductance)								
	RCP 4.5	**RCP 8.5**	**RCP 4.5**	**RCP 8.5**	**RCP 4.5**	**RCP 8.5**	**RCP 4.5**	**RCP 8.5**
1	106 (9%)	126 (29%)*	137 (8%)	158 (25%)**	482 (-3%)	515 (3%)	12 (4%)	11 (-4%)
2	121 (30%)*	180 (94%)**	141 (25%)*	179 (60%)**	447 (-1%)	470 (4%)	11 (-1%)	10 (-5%)
3	106 (0%)	144 (36%)*	131 (-2%)	167 (24%)*	479 (-1%)	498 (3%)	11 (7%)	10 (-5%)
4	124 (37%)**	123 (35%)*	150 (39%)**	139 (29%)*	497 (-3%)	499 (-3%)	12 (-12%)*	13 (-12%)*
5	85 (1%)	81 (-4%)	75 (-4%)	62 (-21%)	487 (-6%)	476 (-8%)*	16 (-5%)	16 (-3%)
Historical (Stomatal conductance suppression)								
1	96		125		502		11	
2	92		110		457		11	
3	105		132		487		11	
4	90		105		517		15	
5	83		76		522		17	
Near future (Stomatal conductance suppression)								
	RCP 4.5	**RCP 8.5**	**RCP 4.5**	**RCP 8.5**	**RCP 4.5**	**RCP 8.5**	**RCP 4.5**	**RCP 8.5**
1	110 (14%)	134 (39%)*	142 (14%)	170 (36%)**	472 (-6%)*	493 (-2%)†	11 (-1%)	10 (-14%)*,†
2	125 (36%)*	188 (105%)**	147 (33%)**	191 (73%)**	436 (-4%)	448 (-2%)	10 (-7%)	9 (-16%)**
3	110 (5%)	153 (46%)**	137 (4%)	180 (36%)**	468 (-4%)	475 (-2%)†	11 (0%)	9 (-14%)
4	129 (44%)**	131 (46%)**	157 (49%)**	152 (44%)**	484 (-6%)*	476 (-8%)**,†	12 (-18%)**	11 (-23%)**,†
5	87 (4%)	83 (0%)	80 (4%)	71 (-7%)	480 (-8%)*	463 (-11%)**	15 (-12%)	14 (-16%)†

* p-value < 0.05 for the Wilcoxon rank-sum test with historical and future samples

** p-value < 0.01 for the Wilcoxon rank-sum test with historical and future samples

† p-value < 0.05 for the Wilcoxon rank-sum test with constant and reduced stomatal conductance samples

†† p-value < 0.01 for the Wilcoxon rank-sum test with constant and reduced stomatal conductance samples

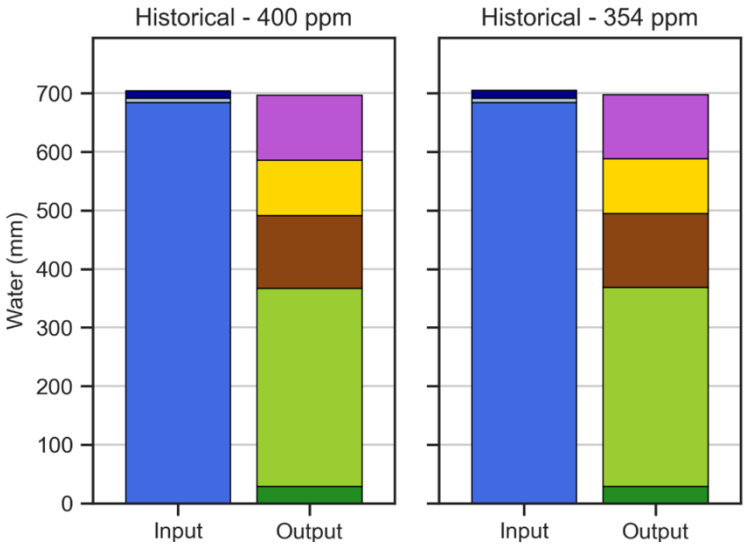

	400 ppm	354 ppm	Δ
Precipitation	684.3		/
Snow	7.7		/
Irrigation	12.6	12.9	-2.3%
Canopy evaporation	28.9	28.9	0%
Transpiration	337.9	339.6	-0.5%
Soil evaporation	124.8	126.6	-1.4%
Water yield	94.0	92.8	1.3%
Percolation	111.4	109.3	1.9%

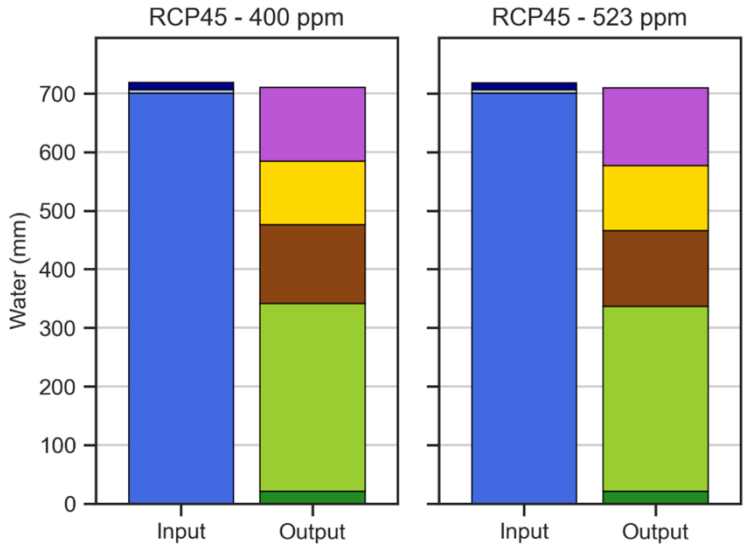

	400 ppm	523 ppm	Δ
Precipitation	701.3		/
Snow	5.6		/
Irrigation	12.3	11.8	4.1%
Canopy evaporation	21.7	21.7	0
Transpiration	319.9	315.0	1.5%
Soil evaporation	135.1	129.6	4.1%
Water yield	107.9	111.5	-3.3%
Percolation	126.1	132.1	-4.8%

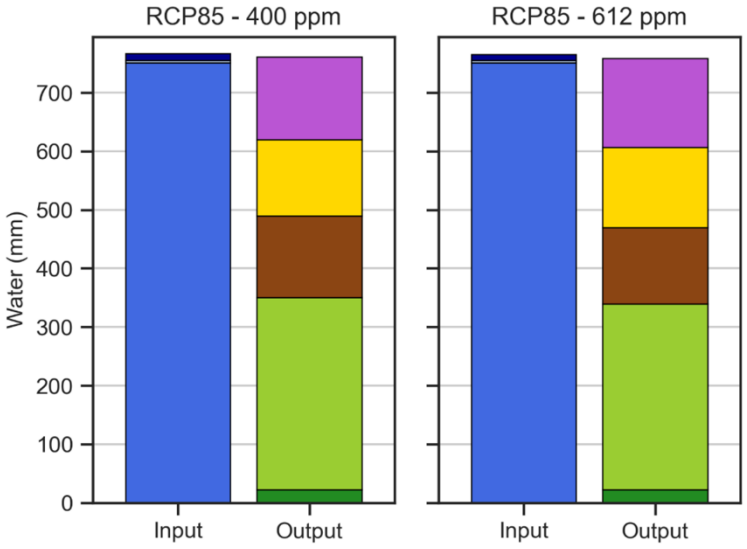

	400 ppm	612 ppm	Δ
Precipitation	751.0		/
Snow	3.9		/
Irrigation	11.9	10.7	10.1%
Canopy evaporation	22.1	22.2	-0.5%
Transpiration	327.9	317.4	3.2%
Soil evaporation	139.7	129.8	7.1%
Water yield	130.3	137.5	-5.5%
Percolation	140.7	151.9	-8.0%

Figure 3.6: Bar plots and tables with the water balance components of the various simulations carried out in this study. The water balance values used are the ensembles of the five climate models. The cases of constant stomatal conductance (400 ppm) and modified CO_2 concentration are reported with the amounts and the percentage changes (Δ column in the table).

3.5 Discussion

3.5.1 Climate models' uncertainty in the Northern Mediterranean area

Our study further confirmed that the projected increases in temperatures in the study region are significant, and especially high for RCP 8.5 and during summer, consistent with previous research (e.g., Spano et al., 2020). On the other hand, results revealed even more uncertainty regarding the future precipitation predicted by climate models for the Northern Mediterranean area. The ensemble mean of the five climate models considered in this study indicated an increase in precipitation, more accentuated during winter and for RCP 4.5. These results look contradictory as compared to the projections for the overall Mediterranean region. Nevertheless, Central and Northern Italy are in a transition zone between the arid North African and the humid Central European climate zones, and the zero-change line predicted in past studies usually crosses this area (e.g., Coppola et al., 2021; Mariotti et al., 2015; Spano et al., 2020). A deeper analysis of the literature regarding only the Northern Mediterranean area showed very high uncertainty, and in particular when considering Central and Northern Italy. For example, Mariotti et al. (2015) analysed the outputs of CMIP5 experiments, using an ensemble of climate models for RCP 4.5, and found only a minor decrease of 0.2 mm/day during summer by the end of the 21st century, and no decrease when considering winter or annual precipitation over the Northern Mediterranean area. Instead, Lionello and Scarascia (2018) considered RCP 8.5 of CMIP5 experiments and found an overall reduction of precipitation except for winter and, to a lower extent, spring months in the Northern Mediterranean area. The analysis of the outputs of the first EURO-CORDEX RCMs ensemble showed that, for Italy, the climate change signal for precipitation was uncertain under RCP 4.5, while it was negative for Central and Southern Italy under RCP 8.5, again with a distinct gradient increasing southward (Jacob et al., 2014). More recently, Coppola et al. (2021) used a much larger ensemble of EURO-CORDEX RCMs and compared the outputs with those of CMIP5 and CMIP6 GCMs, considering RCP 8.5. The three ensembles agreed to show the precipitation zero-change line over the Northern Mediterranean during winter, while it shifted northward in summer, meaning that a decrease in precipitation is projected for summer months over Italy. Evin et al. (2021) also used a large ensemble of EURO-CORDEX RCMs considering RCPs 2.6, 4.5, and 8.5 to estimate future temperatures and precipitation and the relative uncertainty. For Italy, they projected slight increases in winter precipitation and significant decreases in summer precipitation, yet with very large uncertainties. It is interesting to underline that, in this study, Italy emerged as the country with the lowest reduction in precipitation among the Mediterranean countries. Focusing only on the Italian territory, CMCC carried out a climate change analysis considering an ensemble of EURO-CORDEX RCMs (Spano et al., 2020). The main results confirmed the North-South gradient for precipitation since a reduction was found for Southern and Central Italy, mainly in summer and, to a lower extent, in spring months, while an increase in winter precipitation over Northern Italy. Moreover, an increasing trend in maximum daily precipitation was found for summer and autumn. Studies summarized in the draft of the National Climate Change Adaptation Plan (PNACC, 2018) reported instead a reduction in total precipitation, more pronounced in the Southern areas, in the summer season, and when considering RCP 8.5. A robust decrease in total precipitation, with similar patterns, was also found in the analysis carried out by Padulano et al. (2020) which also used an ensemble of EURO-CORDEX RCMs in Italy. The overall picture of increasing precipitation during winter and decreasing precipitation in summer is confirmed also by our analysis when considering RCP 8.5, but the winter increases were higher as compared to the spring and summer decreases, resulting in an overall, yet minor, increase. Instead, for RCP 4.5, minor increases were found also for the summer season. Notably, most precipitation changes in our study were not statistically significant.

For water yield and percolation, the sign of change was in line with the predicted change in precipitation, consistent with other studies that coupled the SWAT model with climate models in Italy. For example, Fiseha et al. (2014) used climate variables from one GCM downscaled with three RCMs as input to simulate future precipitation and hydrological water balance components in the upper Tiber basin, in Central Italy, considering two different scenarios of future CO_2 concentrations. Except for one climate model in the lower emission scenario, their results showed a general decrease in precipitation and related variables, mostly during summer. Decreasing trends in precipitation and related water balance components such as water yield, groundwater recharge, and evapotranspiration were also found for the Candelaro catchment in Southern Italy, considering three RCMs (De Girolamo et al., 2017). Pulighe et al. (2021) applied the SWAT+ model to simulate the future climate in the Sulcis catchment in Sardinia with two RCMs and RCPs 4.5 and 8.5. Their results showed a clear decrease in precipitation only for one climate model with RCP 4.5, while slight increases for the other simulations. PET was predicted to significantly increase and the other water balance components such as surface runoff and percolation decreased because of the increased water loss to the atmosphere. In a small catchment of the Po River delta in Northern Italy, Pesce et al. (2019) used 10 different GCM-RCM combinations and found an average decrease in future precipitation, although with an unclear tendency, especially for RCP 4.5 in the medium-term future (2041-2070). Future water flow was projected to increase in the wet season and decrease during spring and summer. Finally, Glavan et al. (2015) simulated climate change impacts with six different climate models in a small Slovenian catchment, very close to the Italian border. Their results showed that PET increased as well as actual evapotranspiration if precipitation also increased. Also, precipitation was projected to increase with few exceptions by the end of the century, and stream flows showed consistent increases but higher in magnitude. This is in line with our study since we also observed that the percentage change in water yield was much higher as compared to the increase in precipitation. It is worth noting that in our study and the ones previously discussed, a subset of the available climate models was used, which might lead to under-representative estimates enhancing the uncertainty (Evin et al., 2021).

3.5.2 Impacts of vegetation responses to CO_2

The roles of the stomatal conductance reduction and the CO_2 fertilization effects caused by the CO_2 concentration rising are still unclear and debated. Experiments using earth system models showed that the CO_2 physiological response of vegetation on evapotranspiration and long-term runoff had higher impacts compared to radiative or precipitation changes caused by CO_2 rising (Lemordant et al., 2018). Furthermore, plant physiological responses to CO_2 were also found to reduce future drought-stress predictions (Swann et al., 2016). Moreover, Skinner et al. (2018) demonstrated that the CO_2-driven vegetation changes amplified the frequency and intensity of summer heat waves. GCMs predict higher temperatures compared to RCMs, and this was explained by the fact that the latter generally do not include the vegetation response to CO_2 rising since when including this effect, the temperature predicted by RCMs increased (Schwingshackl et al., 2019). However, the study of Taranu et al. (2022) showed that plant physiology had a limited effect and did not explain the large discrepancies observed between GCMs and RCMs. Finally, Vicente-Serrano et al. (2022a) argued that the physiological effect of vegetation as included in climate models might be overestimated and that their outputs should be used with caution when studying future droughts.

The CO_2 rising effect on PET and therefore on all the indices that use it to infer future drought and aridity conditions are remarkable, yet not completely understood (Scheff, 2018; Vicente-Serrano et al., 2022b). The effect of CO_2 rising on future mechanisms and processes relevant to the estimation of future aridity conditions was also analysed quantitatively in climate and hydrological studies, proving that the impacts are not

negligible, and stressing the importance of understanding and quantifying them better to obtain reliable future projections of drought and aridity. For example, Greve et al. (2019) demonstrated that the future estimation of PET was largely influenced by the method used to calculate it and that this uncertainty also affects the validity of indexes such as AI. Zhou et al. (2022) found opposite trends for past conditions in China when calculating PET using modified and traditional Penman-Monteith equations by including or excluding stomatal conductance reduction. They concluded that ignoring this effect results in a significant PET overestimation, especially in arid regions. However, actual evapotranspiration in arid and semi-arid regions is mainly controlled by soil moisture and is not very sensitive to PET (Dakhlaoui et al., 2020), meaning that this overestimation might be a problem in humid regions. Our analysis confirmed that the increase in PET did not lead to a proportional increase in actual evapotranspiration. More in detail, in our study the difference in annual actual evapotranspiration between the two cases considered under RCP 4.5 and 8.5 in the near future was around 5% (Fig. 3.6). This is consistent with the compensative effect caused by CO_2 fertilization (Manzoni et al., 2022) and in line with the magnitudes of changes of less than 8% reported by Fatichi et al. (2016). Lemaitre-Basset et al. (2022) showed that the stomatal conductance reduction effect has a significant impact on future runoff projections over France, while Boé (2021) reported that the decrease in evapotranspiration caused by the physiological effect of CO_2 did not result in an increase in river flows and soil moisture due to reduced precipitation in summer over France. Yang et al. (2019) demonstrated that the outputs of climate models are similar to those of hydrological models when accounting for the suppression effect in the calculation of PET. Using SWAT, multiple studies showed that evapotranspiration was reduced by the plant physiological responses to CO_2, leading to substantial increases in runoff, recharge and discharge (Ficklin et al., 2009; Kishawi et al., 2022; Lee et al., 2018; van Liew et al., 2012). Other studies evaluated the impact of the stomatal conductance reduction and CO_2 fertilization by modifying SWAT to include dynamic CO_2 concentration as input, finding similar results in terms of increased streamflow and reduced evaporation (Butcher et al., 2014; Wang et al., 2017; Wu et al., 2012). Notably, all these studies were conducted with the older SWAT model versions and run over the United States.

Our results are in line with previous studies, since the impact of vegetation responses to CO_2 on future PET, and therefore on future water fluxes and aridity, was high when considering RCP 8.5. Particularly, Lemaitre-Basset et al. (2022) applied the two methods that we used to estimate PET, namely the non-modified Penman-Monteith equation and the modified Penman-Monteith as proposed by Stockle et al. (1992), finding very similar future trends to those we identified. In our study, differences in PET estimation ranged from more than 200 mm increases when considering constant stomatal conductance to decreases of the same magnitude when considering stomatal conductance reduction under RCP 8.5. The magnitude and sign of changes when considering plant physiological responses caused by CO_2 concentration rising were consistent with other studies that applied SWAT. It is interesting to note that when past studies considered CO_2 concentration beyond 660 ppm they found significant percentage decreases in future actual evapotranspiration as compared to baseline periods. More specifically, Ficklin et al. (2009), Lee et al. (2018) and Kishawi et al. (2022) used 970 ppm, 850 ppm, and 935 ppm, obtaining decreases of 40%, 30% and 32% respectively. It has been already hypothesized that the simulated reduction of actual evapotranspiration caused by the plant physiological responses to CO_2 is overestimated by SWAT, but this was attributed to several simplifications in the equations used by the model and not by the invalidity of the equations used over 660 ppm (Butcher et al., 2014; Eckhardt and Ulbrich, 2003; Lee et al., 2018). Considering the findings of Lemaitre-Basset et al. (2022), we confirm that the method included in the SWAT/SWAT+ modelling suite for CO_2 concentrations higher than the 660 ppm threshold is questionable, and simulation outcomes should be interpreted with caution. On the other hand, PET increases with constant stomatal conductance in our study amounted to 225 mm, which corresponds to more than 20% in relative change. Regarding water yield changes

caused by the inclusion of the plant physiological responses to CO_2, our results agree with those of previous studies in the positive sign of change. As shown in Fig. 3.6, the magnitude of change in water yield, comparing simulations considering and ignoring the physiological responses, was approximately 5% under RCP 4.5, while it reached more than 20% under RCP 8.5 (Fig. A3.2). Butcher et al. (2014) reported increases ranging from 3 to 38% and a median of 11%. The contribution of the plant physiological responses to CO_2 estimated by Wu et al. (2012) amounted to 22% for streamflow by the end of this century, much higher than the effect quantified at 1-4% of the recent decades. Marginal increases in streamflow of approximately 1% were instead reported in the study conducted by Wang et al. (2017).

In SWAT+, both the CO_2 suppression effect on stomatal conductance and the CO_2 fertilization effect are considered. Nevertheless, they are calculated in different steps since the stomatal conductance is reduced when using the Penman-Monteith equation to retrieve PET and the fertilization effect when calculating daily accumulated biomass. This might cause some inconsistencies due to the leaf- and canopy-levels transpiration changes caused by these two effects (Manzoni et al., 2022), but the magnitudes of the reductions in actual evapotranspiration and the other variables seem to confirm that the increase in biomass partially compensates the decrease in transpiration caused by reduced stomatal conductance. Furthermore, the approach of using climate inputs from GCMs or RCMs to force a hydrological model, used in our study and the papers previously discussed, has some limitations that need to be considered. With this one-way coupling, the interactions and feedback between climate and vegetation are mostly neglected (Wu et al., 2012). Coupling offline hydrological models which do not account for physiological responses of vegetation with climate models is questionable (Milly and Dunne, 2017), especially when the climate models consider these effects (Boé, 2021). As reported by Schwingshackl et al. (2019), most of the GCMs that they used in their study included the CO_2 vegetation response while none of the RCMs considered it. Indeed, the physiological effect of vegetation induces a larger decrease in precipitation which should be compensated by a decrease in evapotranspiration (Boé, 2021). The opposite problem might occur if the offline hydrological model simulation of the physiological effect of CO_2 on evapotranspiration is inconsistent with the strength of the vegetation response as simulated by the climate model (Boé, 2021). Furthermore, Swann et al. (2016) suggested that using outputs of earth system models in hydrological models may lead to overestimation of the future drought stress due to double counting of plant feedback on surface humidity, temperature and net radiation.

3.6 Conclusion

In this study, the SWAT+ model was forced with climate data from five EURO-CORDEX climate models to estimate future climate change impacts in a typical Mediterranean catchment, the Ombrone catchment in Central Italy. Future aridity conditions were also estimated considering constant and decreasing stomatal conductance. The model performed well after the multi-site calibration carried out for three gauging stations, considering monthly streamflow.

In contrast to temperature, high uncertainties exist in the future trends of precipitation. Only one climate model predicted a clear decrease in future precipitation following RCP 8.5, while the others showed minor increases or constant values. The ensemble mean of winter precipitation increased, while summer precipitation remained almost constant or slightly decreased, with an overall increase in annual average precipitation.

The impact of stomatal conductance suppression on future PET was significant and should be taken into account. Upon disregarding, high increases in PET were obtained, while minor PET increases or even

decreasing values were found upon consideration of the suppression effect. Under RCP 8.5 in the far future period, the differences between disregarding/including the vegetation responses to CO_2 were nearly 50% in PET and ranged from 20 to 30% for the other water balance components (Fig. A3.2).

The SWAT+ model considers the CO_2 effect on future PET with a modification of the Penman-Monteith equation based on an experiment that was conducted for a range of CO_2 values between 330 and 660 ppm. RCP 8.5 predicts much higher CO_2 concentration values by the end of the century. For RCP 8.5, when considering stomatal conductance suppression, we found a dubious drop in PET of more than 200 mm. Further research is certainly needed, but the outputs of the SWAT+ model when excluding vegetation responses to CO_2 and when considering CO_2 concentrations much higher than 660 ppm are prone to large uncertainties. Nevertheless, the Penman-Monteith equation is recommended when using SWAT+ to assess future climate change impacts to account for the effect of reduced stomatal conductance.

The uncertainty in future precipitation and atmospheric evaporative demand patterns strongly increases when considering measures such as the Aridity Index and, consequently, highly influences future climate classification. Unravelling the uncertainties related to future precipitation in transition zones, like the Northern Mediterranean area, and the plant physiological responses caused by rising CO_2 concentration on future atmospheric evaporative demand is crucial to better understanding climate change impacts and planning more effective adaptation strategies.

Chapter 4 Management change impact assessment

The manuscript reported as Chapter 4 was submitted to Agricultural Systems with the title “Exploring Adaptive Capacities in Mediterranean Agriculture: Insights from Central Italy's Ombrone Catchment” and is currently under revision.

4.1 Abstract

Climate change's profound implications for Mediterranean agriculture underscores the urgency of adaptation strategies. These strategies, whether incentivized or farmer-driven, are pivotal in mitigating yield losses and harnessing evolving climatic conditions. While agronomic adaptations’ influence on crop yields is well-explored, its implications for water footprint and hydrological mass balance components remain largely unexplored. With this study, we aim to conduct a comprehensive assessment of the adaptive capacity of agricultural systems in the Ombrone catchment, Tuscany. We estimate the impacts of both climate and management changes on crop yield, water footprint and water balance components by comparing simulations with current and future climate and with and without adaptation strategies. An existing SWAT+ agro-hydrological model of the Ombrone catchment is re-calibrated for crop yields of durum wheat, sunflower and irrigated maize. The impacts of climate change are then assessed by forcing the model with five bias-corrected climate models. Subsequently, we simulate six autonomous agronomic adaptation strategies both individually and in combinations. We quantify their impacts on crop yield, water footprint, and water balance components, such as evaporation, water yield and soil moisture. Notably, our findings reveal variable and adverse impacts on crop yields under RCPs 4.5 and 8.5. Conversely, water footprints exhibit consistent opposing trends. Agricultural systems exhibit robust adaptive capabilities, particularly when multiple strategies are combined. The most impactful strategies revolve around earlier sowing and extended crop cycles. Supplemental irrigation and cover crops are beneficial only in specific scenarios. While adaptation strategies have a limited impact on basin-scale water balance components, they induce an average 27% reduction in water yield at the cropland scale, attributed to practices like zero tillage and cover crops. In conclusion, our research underscores the non-negligible influence of management changes on water balance components in primarily agricultural catchments. Future adaptation strategy assessments should encompass comprehensive integration to evaluate broader impacts on water resources.

4.2 Introduction

Mediterranean agriculture is highly susceptible to climate change, and yield losses are projected for most crops, mainly caused by the expected impacts on water resources (Iglesias et al., 2011; Ludwig et al., 2011; Pasqui and Di Giuseppe, 2019). Increasing temperatures will shorten crop cycle length, reducing yields due to the shorter time to accumulate biomass, while water deficiencies will affect future yields, especially when occurring during sensible phases of the crop cycle. Pests, diseases, weeds, droughts, floods, and cold and heat waves are other factors that will be possibly influenced by climate change and that will harm crop yields (Bindi and Olesen, 2011; Ciscar et al., 2018; Giannakopoulos et al., 2009; Spano et al., 2020). In general, summer crops are expected to be more affected compared to winter crops, mainly due to drought stress (Webber et al., 2018). On the other hand, CO_2 rising will benefit crop yields, especially C3 crops (Ainsworth and Long, 2005; Webber et al., 2018). Also, local processes or characteristics might have a positive effect on crop yields and, since adaptation strategies are planned considering the local characteristics, climate change impacts need to be addressed at the local scale (Iglesias et al., 2010; Pasqui and Di Giuseppe, 2019). In Northern and Central Italy, climate change impacts are uncertain since the General Circulation Models (GCMs) and the

downscaled Regional Climate Models (RCMs) do not provide clear and robust projections regarding precipitation. This area is in the transition zone between the arid North African and the humid Central European climates, and past studies found that the zero-change precipitation line usually crosses this area (Mariotti et al., 2015; Spano et al., 2020). Regardless of the sign and magnitude of climate change, adaptation strategies will have a crucial role in limiting crop yield losses or enhancing the unlikely positive climate changes (Bindi and Olesen, 2011; Reidsma et al., 2015).

Agricultural adaptation strategies can be categorized as planned and autonomous - sometimes referred to as hard and soft adaptations - where planned adaptations refer to major structural changes at larger scales that generally require huge investments and longer times, while autonomous adaptations consist of adjustments at smaller and shorter scales to optimize production (Bindi and Olesen, 2011). Numerous agronomic practices have been proposed to adapt to climate change as it was demonstrated that they can improve crop yield, crop water productivity and water savings (Jovanovic et al., 2020; van Opstal et al., 2021). Developing or selecting crops and varieties that perform better in modified climate conditions is usually indicated as a very promising strategy (Monaco et al., 2014), as well as shifting the crop calendar to better match the plant requirements with the climate. Conservation tillage, either reduced or completely avoided, showed to reinforce the small water cycle, enhance water storage, and increase soil organic carbon (Iocola et al., 2017; Liebhard et al., 2022; Noreika et al., 2022; Sapkota et al., 2012). Mulching is another practice that reduces evaporation and alleviates water scarcity (Nouri et al., 2019; Stewart and Peterson, 2015). Adjusting plant densities is an option to adapt the crop water needs to the actual availability (Stewart and Peterson, 2015). The inclusion of cover crops in the rotation resulted in gains in crop productivity and the provision of several ecosystem services (Adeux et al., 2021; Schipanski et al., 2014). These and other autonomous agronomic adaptation strategies, which are generally overlooked by decision-makers, might have a crucial role as they are, in most cases, highly accepted and will be easily implemented by farmers themselves (Bonzanigo et al., 2016; Varela-Ortega et al., 2016).

In combination with climate models such as GCMs or RCMs, crop-growth models are typically used to estimate future crop yields and the effects of agronomic adaptation strategies. These dynamic and process-based models represent the state of the art over the current understanding of crop processes to simulate crop growth according to the specific weather, soil, management, and crop genetic characteristics (Ewert et al., 2015). Despite the great improvements in the last decades, these models still have important weaknesses that limit their application in integrated assessments. For example, some processes that might affect future crop yield are ignored or simplistically represented, most of the studies focus on few crops, and the required data to accurately set up, calibrate and validate these models are often not available (Ewert et al., 2015). Another major issue is the scaling up to field and catchment scales of the point-scale outputs of crop-growth models, necessary to obtain more meaningful assessments by considering soil, crop, climate, and management variabilities (Ahuja et al., 2019; Tenreiro et al., 2020).

To carry out useful impact assessments concerning food security, the output variables of crop-growth models might not be sufficient. When dealing with climate change impact assessments, integrated assessments are usually preferred to better evaluate the whole spectrum of consequences of climate change, building modelling frameworks that include not only biophysical aspects, but also social, political, and economic ones (Ewert et al., 2015; Reidsma et al., 2015). Nevertheless, the integration of different models is usually challenging. Even focusing only on biophysical aspects, the outputs of crop-growth models are limited for a comprehensive analysis when considering broader environmental and water resource assessments. For example, in addition to crop yield, a typical output derived from crop-growth models commonly used in agricultural water management is the Water Footprint (WF) (Gobin et al., 2017; Kersebaum et al., 2016). WF,

defined as “the volume of freshwater used to produce the product, measured over the full supply chain” (Hoekstra et al., 2011), is a simple and universal metric that can be easily applied. However, it has some shortcomings when trying to analyse the local contexts or consider the impacts of water use downstream (van Noordwijk et al., 2022). More specifically, WF is limited to vertical exchanges of water and does not consider the lateral, or horizontal, flows that are instead included when applying hydrological models (Van Noordwijk et al., 2022). Hence, considering the processes and the outputs of hydrological models is surely helpful to better describe the soil-water interactions at scales larger than the point scale (Tenreiro et al., 2020), and the coupling of crop-growth and hydrological models is often promoted as an optimal solution (Siad et al., 2019, van Gaelen et al., 2017).

Integrated, (semi)-distributed hydrological models, such as the Soil and Water Assessment Tool (SWAT) (Arnold et al., 1998), might offer a solution to most of the issues highlighted in the previous paragraphs. Integrated agro-hydrological models generate a higher number of outputs that can be used to assess more comprehensively the impacts of climate change on food security and water resources, such as crop yield, WF, and water balance components. By using the discretization of the hydrological model, crop yields can be spatially simulated for each specific crop, variety, soil, climate, and management conditions. As integrated models are directly created with multiple modules, the problems related to coupling and the compatibility of the different processes, inputs, and outputs are largely avoided. The SWAT/SWAT+ modelling suite has been already used to evaluate not only climate change impacts on crop yield, WF, and water balance components but also the effect of some adaptation strategies. Numerous studies focused on assessing and optimizing irrigation with SWAT (e.g. Panagopoulos et al., 2012, 2014; Udias et al., 2018). The impact on crop yields of land management practices, such as crop rotation and tillage, have been also simulated (Parajuli et al., 2013), as well as the effects of climate change on the crop calendar (Marcinkowski and Piniewski, 2018). Nkwasa et al. (2023) applied the restructured SWAT+ version (Bieger et al., 2017) to assess climate change impacts on crop production and the effects of longer crop cycles. SWAT has been also applied for WF and water productivity assessments of improved management practices (Garg et al., 2012; Salmoral et al., 2017; Sun and Ren, 2014; Vaghefi et al., 2017) and proposed for integrated water resources management (D’Ambrosio et al., 2020; Luan et al., 2018). Pacetti et al. (2021) quantified the water supply with SWAT to estimate the water-related ecosystem service footprint after coupling the model outputs with indicators of green, blue and grey WF.

Climate and land cover changes are known to affect the water balance and their impacts have been largely studied also with the SWAT model (e.g. Castelli et al., 2017; Mori et al., 2021). In the previous paragraph, we reported some applications of SWAT to assess the effects of agronomic adaptation strategies on crop yield and WF. However, the effects of the future adaptation strategies – the management changes – on the water balance have been mostly neglected (Noreika et al., 2021), especially when focusing on autonomous, farmer-led, agronomic adaptation strategies (Chen et al., 2021). These effects need to be assessed as they might be significant, possibly changing the evaluation of the adaptation strategies if we were to consider only crop yield and WF. For example, it was demonstrated that the mechanization of agriculture in hilly areas led to increased runoff and erosion, reducing the resilience of the catchments (Napoli et al., 2017; Tarolli et al., 2014). Most of the studies that attempted to study the impacts of management changes on water balance components or catchment resilience with SWAT were related to irrigation. For example, Panagopoulos et al. (2014) and Udias et al. (2018) estimated the effects of best management practices to optimize and reduce irrigation water. Similarly, Dechmi and Skhiri (2013) considered several best management scenarios and evaluated their effects on irrigation return flows, suspended sediments, and nutrient loads. Haro-Monteagudo et al. (2020) performed a comprehensive multi-model analysis, including SWAT, to assess the

impacts of climate change on future irrigated agriculture and evaluated the sustainability of the current reservoir management. Taye et al. (2022) evaluated the sustainability of the intensification of groundwater-based irrigation systems coupling SWAT and MODFLOW. A further application of the SWAT model was proposed by Dile et al. (2016) in which they used the model to identify suitable areas for water harvesting ponds and evaluate the implications of these systems on upstream and downstream ecosystem services, including crop yield and water productivity. Yimer et al. (2023) applied SWAT+ coupled with the gwflow groundwater module to assess the impact of drainage from agricultural fields. Furthermore, the impacts on the water balance were largely studied in the Czech Republic by considering a large-scale adoption of rapeseed for biofuel (Noreika et al., 2020), land use and management changes occurred in the last centuries (Noreika et al., 2021) and agricultural conservation practices such as conservation tillage, contour farming, residue incorporation, and reducing field sizes (Noreika et al., 2022). Brouziyne et al. (2018) applied SWAT not only to assess the impacts of climate change on water productivity and water yield but also to simulate the effects of two agronomic adaptation practices, namely earlier sowing and conservation tillage. Finally, Chen et al. (2021) performed a comprehensive assessment of agricultural practices, namely irrigation and early and late sowing, evaluating the impacts on water balance components and crop yields.

Applying the integrated SWAT+ model in an agricultural catchment in Central Italy, this study aims to evaluate climate change impacts on crop yield and WF of three representative crops and the adaptive capacity of the agricultural system through autonomous agronomic adaptation strategies. We re-calibrate an existing model in which durum wheat is selected as the representative rainfed winter crop, while sunflower and maize as the rainfed and irrigated spring crops, respectively. A previous drought risk assessment (Chapter 2) showed that the Ombrone catchment and Southern Tuscany are vulnerable and exposed to drought hazards, even though future projections related to precipitation are highly uncertain (Chapter 3). The adaptive capacity of the agricultural system is then evaluated with scenarios simulating changes in sowing dates, supplemental irrigation, conservation tillage, cover crops, and longer cycle varieties. The most promising combinations of adaptation strategies, an aspect which is also often overlooked, are explored by analysing the synergies and trade-offs among them. Finally, the impacts on water balance components of the management changes via the proposed adaptation strategies are assessed, verifying the hypothesis that management changes can have a significant impact on the water balance in agricultural catchments comparable to climate and land cover changes.

4.3 Methodology

4.3.1 The SWAT+ model

The SWAT+ model is a renovated and improved version of the SWAT model (Bieger et al., 2017; Čerkasova et al., 2023). SWAT+ discretizes the catchment into sub-catchments and Hydrological Response Units (HRUs), which are spatial units with homogeneous characteristics of soil, land use and slope. Compared to the previous version, SWAT+ offers greater flexibility in the definition of water and agricultural management practices, since it includes the possibility to use decision tables, which allow for the specification of complex rules to simulate more realistic operations (Arnold et al., 2018; Čerkasova et al., 2023; Nkwasa et al., 2022).

To simulate crop yield, SWAT+ uses a module which is a simplified version of the EPIC model (Neitsch et al., 2011). Daily biomass accumulation (Δbio_{act}), simulated with equation 1, is adjusted for the plant growth factor (yr) that quantifies the water, temperature and nutrient stresses (equation 2). The total biomass (bio) and crop yield (yld) are then calculated with equations 3 and 4.

$$\Delta bio_{act} = \left(0.5 \cdot I_d \cdot RUE \cdot \left(1 - exp\ \left(-k_j \cdot LD\right)\right)\right) \cdot \gamma_r \quad (1)$$

$$\gamma_r = 1 - MAX(wstrs, tstrs, nstrs, pstrs) \quad (2)$$

$$bio = \sum_{i=1}^{d} \Delta bio_{act} \quad (3)$$

$$yld = bio_{agg} \cdot HI\ for\ HI \leq 1 \quad (4)$$

where I_d is the photosynthetically active radiation, *RUE* is the radiation use efficiency, K_j is the light interception and *LD* is the leaf area index development. *wstrs*, *tstrs*, *nstrs* and *pstrs* represent water, temperature, nitrogen and phosphorous stresses, respectively. "MAX" is a mathematical function that returns the maximum value. *d* is days, bio_{agg} is the above-ground biomass and *HI* is the Harvest Index.

SWAT+ also simulates the CO_2 fertilization and stomatal conductance suppression modifying *RUE* and canopy resistance (r_c) with equations 5 (Stockle et al., 1992) and 6 (Easterling et al., 1992), respectively. The CO_2 effect on stomatal conductance is only included when using the Penman-Monteith approach to calculate potential evapotranspiration. It is important to underline that the equation is based on an experiment that reached 660 ppm (Morison, 1987) and that its validity above this threshold is dubious (Lemaitre-Basset et al., 2022).

$$RUE = \frac{100 \cdot CO_2}{CO_2 + exp\ (r_1 - r_2 \cdot CO_2)} \quad (5)$$

$$r_c = \frac{r_l}{(0.5 \cdot LD) \cdot (1.4 - 0.4 \cdot \frac{CO_2}{330})} \quad (6)$$

where CO_2 is the concentration of carbon dioxide in the atmosphere, r_l is the minimum effective stomatal resistance of a single leaf, r_1 and r_2 are the shape coefficients.

4.3.2 The Ombrone catchment model

The study area is the Ombrone catchment, a medium-sized coastal catchment located in Central and Southern Tuscany (Fig. 4.1). The catchment is almost entirely included in the Grosseto and Siena provinces, has a maximum elevation of 1738 m a.s.l. and an area of 3552 km^2. Significant parts of the catchment are characterized by hilly and mountainous areas with slopes of over 20% (Diodato et al., 2023), where the most cultivated crops are grapevine and olives (Napoli et al., 2014; Napoli and Orlandini, 2015). Cereals are also widespread, while in the coastal areas horticultural and irrigated crops are present. The Ombrone catchment is considered prone to agricultural drought (Diodato and Bellocchi, 2008) as it receives lower precipitation and experiences increased dry spell occurrence compared to other parts of Tuscany (Bartolini et al., 2022). Herbaceous annual crops cover an area of 46.9% according to the Corine Land Cover of 2018 used in this study.

The same model of the Ombrone catchment prepared for the previous hydrological and climatological study was used for the simulations. For this study, the model was initially set up for 13 years for calibration and validation with one year of warm-up. The 2637 HRUs with herbaceous cropland were split to represent the typical cropping pattern of the area, considering durum wheat as the rainfed winter crop (30% of the HRU), sunflower as the rainfed spring crop (15%), maize as irrigated spring crop (15%), and alfalfa as the forage crop (40%).

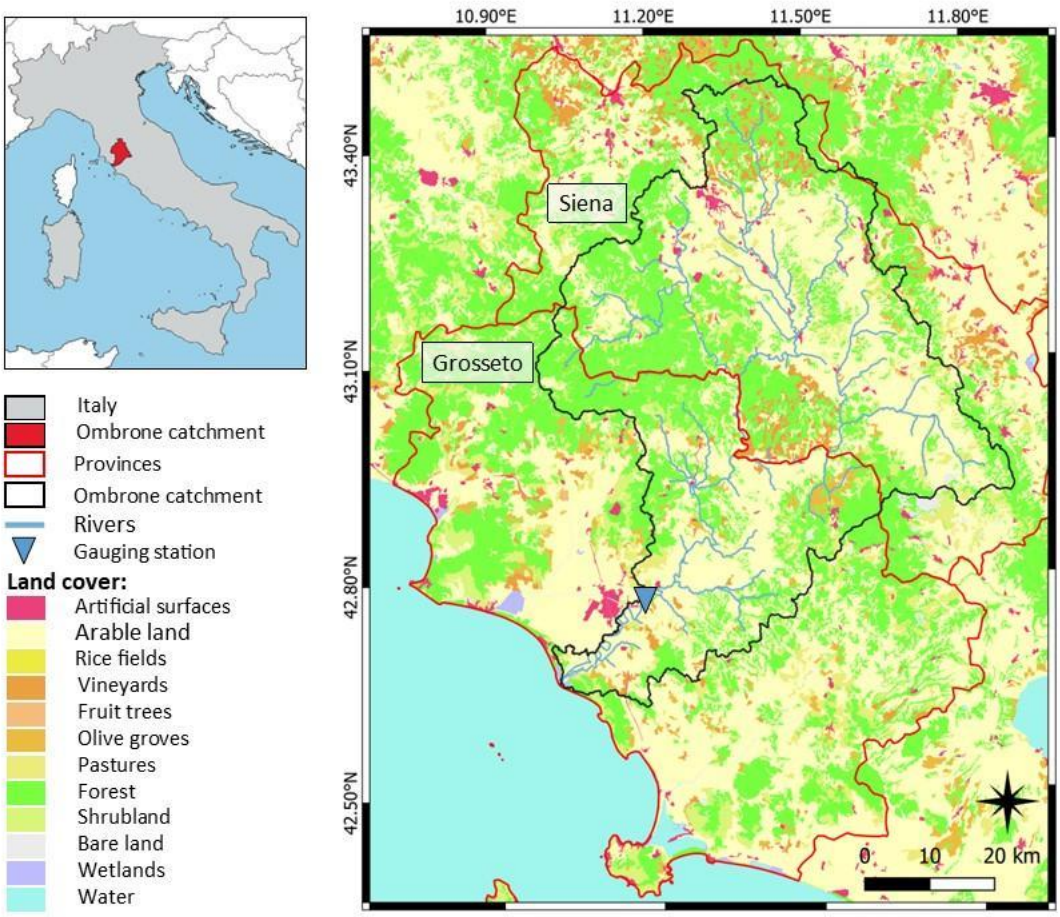

Figure 4.1: The Ombrone catchment with the provinces of Siena and Grosseto, the catchment boundaries, the Istia gauging station and the land cover retrieved from the Corine Land Cover of 2018 used in this study.

4.3.3 Calibration and validation

In this study, we performed a new calibration and validation for crop yield. We used 12 years of provincial crop yield, spanning from 2010 to 2021, retrieved from the National Institute of Statistics (ISTAT) for the provinces of Siena and Grosseto; odd years were used for calibration while even for validation. Since the focus of this study was on crop yield, in addition to the sensitive crop parameters selected in the previous study (Table A4.2), we also included the soil evaporation compensation factor (*esco*), the plant evaporation compensation factor (*epco*) and available water capacity (*awc*) to calibrate the model as in Sinnathamby et al. (2017). *Esco* and *epco* in the previous study were included in the automatic calibration performed for streamflow, while *awc* was not considered since it was not sensitive enough. As we modified two parameters that were originally included in the calibration for streamflow, we performed an additional calibration and validation also for monthly streamflow modifying the *cn2* parameter of the whole catchment and *esco* and *epco* of the HRU other than cropland. To evaluate model performance, we used the Nash-Sutcliffe Efficiency (NSE), the Normalized Root Mean Square Error (NRMSE) and the per cent bias (Pbias) and the criteria of Jamieson et al. (1991) for NRMSE and Moriasi et al. (2007) for NSE and Pbias, reported in Table A4.2.

4.3.4 Climate projections and management

We used five bias-corrected EURO-CORDEX climate models to simulate the future climate referred to as (1) CNRM-CM5-ALADIN63, (2) CNRM-CM5-RACMO22E, (3) EC-EARTH-RACMO22E, (4) MPI-ESM-LR-RCA4 and (5)

NorESM1-M-REMO2015. We performed the simulations for 30-year periods comparing the historical simulation (1976-2005) with the long-term future period (2071-2100) of the same climate model for the Representative Concentration Pathways (RCPs) 4.5 and 8.5. Considering two years of warm-up, the analyses were performed for periods of 28 years. The CO_2 value that could be used as input was constant for each simulation, and therefore we considered the average value for the different periods and RCPs considered in the study. We used the most updated values about CO_2 concentration projections (Büchner and Reyer, 2022), and it is important to underline that the value for the period 2071-2100 under RCP 8.5 is 939 ppm, much higher than the upper threshold of 660 ppm of the Morison experiment (Morison, 1987).

The climatological analysis performed in Chapter 3 showed that the temperature is predicted to increase consistently according to the five climate models, more when considering RCP 8.5. On the other hand, precipitation projections are much more uncertain, with the models showing constant or slightly increasing values, except for NorESM1-M-REMO2015 which predicts decreasing values under RCP 8.5. The precipitation-related variables such as soil moisture, percolation, streamflow, and water yield vary accordingly with rainfall. The uncertainty when using climate models is further increased when dealing with evapotranspiration since it is highly influenced by CO_2 concentration (Lemaitre-Basset et al., 2022). As shown in Chapter 3, when considering the CO_2 increase, the potential evapotranspiration is predicted to have similar average values in the long-term future for RCP 4.5, while lower and probably unrealistic for RCP 8.5.

The crop module of the SWAT+ model is based on heat units but, differently from the original SWAT model, the input to specify the length of the crop cycle is days to maturity (Nkwasa et al., 2023). Hence, to consider the same variety with the future increase in temperature, we calculated the heat units required by the crops for the calibration period 2010-2021, and then we retrieved the days to maturity for the historical (1976-2005) and future (2071-2100) periods, both for RCPs 4.5 and 8.5. We calculated the days to maturity averaging the maximum and minimum temperatures of the five climate models since they were very similar after bias correction.

The crop management applied for calibration and validation and in the “no adaptation” (0.NA) scenario simulations is reported in Table A4.4. The management for the three crops considered is representative of the current practices and was checked with published papers and guidelines from the Tuscany Region (Dalla Marta et al., 2010; Giannini and Bagnoni, 2000; Orlando et al., 2015, Tuscany Region, 2010). Since detailed information about the irrigation schedule was not available, we applied automatic sprinkler irrigation for maize using the default decision table available in the model, with a water stress threshold of 0.6. We adjusted this value during calibration for maize yield. To simulate the optimal soil humidity conditions for sowing, we used the default decision tables automatically generated by the model, adjusted to obtain realistic sowing dates. Moreover, in SWAT+ the crops are automatically harvested at the end of the crop cycle, but we also specified the latest harvesting dates in the decision tables.

4.3.5 Simulation of adaptation strategies

To estimate the adaptive capacity of agricultural systems, we simulated several agronomic adaptation strategies (Table 4.1) such as earlier and later sowing dates (1.ES, 2.LS), supplemental irrigation (3.SI), longer crop cycle (4.LCC), and practices belonging to conservation agriculture, such as zero tillage (5.ZT) and cover crops (6.CC). In addition, we simulated the effect of combining the most effective adaptation strategies (7.SI-LCC, 8.ES-LCC, 9.LCC-CC, 10.ES-SI-LCC, 11.ES-LCC-CC, 12.ES-SI-LCC-CC). Considering the RCPs, periods and management scenarios, we conducted a total of 135 simulations (5 historical simulations + 2 RCPs x 13 management scenarios x 5 climate models). Overall, most of the strategies considered are simple and will be

easily and autonomously adopted by farmers, while others might need institutional support. The supplemental irrigation scenario is simulated regardless of water availability. Even if this is a simplification, the analysis of the outcomes of these simulations is certainly valid for crops at the field scale. It is also important to note that we simulated supplemental and not full irrigation, as the irrigation events were triggered by the water stress threshold. Furthermore, lower irrigation amounts were expected because the ensemble mean of the five climate models showed an increasing sign in annual precipitation and the crop cycles were shortened. Conservation agriculture practices are simulated as indicated in Arabi et al. (2008) and Kalcic et al. (2015) by reducing CN by 2 points, modifying Manning's roughness coefficient for overland flow (OV_N) and including a cover crop. We did not modify the USLE cover factor as it was not relevant to our research objectives.

Table 4.1: The adaptation strategies scenarios considered in the study, with the description and SWAT+ input files change.

	Adaptation Strategy	**Description**	**Input files changed**
1.ES	Earlier sowing	Sowing window anticipated by 15 days, as well as tillage and fertilization operations	lum.dtl management.sch
2.LS	Later sowing	Sowing window delayed by 15 days, as well as tillage and fertilization operations	lum.dtl management.sch
3.SI	Supplemental irrigation	Automatic irrigation applied also to wheat and sunflower	management.sch
4.LCC	Longer crop cycles	Crop cycle increased by 15 days	plants.plt
5.ZT	Zero tillage	Conventional tillage changed to zero tillage. OV_N changed to "notill_2-9res". CN reduced by 2 points	landuse.lum management.sch cntable.lum
6.CC	Cover crops	Sowing and killing a leguminous crop (clover) when the main crop is not cultivated. Mouldboard tillage is also removed and harrow tillage is maintained. OV_N changed to "notill_2-9res". CN reduced by 2 points	landuse.lum management.sch plant.ini cntable.lum

After the simulations, we elaborated the outputs of the model for each RCP and adaptation strategy. In this study, we report the impacts of climate change, with and without adaptation strategies, on crop yield and WF and the effect of the adaptation strategies on the water balance components. The impacts of climate change on crop yields were evaluated by analysing the 28-year average yield for each HRU and comparing the future period (2071-2100) with the historical simulation of the same climate model, considering RCPs 4.5 and 8.5. A similar comparison was carried out for WF, which was calculated as the ratio of evapotranspiration and crop yield, expressed in m^3 kg^{-1}, considering the annual average output files. To evaluate the effect of the adaptation strategies, we evaluated the relative percentage difference between the outputs of the no adaptation and adaptation scenarios. We performed this analysis only for the 2071-2100 future period, for both RCPs, without considering the historical period. Concerning the agricultural impacts, we considered annual average crop yield and WF. Additionally, we analysed the drought and temperature stresses (DS, TS) that are direct outputs of the SWAT+ model. For the impacts on the water balance, we evaluated annual average evaporation, actual evapotranspiration, soil moisture, water yield and percolation at the cropland and catchment scales. The cropland is represented by the HRUs with durum wheat, sunflower and maize where the adaptation strategies were implemented. Synergies (trade-offs) were investigated by assessing if the effect of combinations of adaptation strategies was higher (lower) than the algebraic sum of the individual adaptation strategies. For agricultural outputs, we considered a synergy (trade-off) if the values were higher (lower) than 3%, while for water balance components if they were higher (lower) than 2%. Of course, we considered the opposite when the negative changes were the beneficial ones, like evaporation and water footprint. We also analysed the outputs in terms of beneficial changes, namely increasing crop yield and

decreasing WF, evaporation and water yield. Finally, we evaluated the magnitude of the changes caused by management and climate on the agricultural – yield, WF, DS and TS – and hydrological – the water balance components at the cropland scale – variables, by comparing the absolute maximum percentage changes considering all the simulations performed.

4.4 Results

4.4.1 SWAT+ calibration and validation

The calibrated values for crop yields are reported in Table 4.2, while the results in terms of calibration and validation performances are in Table 4.3. Overall, we obtained at least satisfactory performances for the three crops in the two provinces. For durum wheat and sunflower, changing only the days to maturity, *esco* and *epco* was almost sufficient to obtain the best parameter set, and few additional modifications were needed. On the other hand, for maize, we had to strongly reduce most of the parameters since the model overestimated yields. Because of the known limitations of the model, the aggregated statistical data used and the approximations in the model setup, we consider our model validated for the average annual crop yield, as done in other studies that applied the SWAT/SWAT+ model for crop yield estimation (Musyoka et al., 2021; Nkwasa et al., 2023; Srinivasan et al., 2010). Then, we calculated the heat units to retrieve the days to maturity for the historical (1976-2005) and future (2071-2100) periods, which were drastically reduced, in particular for RCP 8.5 (Table 4.4). Finally, modifying *cn2* of the whole catchment and *esco* and *epco* of the HRUs other than cropland, we obtained at least satisfactory performances for monthly streamflow (NSE > 0.5 and Pbias < 25%) according to Moriasi et al. (2007) as shown in Table A4.4, except for Pbias during calibration in the most downstream gauging station of Istia, for which there is probably an error in the reported observed flows.

Table 4.2: The parameters selected for calibration, the type of change, and the change in terms of percentage or new value.

Parameters crop yield	Type of change	Final change					
		Durum wheat		Sunflower		Maize	
		Siena	*Grosseto*	*Siena*	*Grosseto*	*Siena*	*Grosseto*
days_mat	*Replace*	180	180	110	90	120	120
bm_e	*Percentage*	-	-	5%	-	- 15%	- 10%
harv_idx	*Percentage*	-	- 2.5%	5%	-	- 17.5%	- 10%
lai_pot	*Percentage*	-	- 2.5%	5%	-	- 17.5%	- 10%
ext_co	*Percentage*	-	-	5%	-	- 15%	- 10%
hu_lai_decl	*Percentage*	-	-	5%	-	-	-
dlai_rate	*Percentage*	-	-	- 5%	-	-	-
frac_hu1	*Replace*	-	-	-	-	0.17	0.17
frac_hu2	*Replace*	-	-	-	-	0.55	0.55
lai_max1	*Replace*	-	-	-	-	0.13	0.14
lai_max2	*Replace*	-	-	-	-	0.9	0.92
esco	*Replace*	0.5	0.9	1	0.35	0.70	1
epco	*Replace*	1	0.6	1	0.60	1	1

Table 4.3: Model performances expressed as NRMSE (%) and Pbias (%) for calibration and validation for durum wheat, sunflower, and maize in the Siena and Grosseto provinces.

Crop	Province	Calibration		Validation	
		NRMSE	*Pbias*	*NRMSE*	*Pbias*
Durum wheat	*Siena*	27.50% [3]	-5.08% [1]	28.61% [3]	7.23% [1]
	Grosseto	26.21% [3]	2.97% [1]	17.41% [2]	-0.05% [1]
Sunflower	*Siena*	6.68% [1]	-1.97% [1]	24.23% [3]	2.08% [1]
	Grosseto	20.26% [3]	15.97% [3]	28.86% [3]	-2.97% [1]
Maize	*Siena*	16.87% [2]	-0.27% [1]	22.09% [3]	0.17% [1]
	Grosseto	9.34% [1]	-0.22% [1]	15.32% [2]	-0.84% [1]

[1] Very good; [2] Good; [3] Satisfactory.

Table 4.4: Days to maturity for durum wheat, sunflower and maize used in the simulations.

Crop	Province	Calibrated (2010-2021)	Historical (1976-2005)	Future (2071-2100)	
				RCP 4.5	*RCP 8.5*
Durum wheat	*Siena*	180	187	163	143
	Grosseto	180	187	163	143
Sunflower	*Siena*	110	112	99	89
	Grosseto	90	91	80	72
Maize	*Siena*	120	122	107	96
	Grosseto	120	122	107	96

4.4.2 Climate change impacts on crop yield and water footprint

For durum wheat, the rainfed winter crop, three climate models (CNRM-CM5-ALADIN63, CNRM-CM5-RACMO22E, and EC-EARTH-RACMO22E) predicted decreases in crop yield up to -16.4% under RCP 4.5 and -63.4% for RCP 8.5 considering the most pessimistic model. MPI-ESM-LR-RCA4 simulations disagreed since when considering RCP 4.5 yields were predicted to slightly increase, while they dropped under RCP 8.5. Instead, wheat yields simulated with NorESM1-M-REMO2015 increased by almost 30% under both RCPs. The ensemble mean for durum wheat yield was predicted to remain constant under RCP 4.5 and to decrease by almost -40% under RCP 8.5 (Fig. 4.2). As expected, wheat WF showed the opposite trend of crop yield, with the ensemble mean increasing by 24.1% and 265.3% under RCPs 4.5 and 8.5, respectively (Fig. 4.3). Analysing the distributions, we can assess that low values for wheat yield will be much more frequent compared to the historical simulations under RCP 8.5, explaining the significant increase observed for WF. Specifically, in the worst-case scenario (EC-EARTH-RACMO22E, RCP 8.5), a sevenfold increase in mean WF was predicted as a result of the very low yield, in many HRUs below 1 ton/ha. Considering most of the simulations, because of the very low annual average yields in many HRUs, especially under RCP 8.5, we can affirm that some parts of cropland will become unsuitable for wheat growth.

For sunflower, the absolute magnitudes of changes were much smaller compared to durum wheat. Under RCP 4.5, sunflower yields were predicted to remain constant or increase, with ensemble mean increases of almost 5.1%. On the other hand, under RCP 8.5 all the models predicted decreasing yields except for NorESM1-M-REMO2015. The ensemble mean was predicted to decrease by almost -21.7% under RCP 8.5 (Fig. 4.2). Considering WF under RCP 4.5, CNRM-CM5-ALADIN63, CNRM-CM5-RACMO22E and EC-EARTH-

RACMO22E predicted increasing values by up to 53.8%, while MPI-ESM-LR-RCA4 and NorESM1-M-REMO2015 decreasing values by up to -15.9%. Under RCP 8.5, all the models predicted increases in sunflower WF up to 313% for EC-EARTH-RACMO22E except for NorESM1-M-REMO2015 which showed decreased WF by -26%. The ensemble means for sunflower WF were predicted to increase by 20.6% under RCPs 4.5 and to double under RCP 8.5 (Fig. 4.3). The reductions in sunflower yield predicted in the simulations were not as widespread and significant in magnitude as for durum wheat. Hence, no cropland is expected to become unsuitable for sunflower cultivation.

Maize is an irrigated spring crop and, therefore, it is not drastically affected by changes in precipitation. In our study, the role of irrigation was not as important as depicted by other studies in the Mediterranean. Considering RCP 4.5, maize yields remained almost constant with all the climate models, while for RCP 8.5 yields were predicted to significantly decrease. The decrease reached almost -40% for EC-EARTH-RACMO22E, with an ensemble-mean decrease of -21.2% (Fig. 4.2). WF was consistent with maize yield and, overall, higher variability in WF is expected in the future, but the magnitude of changes (absolute and relative) was not as high as for sunflower and durum wheat. In particular, under RCP 8.5 the maximum increase and decrease in maize WF were simulated by EC-EARTH-RACMO22E (more than 75% increase) and NorESM1-M-REMO2015 (almost -30% decrease), respectively, with a moderate ensemble-mean increase of 14.9% (Fig. 4.3). Even if in some simulations strong reductions in maize yield were predicted, regardless of economic considerations no cropland is expected to become unsuitable for maize cultivation.

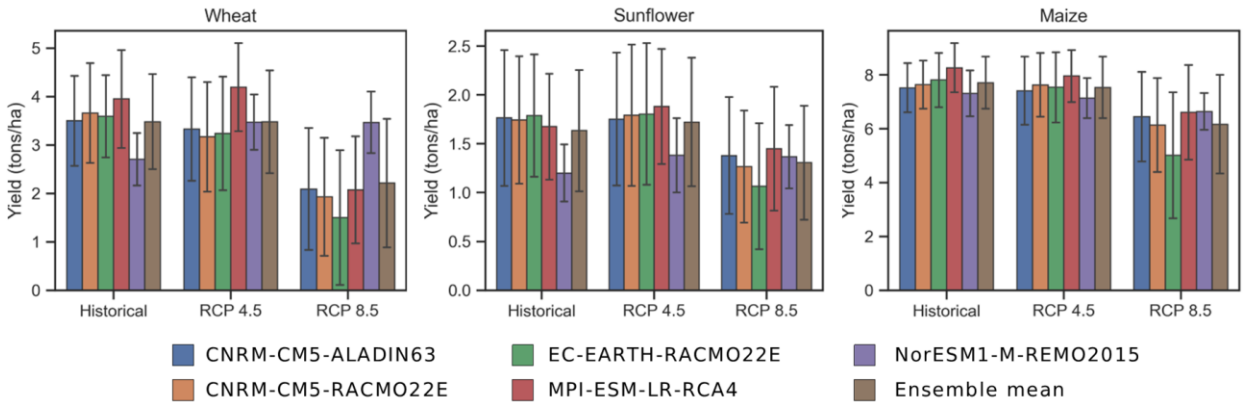

Figure 4.2: Climate change impact on crop yield. Durum wheat, sunflower and maize yield plots are created with the absolute values for the historical and RCPs 4.5 and 8.5 simulations. The plots are created using the annual average yield for the respective periods considering all the HRUs with cropland.

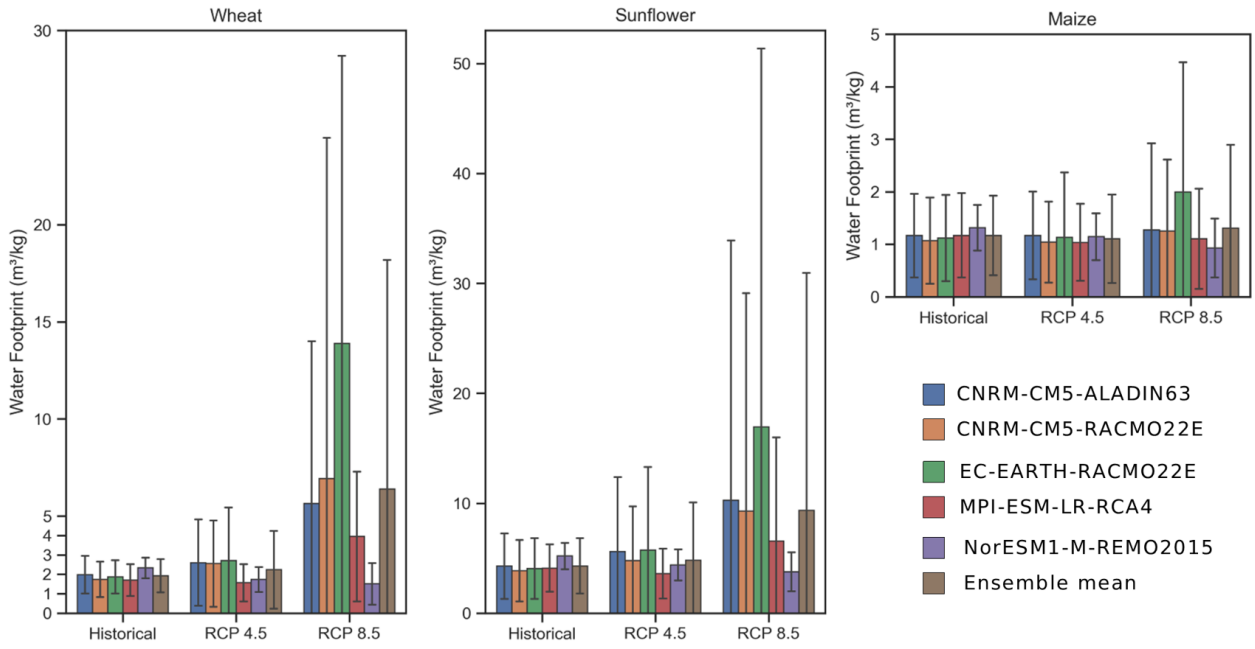

Figure 4.3: Climate change impacts on water footprint. Durum wheat, sunflower and maize water footprint plots are created with the absolute values for the historical and RCPs 4.5 and 8.5 simulations. The plots are created using the annual average water footprint for the respective periods considering all the HRUs with cropland.

4.4.3 The adaptive capacity of agricultural systems

The effects of adaptation strategies on crop yield, WF, DS, TS, evaporation, actual evapotranspiration, soil moisture, water yield, percolation and streamflow are reported as heatmaps in Figures 4.4, 4.5, 4.6 and 4.8. We opted to report only RCP 4.5 outputs since the calculation of potential evapotranspiration was not affected by the increase in CO_2 concentration above the 660 ppm threshold of the Morison experiment. Still, some outputs of RCP 8.5 simulations are discussed, and the heatmaps are available in the supplementary materials (Fig. A4.4-A4.7). In Fig. 4.7 the effect of adaptation strategies on water balance components at catchment and cropland scales are reported. Fig. 4.9 shows the maximum absolute impacts caused by climate and management changes on each variable that we considered in this study, under RCP 4.5. The beneficial effects of the use of adaptation strategies and their combination are plotted in Fig. 4.10 for wheat, sunflower and maize. We considered as beneficial effects increased crop yield and reduced WF, evaporation and water yield. For this figure, again we considered only the outputs of RCP 4.5.

4.4.3.1 Effect of adaptation strategies on crop yield

Overall, durum wheat yield had the highest relative losses predicted without adaptation strategies (Fig. 4.2). Nonetheless, the adaptive capacity for this crop was high (Fig. 4.4), reaching similar or increased yields compared to the historical simulations. The most effective adaptation strategy was 4.LCC, especially when considering the climate models that predicted yield decreases (CNRM-CM5-ALADIN63, CNRM-CM5-RACMO22E and EC-EARTH-RACMO22E). Among the crops that we considered, wheat had the longest crop cycle and, consequently, also the higher reductions due to increased temperatures, explaining why 4.LCC was particularly beneficial. 1.ES also had positive effects, higher when considering MPI-ESM-LR-RCA4 and NorESM1-M-REMO2015, while 5.ZT and 6.CC had a negligible effect. 3.SI was particularly useful in NorESM1-M-REMO2015, but it had little or no positive effect when considering the other models. For the individual adaptation strategies, the magnitudes of change were higher when considering RCP 8.5, except for 3.SI. The

effect of the combinations of adaptation strategies allowed to achieve more than 70% gained yields. Furthermore, we observed some significant synergies combining 3.SI with 1.ES and 4.LCC. As a final recommendation, 1.ES and 4.LCC should be always implemented regardless of the climate model, while 3.SI is suggested only with drier conditions.

A good adaptive capacity was observed for sunflower (Fig. 4.4). 4.LCC was effective with CNRM-CM5-ALADIN63, CNRM-CM5-RACMO22E and EC-EARTH-RACMO22E, even if percentages of gained yields were lower compared to durum wheat. 1.ES, 3.SI and 6.CC had positive effects when considering MPI-ESM-LR-RCA4 and even more NorESM1-M-REMO2015. The change in sowing date had no significant effect in CNRM-CM5-ALADIN63, CNRM-CM5-RACMO22E and EC-EARTH-RACMO22E. In MPI-ESM-LR-RCA4 and NorESM1-M-REMO2015, under RCP 4.5, the effect of 4.LCC was negligible. However, we observed synergies when 4.LCC was combined with 3.SI and 6.CC. Overall, the potential gained yields with adaptation strategies were lower compared to durum wheat, but the maximum reached more than 90% when considering the complete combination of adaptation strategies, RCP 4.5, and NorESM1-M-REMO2015. Different from durum wheat, for sunflower the positive effect of combining 3.SI and 6.CC was much clearer and not alternative, especially for the MPI-ESM-LR-RCA4 and NorESM1-M-REMO2015. Resuming the outcomes for sunflower, we can affirm that 4.LCC should always be taken into consideration, while 1.ES, 3.SI, and 6.CC especially if the climate will get drier.

The climate change impacts on irrigated maize yields were mainly determined by the changes in the climate variables other than precipitation. Hence, the adaptive capacity for this crop was lower and it was strictly linked with the crop cycle start and length (Fig. 4.4). As expected, the magnitude of gained yields was much lower, reaching no more than 25.9% under RCP 8.5. Compared to sunflower, the positive effects of 4.LCC under both RCPs and 1.ES under RCP 8.5 were much clearer (Fig. A4.4). No significant synergies or trade-offs were observed for maize.

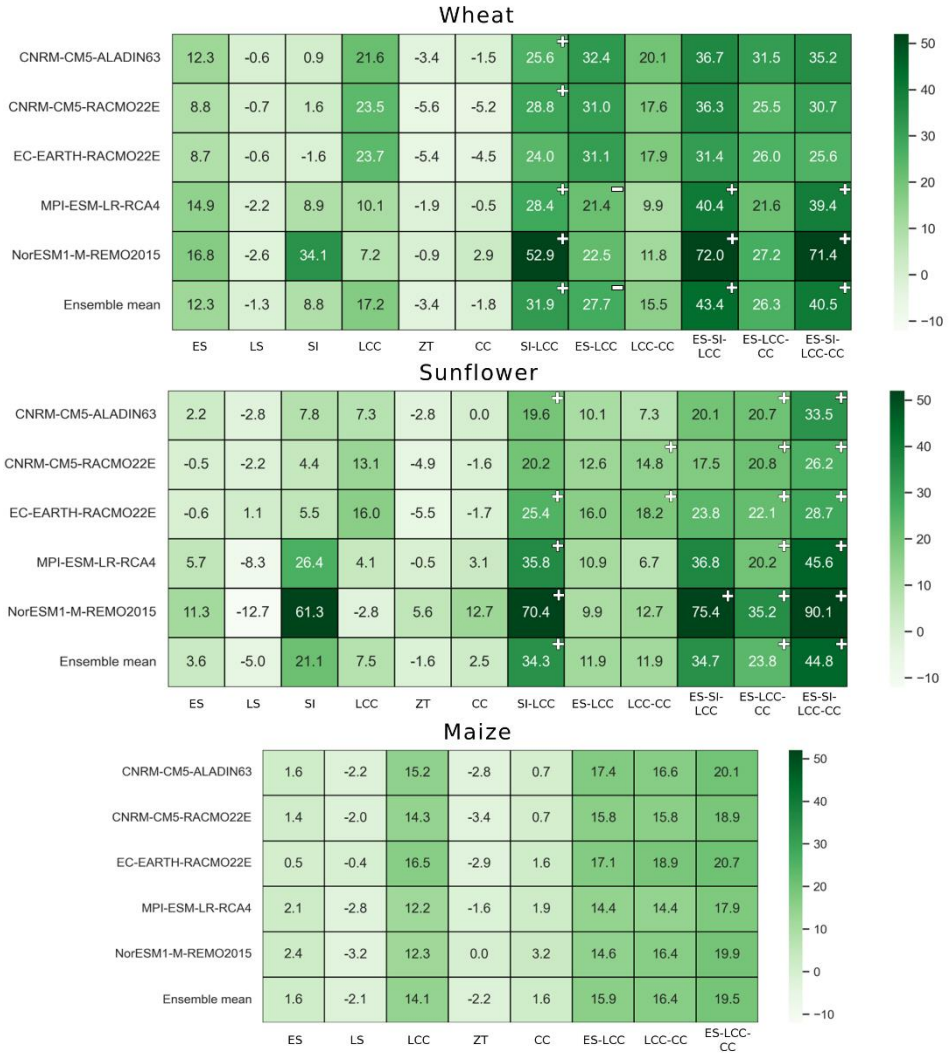

Figure 4.4: Effect of adaptation strategies on crop yield. Heatmaps created with the percentage changes for durum wheat, sunflower and maize yields, calculated considering the "no adaptation" and the different adaptation scenarios, for RCP 4.5. In the combinations of adaptation strategies, the synergies are indicated with the "+" symbol and trade-offs with "-".

4.4.3.2 Effect of adaptation strategies on water footprint

WF showed consistent opposite values compared to crop yield (Fig. 4.5). Overall, the changes reported for RCP 4.5 for the three crops considered were slightly lower in magnitude compared to RCP 8.5 (Fig. A4.5). The strategies with increased water use, such as 3.SI and 6.CC, showed an increase in WF, more accentuated when these strategies had no significant positive impact on yields. Instead, it is interesting to point out that WF decreased for sunflower when considering NorESM1-M-REMO2015, meaning that the increase in water used by these strategies was justified by the increase in crop yield. WF decreased also for wheat with NorESM1-M-REMO2015 when applying supplemental irrigation. 4.LCC showed to be crucial to reducing WF, since it increased crop yield without significantly increasing the annual evapotranspiration, with beneficial effects that were higher in CNRM-CM5-ALADIN63, CNRM-CM5-RACMO22E and EC-EARTH-RACMO22E. In MPI-ESM-LR-RCA4 and NorESM1-M-REMO2015, 1.ES was effective in reducing the WF of durum wheat and sunflower. For durum wheat, a reduction was also observed with the other climate models. In CNRM-CM5-ALADIN63, CNRM-CM5-RACMO22E and EC-EARTH-RACMO22E, for sunflower and under RCP 4.5, 2.LS was more beneficial than 1.ES, even if with low-magnitude changes. Under RCP 8.5 for sunflower, 2.LS consistently reduced WF while 1.ES increased it, according to all climate models except for NorESM1-M-REMO2015 (Fig. A4.5). Due to lower crop yields and increased water retention, 5.ZT always showed minor increases in WF, negligible for NorESM1-M-REMO2015 for sunflower and maize. For durum wheat, a huge ensemble decrease in WF of -39.1% was achieved when simultaneously implementing 1.ES and 4.LCC under RCP 8.5 (Fig. A4.5), even if a trade-off was observed under RCP 4.5 (Fig. 4.5). On the other hand, when combining adaptation

strategies that decreased WF with others that increased it, such as 4.LCC with 3.SI or 6.CC, synergies were observed for the three crops. For sunflower, the best outcomes regarding WF were obtained mainly because of 4.LCC, with the highest decrease being -25% considering the ensemble mean and RCP 8.5 (Fig. A4.5). Similarly, for maize, the strongest reductions in WF were also achieved with 4.LCC, with a maximum decrease of -18.2% considering the ensemble mean and RCP 8.5 (Fig. A4.5).

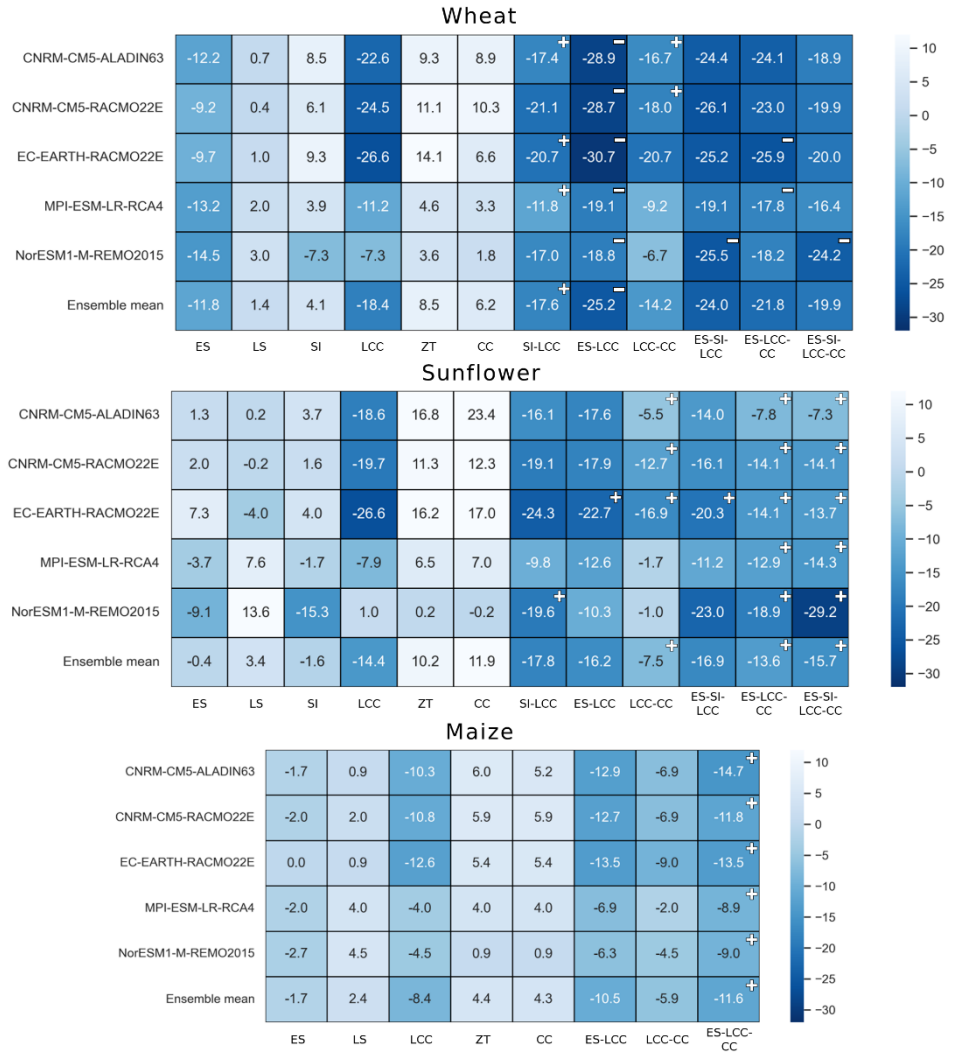

Figure 4.5: Effect of adaptation strategies on water footprint. Heatmaps created with the percentage changes in WF of wheat, sunflower, and maize, calculated considering the "no adaptation" and the different adaptation scenarios, for RCP 4.5. In the combinations of adaptation strategies, the synergies are indicated with the "+" symbol and trade-offs with "-".

4.4.3.3 Effect of adaptation strategies on drought and temperature stress

Overall, DS and TS decreased compared to historical simulations. This was expected for DS, since most climate models predicted minor increases in precipitation and the crop cycles were shortened due to the heat units' requirements that were reached much faster in a warmer climate. Instead, for TS this was surprising since the decrease was only partially explained by the shorter crop cycles. Hence, the TS was largely caused by low temperatures, as also discussed by Wang et al. (2017). The results for TS are similar when considering the two RCPs and the spring crops maize and sunflower. Hence, in Fig. 4.6, we reported only the outputs of the simulations under RCP 4.5 for durum wheat and sunflower.

DS was significantly influenced by the change in the sowing date, especially for wheat. As expected, 1.ES increased the DS for the winter crop and decreased it for the spring crop, while 2.LS showed consistent opposite results. 3.SI strongly reduced DS with ensemble-mean reductions of -41.1% and -54.8% for wheat and sunflower, respectively. Furthermore, 4.LCC significantly increased DS by 29% and 45.4% for wheat and

sunflower, respectively. Notably, 6.CC did not increase DS but slightly reduced it. Regarding TS, 1.ES increased while 2.LS decreased it, especially for the spring crop, confirming that lower temperature mainly contributed to TS. Moreover, 4.LCC increased TS mainly for the winter crop with an ensemble-mean increase of 19.2%. Consistently with the synergies observed for crop yield, we found synergies between 1.ES and 4.LCC only for sunflower, while between 3.SI and 4.LCC for both crops. Instead, no synergies or trade-offs were found for TS.

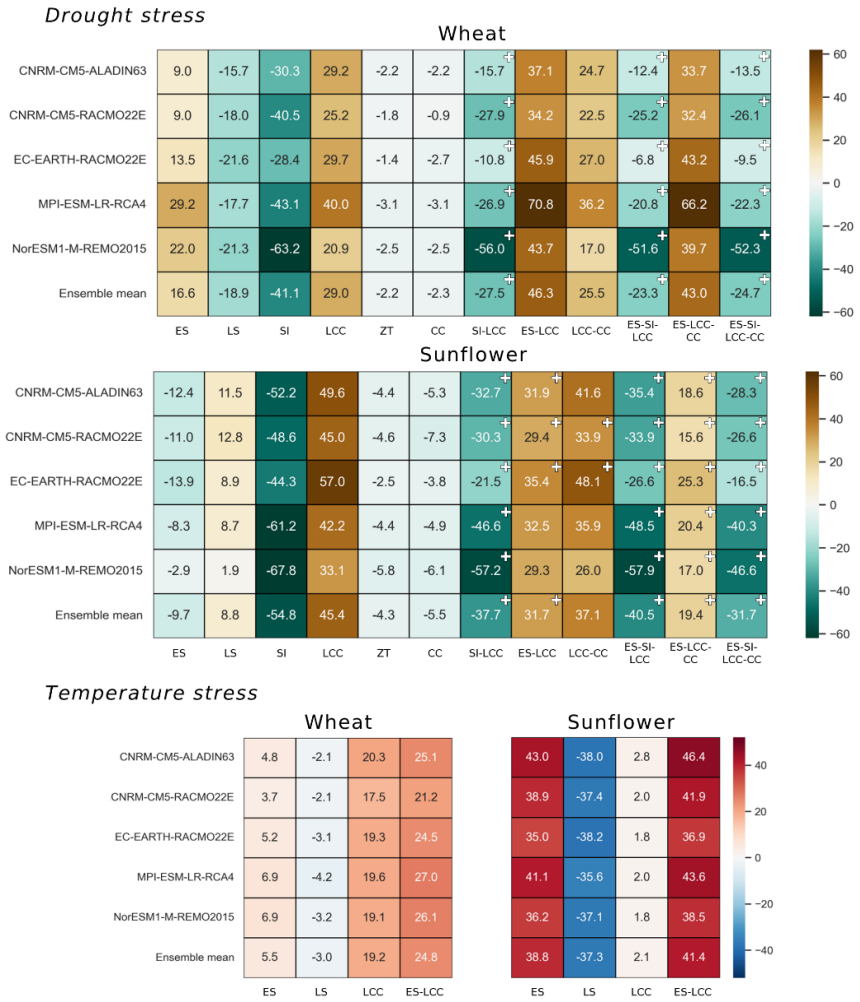

Figure 4.6: Effect of adaptation strategies on drought and temperature stress. Heatmaps created with the percentage changes in DS and TS of wheat and sunflower, calculated considering the "no adaptation" and the different adaptation scenarios, for RCP 4.5. For TS, we reported only the strategies that had an effect on it. In the combinations of adaptation strategies, the synergies are indicated with the "+" symbol and trade-offs with "-".

4.4.4 Effects of adaptation strategies on water balance components

Results showed that the impacts of some adaptation strategies on some components of the water balance were significant, especially at the cropland scale (Fig. 4.7, 4.8) but also at the catchment scale (Fig. 4.7).

At the cropland scale (Fig. 4.7, 4.8), the impacts of adaptation strategies on the water balance components were consistent in sign and generally higher in magnitude compared to the catchment scale (Fig. 4.7). The impact of 3.SI was reduced when considering the catchment scale, especially for evapotranspiration, water yield, soil moisture and percolation, while it remained almost the same for evaporation. For 4.LCC, 5.ZT and 6.CC we also observed reduced changes for evapotranspiration, as well as for soil moisture and percolation for 5.ZT and 6.CC. However, these described percentage changes refer to magnitudes lower than 5%. Instead, the effect of 5.ZT and 6.CC on water yield was very high in cropland, with average reductions of more than -27% under RCP 4.5. This effect was drastically reduced to approximately -5% at the catchment scale. Synergies between adaptation strategies were found for evaporation and evapotranspiration, mainly with 3.SI and 4.LCC (Fig. 4.8).

The most impacted water balance component at the catchment scale was evaporation, which was affected mainly by 1.ES and 3.SI in some specific simulations (Fig. 4.7). More precisely, evaporation was decreased by earlier sowing, longer crop cycle varieties and cover crops, while it was increased mainly with supplemental irrigation, but also with later sowing dates and zero tillage. Supplemental irrigation also increased catchment actual evapotranspiration. Water yield was affected to some extent by 5.ZT and 6.CC, while for evapotranspiration, percolation and soil moisture the impacts were negligible.

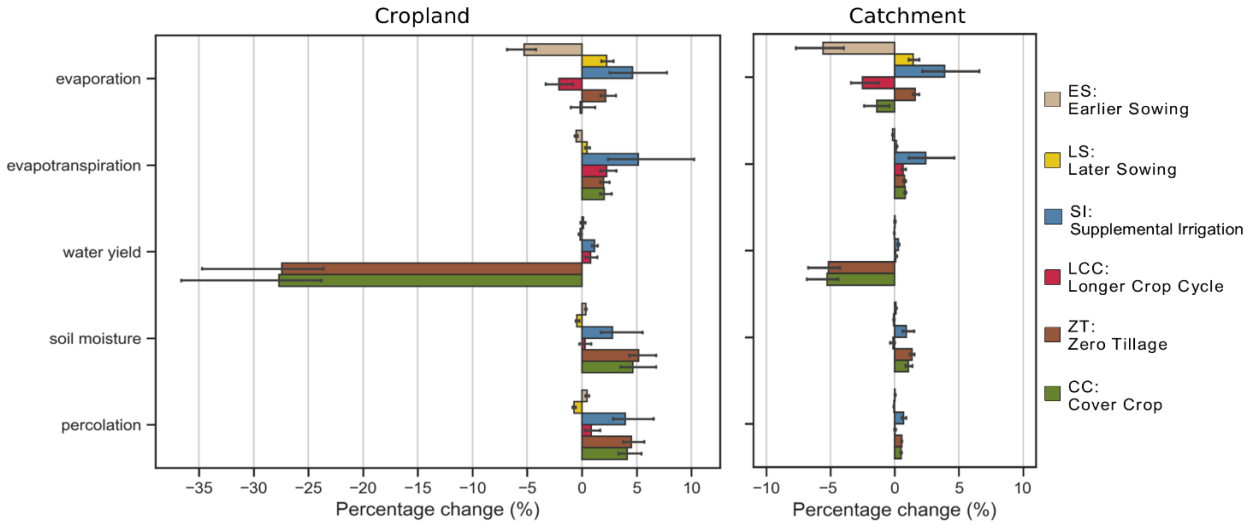

Figure 4.7: Comparison of the effects of adaptation strategies on water balance components for the whole catchment and only for cropland where the adaptation strategies are implemented. The bar plots are created considering the percentage relative differences between adaptation and no adaptation scenarios. The graphs use outputs of RCP 4.5 simulations.

4.5 Discussion

4.5.1 Crop yield estimation with SWAT+

Model performances for estimating crop yield are generally lower compared to monthly streamflow. This is a known issue reported in other studies in which the long-term annual average was coherent with the observed data, but not the inter-annual variation (Musyoka et al., 2021; Nkwasa et al., 2023). Certainly, using an aggregated representation of cropland and management is an approximation that has an impact on the model performance (Abbaspour et al., 2015; Srinivasan et al., 2010). Also, controlled experimental yields are usually preferred to actual yields since agricultural models cannot simulate yield losses due to pests and factors other than nutrients, water, and temperature stresses. Finally, it is important to consider that the provincial average yields provided by ISTAT have large uncertainties, even if they are commonly used in research conducted in Italy (Bocchiola et al., 2013; Diodato and Bellocchi, 2008; Monteleone et al., 2022; Toscano et al., 2012). The higher variability of the simulated yields compared to observed yields can be also explained by the fact that aggregated observed data tend to reduce the variability of the farm scale (Eini et al. 2023). Often, the simulated larger variability is caused by a higher number of extremely low yields (Wang et al., 2017), as in our study. Nevertheless, given all these limitations, the performances of the SWAT+ model were overall at least satisfactory according to the performance criteria selected for this research.

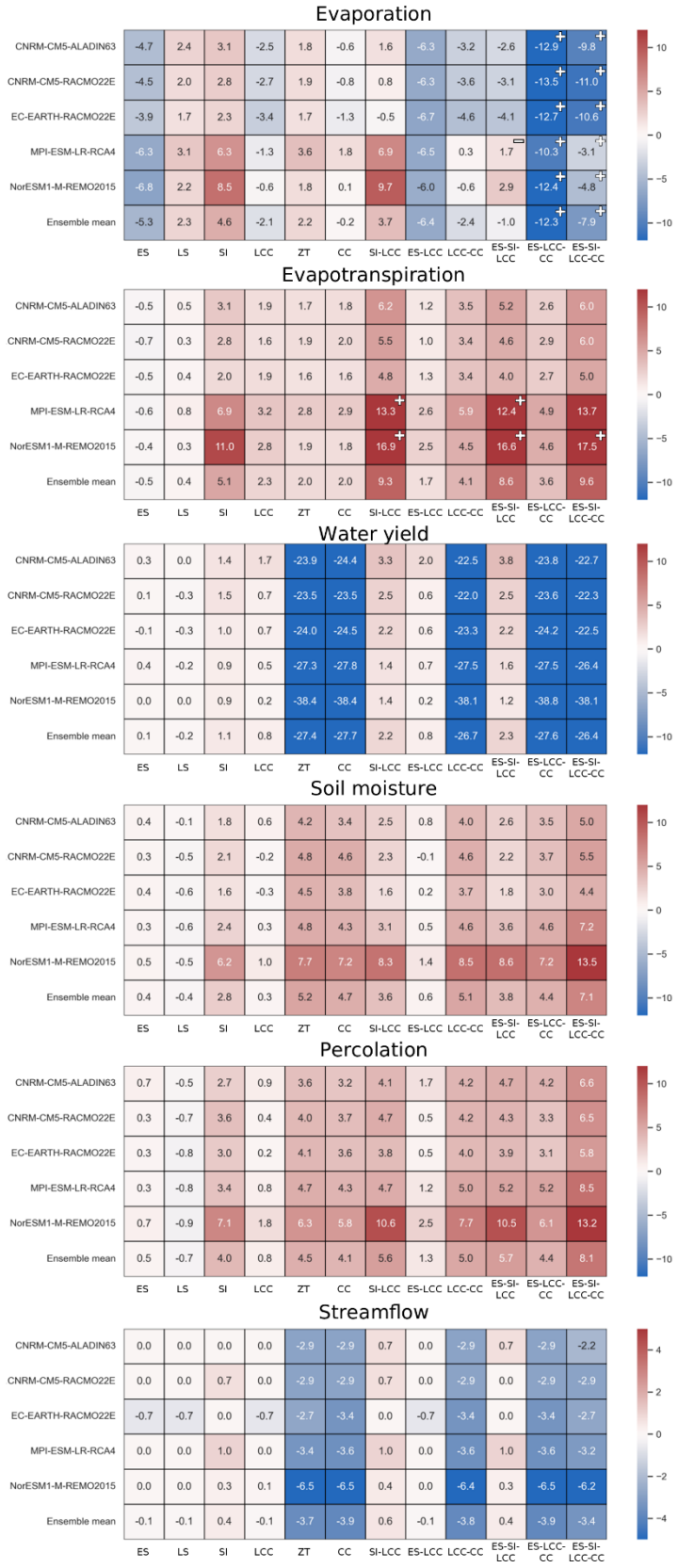

Figure 4.8: Effect of adaptation strategies on evaporation, evapotranspiration, water yield, soil moisture and percolation, considering only cropland, and streamflow at the outlet. Heatmaps created with the percentage changes, calculated considering the adaptation and no adaptation scenarios, for RCP 4.5. In the combinations of adaptation strategies, the synergies are indicated with the "+" symbol and trade-offs with "-".

4.5.2 Uncertain impacts of climate change on crops

In our study, the ensemble means showed negligible changes for future yields under RCP 4.5 while strong decreases (>20%) under RCP 8.5. Nonetheless, crop yields were highly dependent on the different climate models used. More in detail, NorESM1-M-REMO2015 showed contrasting values with the other climate models. This was mainly caused by the very low historical yields simulated, which resulted in considerable percentage increases in the future even if the absolute values were in line with the observed yields and the other simulations (Fig. 4.2). The uncertainty is also reflected in analysing literature about climate change impacts in the Mediterranean region. For general cereals in different areas of Spain, Iglesias et al. (2010) reported yield changes from -60% to +30%. More specifically for winter wheat, the uncertainty in future yield is very high and our estimations of constant yields under RCP 4.5 and strongly decreasing values under RCP 8.5 are within the ranges reported in the literature. For example, Ventrella et al. (2015) found increasing winter wheat yields in Southern Italy with the DSSAT model, while Garofalo et al. (2019) reported that yields are expected to remain constant in the future in the same area applying an ensemble of crop models. In the Italian island of Sardinia, Bird et al. (2016) simulated huge variations in future yield according to the soil considered in the simulations with the Aquacrop model, with a reduction in future yield of -64% in clay loam soils and increases of 8% and 26% on sandy loams and sandy clay loams. Interestingly, they estimated a 15% chance of crop failure in clay loam soils for winter wheat, and this is consistent with our consideration about part of the catchment that will become unsuitable for winter wheat cultivation due to extremely low annual average yields, for some climate models. The multi-model climate sensitivity analysis performed by Pirttioja et al. (2015) showed that in Spain wheat yields are expected to increase up to 30% if precipitation increases and with constant temperatures and to decrease with lower precipitation with magnitudes of change up to -60% in the worst scenarios. Negative impacts on wheat yield were also reported in the study of Ruiz-Ramos et al. (2018) in Spain. In Egypt, El Afandi et al. (2010) found significant yield decreases of -41% for wheat. For our study area, the European-scale study of Moriondo et al. (2010) simulated minor changes in wheat yield, while in the analysis at the national scale reported by Spano et al. (2020), moderate increases were predicted under RCP 8.5. The moderate increases were confirmed also by the draft of the PNACC (2018) while constant values were predicted for RCP 4.5. Fewer specific studies are available for sunflower, which is considered highly vulnerable since it is a rainfed spring crop (PNACC, 2018; Spano et al., 2020). However, the climate change analysis of Moriondo et al. (2010) reported minor changes in sunflower yields for our study area. This is in line with our outputs that showed constant and decreasing sunflower yields for RCPs 4.5 and 8.5, respectively. Many studies evaluated the impacts of climate change on maize and, in general, more consistent values are reported in the literature. This can be attributed to the fact that maize as an irrigated crop is less affected by precipitation variability. Decreasing maize yields were found in the studies of Torriani et al. (2007), Tubiello et al. (2000) and Bocchiola et al. (2013). However, in this last study, with sufficient irrigation or precipitation and increases in temperature of less than 2°C, constant or increasing maize yields were predicted (Bocchiola et al., 2013). Moderate decreases were found also by Rey et al. (2011) and Gabaldon-Leal et al. (2015) in Spain, while strong decreases of -56% were instead reported in the study of El Afandi et al. (2010) in Egypt. The outcomes of the simulations summarized in Spano et al. (2020) and PNACC (2018) confirmed the moderate decreases in maize yields in Southern Tuscany. Our results are in line with those reported in maize literature since we found yield decreases under RCP 8.5 and minor changes under RCP 4.5.

WF is a common metric to estimate agricultural water consumption which entails a high degree of uncertainty due to the different approaches to account for the water used (Feng et al., 2021). This uncertainty escalates when considering future WF in the context of climate change (Wang et al., 2023) and the large range observed in our results seems to confirm this statement (Fig. 4.3). Global estimates of WF, considering the sum of blue

and green water, were estimated by Mekonnen and Hoekstra (2011) as 1.6 $m^3\ kg^{-1}$ and 1.0 $m^3\ kg^{-1}$ for wheat and maize, respectively. In a following publication, Mekonnen and Hoekstra (2012) estimated the WF of oil crops at 2.2 $m^3\ kg^{-1}$. Feng et al. (2021) reported lower values for WF global averages, estimated at 1.1 $m^3\ kg^{-1}$ and 0.7 $m^3\ kg^{-1}$ for wheat and maize, respectively, with the ranges of uncertainty that increased considerably when considering smaller scales. At the European scale, a WF of 1.4 $m^3\ kg^{-1}$ and 0.6 $m^3\ kg^{-1}$ was reported in the analysis based on the Aquacrop model of Gobin et al. (2017). Focusing only on Italy, reported WF values have a broad range of uncertainty. For example, in the multi-model ensemble analysis of Kersebaum et al. (2016), durum wheat WF in Southern Italy calculated with observed yield and simulated evapotranspiration was estimated within the range of 1.3-1.7 $m^3\ kg^{-1}$. For the same area, Garofalo et al. (2019) reported WF values of 0.9 $m^3\ kg^{-1}$, while Ventrella et al. (2015) found values up to 2.7 $m^3\ kg^{-1}$ for rainfed winter durum wheat. When simulating future scenarios, these studies estimated a reduced WF of 0.9 $m^3\ kg^{-1}$ (Garofalo et al., 2019; Ventrella et al., 2015). The irrigated maize WF in Northern Italy was estimated by Nana et al. (2014) at 0.5 $m^3\ kg^{-1}$. Bocchiola et al. (2013) found minor changes in future total WF, with green and blue water compensating for each other in response to precipitation variability. Nevertheless, in the worst-case scenario, WF decreased due to the drop in maize yield (Bocchiola et al., 2013). Specific studies on sunflower are less common and the WF varies a lot according to the different climates. In the studies discussed by Bulut (2023) about sunflower WF, the values range between 1.3-3.3 $m^3\ kg^{-1}$, with huge differences in green and blue WFs. Brouziyne et al. (2018) performed a water productivity analysis in Morocco and found a decrease in future water productivity for both rainfed wheat and sunflower due to climate change. The ensemble mean of total WFs estimated in our study were 1.9 $m^3\ kg^{-1}$, 4.2 $m^3\ kg^{-1}$ and 1.1 $m^3\ kg^{-1}$ for durum wheat, sunflower and maize, respectively, slightly higher than WF values found in the literature. Nonetheless, our WF values are still in the range of uncertainty reported in the literature, and it is important to keep in mind that we calculated WF considering the annual average actual evapotranspiration as water used, and not only referring to the months in which the crop is grown. This approach allowed us to compare the WF of other adaptation strategies such as cover crops. Considering RCP 4.5, WFs slightly decreased for maize and increased for the rainfed crops, while for RCP 8.5 the ensemble means showed minor increases for maize but increased substantially for durum wheat and sunflower due to the significant drop in crop yield in many HRUs.

The analysis reported by Webber et al. (2018) showed that heat stress will not harm future wheat and maize yields. These results are consistent with our study since we found decreasing temperature stress due to reduced crop cycle length and increased temperature. This seems counterintuitive but the optimal temperatures are quite high – 15 °C for durum wheat and 25 °C for sunflower and maize – and, consequently, the temperature stress is largely caused by low temperatures, as found and discussed also in Wang et al. (2017). Considering drought stress, Webber et al. (2018) reported negative impacts on maize yield in our study area. Our results showed maize yield reduction under RCP 8.5, but these were not strictly related to drought stress which was negligible due to supplemental irrigation. Regarding future irrigation, despite the rising temperatures and the consequent increase in evapotranspiration, other studies found reduced irrigation requirements for maize by up to -25% mainly due to the shortening of the crop cycle (Gabaldon-Leal et al., 2015; Rey et al., 2011). These reductions were confirmed also in our study and the role of supplemental irrigation was not so important since climate models predicted slight increases in precipitation.

4.5.3 The effectiveness of adaptation strategies

In response to reduced precipitation, irrigation is likely to be needed in the Northern Mediterranean countries for typically rainfed crops, such as wheat (Saadi et al., 2015) and sunflower (Giannini et al., 2022). In Southern Italy, irrigation was predicted to increase future wheat yield by 11-15% (Ventrella et al., 2015) and 18%

(Garofalo et al., 2019) and to reduce yield variability (Ventrella et al., 2012b). Other studies conducted in the Mediterranean confirmed the positive effects of supplemental irrigation, such as El Afandi et al. (2010) in Egypt, Bird et al. (2016) in Sardinia, Ruiz-Ramos et al. (2018) in Spain, and Moriondo et al. (2010) at European scale. Furthermore, changes in sowing date drastically affect future yields, with variations of up to 40% found in Southern Italy in the study of Ventrella et al. (2012a). However, contrasting results can be found in the literature. For example, El Afandi et al. (2010) reported positive effects of earlier sowings, while Bird et al. (2016) and Moriondo et al. (2010) claimed the benefits of delayed sowing. Crop rotation (Ventrella et al., 2012c), mulching (Bird et al. 2016) and longer crop cycles (Moriondo et al., 2010) also showed positive effects on wheat yield. For sunflower, the study of Giannini et al. (2022) in Sardinia reported that earlier sowing and supplemental irrigation have beneficial effects on yield. Focusing on our study area, the analysis of Moriondo et al. (2010) confirmed that anticipated sowing dates led to moderate increases in sunflower yields, comparable to those of longer crop cycle varieties. In the same study, the increase caused by the application of supplemental irrigation on future sunflower yields was higher than 75%. Maize is typically irrigated in Italy and an appropriate irrigation strategy is fundamental to avoid water stresses during the most critical phases (El Afandi et al., 2010; Gabaldon-Leal et al., 2015; Monteleone et al., 2022). Furthermore, longer crop cycles and earlier sowing dates showed positive effects on maize yield (Rey et al., 2011; Torriani et al., 2007; Tubiello et al., 2000), quantified in an increase of 14% in the study of Gabaldon-Leal et al. (2015). Regarding the impacts of irrigation on WF, Bocchiola et al. (2013) demonstrated the strong relation between blue water and precipitation for maize in Northern Italy. The historical and future WFs of the irrigated simulations for winter wheat in Southern Italy reported in the studies of Ventrella et al. (2015) and Garofalo et al. (2019) were lower as compared to the WFs of the rainfed crop, demonstrating the beneficial impact of irrigation reducing WF by increasing crop yields. Our results confirmed that, when irrigation increased crop yield for wheat and sunflower, WF consistently decreased. The water productivity analysis of Brouziyne et al. (2018) in Morocco showed the beneficial impact of no-tillage on the water productivity of wheat and sunflower, while anticipating sowing of 10 days was beneficial for wheat and unclear for sunflower. Their results about earlier sowing were consistent with our WF outcomes, while the beneficial impacts of zero tillage were not confirmed in our study.

According to our results, adaptation strategies showed to be essential to maintain the historical crop yields. Furthermore, in some cases, especially when considering combinations of adaptation strategies, the SWAT+ model predicted increases in future yields and decreases in WF (Fig. 4.10). Considering the effect of adaptation strategies on agricultural outputs, namely crop yield and WF, the most promising adaptation strategies for durum wheat were earlier sowing and longer crop cycles, while supplemental irrigation had beneficial effects only with MPI-ESM-LR-RCA4 and NorESM1-M-REMO2015. For sunflower, longer crop cycles were always useful while earlier sowing, supplemental irrigation and cover crops only with MPI-ESM-LR-RCA4 and NorESM1-M-REMO2015. Similar recommendations can be provided for maize, with longer crop cycles being the most effective strategy both in increasing crop yield and in reducing WF. Overall, we can affirm that in our case study, the effect of some adaptation strategies was comparable to the impacts of climate change. Comparing the magnitudes of change in Fig. 4.9, it is possible to observe that the maximum absolute percentage increases for crop yields are much higher for management changes than the changes caused by climate change under RCP 4.5. The increased magnitude of changes in management as compared to climate is more evident when considering combinations of adaptation strategies in some climate models, mainly NorESM1-M-REMO2015. On the other hand, the impacts of climate change on WF are much higher compared to those of adaptation strategies, except for total WF for maize that showed similar magnitudes of change as compared to the maximum management changes (Fig. 4.9). Finally, the maximum absolute changes were also similar when considering DS and TS (Fig. 4.9).

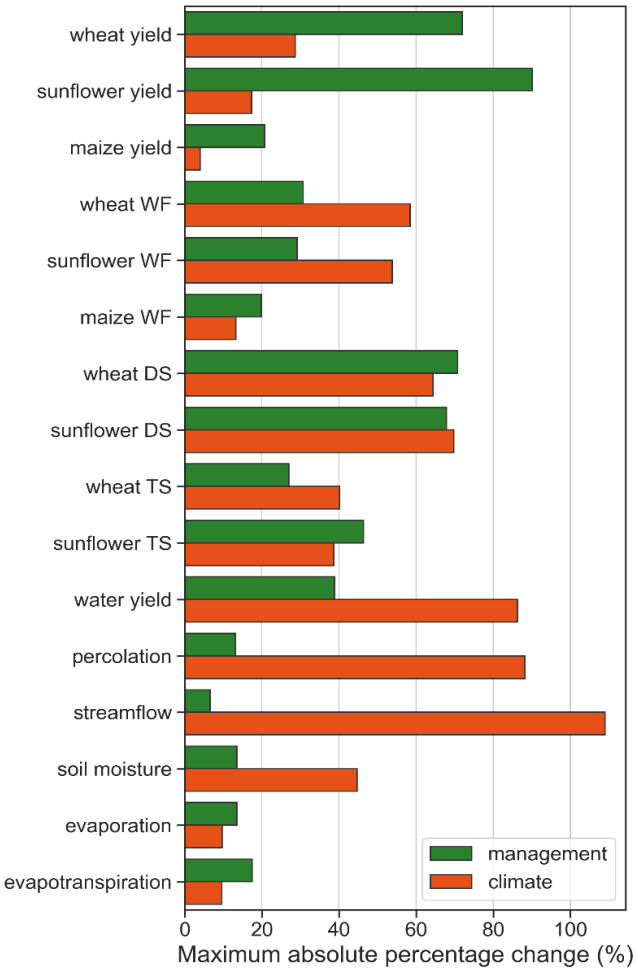

Figure 4.9: Comparison of the management and climate change effects on the agricultural and hydrological variables considered in this study, under RCP 4.5. The bar plot is created using the maximum absolute percentage change of the simulations performed in this study. For the water balance components, we are considering the outputs at the cropland scale and for streamflow the Sasso d'Ombrone gauging station.

4.5.4 The impact of adaptation strategies on water balance components

The use of an agro-hydrological model to spatially simulate crop growth and the possible management changes allowed for the evaluation of their impacts on water balance components, such as evaporation, actual evapotranspiration, water yield, percolation and soil moisture. Certainly, the SWAT+ model simplifies the processes influenced by management changes and further research is necessary. In our study, the area with herbaceous crops where the adaptation strategies were implemented corresponds to approximately one-third of the whole catchment, and it is interesting to note that the changes were not always reduced proportionally (Fig. 4.7). The outputs regarding the beneficial effects of the simulations on evaporation and water yield are also plotted in Fig. 4.10. To quantify how much the management changes influenced the water balance components, we compared them with the changes induced by climate change (Fig. 4.9).

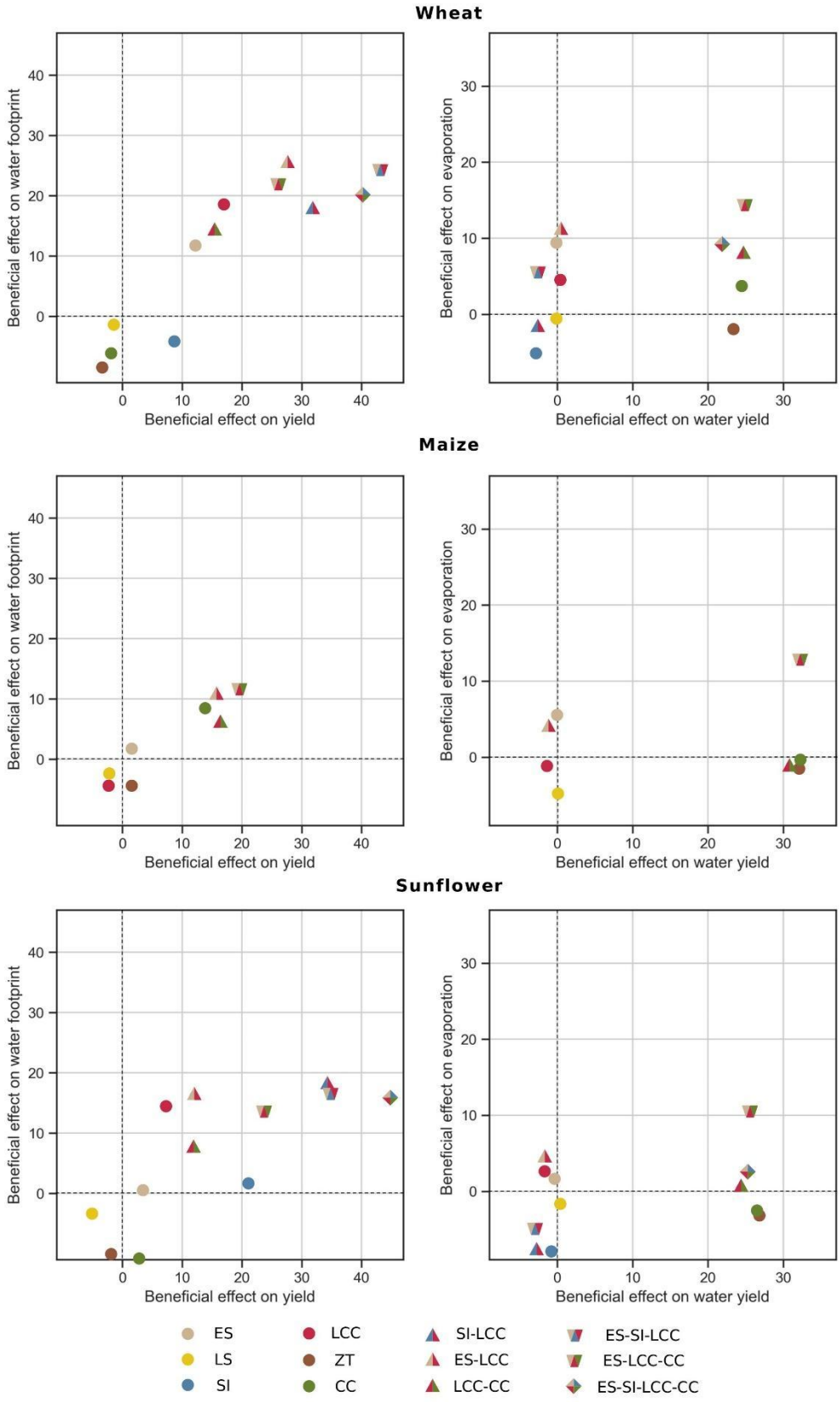

Figure 4.10: The beneficial effects of adaptation strategies and of their combinations expressed in percentage changes for wheat, sunflower and maize, considering the ensemble mean. We selected as beneficial effect on agricultural outputs increased crop yield and reduced WF, while for the water balance reduced evaporation and increased water yield. For this figure, we considered only the outputs of RCP 4.5 and the cropland scale.

The impacts of adaptation strategies on water balance components are usually neglected and there are few studies in the literature. One example is the water productivity analysis carried out with the SWAT model by Brouziyne et al. (2018), which showed that earlier sowing caused a reduction in water yield lower than 5%, while zero tillage yielded minor changes (<1%). Salmoral et al. (2017) evaluated the impact of contour tillage on water balance components and found no significant changes, different from when considering afforestation – a land cover change – which drastically influenced basin evapotranspiration and evaporation. In a field-scale study about the full adoption of rapeseed for biofuel, Noreika et al. (2020) found significant changes in evapotranspiration, soil moisture and flow by -11.8%, 16.6% and 36.1%, respectively. According to Noreika et al. (2022), residue incorporation, contour farming and conservative tillage reinforced the small water cycle both at the field and catchment scales, except for streamflow at the outlet. Their results showed that soil moisture and evapotranspiration were higher with conservation practices compared to conventional tillage, while the opposite occurred for runoff and lateral flow, with the runoff that was more than double. Interestingly, they found that the scale of adoption of the practices and the distribution in the catchment did not affect the water balance components. Ullrich and Volk (2009) found decreases of up to -30% in surface runoff and more than -10% in water yield applying no-tillage compared to conventional tillage, with differences according to the crops and tillage dates considered. Chen et al. (2021) performed a comprehensive analysis of irrigation at different depths, earlier and later sowing. For irrigated maize, they found that earlier sowing moderately increased (<5%) evapotranspiration, soil moisture, runoff and water yield, while later sowing decreased them by almost the same magnitude, except for soil water for which they reported a decrease of -7.8%. For irrigated wheat, with earlier sowing they observed an increase of 7.3% in evapotranspiration and decreases of more than -10% in soil moisture, runoff and water yield, while opposite changes were found for later sowing dates. For rainfed wheat, except for evapotranspiration which remained almost constant, they reported significant decreases in soil moisture, runoff and water yield for earlier sowing, while consistent opposite for later sowing, with increases reaching 77.3% in soil moisture.

In our study, while the effects of adaptation strategies on crop yield and WF were significant, the impacts on the water balance were generally low when considering the relative changes at the catchment scale (Fig. 4.7). However, in some cases and especially when considering the cropland scale, the impacts were significant and should not be neglected when comprehensively evaluating agronomic adaptation strategies. For example, water yield in cropland was significantly reduced by almost -40% when applying zero tillage and cover crops in one specific climate model under RCP 4.5 (Fig. 4.8). Combinations of adaptation strategies were more beneficial compared to individual ones (Fig. 4.10), and some synergies were observed. Furthermore, for some water balance components such as evaporation and actual evapotranspiration, we observed minor changes caused by climate change, comparable to the ones obtained for management changes, while the impacts of climate change were much higher as compared to those caused by management changes for water yield, soil moisture, percolation and streamflow (Fig. 4.9). At the catchment scale, the adaptation strategies had impacts of a few percentiles, with ensemble-mean changes mostly lower than 5%, with some exceptions (Fig. 4.7). These changes might seem negligible, but it is important to underline that we simulated very small changes. For example, sowing dates were shifted by only 15 days and the crop cycles were increased by the same number of days. As already discussed, supplemental irrigation was not so important in our study, but still, we could observe some impact on the water balance. With more significant management changes the impacts on the water balance components at the catchment scale could further escalate.

4.6 Conclusion

We applied an integrated agro-hydrological model to perform a comprehensive climate change impact assessment and to evaluate the adaptive capacity of agricultural systems in the Ombrone catchment. Despite the limitations of integrated models, distributed agro-hydrological models such as SWAT+ can be very useful for carrying out comprehensive climate change impact assessments since their outputs are related to food security and water resources at both field- and catchment scales.

Projected crop yield changes were highly variable and dependent on the crop, RCP and climate model considered. With RCP 8.5, the ensembles showed strong decreases in crop yields, while constant values with RCP 4.5. On the other hand, WF showed consistent opposite values with very high percentage changes in particular for durum wheat with RCP 8.5. This was the result of the very low yields (<1 ton/ha) predicted for durum wheat in many HRUs of the Ombrone catchment, which led us to conclude that, without adaptation, part of the catchment will become unsuitable for wheat growth under the worst scenarios. With the application of some adaptation strategies, we obtained similar or even improved yields and WFs compared to the historical simulations, demonstrating the high adaptive capacity of the agricultural systems. Longer crop cycles were found to be beneficial for the three crops considered. Earlier sowing was useful in particular for durum wheat and with some specific climate models and simulations also for maize and sunflower. Supplemental irrigation was beneficial for the rainfed crops but only with some climate models. For sunflower, some simulations showed the positive effect of cover crops. Many combinations of adaptation strategies showed interesting synergies that enhanced the positive effects or reduced the negative ones, but in some cases, we also observed trade-offs that should be considered. At the catchment scale, the impacts of management changes on water balance components were mostly lower than 5%, with some exceptions. However, considering only cropland we obtained more significant impacts, such as the reduction in water yield by almost -40% when applying zero tillage and cover crops for one specific climate model. Also, we simulated minor management changes and we concluded that with stronger changes the impacts on some water balance components could escalate. Hence, the impacts of some management changes in some agricultural catchments cannot be neglected when trying to assess the adaptive capacity of agricultural systems. To conclude, climate change impact assessment should be as integrated and comprehensive as possible by also considering the impacts at scales larger than the field scale, not only to include more climate, soil, crop, and management variabilities but also to simulate catchment-scale processes and impacts.

Chapter 5 Integration of the approaches

5.1 Abstract

Global agendas highlight how the challenges related to disaster risk reduction, sustainable development and climate change adaptation overlap. Despite common goals, there exist multiple approaches to risk estimation and management. In this study, we integrate climate risk and impact assessment methodologies to estimate future climate risk. We apply this framework in a sensible case study, Somalia, a country exposed to extreme events with a highly vulnerable population, where this kind of study is low. Considering risk as a function of hazard, exposure and vulnerability, we included indicators typically used in other climate risk assessments, mostly derived from the Shared Socio-economic Pathways (SSP) narratives, but also integrating them with the outputs of an agro-hydrological model forced with two climate models. In this way, we estimate future hazard, coping and adaptive capacity based on physical processes, instead of static proxy indicators.

Our results show that climate risk in Somalia will decrease in the future under the "Sustainability" and "Conventional development" scenarios, while it will remain similar to the present for the scenarios with significant adaptation challenges. By the end of the century, the climate is projected to be hotter and wetter, with decreasing dry extreme events for all SSPs, even if with variable magnitudes. Irrigated maize yield is projected to be severely affected by increased temperatures, even if adaptation strategies reduce yield losses. Conversely, rainfed sorghum yield will mostly benefit from increased rainfall. Nevertheless, even under the most optimistic scenarios, sorghum and maize yields will remain very low. Consistently with the so-called "Scenario optimism" of the SSP narratives, the vulnerability will decrease compared to the present, while exposure will highly increase in "Middle of the road", "Regional rivalry" and "Inequality" scenarios due to the demographic increase.

The outcomes of this assessment can be used to understand patterns, trends and main drivers of future climate risk under plausible scenarios for Somalia and neighbouring countries. Future applications should focus on developing local narratives including relevant stakeholders and on the improvement of the representation of resilience by simulating additional adaptation strategies and, more importantly, the transformative capacity. Avoiding further integration between approaches would be a missing opportunity to achieve greater policy impact.

5.2 Introduction

Climate, demographic and socio-economic changes pose tremendous risks for the population of low-income countries (FAO, 2021). These vulnerabilities are exacerbated for the small-holder farmers who rely on agropastoral activities and live in remote rural areas (Abdi-Soojeede, 2018). The challenges related to future climate risk have been thoroughly studied by the development, disaster and climate change research communities (Mochizuki et al., 2018; Savelli et al., 2022), each one characterized by specific approaches, agendas, definitions and methodologies (e.g. IPCC, 2022; UNISDR, 2015). For example, the disaster risk reduction community applies the contextual/factor approach, which generally relies on combined indicators, while the climate change adaptation community focuses on the outcome/impact approach, mainly based on quantitative measures of the relationship between stressor and response (Vogt et al., 2018). The risk and vulnerability concepts are also highly intertwined with the UN Sustainable Development Goals (UN, 2015) and the social-ecological resilience perspective (Folke, 2006; Mochizuki et al., 2018). Even if the challenges addressed by the disaster, climate adaptation and sustainable development communities strongly overlap, more efforts are required to enhance coherence among policies, goals, indicators and measurements

(UNISDR, 2015). A fundamental step towards an increased integration of approaches and a clearer understanding of alternative future scenarios is represented by the Shared Socio-economic Pathways (SSPs, O'Neill et al., 2017; van Ruijven et al., 2014). Further integration between methodologies, approaches and collaborations between research communities is necessary to achieve greater policy impact (Challinor et al., 2010; Marzi et al., 2021).

The definition and conceptualization of climate risk are highly variable according to the respective research communities. In the last years, some agreement was reached after the IPCC framed risk as the interaction of hazard, exposure and vulnerability (IPCC, 2014; 2022). Estimating climate risk or vulnerability related to single or multi-hazards with this conceptualization is nowadays an established framework (Hagenlocher et al., 2019; Jurgilevich et al., 2017; Merz et al., 2014) applied at global (Carrão et al., 2016; De Groeve et al. 2015), continental (Ahmadalipour et al., 2019), national (Mysiak et al. 2018; Song and Lee, 2021) and regional scales (Cotti et al., 2022). Many risk indexes and assessments address only past and present conditions (Hagenlocher et al., 2019). For example, the Index for Risk Management (InfoRM) supports global humanitarian risk analysis by combining hazard, exposure, vulnerability and lack of coping capacity dimensions (De Groeve et al., 2015). To monitor agricultural drought, the Global Drought Observatory developed the Risk of Drought Impacts for Agriculture (RDrI-Agri), which includes similar indicators (GDO, 2021). When dealing with future climate risk, the assessments usually consider only the dynamics of biophysical hazards, while the socio-economic exposure and vulnerability are maintained constant (Birkmann et al., 2015; Jurgilevich et al., 2017). An exception is represented by Tabari et al. (2021), who performed a global drought and flood risk assessment including dynamic hazard, exposure and vulnerability indicators. In a following study, Tabari and Willems (2023b) assessed future drought impacts considering future exposure and vulnerability dynamics, with the Human Development Index projected by Cuaresma and Lutz (2015) used as a proxy for vulnerability. The same authors evaluated the risk of compound hot and dry events considering future population and cropland as exposed elements and a governance indicator developed by Andrijevic et al. (2020) as a proxy for future vulnerability (Tabari and Willems, 2023a). Finally, Marzi et al. (2021) integrated into the InfoRM framework future climate-related hazards and exposure dynamics while maintaining constant vulnerability.

Applying the outcome/impact approach, researchers also study crop risk and vulnerability in response to hazards such as drought, usually relying on process-based crop models (Monteleone et al., 2022; Richter and Semenov, 2005; Yin et al., 2014). Similarly, for future scenarios, climate change impacts and adaptation strategies to reduce risk in agricultural systems are often studied with crop models (Ewert et al., 2015; Jägermeyr et al., 2021). Although the IPCC risk framework is not widely adopted by crop modellers, the coupling of the biophysical outputs such as yield with socio-economic data or models is common (Antle et al., 2021; Ewert et al., 2015; Ruane et al., 2017). An interesting application was performed by Simelton et al. (2009), who analysed vulnerability typologies based on socioeconomic characteristics with a crop failure index and a drought index using collected yield data. Similarly, Fraser et al. (2013) combined a crop vulnerability index, a hydrological model, and socioeconomic projections to identify vulnerability hotspots for cereal production in the world. Furthermore, De Vos et al. (2023) applied an integrated framework considering socio-economic development, gradual climate change and climate anomalies to evaluate future rice availability and stability in Africa. Despite some interesting examples, in conventional climate change assessments socio-economic conditions are generally assumed to remain constant (Valdivia et al., 2021). In the last years, a decisive step towards increased integration between biophysical and socio-economic dimensions was carried out by the Agricultural Model Intercomparison and Improvement Project (AGMIP), which produced frameworks, protocols and guidelines regarding Integrated Assessment Modelling (Ruane et

al., 2017), Representative Agricultural Pathways (Valdivia et al., 2015; 2021) and Regional Integrated Assessments (Antle et al., 2021; Rosenzweig et al., 2016).

Compared to the risk concept, the interpretation of the resilience concept is even more open in different fields (Mochizuki et al., 2018). After the first introduction of the term in ecology in the early 70s, in which resilience was defined as a property of the systems (Holling, 1973), the concept has evolved and largely applied in social-ecological systems research, including the notions of adaptive and transformative capacities (Folke, 2006). The term resilience is also widely applied and operationalized in sustainable development research and policies (Barron et al., 2021; Jeans et al., 2017) and risk assessment frameworks (Marzi et al., 2019), where is often conceptualized as the "flip side" of vulnerability (Manyena, 2006; Mochizuki et al., 2018). Although defined and interpreted slightly differently, nowadays there is consensus that the concept of resilience should involve the coping, adaptive and transformative capacities of the systems, even if the distinction between these capacities remains vague (Mochizuki et al., 2018). Inferring from impact research in agriculture, these three capacities can be broadly associated with the scenarios considered when simulating future management. The coping capacity of the agricultural system resembles the behaviour of the so-called "dumb" farmer, who does not apply any change in the management (Cline, 1996). Despite being unrealistic, this scenario is by far the most applied in future agricultural simulations. When considering adaptation, a typical categorization divides the strategies into autonomous (also referred to as soft or farmer-led) and planned (hard or institutional) adaptations, where autonomous adaptation strategies are the adjustments at the field or farm scales that farmers will adopt autonomously, while planned adaptations refer to deep transformations out of the scope of farmers' influence that will need institutional interventions (Bindi and Olesen, 2011). To operationalise the resilience concept, these two categories of strategies can represent the adaptive and transformative capacities of agricultural systems.

Despite the great advancements of the research communities dealing with risk, the explicit coupling of the approaches described in the previous paragraphs is largely missing. Combined indicators are very powerful tools that allow communication between academics and policymakers. Nevertheless, estimating some indicators using crop models can improve the representativeness and effectiveness of the combined indicators, especially for future conditions. The theoretical justification for the inclusion of crop indicators in the IPCC risk framework relies on the fact that climate change itself can be explicitly considered a hazard, resembling other vulnerability/risk assessments (ESCWA et al., 2017). Also, according to the IPCC, hazards are not defined solely as extreme events, but also as trends or physical impacts (IPCC, 2014). More specifically, crop models based on real physical processes could contribute to simulating future climate hazard and resilience. For example, agricultural drought is generally inferred considering vegetation status and deficits or anomalies in precipitation, soil moisture or evapotranspiration with indexes such as the Standardized Precipitation Evapotranspiration Index (SPEI, Vicente-Serrano et al., 2010; Yimer et al., 2022). The rationale for considering a drought indicator representative is to check how it correlates with drought impacts (Hall and Leng, 2019). Despite being widely adopted and useful, these indexes generalize drought drivers and ignore local contexts that are crucial for the propagation towards drought impacts (Kchouk et al., 2022), a problem which is amplified where these relations are unexplored, such as the African continent (Lam et al., 2023). Furthermore, they do not consider some important characteristics of agricultural systems, such as the crop type or their growth stage and if they are under irrigated or rainfed management. As a result, different accumulation periods were found to be best correlated with drought impacts in different regions or countries (Bachmair et al., 2018; Huang et al., 2018; Stagge et al., 2015). Further proof of the uncertainty in the hazard assessment was shown in the comparative analysis of global risk indexes performed by Garschagen et al. (2021) where, differently to vulnerability patterns, little agreement was found for the hazard component. This

uncertain correlation is exacerbated when dealing with the impacts of climate change on agriculture, since the effects on crops are numerous and, in some cases, positive. Process-based crop models offer a valuable methodology to estimate crop yield and its change under future climate. Moreover, resilience is also typically estimated with proxy indicators using socio-economic or biophysical data, which sometimes are considered as general vulnerability indicators. Using crop models to derive indicators by simulating the coping, adaptive and transformative capacities can be a valuable alternative to quantify resilience, which is the first necessary step for planning resilience interventions.

In this study, we proposed further and explicit integration between approaches to estimate current and future climate risk, mainly following the conceptualization and methodology of the InfoRM indexes (De Groeve et al., 2015; Marzi et al., 2021). More specifically, we used an agro-hydrological model – the Soil and Water Assessment Tool Plus (SWAT+, Bieger et al., 2017) – to retrieve hazard and resilience indicators considering future climate projections by the end of the century. These indicators were then combined with dynamic socio-economic indicators representing future exposure and vulnerability, relying on the variables derived from the five SSP narratives (O'Neill et al., 2017). We test the coupling of the risk-related approaches in Somalia, which is a country highly exposed to climate hazards and with an extremely vulnerable population, where extreme events are recurrent and devastating (Abdullahi et al., 2022; Ogallo et al., 2017). According to the EM-DAT database, 17 major droughts and 48 floods occurred since 1961, with an increasing trend in the last years. In Somalia, these kinds of risk-related assessments and modelling exercises are largely missing. Here, we aim to provide valuable insights to better understand the main trends and patterns characterising plausible future conditions and challenges in Somalia and other similar countries to better prepare adaptation strategies, demonstrating the potential of coupling different risk-related approaches towards greater policy impact.

5.3 Methods

The methodological steps were prepared based on the composite indicators' guidelines of OECD (2008) and Chapter 2 and other risk assessments (De Groeve et al., 2015; Marzi et al., 2021; Hagenlocher et al., 2018).

1. Conceptual and methodological framework definition
2. Study area definition
3. Indicator analysis and selection
4. Normalization and weighted aggregation
5. Robustness evaluation

5.3.1 Conceptual and methodological framework definition

We estimated climate risk for the historical and long-term future (2071-2100) periods in Somalia considering the five SSPs narratives and variables produced within them. With historical period, here we refer to the period 1985-2014 when using outputs produced with the agro-hydrological model, while to the recent past when considering SSP-based indicators. More details are available in the supplementary materials, part 1 and 2. The main characteristics describing the SSP narratives useful for this study from reference papers (O'Neill et al., 2016; 2017) are reported in Table 5.1. We considered the framework proposed by IPCC, with risk being a function of hazard, exposure and vulnerability. The definitions and their references used in this study are reported in Table 5.2. Our focus was on agriculture and food security in conditions of water scarcity and drought, but we referred to a general climate risk assessment as we included mostly general exposure and vulnerability indicators and other extreme events, such as heat waves and heavy precipitation. Consistently

with the InfoRM risk index, we referred to hazard, vulnerability and exposure as dimensions, each of them composed eventually by multiple categories (De Groeve et al., 2015). In this study, we considered extreme events and crop yield change as hazard categories, while resilience, socio-economic and environmental susceptibilities as vulnerability categories. Finally, dimensions and categories aggregated the selected indicators. The scheme with the categories for each dimension, with the respective indicators and data source or methodology used for this assessment is reported in Fig. 5.1, while the full set of indicators is reported in Table 5.3.

Table 5.1: The five SSP narratives and their main characteristics used in this study, adapted from O'Neill et al. (2016, 2017).

General	*Code*	SSP126	SSP245	SSP370	SSP460	SSP585
	SSP	1	2	3	4	5
	Name	Sustainability	Middle of the road	Regional rivalry	Inequality	Conventional development
	Socio-economic challenges	Low	Intermediate	High	High for adaptation, low for mitigation	Low for adaptation, high for mitigation
Forcing	*Category*	Low	Medium	High	Medium	High
	2100 W m^{-2}	2.6	4.5	7.0	6.0	8.5
Demography	*Population growth*	Relatively low	Medium	High [a]	Relatively high	Relatively low
	Urbanization	High	Medium	Low	High	High
Human development	*Education*	High	Medium	Low	Very low/unequal [a]	High
Economy	*Growth per capita*	High [b]	Medium, uneven	Slow	Low [b]	High
Technology	*Development*	Rapid	Medium, uneven	Slow	Slow [c]	Rapid
Environment and natural resources	*Environment*	Improving conditions over time	Continued degradation	Serious degradation	Continued degradation [d]	Highly engineered approaches, successful management of local issues
	Agriculture	Productivity improvement, diffusion of best practices	Medium pace of technology changes, entry barriers to markets reduced slowly	Low technology development, restricted trade	High agricultural productivity for large-scale industrial farming, low for small-scale farming	Highly managed, resource-intensive, rapid increase in productivity

[a] for high-fertility countries
[b] in low-income countries
[c] in non-high-tech economies and sectors
[d] in low-income living areas

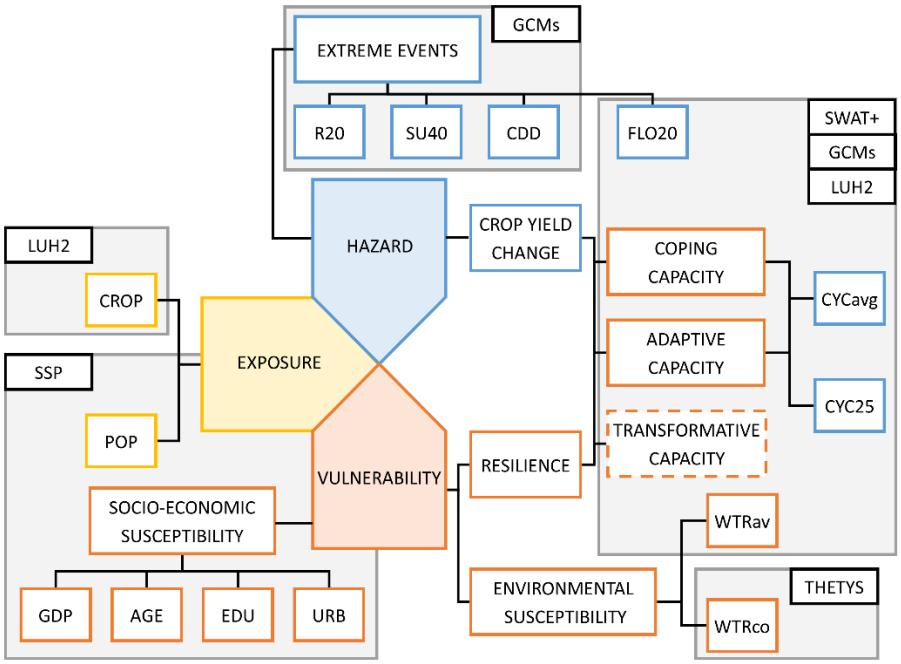

Figure 5.1: Schematic representation of the conceptual and methodological risk framework, with the components, indicators, and data source or methodology used. Indicators abbreviations are defined in Table 5.3.

Table 5.2: Definitions used in the study.

Concept	Definition	Reference
Risk	The potential for adverse consequences on lives, livelihoods, health, ecosystems and species, economic, social and cultural assets, services (including environmental services) and infrastructure.	IPCC, 2014
Hazard	The potential occurrence of a natural or human-induced physical event or trend or physical impact that may cause loss of life, injury, or other health impacts, as well as damage and loss to property, infrastructure, livelihoods, service provision, ecosystems and environmental resources.	IPCC, 2014
Exposure	The presence of people, livelihoods, species or ecosystems, environmental functions, services, and resources, infrastructure, or economic, social, or cultural assets in places and settings that could be adversely affected.	IPCC, 2014
Vulnerability	The propensity or predisposition to be adversely affected. Vulnerability encompasses a variety of concepts and elements including sensitivity or susceptibility to harm and lack of capacity to cope and adapt.	IPCC, 2014
Susceptibility	The physical predisposition of human beings, infrastructure, and environment to be affected by a dangerous phenomenon due to lack of resistance and predisposition of society and ecosystems to suffer harm.	Cardona et al., 2012
Resilience	The capacity of social, economic and environmental systems to cope with a hazardous event or trend or disturbance, responding or reorganizing in ways that maintain their essential function, identity and structure, while also maintaining the capacity for adaptation, learning and transformation.	IPCC, 2014
Coping capacity	The ability of a system or individual to respond to adverse shocks, which affects how direct risk translates into indirect risk.	Mochizuki et al., 2018
Adaptive capacity	The ability of a system or individual to reduce direct and indirect risk through marginal or incremental changes to the system (that is, changes that occur within the scale of interest).	Mochizuki et al., 2018
Transformative capacity	The ability of a system and individuals to address fundamental drivers of risk that are outside of the scale of interest or to amend the major functioning of a system, thereby changing mechanisms and modifying the ramifications of direct and indirect drivers of risk.	Mochizuki et al., 2018

Table 5.3: Indicators used in the risk assessment, with the abbreviation, dimension, method, description, functional relationship with the dimension and data source.

N	Indicator	Code	Dimension	Method	Description	Functional relationship	Data source
1	Extreme precipitation	R20	Hazard	GCMs	Annual number of days with P > 20 mm	The highest the number of days above the threshold, the highest the hazard	ISIMIP repository (data.isimip.org/search/), Lange and Büchner, 2021, elaborated in this study
2	Extreme temperature	SU40	Hazard	GCMs	Annual number of days with TMAX > 40 °C	The highest the number of days above the threshold, the highest the hazard	ISIMIP repository (data.isimip.org/search/), Lange and Büchner, 2021, elaborated in this study
3	Meteorological drought	CDD	Hazard	GCMs	Longest dry spell, the maximum number of consecutive dry days with P < 1 mm	The longest the maximum dry spell, the highest the hazard	ISIMIP repository (data.isimip.org/search/), Lange and Büchner, 2021, elaborated in this study
4	Hydrological drought	FLO20	Hazard	SWAT+ (GCMs + LUH2)	Number of months below the 20th percentile threshold calculated in the historical period	The highest the number of months below the threshold, the highest the hazard	This study
5	Crop yield change (average)	CYCavg	Hazard, resilience	SWAT+ (GCMs + LUH2)	Average yield (t/ha), to take into account climate change impacts	The lowest the crop yield, the highest the hazard	This study
6	Crop yield change (low)	CYC25	Hazard, resilience	SWAT+ (GCMs + LUH2)	First quartile yield (t/ha), to take into account yield variability	The lowest the crop yield, the highest the hazard	This study
7	Water availability	WTRav	Environmental susceptibility	SWAT+ (GCMs + LUH2)	Sum of annual average water yield and recharge (mm/year)	The lowest water available, the highest the vulnerability	This study
8	Water consumption	WTRco	Environmental susceptibility	Tethys	Total water consumption (km^3)	The highest the water consumption, the highest the vulnerability	Khan et al., 2023
9	Gross Domestic Product	GDP	Socio-economic susceptibility	SSP	GDP per capita (billion US$2005/year)	The lowest the GPD, the highest the vulnerability	SSP database (tntcat.iiasa.ac.at/SspDb/), Riahi et al., 2017, IIASA, Cuaresma, 2017
10	Age	AGE	Socio-economic susceptibility	SSP	% of young, adult, and old population (<15 years, between 15 and 65 years, >65 years, respectively)	The highest the share of young and old population, the highest the vulnerability	SSP database (tntcat.iiasa.ac.at/SspDb/), Riahi et al., 2017, IAASA, Samir and Lutz, 2017
11	Education	EDU	Socio-economic susceptibility	SSP	% of the population without education and with primary, secondary and tertiary education	The lowest the education, the highest the vulnerability	SSP database (tntcat.iiasa.ac.at/SspDb/), Riahi et al., 2017, IAASA, Samir and Lutz, 2017
12	Urbanization	URB	Socio-economic susceptibility	SSP	% of the population living in urban areas	The lowest the share of population living in cities, the highest the vulnerability	SSP database (tntcat.iiasa.ac.at/SspDb/), Riahi et al., 2017, NCAR, Jiang and O'Neill, 2017
13	Total population	POP	Exposure	SSP	Total population (million)	The highest the population, the highest the exposure	SSP database (tntcat.iiasa.ac.at/SspDb/), Riahi et al., 2017, IAASA, Samir and Lutz, 2017
14	Cropland	CROP	Exposure	LUH2	Total area (ha) with C4 annual crops	The highest the cultivated area, the highest the exposure	Land Use Harmonization 2 (luh.umd.edu/), Hurtt et al., 2020

As hazard indicators, for the “extreme events” category, we included extreme precipitation (R20) and temperatures (SU40), longest dry spell (CDD) and low river flow (FLO20). Additionally, we framed climate change as a hazard itself and included “crop yield change” as a category. For vulnerability, many conceptual approaches exist to define it. In this study, we used the “vulnerability as an outcome”, as framed by Jurgilevich et al. (2017), since we considered dynamic socio-economic scenarios and adaptation strategies. Following the IPCC framework, we relied on indicators of susceptibility, either social, economic or ecological, and coping and adaptive capacities (Hagenlocher et al., 2019). We used indicators derived from the five SSP narratives, representing the “socio-economic susceptibility” category. Additionally, we included in the “environmental susceptibility” category indicators with a clear focus on water availability and consumption, which in some drought risk assessments are considered within physical susceptibility (Hagenlocher et al., 2019), exposure (GDO, 2021) or coping capacity. To consider the coping and adaptive capacities, we referred to the concept of resilience, which also includes the transformative capacity (Folke, 2006; Mochizuki et al., 2018). As we focused mainly on agriculture, we used the agro-hydrological SWAT+ model to simulate the capacity of the system to maintain good crop yields or increase them, considering different scenarios. More in detail, the coping capacity was represented in the simulations with constant fertilization and without any other management change, following the “dumb” farmer scenario. For adaptive capacity, we ran simulations considering simple agronomic autonomous adaptation strategies that will be easily implemented by farmers, such as changing the sowing and harvesting dates and adopting longer crop cycle varieties. Furthermore, in the adaptive capacity simulations, we also included the expected management changes in fertilization as projected in the datasets that we used. In this modelling exercise, we did not simulate any transformative capacity with the agro-hydrological model, even if the effects of some transformations are inherently included in the SSP narratives (Table 5.1). Hence, in our framework, we indirectly considered resilience indicators reflecting the coping and adaptive capacities through the process-based model, which was used to estimate future hazards. Here, resilience is considered a neutral concept in the coping capacity simulation and desirable resilience for the adaptive capacity simulations (Mochizuki et al., 2018) since we considered the best-performing adaptation strategies to calculate the final climate risk index. Finally, for exposure, we included the potentially affected population (POP) and cropland (CROP). Even if we recognize that cropland has a positive role from a food security point of view, this indicator is typically included in many climate risk assessments (e.g. GDO, 2021; Meza et al., 2020) and we decided to remain consistent with them.

5.3.2 Study area definition

Somalia is a country in the Horn of Africa with a prevalent arid and semi-arid climate (Fig. 5.2). As the average annual precipitation ranges from 100 to 700 mm, water resource management is fundamental in Somalia (Basnyat, 2007). Annual rainfall is distributed in a bimodal pattern, with long rains from March to June and short rains from October to November, locally known as Gu and Deyr, respectively, which corresponds to the growing periods when rainfed agriculture is practised (Basnyat, 2007). The interannual variability characterizes precipitation patterns, with recurrent extreme events such as droughts and floods (Ogallo et al., 2017). The Juba and Shabelle rivers are the only two perennial rivers of Somalia, which originate in the Bale mountains of Ethiopian highlands and flow southwards towards the Indian Ocean. Their catchment areas are 216,728 and 297,455 km^2 for the Juba and Shabelle rivers respectively. These two rivers are fundamental for the Somali economy and social and environmental well-being (Sebhat, 2015). About two-thirds of their catchment area is in Ethiopia and Kenya, where more than 90% of the runoff is generated (Basnyat, 2007).

Agriculture and livestock are the main sectors contributing to the Somali GDP (Mourad, 2022). Even if urbanization is increasing, the largest part of the population still lives in rural areas, with a significant

percentage of nomadic pastoralists (Basnyat, 2007; Michalscheck et al. 2016). The rural population has little access to clean water, and conflicts between different users of scarce water resources are increasing (Hashi, 2017). The instability of the country led to a war of almost 30 years that further weakened the Somali institutions and increased the vulnerability of the local population (Houghton-Carr et al., 2011; Sebhat and Wenninger, 2014; Mourad, 2022). The vulnerability of Somalia is also enhanced by the decreasing and increasing trends in exports and imports at 13% and 16%, respectively (Mourad, 2022).

The alluvial plains of the Juba and Shabelle rivers are the food basket of Somalia accounting for 90% of food production and 70% of cereal production (Basnyat, 2007). The main crops are maize and sorghum, cultivated both in rainfed and irrigated areas, with the share of land cultivated with sorghum increasing where water is scarcer (Basnyat, 2007; Warsame et al., 2022; 2023). The outbreak of the civil war and recurrent droughts and floods drastically reduced the area under irrigation, estimated in the pre-war period to be 1100 km^2 under recession cropping and 1130 km^2 under gravity and pump irrigation (Houghton-Carr et al., 2011).

For this study, we set up the SWAT+ model for the whole Juba and Shabelle catchments (Fig. 5.2), but in the analysis, we calculate the physical indicators only with the outputs generated within the Somalian parts. As the socio-economic indicators from SSP narratives are downscaled at the national scale, we considered the data for the whole of Somalia, justified by the fact that the Juba and Shabelle valleys are the food basket of the country, accounting for most of the cereal, fruit and vegetable production.

5.3.3 Indicator analysis and selection

In this climate risk assessment, we retrieved indicators mainly from agro-hydrological modelling and using the data derived from SSP narratives (Fig. 5.1, Table 5.3). In the SWAT+ model, we divided cropland in Somalia based on reports from FAO and EU (Basnyat, 2007; FAO and WFP, 1997; EU, 2010). We considered sorghum as only rainfed, while maize was both rainfed and irrigated. To realistically represent crop cycles in the two rainy seasons, we considered the FAO crop calendar and then adjusted it using the monthly average Leaf Area Index (LAI). Then, we calibrated and validated the model for monthly streamflow at the Luuq gauging station. Finally, we considered two representative Hydrological Response Units (HRUs) with irrigated maize and rainfed sorghum and calibrated the model outputs of crop yields. More details about the model set-up, calibration, validation, and simulations are available in the supplementary material, part 1. We then ran the SWAT+ model with different inputs obtained from the Land Use Harmonization 2 (LUH2) and simulated different adaptation strategies reflecting the coping capacity and the adaptive changes (Table 5.4). Moreover, we calculated water availability with the outputs of the SWAT+ model. The dataset produced by Khan et al. (2023) was used to estimate historical and future water consumption. Finally, the outputs derived from SWAT+, climate models, LUH2 and the dataset produced by Khan et al. (2023) represented hazard, environmental susceptibility and, indirectly, resilience, to be coupled with the socio-economic indicators that represented exposure and vulnerability (Table 5.3). As discussed in section 2.1, we also included cropland from LUH2 as an indicator of exposure.

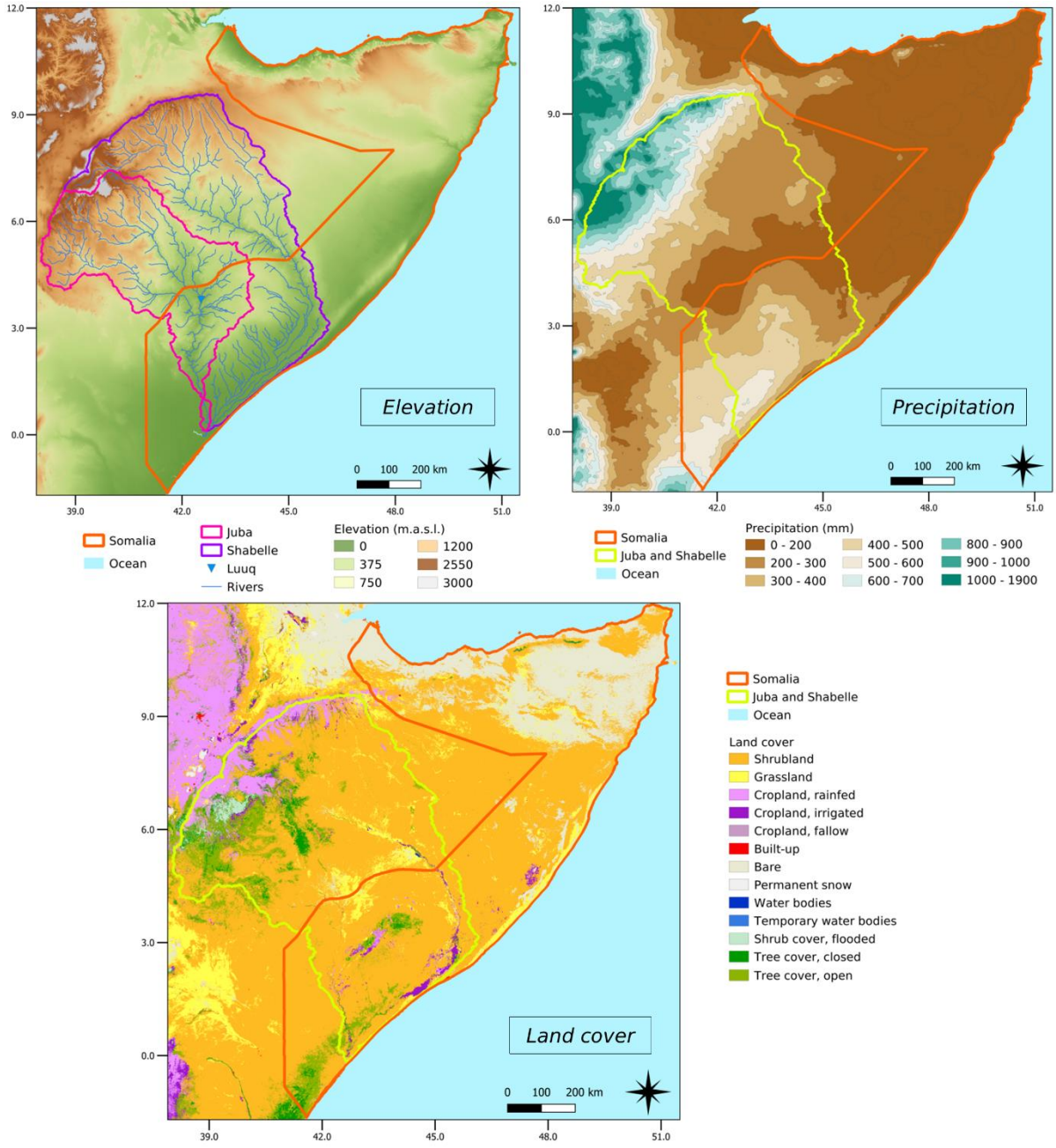

Figure 5.2: Elevation, precipitation and land cover maps of the Juba and Shabelle catchments and Somalia. The DEM (from the Shuttle Radar Topography Mission) and the land cover (the Copernicus Global Land cover map) are created with the data used for the SWAT+ model, while the precipitation map considers the long-term average of the Climate Hazards Infrared Precipitation with Stations (CHIRPS, Funk et al., 2015).

Even if we performed an analysis with and without agronomic adaptation to quantify the adaptive capacities, in the final composite indicator we considered as the main option the yield outputs of the best-performing adaptation simulation, hence avoiding the "dumb" farmer scenario. For the crop yield indicators, we used the average and first quartile crop yields of the representative HRUs, and we applied a weighted average considering the percentage of irrigated area as reported in the LUH2 dataset (Table 5.4). As climate models, we considered the outputs of the GCMs ipsl-cm6a-lr and mri-esm2-0, the only two models available for all five SSPs in the ISIMIP repository (Lange and Büchner, 2021). From the dataset of Khan et al. (2023), we included only the ipsl-cm5a-lr climate model to remain consistent with the SWAT+ simulations.

As socio-economic indicators, we analysed 8 possible indicators and, finally, we considered only 5, excluding the “female population”, the “income Gini coefficient” and the “conflict probability”, due to data redundancy and similar values across the five SSP narratives and the historical period. More details about the exploratory analysis and the reason for inclusion or exclusion are discussed in the supplementary materials, part 2. As we estimated the climate risk for only one country, we did not perform any further multi-collinearity analysis.

Table 5.4: Management schedule for the SWAT+ simulations considering the base, coping and adaptive scenarios.

Simulation	Resilience	Description	Irrigation maize	Fertilization (kg/ha/yr)
Base	/	/	Historical: 6%	Historical: 13
No Adaptation	Coping capacity	Considering only climate and CO_2 concentration changes		
Adaptive changes: LCC	Adaptive capacity	Considering the fertilization and irrigation changes as reported in LUH2, and longer crop cycles	SSP126: 20% SSP245: 1% SSP370: 2% SSP460: 2% SSP585: 30%	SSP126: 24 SSP245: 100.1 SSP370: 10 SSP460: 14.9 SSP585: 37.1
Adaptive changes: LCC - ES	Adaptive capacity	Considering earlier sowing (20 days) in addition to LCC		
Adaptive changes: LCC - LS	Adaptive capacity	Considering later sowing (20 days) in addition to LCC		

5.3.4 Normalization and weighted aggregation

As the main normalization method, we considered the widely used min-max normalization method using values between 1 and 10. As the main weighting scheme, we applied equal weights, except for crop yield indicators where we considered the irrigated area as weight, as discussed in section 2.3. To aggregate indicators, we used both arithmetic and geometric means. The geometric mean is used instead of arithmetic mean to allow some degree of non-compensability (OECD, 2008). Since the geometric mean is always lower than the arithmetic mean, to reward the scenarios with higher scores, we largely followed the procedure of the InfoRM risk index (De Groeve et al., 2015). More in detail, we applied these steps to calculate risk:

1. Calculate the arithmetic mean of the indicators with the two climate models and for the two growing seasons for crops.
2. Normalize the indicators between 1 and 10, following the notion the higher the better.
3. Calculate the geometric mean for the two crops, then for the categories, and finally for the dimensions.
4. Reverse scale to reclassify following the notion the higher the worse.
5. Calculate the risk index with equation 1, similar to the InfoRM risk index (De Groeve et al., 2015), combining the three dimensions of risk.

$$Risk = Hazard^{1/3} \cdot Exposure^{1/3} \cdot Vulnerability^{1/3} \quad (1)$$

To allow a simple analysis and discussion of the outcomes of the analysis, we reported the relative rank of the six scenarios and classified climate risk, hazard, vulnerability and exposure as “very high” (>8), “high” (6-8), “intermediate” (4-6), “low” (2-4), “very low” (<2). Furthermore, since we conducted a study on an individual country and we wanted to quantify the future risk compared to the current situation, we also considered the percentage relative differences between projected and historical scenarios. This can be also considered a normalization approach as proposed by OECD (2008), defined as “distance to a reference measure”.

5.3.5 Robustness evaluation

When constructing a composite index, multiple choices are made, which involve a high level of uncertainty (OECD, 2008). In the sensitivity/uncertainty analysis, we considered different weighting and aggregation strategies and excluded individual indicators. As different weighting methods, we attributed equal importance to all the indicators, calculating the final risk index as the arithmetic mean of all the indicators without considering the categories and dimensions, referred to as proportional weights (as in Chapter 2). As an alternative aggregation method, we used arithmetic mean for all the aggregation steps. Moreover, we considered coping capacity simulations instead of the best-performing adaptive capacity simulation. Finally, we excluded each crop, GCM and indicator to evaluate their effects on the final risk and the intermediate dimensions. The 21 alternatives considered for the robustness evaluation, in addition to the main option, are reported in Table 5.5.

Table 5.5: The main and 21 alternative options that we considered to evaluate the robustness of the assessment.

N	Alternative	Abbreviation	Description
0	Main option	MAIN	/
1	Arithmetic mean	AM	Aggregating the GCM outputs, crops and categories with arithmetic mean
2	Proportional weights	PW	Not considering the categories and aggregating the whole set of indicators with geometric mean, and not with Equation 1
3	Coping capacity	CC	Using the crop yield outputs of the simulation without adaptation strategies
4-5	One GCM	IPSL, MRI	Considering only the outputs of one GCM
6-7	One crop	MAIZE, SORG	Considering only the outputs of one crop
8-21	Excluding individual indicators	NOx (NO1, NO2, …, NO14)	Excluding one indicator at a time. The *x* in NO*x* refers to the indicators in Table 5.3.

At the end of the process, it is important to reflect on the different steps applied in the risk assessment, to focus on relevant inputs and outputs (OECD, 2008) and to understand the implications of the assessment and discuss possible adaptation strategies (Hagenlocher et al., 2019). In this study, we mainly focused on the relative changes compared to the historical simulations to investigate which aspects should be prioritized in the planning of adaptation/development policies. Nevertheless, we did not conduct any additional analysis or propose any specific adaptation strategy, as we focused on one single country and we based the assessment on SSP narratives, interested in future climate risk trends. Finally, we discussed the limitations of the approach.

5.4 Results

5.4.1 SWAT+ calibration

Despite the poor input data used to set up and calibrate the model, SWAT+ was able to represent satisfactorily the monthly discharge at the Luuq gauging station and irrigated maize and rainfed sorghum crop yields in Lower Shabelle and Bakool regions, respectively (Fig. 5.3). Streamflow was underestimated by the model, but all the performance indicators were more than satisfactory according to the criteria of Moriasi et al. (2007). Moreover, SWAT+ simulated satisfactorily the crop yield and during calibration the yield variability. We considered the model validated for the exploratory analysis performed in this study, keeping in mind that most applications of the SWAT model for crop yield validate it considering the long-term annual average.

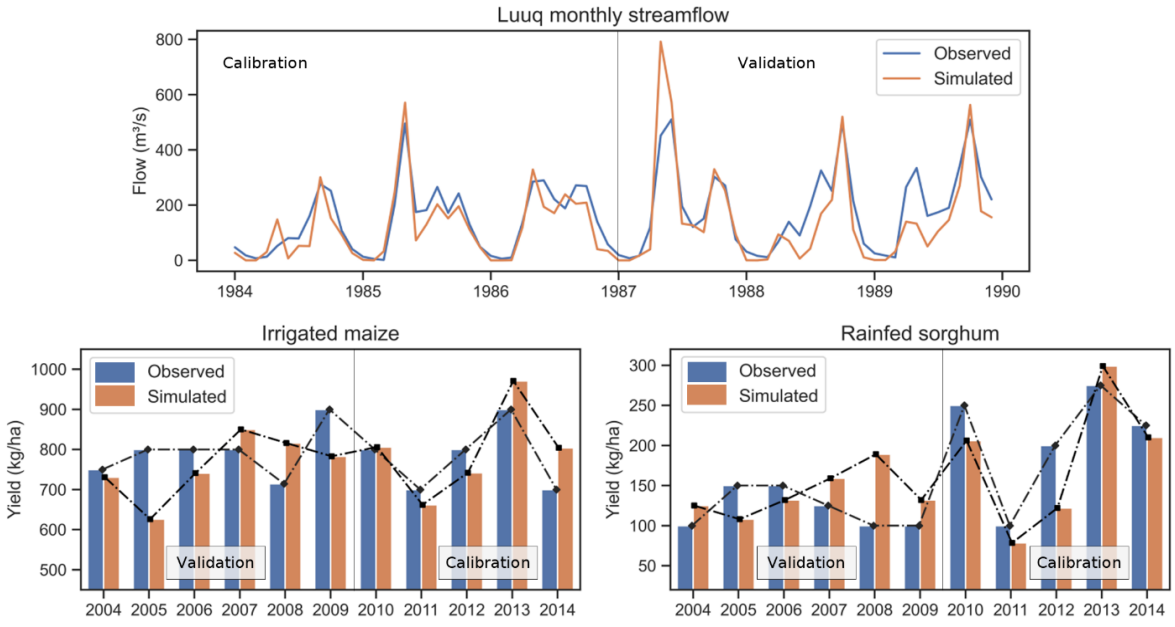

Streamflow	Calibration	Validation
NSE	0.79	0.65
Pbias	15.4%	18.1%
RSR	0.46	0.62
R^2	0.84	0.79

Maize	Calibration	Validation
Pbias	-2.2%	4.6%
RMSE	64.3 kg/ha	100.5 kg/ha
R^2	0.63	0.00

Sorghum	Calibration	Validation
Pbias	12.8%	-16.6%
RMSE	43.1 kg/ha	46.2 kg/ha
R^2	0.82	0.21

Figure 5.3: Calibration and validation plots and tables with performance indicators. The hydrograph with monthly streamflow refers to the Luuq gauging stations on the Juba River. The bar plots represent respectively irrigated maize and rainfed sorghum crop yields. For crop yield, the performance indicators are the per cent bias (Pbias), the root mean square error (RMSE) and the coefficient of determination (R^2), while for streamflow, they are the Nash-Sutcliffe Efficiency (NSE), the RMSE-observations standard deviation ratio (RSR), Pbias and R^2.

5.4.2 Future climate and crop yield

The two climate models showed increasing temperatures and precipitation under all SSP scenarios. Temperature increases were predicted to be similar considering annual or seasonal (Gu and Deyr) averages, with the magnitude being higher for SSPs with higher radiative forcings. For precipitation, both climate models projected increases in annual precipitation, but with different magnitudes and different seasonal patterns. For ipsl-cm6a-lr the increases reached 73.5% for annual average precipitation, while for mri-esm2-0 they were always around 10%. In the Gu season, mri-esm2-0 projected slightly decreasing precipitation, compensated by the increase during the Deyr season. More detailed information about future temperature and precipitation can be found in the supplementary materials, part 3.

The crop yields estimated after the coping and adaptive capacities simulations are summarized in Figure 5.4. Since maize was simulated as an irrigated crop, the increases in precipitation were not beneficial for crop yield (Fig. 5.4a,c). Instead, we observed declining crop yields mainly due to the decrease in crop cycle length as a result of increased temperatures. The reduction was higher for SSPs with the strongest temperature increases, while they were reduced, especially in the Deyr season, for SSPs 126 and 245. Sorghum crop yield reductions were also found for SSPs 460 and 585 in the Gu season, while for the other SSPs, slight increases were predicted (Fig. 5.4b). Instead, for the Deyr season, the increased precipitation will be highly beneficial for sorghum yield, with increases for all SSPs (Fig. 5.4d). Considering the adaptive capacity, which is the best adaptation strategy combining longer crop cycles and/or shifted sowing dates and modified fertilization, we obtained increases in crop yield compared to the coping capacity simulations for all SSPs, crops and climate

models. The only exception was rainfed sorghum in the Deyr season for SSPs 126 and 245, for which adaptation strategies were not effective (Fig. 5.4d). Often, the increase was sufficient to achieve yield increases compared to the historical simulations.

The best-performing adaptation strategy was longer crop cycles with delayed sowing dates for irrigated maize under all SSPs and climate models, except for ipsl-cm6a-lr under SSPs 126 and 585 where earlier sowing was more beneficial. Maintaining the same sowing date but adopting longer crop cycle varieties was the best adaptation strategy for rainfed sorghum, except for mri-esm2-0 under SSP585 in the Deyr season and under SSPs 460 and 585 in the Gu season, where simulations with delayed sowing showed the highest crop yield. Finally, interesting indications were obtained by analysing the 1st quartile yield values (Fig. 5.4). While for irrigated maize the behaviour was similar to the average yield, for rainfed sorghum it was much more variable. Very importantly, the 1st quartile yield was simulated to be much higher in the Deyr season under all SSPs and climate models considered in this study (Fig. 5.4d). Finally, as a general comment, it is important to remember that the values of maize and sorghum yields were very low, around 800 kg ha^{-1} for irrigated maize and 160 kg ha^{-1} for rainfed sorghum. Even if the climate change hazard will be mitigated by adaptive changes, the simulated future yields will remain very low and the yield gap will remain unfilled.

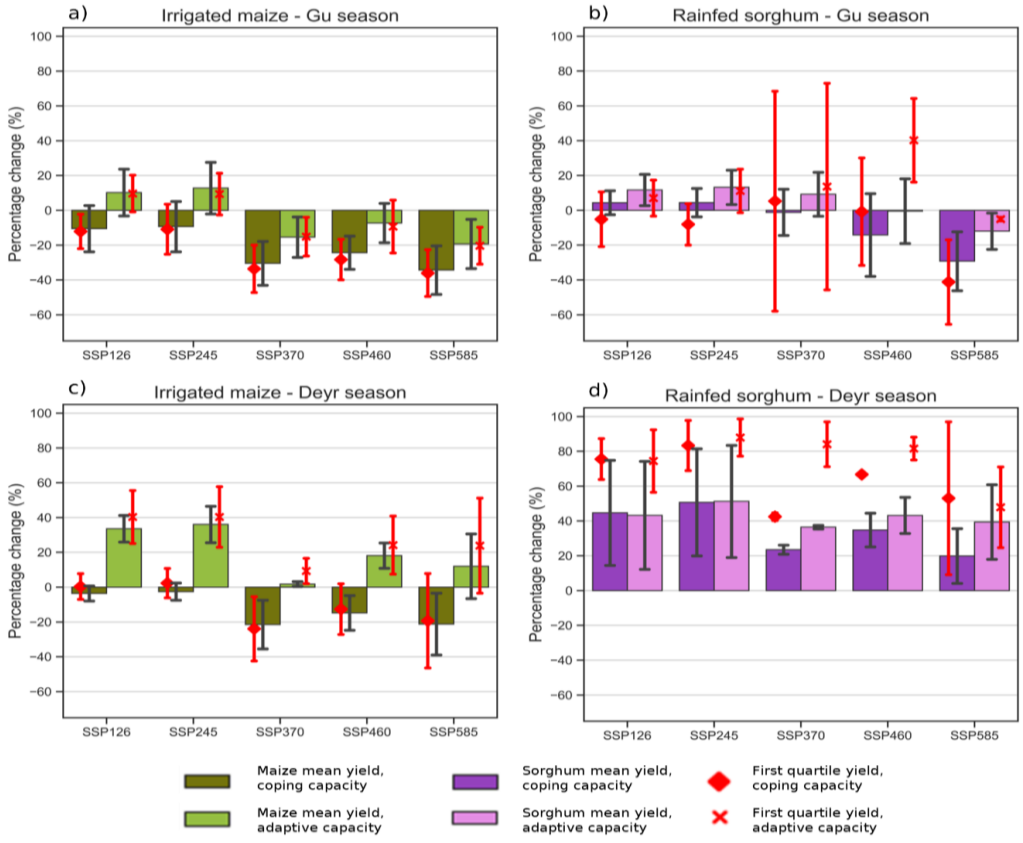

Figure 5.4: Irrigated maize and rainfed sorghum crop yields considering the coping and adaptive capacity simulations. In the coping capacity, the management is maintained equal for all scenarios. For the adaptive capacity, changes in sowing date, different fertilization amounts and increased longer crop cycles are also simulated. In the figure, the best adaptation strategy is reported. The bar plots show the average crop yields, while the red point plots the 1st quartile yields. The uncertainty is drawn considering the maximum and minimum crop yields simulated with climate inputs of the two models used. In a) and b), results are referred to the Gu season, while in c) and d) to the Deyr season.

5.4.3 Indicators' analysis

The analysis of the relative percentage changes compared to the historical period for the individual indicators is useful to understand the main drivers that will affect how risk and its dimensions will evolve (Figure 5.5).

Regarding the extreme events indicators, extreme precipitation will mostly increase, especially for the ipsl-cm6a-lr model that predicted higher precipitation. For mri-esm2-0, the increases in R20 were found to be generally lower, and under SSP370 a decrease was predicted. Extreme temperatures (SU40) will increase according to both climate models. The indicators related to dry conditions showed beneficial changes, with a lower number of longest dry spells and low flows predicted. Considering average and 1st quartile yields, the percentage change of the averaged values for the seasons, the crops and the climate models showed yield increases. Beneficial changes were always found for SSPs 126 and 245, while there was more uncertainty for the other scenarios, with some decreasing yield values. For the water availability indicator, future conditions will improve under all scenarios according to the ipsl-cm6a-lr climate model, while for mri-esm2-0 only under SSP585. Water consumption will increase compared to the historical period under all scenarios considered. For the indicators belonging to the socioeconomic susceptibility category, significant beneficial effects were predicted according to the datasets used in our study, mainly due to the very low performances of the indicators for the historical period and the so-called "Scenario optimism" of the SSP narratives. The population will increase for all scenarios except for SSP585, while cropland will have beneficial changes under SSPs 126 and 370.

5.4.4 Future climate risk, hazard, vulnerability and exposure

In line with the mostly negative percentage changes of Figure 5.5, indicating a decreasing risk, results showed that climate risk will decrease in the future under all scenarios considered (Fig. 5.6, Table 5.6). The lowest risk was found for SSPs 126 – Sustainability – and 585 – Conventional development (the green and purple bars in Figure 5.5). This is consistent with the narratives on which the SSPs themselves are based (Table 5.1), as scenarios with low adaptation challenges had the lowest climate risk. The categorization of the climate risk ranged from "intermediate" to "low", with low differences in magnitudes due to the compensating effect of the various indicators. However, as shown in Figure 5.5 and Table 5.6, the individual drivers or indicators, as well as the dimensions, were highly different.

Hazard was found to be the highest in the historical period and SSP585 – Conventional development - while low for the other SSPs (Fig. 5.7, Table 5.6). In the historical period, the "high" hazard was driven by the FLO20 and CDD indicators, the ones reflecting dry conditions, and by low crop yields, especially for rainfed sorghum in the Deyr season (Fig. 5.4). High values of SU40 and R20, the indicators related to extreme wet and hot events, and low performance for maize yield were the main cause for the "high" hazard for SSP585 (Fig. 5.4, Table 5.6). For the other SSPs, the increase in temperature and precipitation was not as detrimental as for SSP585 in the calculation of the hazard index. Vulnerability was shown to be highest in the historical period, mainly driven by low water availability and low values for the indicators calculated with the outputs of the SSP narratives. Intermediate vulnerability scores were found for SSPs 245, 370 and 460. "Low" and "very low" vulnerability scores were instead retrieved for SSPs 585 and 126 respectively (Fig. 5.7, Table 5.6). Finally, exposure was found to be the highest in SSP245, followed by SSPs 460 and 370, while SSPs 126 and 585 showed the lowest values (Fig. 5.7, Table 5.6).

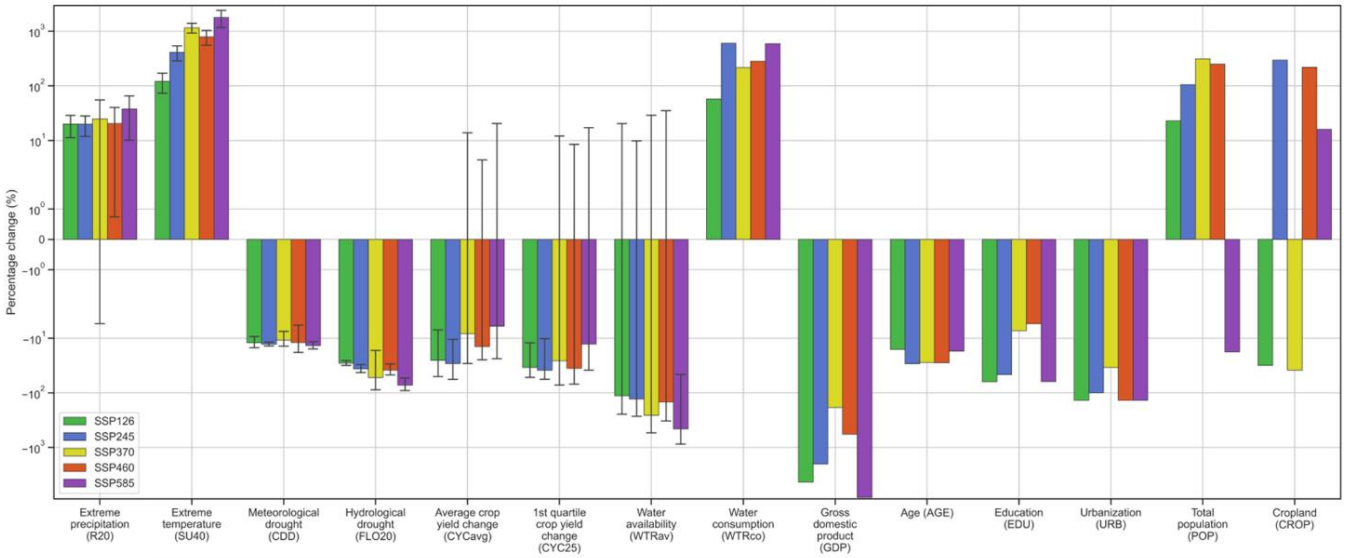

Dimension	hazard															
Category	extreme events								climate change							
Number	1		2		3		4		5				6			
Indicator	*R20*		*SU40*		*CDD*		*FLO20*		*CYCavg*		*CYCavg*		*CYC25*		*CYC25*	
Crop									*maize*		*sorghum*		*maize*		*sorghum*	
Climate model	*ipsl*	*mri*	*ipsl*	*mri*	*ipsl*	*mri*	*ipsl*	*mri*	*ipsl*	*mri*	*ipsl*	*mri*	*ipsl*	*mri*	*ipsl*	*mri*
Historical	108	148	68	132	151	187	6.0	6.0	780	784	143	129	694	687	65	52
SSP126	139	165	184	229	137	159	4.5	4.1	865	1042	153	195	778	947	88	79
SSP245	138	166	436	510	133	161	4.2	3.4	868	1078	158	203	764	958	96	81
SSP370	168	140	1019	1357	130	173	0.7	5.0	672	783	184	153	610	730	112	71
SSP460	151	149	772	865	142	153	3.2	4.2	746	904	178	157	635	847	110	82
SSP585	179	163	1714	1684	127	165	0.5	2.8	620	890	153	160	575	829	71	72

Dimension	vulnerability						Exposure	
Category	environmental susceptibility			socio-economic susceptibility				
Number	7		8	9	10	11	12	13	14
Indicator	*WTRav*		*WTRco*	*GDP*	*AGE*	*EDU*	*URB*	*POP*	*CROP*
Climate model	*ipsl*	*mri*	*ipsl*						
Historical	10.6	26.8	0.013	0.5	47.6	8.6	37.4	9.3	6543
SSP126	36.7	21.3	0.021	20.9	40.0	3.2	88.6	11.5	4482
SSP245	39.1	24.1	0.092	9.9	33.7	4.6	74.8	19.2	25973
SSP370	68.1	19.0	0.041	1.3	34.4	8.0	50.2	38.6	4040
SSP460	45.5	17.3	0.050	3.2	34.2	8.1	88.6	32.7	20949
SSP585	102.7	39.1	0.091	39.2	39.4	3.3	88.6	7.7	7599

Figure 5.5: The relative percentage changes compared to the historical situation of individual indicators. The changes are expressed considering their functional relationship with the risk. Hence, negative changes indicate a decreasing risk and vice versa. The y-axis has a "symlog" scale. Where more values were used for each indicator (i.e. climate models, seasons and crops), the error bar consists of the full range of the simulated outputs. The tables report the full set of indicators and their values.

Table 5.6: Hazard, vulnerability, exposure and risk of the scenarios considered in this study. The relative rank is reported as well as a categorization (>8 very high, 6-8 high, 4-6 intermediate, 2-4 low, <2 very low). For each dimension, the beneficial (↓, decreasing risk) and detrimental (↑, increasing risk) drivers (indicators) are also reported. Beneficial (detrimental) drivers are individuated as those >8 (<3) after the normalization step 2 in paragraph 2.4.

	Historical	SSP126 – Sustainability	SSP245 – Middle of the road	SSP370 – Regional rivalry	SSP460 – Inequality	SSP585 – Conventional development
Hazard (rank)	**High (1)**	**Low (4)**	**Very low (6)**	**Low (3)**	**Low (5)**	**High (2)**
↑ Drivers	*Dry events, crop yields*			*Maize yield*		*Wet and hot events, maize yield*
↓ Drivers	*Wet and hot events*	*Hot and dry events, crop yields*	*Dry events, crop yields*	*Sorghum 1st quartile yields*	*Dry events, sorghum 1st quartile yields*	*Dry events*
Vulnerability (rank)	**High (1)**	**Very low (6)**	**Intermediate (2)**	**Intermediate (4)**	**Intermediate (3)**	**Low (5)**
↑ Drivers	*Water availability, GDP, age, education, urbanization*	*Water availability*	*Water consumption*	*GDP, education*	*GDP, education*	*Water consumption*
↓ Drivers	*Water consumption*	*Water consumption, education, urbanization*	*Age*	*Age*	*Age, urbanization*	*Water availability, GDP, education, urbanization*
Exposure (rank)	**Low (4)**	**Low (6)**	**Very high (1)**	**Very high (3)**	**Very high (2)**	**Low (5)**
↑ Drivers			*Cropland*	*Population*	*Population, cropland*	
↓ Drivers	*Population, cropland*	*Population, cropland*		*Cropland*		*Population, cropland*
Risk (rank)	**Intermediate (1)**	**Low (6)**	**Intermediate (4)**	**Intermediate (2)**	**Intermediate (3)**	**Low (5)**

5.4.5 Robustness evaluation

The uncertainty, expressed by plotting the distributions of the climate risk index (Fig. 5.6) calculated with the 21 alternatives of Table 5.4 (22 with the main option), was quite low only for SSP126 – Sustainability – that remained in the "low" risk category with all the alternative options considered. The other scenarios showed much more variability, with SSP370 – Regional rivalry - the most uncertain scenario. Using proportional weights, considering only the outputs of mri-esm2-0 climate model or the maize crop, and excluding individual indicators, mainly belonging to exposure and vulnerability dimensions, highly influenced the final climate risk score of the different scenarios. Nevertheless, with some exceptions, the scenario rankings for climate risk rarely varied.

As shown in Table 5.6, the individual dimensions showed scores with wider ranges as compared to climate risk, mainly because of the lower number of indicators that reduced the compensative effects. The high range of values with few indicators is particularly evident for exposure that had only "low" or "very high" scores (Fig. 5.7). Being the exposure often represented by few indicators, their choice is a fundamental step as they highly influence the exposure index and therefore the final climate risk index. Excluding either cropland (NO14) or total population (NO13) had a huge effect on the final exposure score. This was particularly evident in SSPs 245 and 370, while the historical period, SSPs 126 and 585 had "low" scores with little uncertainty. Furthermore, allowing more compensation by applying arithmetic mean (AM) resulted in a lower exposure score, especially for the scenarios with "very high" exposure.

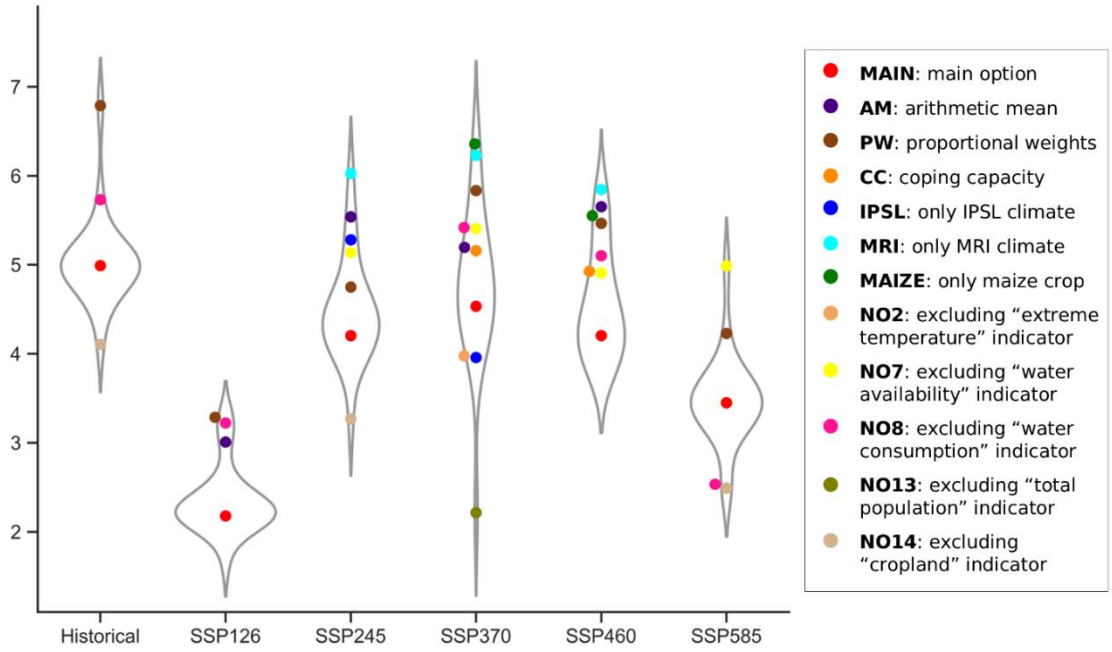

Figure 5.6: Violin plot of risk scores considering the whole set of alternatives used in the uncertainty/sensitivity analysis and the main option. The swarm plot represents the risk scores of the alternative options, with the main option point coloured in red. To ease the visualization and interpretation of the plot, we included only the alternatives that differed > |0.5| as compared to the main option.

For climate hazard, the uncertainty related to climate models was quite high (Fig. 5.7). When considering only mri-esm2-0 (MRI), hazard highly increased for SSPs 245, 370 and 460, while it decreased for the historical period and especially for SSP585. With mri-esm2-0 under SSP585, crop yield changes were mostly beneficial, as well as extreme precipitation increases that were much reduced as compared to ipsl-cm6a-lr. Furthermore, using only the outputs of ipsl-cm6a-lr (IPSL) influenced significantly climate hazard, with for example SSP126 which was ranked as third in climate hazard. Considering the coping capacity simulations (CC) instead of the adaptive capacity affected the magnitude of the scores, even if not that significantly since the two crops showed different responses to adaptation strategies (Fig. 5.4). Finally, considering only the maize crop (MAIZE), the climate hazard highly increased and reached up to "very high" scores for the scenarios in which maize yield mostly decreased, namely SSPs 370, 460 and 585. Here, it is important to consider that, in the construction of the composite indicator, maize yield was weighted with the percentage of the area under irrigation, and therefore it had little impact under most scenarios. When applying arithmetic mean (AM), the scores increased towards "intermediate" values for the SSPs that in the main alternative showed "low" hazard.

Excluding indicators belonging to the environmental susceptibility category, namely water availability and water consumption, strongly influenced both the vulnerability scores and the scenario rankings. Without the water availability indicator (NO7), vulnerability increased for all the scenarios, more for SSPs 245 and 585 which were ranked as more vulnerable compared to the historical period. On the other hand, excluding the water consumption indicator (NO8) worsened the conditions of the historical period and SSP126, while vulnerability for SSP585 was the lowest with a "very low" score. The situation was much less uncertain for the other category of vulnerability, namely socioeconomic susceptibility, where the values for the historical period were found to be the highest for all the indicators considered, followed by SSPs 370 and 460, and excluding individual indicators did not result in significant changes. Allowing compensation by aggregating indicators with the arithmetic mean (AM) had a strong impact on the absolute values of vulnerability, especially on SSP126 which resulted in being slightly more vulnerable as compared to SSP585.

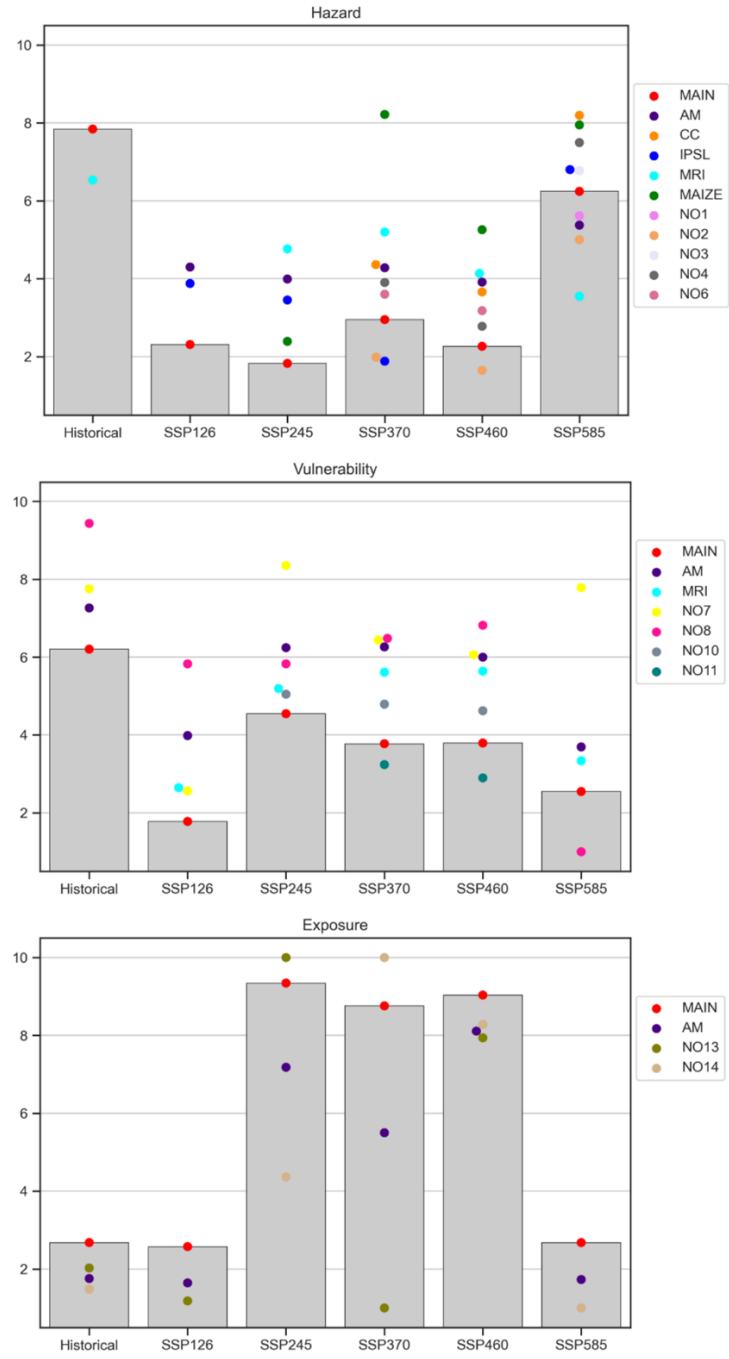

Figure 5.7: The climate risk dimensions (hazard, vulnerability and exposure) for the six scenarios considered in this study. The bar plots and the red points correspond to the scores obtained for the main option, while the points represent the scores of the alternative options used in the uncertainty/sensitivity analysis, considering only the alternatives that differed > |0.5| as compared to the main option.

5.5 Discussion

5.5.1 Climate change impact assessment

The outputs of the two climate models used in this study are comparable to previous climate change analyses, which projected increased temperatures and precipitation by the end of the century specifically for Somalia (FAO et al., 2017; Ogallo et al., 2018). In our analysis, a maximum relative percentage increase for precipitation of more than 90% was found for ipsl-cm6a-lr under SSP585, but it is important to keep in mind that absolute precipitation values are low in Somalia and high percentage increases are common (SMHI, 2017). Consistent results are also reported for Southern Ethiopia by Gebrechorkos et al. (2023), with increased precipitation and streamflow predicted for the upper Juba and Shabelle rivers, and by Murken et al. (2020), who highlighted the projected increased hot days, tropical nights and extreme precipitation events.

Future crop yield predictions are scarce in the area. Zooming in the maps of Jägermeyr et al. (2021), maize yields are predicted to decrease under SSP585. In neighbouring Ethiopia, the impacts of climate change on maize yields are uncertain, with some areas that will have negative effects (Murken et al., 2020). Our study confirms the negative impacts on maize yield, while increased rainfall benefits sorghum yield especially during the Deyr season. Adapting varieties is fundamental to cope with increased temperatures and avoid reductions in the crop cycle length (Zabel et al., 2021), as already discussed in other studies (FAO et al., 2017; Nkwasa et al., 2023). Consistently, our results showed that adopting longer crop cycle varieties and modifying the sowing date is beneficial to cope with climate change, reducing losses or even increasing crop yields. Nevertheless, even under the most optimistic scenarios crop yields remain at very low absolute values, which is worrying as the population is expected to increase in the short term and most scenarios also by the end of the century. Our yield projections corroborate the concerns that emerged from Ray et al. (2013), who demonstrated that current global yield trends are insufficient to cope with future population increases, especially in countries such as Somalia.

Since our analysis is based on similar data (i.e. climate models and SSP-related variables), our results are highly consistent with past research. As we considered mostly dry events as hazard indicators and precipitation was projected to increase, the historical period had high hazard. Past literature which slightly differs from our results considered the SPEI as a drought indicator (Ahmadalipour et al., 2019; Tabari et al., 2021), while climate trends and analyses with indexes considering only precipitation are consistent with our outcomes (Ogallo et al., 2018; Tabari et al., 2023b). High temperatures were directly detrimental to the SU40 indicator, but also indirectly due to the reduced crop cycle length and therefore crop yield. Vulnerability was also the highest in the historical period, mainly due to indicators of socio-economic susceptibility, partially mitigated by the low water consumption. Although at a variable pace, conditions were predicted to improve and vulnerability to decrease, consistent with most of the other assessments and SSP narratives (Ahmadalipour and Moradkhani, 2018; Andrijevic et al., 2020). Finally, exposure was found to highly increase in the future for the scenarios with significant population increase, which correspond to the ones with lower education, while remaining similar for the high-development scenarios. As a result of these dimensions, the climate risk was projected to be higher under “Regional rivalry” and “Inequality” SSP scenarios, consistent with other assessments and with the SSP narratives themselves, as these are the scenarios with high adaptation challenges (Table 5.1).

5.5.2 Study limitations and further research

In this assessment, we used the variables produced within the SSP narratives which are known to have some practical limitations (O'Neill et al., 2020; Marzi et al., 2021). They should be intended as a description of plausible future conditions to enable the research community to develop sensible assessments and not for direct climate policy advice (O'Neill et al., 2017). As these narratives were created focusing on the final outcomes, they do not include by design the feedback of climate change impact, resulting in a "Scenario optimism" in which no country will experience a decline in socio-economic development (Andrijevic et al., 2020). Even if local challenges are strictly related and relevant to global dynamics, SSP narratives ignore local conditions (Birkmann et al., 2020; O'Neill et al., 2017). Furthermore, shocks and disruptions that might significantly alter future development are only implicitly considered within the SSP scenarios without information on causal events (O'Neill et al., 2020). These and other limitations limit the potential of the adoption of SSP narratives in domains beyond climate change, such as sustainable development (Marzi et al., 2021). Despite these issues which will need to be tackled in the future, our study sums to a significant amount of literature that applied SSP narratives to project vulnerability and coping capacity drivers (Andrijevic et al., 2020; Rohat et al., 2018; Yang and Cui, 2019; Tabari and Willems, 2023a, b).

This kind of risk assessment should not be intended as a direct measure to estimate risk but interpreted in relative terms (OECD, 2008). Hence, the final "low" risk found here for SSPs 126 and 585 might be much higher if global or continental scale assessments are performed. Even if country-specific climate risk assessments already exist (Cochrane and Al-Hababi, 2023; Song and Lee, 2021), the risk assessment framework is usually applied to compare multiple spatial units, such as countries, regions or municipalities. In our assessment, we adopted the same methodology to compare future scenarios in a single country. Moreover, we also used a process-based crop model to include yield projections and to partially represent resilience with specific agronomic adaptation strategies. We argue that this provides very valuable insights and that the coupling of risk-related methodologies enhances and multiplies the effectiveness of this kind of assessment. Furthermore, we underline the importance of considering, at least, simple adaptation strategies and avoiding the "dumb" farmer scenario. Despite the adaptive capacity, the crop yield indicator is probably the most worrying for the future, as we noticed that even under the best-performing scenarios where crop yields are predicted to increase, they will remain very low, threatening food security. If we were to exclude this concern about future crop yields, the interpretation of the results of this assessment would be encouraging at least for SSPs 126 and 585. It is also important to keep in mind that agro-hydrological modelling is based on simplified processes. Further improvements would be to consider additional inputs, crops and climate models to optimize the model and the robustness of the assessment methodology. Also, the land use map used in this study showed some inconsistencies compared to the land use produced within the FAO SWALIM project. Moreover, we focused only on agriculture and cereal crops, but in Somalia, a large part of the income and diet depends on livestock. In addition, in our study, we did not simulate any agricultural transformative change such as agroforestry, optimized crop distribution or other practices (Davis et al., 2017; Fedele et al., 2019; Vermeulen et al., 2018) but we argue that process-based crop models should be applied for this scope within the framework of risk assessment. Finally, critical social science that engages with politics and inequalities should start to be included in this kind of climate risk assessment (Savelli et al., 2022).

5.6 Conclusions

Integrating approaches, methodologies and definitions of different research communities, we estimated the current and future climate risk for Somalia. According to our results, future hazard in Somalia will decrease

for all the scenarios considered. Future extreme events will be more related to heavy precipitation and heat waves since a hotter and wetter climate is projected under all scenarios. Without considering adaptation strategies, irrigated crop yields will mostly decrease. Rainfed crop yields might benefit from increased precipitation. Despite improvements after adopting longer crop cycle varieties and shifting the sowing dates, yields will remain very low. Vulnerability will decrease compared to the present even if with different magnitudes, while exposure will highly increase in SSPs 245, 370 and 460 mainly due to the demographic increase.

This paper is, to our knowledge, the first attempt to explicitly include indicators produced with a process-based crop-growth model in the risk assessment framework where risk is defined as the interaction between hazard, exposure and vulnerability. Using the SWAT+ agro-hydrological model, we estimated indicators based on physical processes instead of relying on proxy indicators. We argue that this is a step forward towards a better representation not only of future hazard, but also of future coping and adaptive capacities. Potentially, process-based models can be used to simulate even more complex adaptation strategies and transformative changes, hence providing an interesting methodology to operationalize the resilience concept.

To conclude, we will need all the skills and methodologies developed within the disaster, climate change and development research communities to cope and adapt to future climate change challenges. Avoiding further integration between different approaches would be a missing opportunity to achieve greater policy impact.

Chapter 6 Conclusions

6.1 Discussion

O1. To evaluate the future climate impacts, risk and its components and to quantify the adaptive capacity of agricultural systems in the selected study areas, highlighting uncertainties and neglected issues.

6.1.1 Future climate and risk in the study areas

For the study areas considered, Southern and Central Tuscany in Italy and the Juba and Shabelle catchment in Somalia, future temperatures will increase. The increase is proportional to the radiative forcing, being higher in RCP 8.5 or SSP585. This will have negative implications due to heat waves, contributing to higher evapotranspiration and shortening the crop cycles. However, increased average temperatures below heat stress thresholds might also be beneficial for some crops.

A much higher uncertainty is related instead to future precipitation. This is surprising for the Italian case study since the Mediterranean basin is a hotspot for climate change due to projected decreased precipitation (Lionello and Scarascia, 2018). Nevertheless, this assertion is made considering the whole Mediterranean region. In many climate change studies, Central and Northern Italy are crossed by the zero-change precipitation line (Evin et al., 2021; Mariotti et al., 2015; Spano et al., 2020). This is also confirmed by analysing the RCMs considered in this thesis, which project a minor annual average increase in precipitation. The increase is mainly driven by winter precipitation and this is, interestingly, the opposite of the outcomes of the review of Caporali et al. (2021) for past precipitation trends over Italy. The plausible decrease in summer precipitation is concerning for Southern and Central Tuscany, and even more for the coastal areas. Summer is the season with the highest evapotranspiration and irrigation, which sums up an already critical situation of high water demand for domestic use and groundwater over-abstraction. The climate models used in this thesis and other studies for Somalia indicate a likely increase in annual average precipitation, even if with uncertain magnitudes. This would be an opportunity to enhance food security if the water is used productively both as green and blue water. On the other hand, the increased hazard due to heavy precipitation and hence floods is a concern. Furthermore, for both Italy and Somalia, I analyzed annual and seasonal average trends, but the interannual variability which might increase will also possibly have negative consequences.

Drought and other climate hazards are fundamental drivers of risk, necessary to evaluate future water shortage. The other components of risk, namely exposure and vulnerability, are equally important to understanding the future dynamics of water demand and, hence, scarcity. The population is usually considered the main indicator of exposure and socioeconomic characteristics of vulnerability. Demographic issues are particularly concerning for Somalia and Sub-Saharan Africa in general. The findings of Chapter 5 confirm that increased population is one of the main drivers for future risk. In Italy, I analysed spatial patterns of exposure and vulnerability only for the present due to data unavailability at the required spatial scale. However, it is possible to affirm that agriculture in the Northern Mediterranean will face different, reduced – yet not small – challenges on the water demand side.

6.1.2 The uncertainty in estimating future drought and aridity

In drought analysis, the role of temperature and evapotranspiration is considered always more important. This is the reason why some authors consider the Standardized Precipitation Evapotranspiration Index (SPEI, Vicente-Serrano et al., 2010) more accurate and complete as compared to the simpler Standardized Precipitation Index (McKee et al., 1993). In this thesis, I considered both indicators based solely on precipitation in the drought and climate risk assessments (Chapters 2 and 5) and temperature-related ones (Chapters 2, 3 and 5). How drought is defined influences the selection of the indicators, that for drought are numerous (Kchouk et al., 2022). Indeed, the drought definition is extremely subtle and its choice has tremendous consequences on the outcomes of the studies (Hall and Leng, 2019; Satoh et al., 2021). For example, studies that include the SPEI have much worse predictions compared to those that rely on SPI. In Somalia, the analyses that use SPEI report increasing drought hazard (Ahmadalipour et al., 2019; Tabari et al., 2023b), while those that consider only precipitation show the opposite trend (Ogallo et al., 2018; Tabari et al., 2023a). Results of Spinoni et al. (2021) highlight that, in the worst-case scenario, the global population exposed to drought will increase by 14% and 60% if considering SPI or SPEI respectively.

Including evapotranspiration in the indexes to estimate drought hazard has a remarkable influence. At the same time, the estimation of future evapotranspiration is highly uncertain. As discussed in Chapter 3, there is a discrepancy between the future drought calculated with the outputs of the climate models and simple metrics of water scarcity, such as the aridity index and the SPEI, with the former showing heterogeneous patterns of change while the latter depicting much drier conditions (Berg, 2022). A crucial difference is that the vegetation responses to increased CO_2 concentration are typically not represented when using simple indicators (Greve et al., 2019; Scheff et al., 2022; Yang et al., 2019).

Even if often neglected, there are many approaches to include vegetation responses to CO_2 in the calculation of future evapotranspiration when considering simple metrics. However, as shown in Chapter 3, this entails high uncertainties, especially for very high CO_2 concentrations. The SWAT+ model includes a modification of the Penman-Monteith approach to account for the suppression effect on stomatal conductance, but simulation outcomes beyond 660 ppm are doubtful. The equations included in the SWAT+ model were developed in the nineties (Easterling et al., 1992) based on experiments performed in the eighties (Morison, 1987). Below the 660 ppm threshold, the SWAT+ model simulates hydrological fluxes coherently with the theory and with similar magnitudes of changes compared to other studies. The effects are not too high, as the decrease in evapotranspiration caused by the reduced stomatal conductance is counterbalanced by the CO_2 fertilization effect that increases biomass production and leaf area (Manzoni et al., 2022). Fatichi et al. (2016) quantified the changes in actual evapotranspiration to be lower than 8%, which is consistent with the outputs of the SWAT+ model under RCP 4.5. On the other hand, when considering values much higher than this threshold, the potential evapotranspiration drastically decreases, as well as related variables, highly influencing hydrological fluxes such as water yield that significantly rise. A similar behaviour in future potential evapotranspiration was also reported by Lemaitre-Basset et al. (2022), who applied the equations used by SWAT+ to calculate potential evapotranspiration including vegetation responses to CO_2. It is difficult to evaluate how models simulate future evapotranspiration as there is much uncertainty in the theory, especially for elevated concentrations (Toreti et al., 2020). Other research communities, such as the Agricultural Model Intercomparison Project (AGMIP), are active in finding alternative improved equations. The problem is therefore not strictly related to the SWAT+ model but to the larger research community. It is possible to conclude that vegetation responses are sufficiently known and represented in models, and there is no need anymore to perform simulations without CO_2 increase (Toreti et al., 2020), and the SWAT+ model is no

exception in this. Nevertheless, the model outputs with CO_2 concentration beyond the 660 ppm threshold have to be analysed cautiously.

6.1.3 The adaptive capacity of agricultural systems

Regardless of the climate change impacts on future crop yield and water availability and the dynamics of exposure that influence water demand, adaptation strategies will be fundamental to contain losses by reducing vulnerability. Within sustainable development, the adaptation strategies are framed and promoted as best practices to make better use of resources, increase crop yields and reduce the yield gap. In the study areas considered in this thesis, crop yield decreases are simulated under specific scenarios and for some crops. As precipitation is not projected to reduce, the main reason for the crop yield loss is the shrinking in crop cycle duration caused by increased temperatures. Nevertheless, the adaptive capacity of the agricultural systems analysed in Chapters 4 and 5 is high. Crop yield losses are strongly reduced with simple agronomic, autonomous adaptation strategies. The most effective strategy is the adoption of varieties with longer crop cycles, to balance the reduction induced by increased temperatures. For specific crops, contexts and scenarios, benefits are produced also by other management changes, such as earlier sowing, supplemental irrigation and cover crops. Interestingly, the combination of adaptation strategies shows more beneficial synergies than detrimental trade-offs for crop yields, water footprints and hydrological fluxes. Considering only the ensembles, twelve synergies and only two trade-offs are detected.

Water should be managed at the catchment scale and the field-scale agricultural practices should be evaluated at larger scales (Giordano et al., 2017; Ruane, 2012). Furthermore, agronomic practices should produce real water savings, meaning that water consumed should be reduced and not the water withdrawn as occurs in the apparent water savings (van Opstal et al., 2021; Whiting et al., 2023). In Chapter 4, an integrated, multi-scale climate change impact assessment is performed in which the effects of the management changes are evaluated considering not only crop yields but also the water footprints and hydrological fluxes at the catchment scale. Results show that for some variables, the impacts of the management changes are comparable to those of climate change. This is further evidence proving that the promotion of alternative agronomic strategies should be evaluated not only at the field scale but also at the catchment scale. As also discussed in Villani et al. (2021), more attention should be paid to the management and land cover changes, as they influence the microclimate and might represent a third way to cope with climate change (Ismangil et al., 2016; van Woesik et al., 2023).

Comparing climate and management change impacts, results show that adaptation strategies have a much higher impact on crop yields. The magnitude of changes is higher for rainfed crops, wheat and sunflower, and when combinations of adaptation strategies are considered. On the other hand, the impact of management changes on hydrological variables, when considering the catchment scale, is negligible. However, when evaluating the outputs for cropland, practices belonging to conservation agriculture show a significant impact, mainly in reducing water yield by almost 40% when considering the maximum absolute change. Still, the impacts of climate change are higher for water yield, percolation, streamflow and soil moisture. Also for water footprint the impact of climate change is higher, especially for the rainfed crops. The differences between the effects of management and climate changes are minimal for maize water footprint, drought and temperature stresses, evaporation and evapotranspiration. It is important to underline that, even if the magnitudes of change caused by adaptation strategies on hydrological fluxes are not high, the simulated management changes consist of minor modifications, such as the shift in sowing dates of only two weeks, and still they have some impacts. Concluding, the impacts of management changes on hydrological variables should not be neglected in intensively cultivated catchments.

In this thesis, I evaluated quantitatively the effects of a limited number of agronomic strategies. Of course, there are many other strategies, both autonomous and planned, contributing to the adaptive and transformative capacities which are not quantified in this thesis. During the PhD, I collaborated on projects and co-authored papers that focused on adaptation strategies to drought and climate change. In the AGRIWATER (Innovative and Sustainable Measures for Keeping Water in the Agricultural Landscape) Erasmus+ Project, we listed 40 best practices in six European countries to cope with drought and water scarcity, already implemented by European farmers. These were divided into technological, technical, agronomic and economic/institutional measures. Particularly important were the practices related to water harvesting and those that increased irrigation efficiency. Moreover, in the ongoing AG-WaMED (Advancing non-conventional water management for innovative climate-resilient water governance in the Mediterranean Area) PRIMA project, the Orcia catchment was selected as the Italian case study. After the first participatory phases of the project, farmers and water authorities suggested new reservoirs and farm ponds for supplemental irrigation as the main solutions to cope with water shortage, confirming the usefulness of some adaptations suggested in Chapter 2. These adaptation strategies will be simulated with the SWAT+ model in the remaining years of the project. In a Sub-Saharan context, the FAO's Aquacrop model was applied to quantify the effect of soil bunds to cope with increased temperatures and decreased precipitation (Setti et al., 2023). This autonomous adaptation measure showed to be useful if precipitation drastically decreases. Moreover, in Renzi et al. (2023) SWAT outputs were used to estimate irrigation amount to run Aquacrop simulations and evaluate the performance of a macro-catchment water harvesting technique, Marab farming, in Jordan. Finally, sand dams are extremely promising transformative solutions in drylands that, differently from other strategies, will need institutional support and coordination (Castelli et al., 2022; Villani et al., 2018).

O2. To improve the climate risk assessment methodology and integrate it with agro-hydrological modelling, to perform more relevant and comprehensive climate change risk/impact assessments.

6.1.4 Improving drought/climate risk assessments

Most of the drought risk assessments reviewed by Hagenlocher et al. (2019) did not perform any form of validation. The outcomes of risk assessments highly depend on the procedure applied to calculate the composite index and mainly, but not only, on the selection of indicators and weighting scheme. Validation with external data is useful but usually impossible or not accurate enough. The robustness evaluation introduced in Chapter 2 and improved in Chapter 5 adds valuable information to better interpret and understand the outcomes of the assessment, providing a range of values which represent the uncertainty or the sensitivity. This method also has advantages compared to similar methodologies applied considering distributions of weights and indicators (Marzi et al., 2019; Naumann et al., 2014), which might be more robust from a statistical point of view, but at the cost of less interpretability. The robustness evaluation performed for Chapter 5 was very helpful in understanding the effect of the choice to consider different crops and climate models. Of course, this kind of internal validation should always be coupled with external validation when possible, hence using external data or experts' opinions to validate the results. This could not be applied in Chapters 2 and 5 since for the former no data at the required spatial resolution was available and for the latter, I focused on future conditions. Additionally, robustness evaluation can be very useful and can potentially address most of the decisions that are made in the establishment of the methodology of the drought risk assessment. However, it is also difficult to evaluate which are the "uncertain" decisions and this depends a lot on the expertise and background of those who developed the methodology. A critical aspect consists of the assumptions that are made when selecting indicators and their relationship with risk and its

dimensions. For example, in Chapter 2 I assumed that youngest farmers and organic farms were less vulnerable to drought. This is justified considering the current characteristics of Southern and Central Tuscany, but it might be wrong somewhere else or in a different period. Instead, in Chapter 5 I considered more cropland as a factor that increased exposure, but this could be debated.

Another crucial problem is that most drought risk assessments do not report any hints or suggestions about possible adaptation strategies (Hagenlocher et al., 2019), even if they should be performed to start the discussion about how to shift towards proactive drought risk management. Their final outputs are generally maps or tables that rank the units considered in the assessment. These outputs are surely informative and useful, but at the same time, they can be very confusing and might lead to wrong conclusions and maladaptation. To explicitly link the outcomes of the assessment with actionable adaptation strategies, archetype analysis is proposed as an additional and final step in the drought risk assessment methodology.

Archetype analysis is an emerging methodology to find recurrent patterns within cases and provide a simplified, but contextual, interpretation of results, which is used in sustainability research to ease communication between the academy and decision-makers (Oberlack et al., 2019). For example, Paumgarten et al. (2020) applied archetype analysis to delineate climate risk profiles in South Africa considering households' livelihoods and proposing adaptation strategies according to each profile. Piemontese et al. (2021) coupled cognitive and spatial archetypes to evaluate barriers to the scaling up of sustainable land management strategies. Similarly, Riach et al. (2023) constructed climate risk archetypes for municipalities in Germany to build the knowledge necessary to discuss adaptation strategies. In the application presented in Chapter 2 of this thesis, archetype analysis is suggested as the final methodological step to link the outcomes of the drought risk assessment with possible adaptation strategies. This can be done of course also for the smallest units of analysis, in Chapter 2 the municipalities, but archetype analysis allows an intermediate level of abstraction (Oberlack et al., 2019), which is very useful to ease the interpretation of the results. Archetype analysis would be only the basis to start the discussion about how to shift towards proactive drought management. The actual promotion of adaptation strategies requires extra analysis and specific knowledge of the local experts and decision-makers.

6.1.5 Integrating climate impact and risk assessments

Composite indexes are extremely effective tools with great potential for knowledge transfer between academics and decision-makers (OECD, 2008). Well-known examples are the Human Development Index and the World Press Freedom Index. Composite indexes are largely used in disaster risk research dealing with climate risk to guide the emergency response and the allocation of funds. As a result of the enhanced knowledge-sharing between different academic communities, the InfoRM climate change risk (Marzi et al., 2021) represents one of the first attempts to include information related to climate change impact assessments within composite risk indexes. Here, the authors considered future projections to estimate future hazards such as drought and floods. However, climate change impact assessments are not limited to the estimation of future occurrence of extreme events, but also to many other impacts. For example, agronomists and crop modellers apply crop models to estimate future climate change impacts and possible adaptation strategies.

Risk assessment results are reported as relative statistics, and therefore they are useful to compare the spatial or temporal units considered in the analysis. In this thesis, for example, these are municipalities for the Italian case study and different future scenarios for the Somalian case study. Hence, compared to climate change impact assessments, results are not quantitative estimates. Coupling the outcomes of the two approaches

provides quantitative impacts and the relative rankings of the various units, diminishing the possibility of misunderstanding and maladaptation. In this way, the composite risk index gains in representativeness of climate change impacts on agriculture, which is fundamental for water scarcity issues, especially in countries of the South of the world. At the same time, the integration is useful to present effectively and simply the complex outcomes of climate change impact assessments with standardized maps and rankings. In Chapter 5, for example, average crop yields are not drastically affected by climate change after adaptation. Hence, considering the outcomes as relative statistics, future crop yields would not be a major concern. Nevertheless, the quantitative estimates lead to the conclusion that they remain very low and will unlikely be able to ensure food security.

The direct inclusion of indicators estimated with process-based models is innovative but also critical, as the hazard indicators typically represent only extreme events such as droughts, floods and heat waves. The solution proposed also addresses the concern raised by Enenkel et al. (2020) who argued that researchers focus too much on hazards while the impacts should be studied. In general, the rationale for considering that a drought indicator is representative is to check how it correlates with drought impacts (Hall and Leng, 2019). Recent reports applied a data-driven estimation of drought risk, where drought hazard is linked to impacts with machine learning models (Rossi et al., 2023). In other drought risk assessments, precipitation change has been already considered an indicator of hazard. Furthermore, vegetation status is often used to infer agricultural drought with indexes such as the Vegetation Health Index (Kogan, 1995, 2001). Finally, the IPCC (2014) define hazards as "the potential occurrence of a natural or human-induced physical event or trend or physical impact […]". Climate change is a trend and crop yield change is a physical impact, so the categorization used here is also theoretically sound.

Hall and Leng (2019) argue that calculating drought risk, especially when considering agricultural impacts, is not useful since it is impossible to unambiguously distinguish between drought and non-drought conditions. The problem is mainly related to the estimation of the drought hazard, while exposure and vulnerability patterns can help to target countries, regions or municipalities for drought risk adaptation, since "prioritizing adaptation actions does not actually require calculation of drought risk" (Hall and Leng, 2019). They propose simulations with physically-based models to perform stress tests to understand thresholds of vulnerability or tipping points, when impact data are not available. According to them, it is important to simulate different alternative portfolios of interventions in a wide range of possible hydro-climatic conditions. This is very similar to the approach applied in Chapter 5, where the ambiguous drought hazard definition is not used alone, but a physically-based model is directly used to simulate crop yields and possible adaptation strategies with changed climate variables.

The other critical component that can be better represented using process-based crop models is adaptive capacity, framed in this research as a part of resilience. As previously mentioned, resilience is interpreted differently according to the various academic fields. Similarly, the coping, adaptive and transformative capacities are studied by different communities with variable approaches, interpretations and implications. For example, in the approach of the climate change adaptation community, applied in this thesis in Chapters 3 and 4, the adaptive capacity of agricultural systems is frequently evaluated. The adaptation strategies are typically framed as autonomous, soft, or farmer-led, and planned, hard, or institutional (Bindi and Olesen, 2011). When adaptations are not simulated, the "dumb" farmer scenario is an effective way to name it. Despite being unrealistic, this scenario is by far the most represented in climate change studies (Cline, 1996).

In resilience thinking, there is consensus that resilience should be represented by the coping (or resilience), adaptive and transformative capacities. Following the definitions of Folke et al. (2010), the coping (resilience)

capacity resembles the engineering resilience concept, adaptability refers to minor adjustments of the systems, and transformability involves the capacity of the systems to cross thresholds. These three capacities are also interpreted similarly by the disaster risk reduction community and, in this thesis, I adopted the definitions and interpretations of Mochizuki et al. (2018). Here, the coping, adaptive and transformative capacities are respectively the abilities of systems or individuals to "respond to adverse shocks […]", "reduce direct and indirect risk through marginal or incremental changes to the system", and "to address fundamental drivers of risk that are outside of the scale of interest or to amend the major functioning of a system […]" (Mochizuki et al., 2018).

It is evident how the aspects of resilience, as addressed in resilience thinking and elaborated within the risk community by Mochizuki et al. (2018), resemble the typical scenarios used in crop modelling by the climate change adaptation community and the types of adaptations described by Bindi and Olesen (2011). Hence, in Chapter 5 resilience is represented in climate risk assessments with different sets of model simulations. Specifically, the coping capacity is represented by the "dumb" farmer scenario simulations, the adaptive capacity by simulations with simple, autonomous adaptation strategies, and the transformative capacity by planned, institutional adaptation strategies. Representing adaptations with process-based models is a step forward as nowadays these capacities are typically represented in climate risk assessments with static proxy indicators, which would be better included within the socioeconomic or physical vulnerability dimensions.

6.2 Limitations and future work

The objectives of the thesis were conceived to be broad on purpose, and the four Chapters based on manuscripts are linked by assessment research questions but mainly by the methodological approaches used (Fig. 1.2). Each Chapter also has research questions that cover more generic, but relevant, issues that are interesting for the larger research communities and not only to stakeholders that deal with water resource management in the selected study areas. The answers to these research questions were addressed with the methodologies used and in the study areas considered in this thesis, but more research is necessary to improve the knowledge regarding these topics.

Despite always having the general objective in mind, each study was conceived at different moments of the PhD and experienced multiple rounds of revision and contributions by the co-authors involved in the studies. Hence, in some aspects the consequentiality of the studies is affected. For example, to limit the simulation time and the number of outputs to be reported in the results' sections, at the beginning I mainly focused on the far future period (2071-2100). Most of the studies referenced in this thesis also consider the far future, and it makes sense because the climate change effects are exacerbated by the end of the century. This is the main reason why in Chapters 4 and 5 the far future period is considered. Instead, in Chapter 3 the focus is on the effect of vegetation responses to CO_2 and, as already largely discussed, the SWAT+ model outputs are dubious over the 660 ppm threshold of CO_2 concentration. Hence, in Chapter 3 the whole future period is considered, but the analysis related to the effect of vegetation responses is focused on the near future (2041-2070). In the following studies, the SWAT+ model is used for the far future period and with RCP 8.5, hence with a CO_2 concentration higher than 660 ppm. This is of course mentioned in Chapter 4 and it is also the reason why the main results that are discussed are those related to RCP 4.5, while RCP 8.5 outputs are rarely commented and reported only in the appendix. In Chapter 5, the SWAT+ model outputs for SSPs 370 and 585 are considered in the analysis; nevertheless, here the outputs are normalized and aggregated with many other indicators, and hence it is possible to affirm that the uncertainty related to the stomatal conductance suppression effect is negligible. However, in future studies, until the equations in the model are not updated,

the best solution would probably be to use a maximum CO_2 concentration of 660 ppm (as done in Marcinkowski and Piniewski, 2024). A similar issue emerged in the conceptualization of (drought) hazard in Chapters 2 and 5. Chapter 2 started as a preliminary study to select one of the five catchments to apply the SWAT+ model, hence I mainly used easily retrievable indicators also to represent drought hazard. The selection of many indicators to represent drought hazard was motivated by the fact that there is no single drought index that can perfectly describe it. Hence, by considering many drought indices I expected a better representation of this crucial risk dimension. As with all the choices performed in drought risk assessments, this is reasonable but also has many drawbacks. For example, in Chapter 5 I opted to represent the drought hazard only with one specific indicator. From the criticalities that emerged within Chapter 2 and the following reflections, I decided to find an alternative way to represent the hazard dimension and I applied it in Chapter 5.

One of the main limitations of the studies carried out in the thesis is the lack of involvement of local stakeholders. Especially for the drought and climate risk assessments of Chapters 2 and 5, including interested stakeholders from the very first steps significantly contributes to the final adoption of the outcomes of the studies. Nevertheless, the research questions of the two Chapters were mainly methodological, linked to the improvement of the methodology and the integration of agro-hydrological modelling. Furthermore, an interesting characteristic of drought or climate risk assessment is that they can be easily updated when some changes are required or new datasets emerge. For example, the drought risk assessment of Chapter 2 is based on the sixth agricultural census carried out in 2010, and it could be updated with the results of the new seventh agricultural census that should be published soon. Finally, the studies presented in this thesis are carried out within the activities of the research group and contributed to promoting collaborations with local experts or stakeholders in the selected study areas. For example, the SWAT+ model used in Chapters 3 and 4 for the Ombrone catchment is being improved and applied in the AG-WaMED project, where local stakeholders are involved in the participatory modelling activities.

When the climate change impact assessment was conceived, the idea was to analyze future precipitation and temperatures and then focus on the impacts on crop yield, water footprint and adaptive capacity. The hypothesis was that precipitation would reduce in the future, as indicated in the reports for the Mediterranean region. Results showed that local climate patterns are uncertain also within the Mediterranean region, and further research and improved communication are required when dealing with local climate change dynamics. Furthermore, the role of vegetation responses to CO_2 has a high effect on future evapotranspiration and therefore aridity, which can be used as a proxy for drought conditions. This topic emerges from highly-cited literature (Greve et al., 2019; Milly and Dunne, 2016; Roderick et al., 2015; Vicente Serrano et al., 2022), but surprisingly most drought analyses do not consider it. Coupling climate models with offline hydrological models has some issues when the representation of vegetation responses to CO_2 is accounted for differently (Boé, 2021; Milly and Dunne, 2017). Hence, the different representation of the vegetation responses to CO_2 is one of the main reasons for the discrepancy in future drought representation. Further research is being planned to understand if the role of plant physiological responses to CO_2 is sufficiently considered, or at least known, by researchers involved in assessing drought in a changing climate. The hypothesis is that future drought analyses that use indexes such as SPEI or the aridity index are systematically overestimating drought hazards.

Integrating different types of models is already a common practice to perform, for example, climate change impact assessments. These are generally performed by coupling climate models with crop and hydrological models. Often, studies related to crop yields are separated from those that evaluate future hydrological fluxes. Nevertheless, practices should be evaluated for producing real water savings and therefore water should be

managed at the catchment scale. To accomplish this goal, crop and hydrological models can be coupled or it is possible to use, as in this thesis, integrated hydrological models that include a module to simulate crop growth, such as SWAT+. As shown in Chapter 4, SWAT+ is useful for studying the effects of adaptation strategies both at field and catchment scales, permitting a comprehensive evaluation of management changes. Every crop or hydrological model has a simplified representation of processes and certainly more research is necessary to better quantify the impacts of the management changes especially on hydrological fluxes. Furthermore, applying ensembles of agro-hydrological models, as already common practice in climate research and always more applied in crop modelling (e.g. Jägermeyr et al., 2016), might be an interesting solution for more robust predictions and estimations. An interesting alternative to study the impacts of management changes is to directly use GCMs that allow the simulation of land-atmosphere interactions and land management strategies, though at a coarse resolution. For example, Gormley-Gallagher et al. (2022) used the Community Earth System Model to estimate the effects of irrigation and conservation agriculture on temperature trends. Adaptation strategies in this thesis are not evaluated based on economic or social factors but only for the effects on agricultural and hydrological outputs. Despite the simulated adaptation strategies are mostly autonomous and simple, meaning that they could be easily adopted by farmers themselves without the support of external institutions, there might be some hidden factors that hamper their application. In addition, in this thesis the concepts related to adaptation to climate change are simplified, with management changes and adaptation strategies that are used as synonyms. The effect of the proposed alternative strategies in the current climate was not always considered and, in any case, not used to estimate the "true" adaptation potential as described by Lobell (2014). Even if this might create some confusion, for the applications proposed in this thesis the concept of true adaptation is not fully relevant.

As already discussed in Chapter 5 and Section 6.1.5, the inclusion of indicators calculated with process-based models within the climate risk assessment framework is innovative and critical at the same time. Further research is needed to improve the theoretical justification, enhance the positive aspects of the combination of the approaches and limit the issues that arise due to increased complexity. Furthermore, in agriculture, the hazard and their impacts are studied with many approaches, while this might not be the case for other sectors. Hence, the coupling of the approaches of the disaster and climate communities, as presented in this thesis, might be not possible for sectors other than agriculture. Additionally, agro-hydrological models were used in this thesis to simulate a limited number of simple agronomic adaptation strategies that resembled the adaptive capacity. Nevertheless, it is theoretically possible to simulate more complex adaptations and deep transformations of the agricultural systems. These aspects should be explored in further research.

6.3 Key messages

Uncertain future climate:

- Evaluating future drought hazard is extremely difficult due to the uncertain precipitation projections, the vegetation responses to CO_2, and the ambiguous drought definitions.
- We need to assess climate change impacts at small scales since they might be counterintuitive, as in the case of Central Italy, where climate models did not show decreasing precipitation as compared to the rest of the Mediterranean region.

Agro-hydrological modelling:

- The SWAT+ model is very effective in simulating various aspects of crop growth and hydrological fluxes, taking easily into account management, soil, climate and crop variabilities.
- Integrated agro-hydrological models are extremely useful for evaluating real/apparent water savings at the catchment scale.

Adaptive capacity of agricultural systems:

- In prevalently agricultural catchments, management changes can have impacts that can be compared to those of climate change.
- The adaptive capacity of agricultural systems is generally high, even if crop yields in Sub-Saharan Africa remain very low.
- Combinations of adaptation strategies show interesting synergies that should be studied and considered.

Improving risk assessment frameworks:

- Climate/drought risk/vulnerability assessments are fundamental to fuel the discussion about possible adaptation strategies. It is fundamental to summarize and present the results effectively and the robustness evaluation and archetype analysis are useful for this scope.
- Agro-hydrological modelling can be used to represent climate hazard and resilience within risk assessment frameworks.
- Quantitative estimates of climate change impact assessments can improve the quality, representativeness, and reliability of climate risk assessments.

Final remarks:

- Future water scarcity is expected to be a greater challenge compared to future water shortages in Somalia and very likely in most of Sub-Saharan Africa.
- There are great opportunities to improve current methodologies and approaches if the disaster risk reduction, climate change adaptation and sustainable development research communities share their knowledge and collaborate.

Appendix

A2: Supplementary materials chapter 2

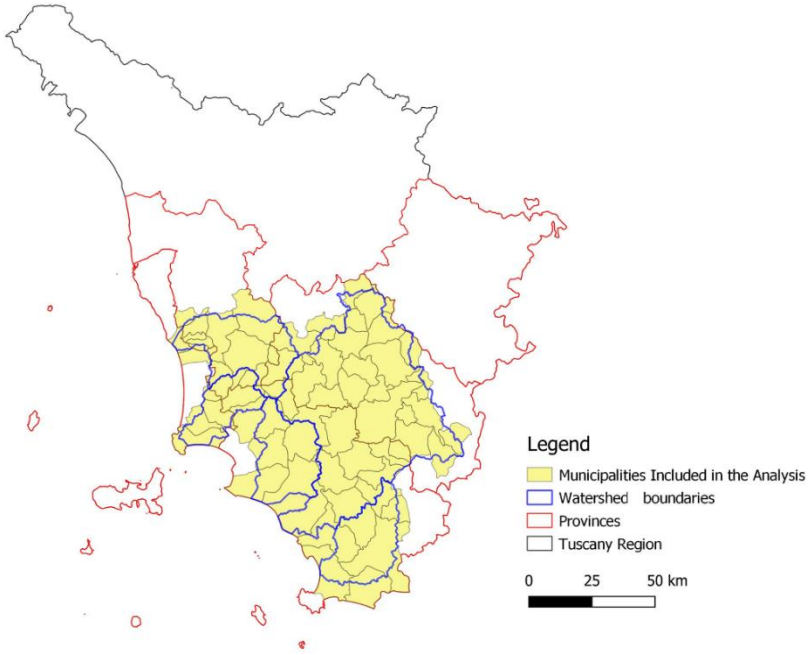

Figure A2.1: Tuscany region with the watersheds and municipalities included in the analysis.

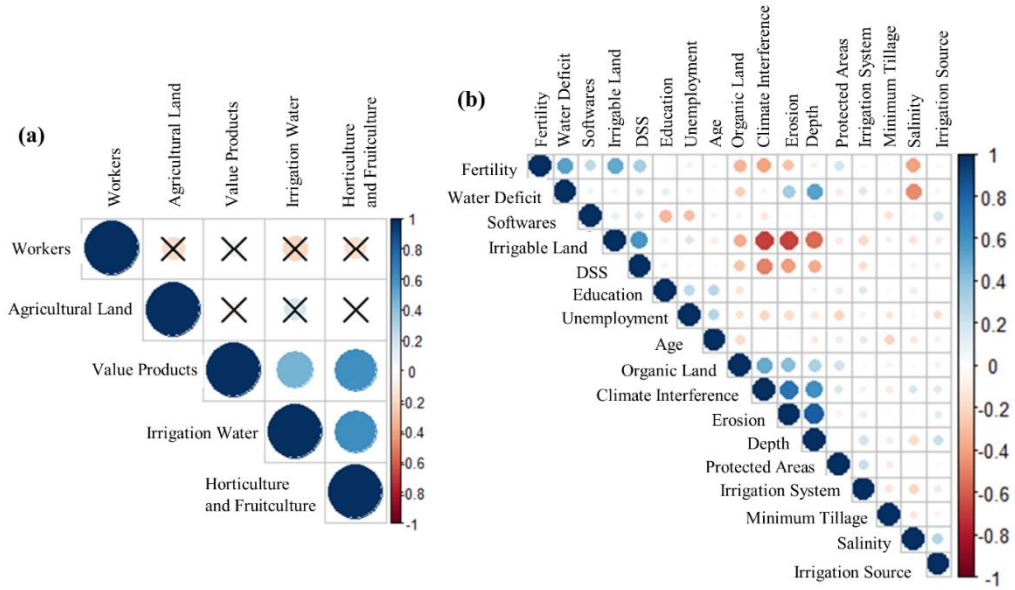

Figure A2.2: Correlograms calculated with the Spearman method for a) exposure and b) vulnerability indicators. Positive and negative values indicate positive and negative correlations, respectively.

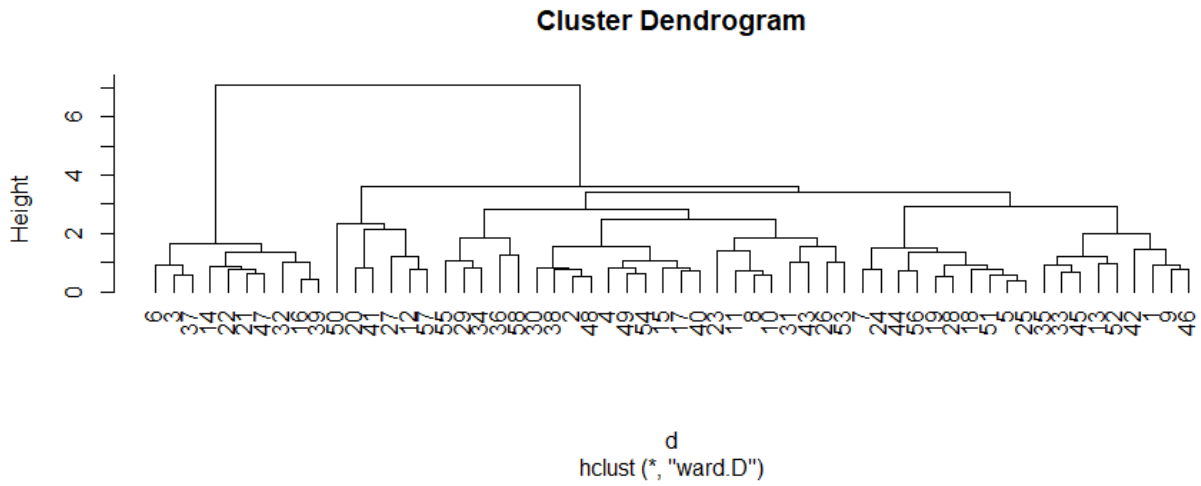

Figure A2.3: Cluster dendrogram created with the Ward method considering the normalized exposure and vulnerability indicators.

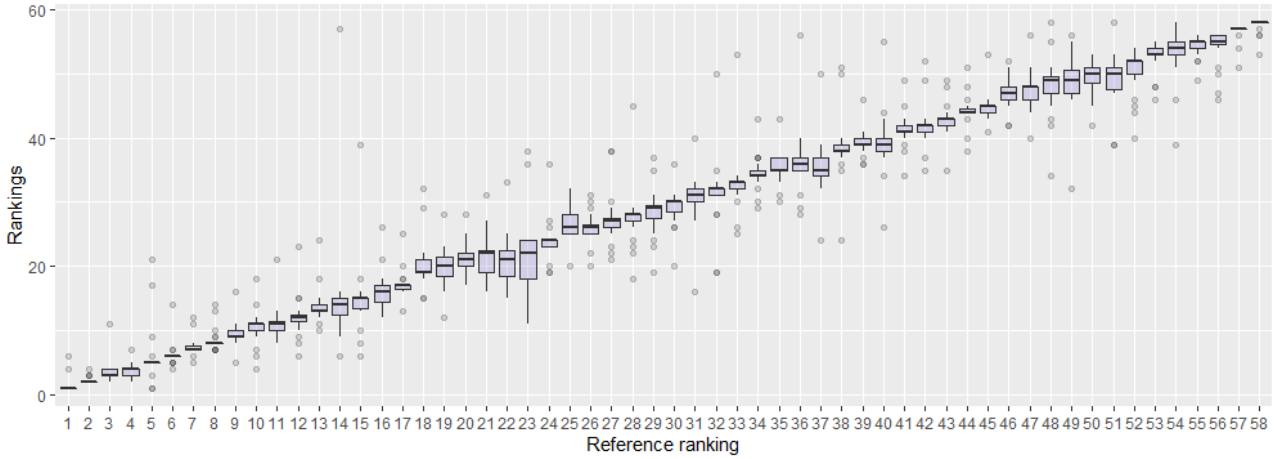

Figure A2.4: Summary boxplot of the uncertainty analysis; in the x-axis, it is reported the reference ranking (the ranking of the municipalities calculated through the main procedure, that is equal weights), while on the y-axis the values of the rankings assigned with the alternative methods considered in the uncertainty analysis. The line represents the median, the box the upper and lower quartiles, the whiskers the highest and lowest values excluding outliers, and dots potential outliers.

A3: Supplementary materials chapter 3

Table A3.1: Code (in the SIR archive), latitude, longitude and elevation of the climate stations used as input data for calibration and validation and bias correction.

ID	SIR CODE	Latitude	Longitude	Elevation (m.a.s.l.)	Calibration and Validation					Bias Correction	
					Precipitation	Temperature	Solar radiation	Relative humidity	Wind speed	Precipitation	Temperature
1	01000831	43.45	11.531	553						X	
2	01001284	43.486	11.379	509	X						
3	01002779	43.102	11.039	490	X	X					
4	03002531	43.016	11.165	494	X						
5	03002613	43.329	11.555	224	X						
6	03002643	43.414	11.456	430	X						
7	03002701	43.050	11.491	592	X						
8	03002733	43.203	11.077	368	X						
9	03002761	43.276	11.230	258	X						
10	03002789	43.062	11.323	318	X						
11	03002801	42.984	11.365	82	X						
12	03002819	42.951	11.853	622	X						
13	03002869	43.067	11.725	492	X						
14	03002888	43.155	11.650	404	X						
15	03002901	42.894	11.527	561	X						
16	03002921	42.940	11.284	71	X						
17	03002941	42.804	11.303	148	X						
18	03002961	42.765	11.166	20	X						
19	03003071	42.694	11.329	548	X						
20	11000005	42.706	11.145	32	X	X	X	X	X	X	X
21	11000008	42.93	11.08	41			X	X			
22	11000013	42.769	11.016	2	X	X		X	X	X	X
23	11000015	43.033	11.064	466	X	X		X		X	X
24	11000019	43.370	11.423	308	X	X			X		
25	11000022	43.512	11.236	436							X
26	11000025	43.366	11.151	229							X
27	11000041	43.021	10.865	186						X	X
28	11000042	42.789	11.176	50	X	X				X	X
29	11000051	42.951	11.439	195	X	X		X	X	X	X
30	11000052	42.854	11.556	812							X
31	11000054	42.796	11.406	363	X	X			X	X	X
32	11000056	43.24	11.42	165			X				
33	11000058	42.961	11.618	670	X	X		X	X		X
34	11000059	43.027	11.582	497	X	X					X
35	11000061	42.948	11.733	612	X	X			X		X
36	11000067	43.092	11.439	188	X	X			X	X	X
37	11000080	43.209	11.18	452		X		X	X	X	X
38	11000082	43.243	11.417	165	X	X	X	X	X		X
39	11000087	43.457	11.422	369	X	X		X			
40	11000103	42.661	11.017	2		X					
41	11000115	42.890	11.625	1671	X	X					
					32	17	4	9	10	10	16

Table A3.2: Parameters considered in the sensitivity analysis and selected for calibration, with the relative sensitivity rankings for monthly streamflow.

Sensitivity ranking	Parameter	Selected for calibration
1	bd	Yes
2	esco	Yes
3	cn2	Yes
4	epco	Yes
5	revap_co	Yes
6	revap_min	No
7	cbn	No
8	canmx	No
9	flo_min	No
10	z	No
11	awc	No
12	perco	No
13	surlag	No
14	biomix	No
15	k	No

Table A3.3: Statistics used for model evaluation.

Statistic	Variable	Time scale	Reference	Performance rating			
				Very good	*Good*	*Satisfactory*	*Unsatisfactory*
NSE	Streamflow	Monthly	*Moriasi et al., 2015*	> 0.8	0.7 – 0.8	0.5 – 0.7	< 0.5
Pbias	Streamflow	Monthly	*Moriasi et al., 2015*	< 5%	5-10%	10-15%	> 15%
RSR	Streamflow	Monthly	*Moriasi et al., 2007*	< 0.5	0.5 – 0.6	0.6 – 0.7	> 0.7

Table A3.4: Multi-site calibration for streamflow, with the parameters selected, the type of change, and the change in terms of percentage or new value.

Parameters streamflow	Type of change	Range	Final change		
			Subbasins Buonconvento	Subbasins Sasso d'Ombrone	Subbasins Istia
bd	*Percentage*	-20, +20%	19.83%	11.02%	19.92%
esco	*Replace*	0.05, 0.99	0.14	0.05	0.08
cn2	*Percentage*	-20, +20%	18.06%	7.96%	19.92%
epco	*Replace*	0.05, 0.99	0.19	0.17	0.05
revap_co	*Replace*	0.02, 0.19	0.11	0.16	0.08

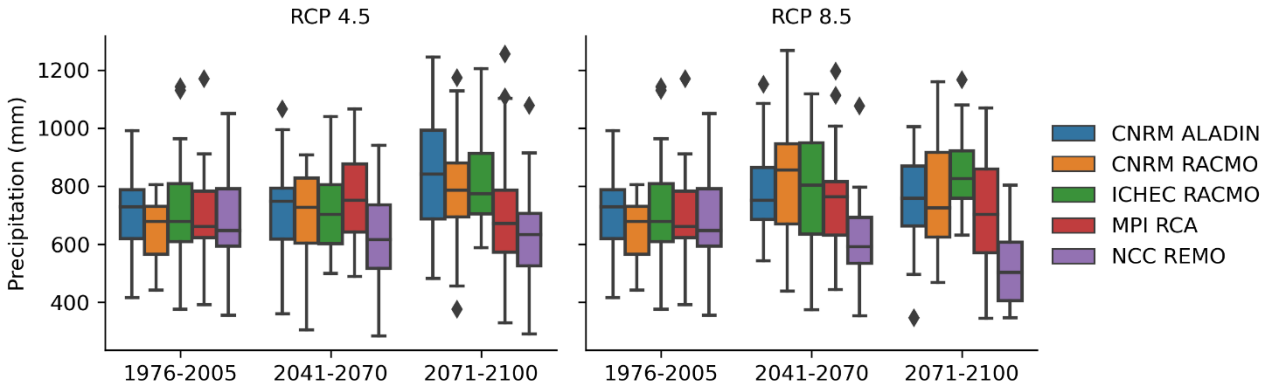

Figure A3.1: Boxplots of average annual precipitation for RCP 4.5 and 8.5 for the five climate models, with the historical period, the medium- and long-term futures, considering the outputs of the 28 years.

Table A3.5: Absolute difference between the long-term future (2071-2100) and historical (1976-2005) periods, considering the average values of precipitation and temperatures of the five climate models considered. Results are reported with the standard deviation for RCPs 4.5 and 8.5 and annual, summer, and winter seasons, in terms of 5th and 95th percentiles and mean. The 5th and 95th percentiles and the mean are calculated considering the 28 years of the 5 climate models.

Variable (unit)	**Period**	**RCP 4.5**			**RCP 8.5**		
		5th percentile	*Mean*	*95th percentile*	*5th percentile*	*Mean*	*95th percentile*
Precipitation (mm)	*Annual*	**32** ± 79.4	**70** ± 66.1	**145** ± 124.9	**36** ± 80.2	**32** ± 98.9	**57** ± 142.9
	DJF	**6** ± 12.6	**34** ± 6.8	**77** ± 42.3	**3** ± 10.5	**22** ± 30.7	**68** ± 80.6
	JJA	**-0.7** ± 2.8	**5** ± 18.9	**20** ± 65.6	**1** ± 4.5	**-7** ± 22.3	**-15** ± 47.4
Maximum temperature (°C)	*Annual*	**2.1** ± 0.26	**2.0** ± 0.26	**2.0** ± 0.43	**3.9** ± 0.36	**3.9** ± 0.34	**4.1** ± 0.56
	DJF	**2.1** ± 0.90	**1.9** ± 0.24	**1.9** ± 0.16	**4.0** ± 0.83	**3.6** ± 0.17	**3.5** ± 0.12
	JJA	**2.2** ± 0.31	**2.1** ± 0.63	**2.3** ± 1.20	**4.6** ± 0.74	**4.4** ± 0.83	**4.3** ± 1.15
Average temperature (°C)	*Annual*	**2.1** ± 0.19	**2.1** ± 0.23	**2.1** ± 0.40	**3.9** ± 0.27	**4.0** ± 0.26	**4.2** ± 0.45
	DJF	**2.0** ± 0.74	**1.9** ± 0.31	**2.0** ± 0.34	**3.7** ± 0.64	**3.5** ± 0.14	**3.6** ± 0.26
	JJA	**2.3** ± 0.32	**2.3** ± 0.47	**2.5** ± 1.00	**4.8** ± 0.54	**4.8** ± 0.62	**4.8** ± 0.97
Minimum temperature (°C)	*Annual*	**2.0** ± 0.12	**2.2** ± 0.23	**2.1** ± 0.34	**3.9** ± 0.20	**4.1** ± 0.19	**4.2** ± 0.45
	DJF	**1.9** ± 0.59	**1.9** ± 0.40	**1.9** ± 0.45	**3.5** ± 0.67	**3.5** ± 0.12	**3.6** ± 0.33
	JJA	**2.4** ± 0.36	**2.5** ± 0.32	**2.8** ± 0.72	**4.9** ± 0.38	**5.1** ± 0.42	**5.3** ± 0.78

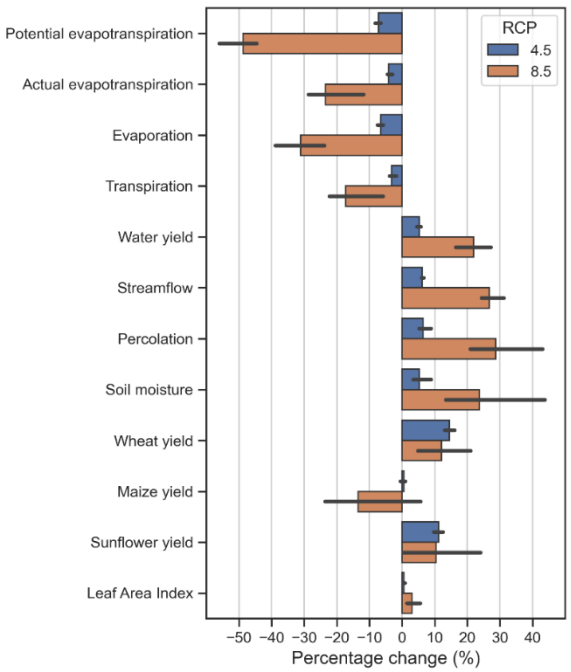

Figure A3.2: Water balance components change (%) of the long-term (2071-2100) climate change between the cases of considering and not considering the plant physiological responses to CO2 for RCPs 4.5 (blue) and 8.5 (orange). The simulated water balance components are potential and actual evapotranspiration, evaporation, streamflow, water yield, percolation, and soil moisture. Crop yields and LAI are also reported in the figure. The uncertainty (black bar) is reported considering the five climate models.

Table A3.6: Absolute difference between the long-term future (2071-2100) and historical (1976-2005) periods, considering the average values of potential and actual evapotranspiration, evaporation, flow, and other water balance components of the five climate models considered. Results are reported with the standard deviation for simulations considering the increase and stable CO2 values, RCPs 4.5 and annual, summer, and winter seasons, in terms of 5th and 95th percentiles and mean. The 5th and 95th percentiles and the mean are calculated considering the 28 years of the 5 climate models.

Variable (unit)	Period	*5th percentile*		*Mean*		*95th percentile*	
		Constant CO_2	**Increasing CO_2**	**Constant CO_2**	**Increasing CO_2**	**Constant CO_2**	**Increasing CO_2**
Potential evapotranspiration (mm)	*Annual*	**123.9** ± 31.3	**37.1** ± 30.2	**110.0** ± 32.9	**16.1** ± 29.6	**106.9** ± 56.5	**6.1** ± 45.7
	DJF	**4.5** ± 2.4	**-3.1** ± 1.8	**5.7** ± 4.3	**-4.8** ± 3.1	**3.7** ± 4.7	**-10.0** ± 3.8
	JJA	**55.6** ± 11.3	**24.2** ± 9.9	**54.4** ± 19.8	**17.0** ± 17.9	**70.7** ± 21.8	**26.6** ± 19.8
Actual evapotranspiration (mm)	*Annual*	**10.5** ± 27.2	**-5.6** ± 26.3	**0.2** ± 23.4	**-23.7** ± 21.7	**-8.1** ± 23.8	**-37.2** ± 24.7
	DJF	**-3.3** ± 2.2	**-7.4** ± 2.3	**-5.5** ± 1.2	**-11.4** ± 1.9	**-10.4** ± 1.7	**-18.4** ± 2.6
	JJA	**4.9** ± 8.7	**4.6** ± 7.4	**6.1** ± 11.5	**1.9** ± 10.3	**2.7** ± 16.8	**-5.6** ± 18.0
Evaporation (mm)	*Annual*	**12.7** ± 7.1	**4.2** ± 7.2	**14.0** ± 4.6	**3.8** ± 5.1	**18.6** ± 4.7	**6.1** ± 4.8
	DJF	**2.8** ± 1.4	**0.7** ± 1.1	**3.7** ± 1.4	**0.8** ± 1.2	**4.8** ± 1.8	**0.8** ± 1.4
	JJA	**3.8** ± 0.8	**3.1** ± 0.8	**8.6** ± 3.5	**7.3** ± 3.5	**12.0** ± 6.6	**9.1** ± 6.8
Istia streamflow (m^3/s)	*Annual*	**2.0** ± 1.6	**2.8** ± 1.9	**5.6** ± 3.2	**7.0** ± 3.5	**13.5** ± 9.0	**15.9** ± 9.5
	DJF	**1.3** ± 2.5	**1.9** ± 2.7	**9.5** ± 4.8	**12.3** ± 5.2	**27.8** ± 11.7	**33.4** ± 11.6
	JJA	**0.1** ± 0.2	**0.1** ± 0.3	**1.0** ± 2.1	**1.3** ± 2.1	**4.9** ± 13.1	**5.6** ± 13.4
Water yield (mm)	*Annual*	**4.9** ± 11.4	**7.6** ± 12.7	**34.9** ± 19.1	**43.2** ± 20.7	**86.6** ± 69.1	**101.8** ± 71.2
	DJF	**0.8** ± 1.6	**1.2** ± 1.8	**14.8** ± 6.7	**18.9** ± 7.1	**44.5** ± 19.8	**54.2** ± 19.6
	JJA	**0.1** ± 0.3	**0.2** ± 0.3	**2.2** ± 4.7	**2.4** ± 4.7	**9.8** ± 33.9	**10.4** ± 34.4
Percolation (mm)	*Annual*	**21.9** ± 16.4	**31.4** ± 17.9	**34.9** ± 21.8	**47.0** ± 22.4	**64.1** ± 37.6	**77.6** ± 37.3
	DJF	**5.6** ± 7.6	**8.4** ± 8.3	**14.0** ± 8.0	**17.9** ± 8.1	**27.1** ± 19.3	**31.4** ± 18.6
	JJA	**1.3** ± 1.6	**2.1** ± 1.8	**1.9** ± 2.4	**3.6** ± 2.6	**4.5** ± 7.0	**7.8** ± 7.3
Soil moisture (mm)	*Annual*	**28.2** ± 20.0	**44.4** ± 18.6	**15.2** ± 12.5	**29.7** ± 10.0	**14.5** ± 11.6	**25.4** ± 9.0
	DJF	**22.4** ± 20.8	**39.0** ± 19.7	**19.7** ± 13.6	**33.1** ± 10.4	**23.6** ± 23.9	**32.0** ± 20.7
	JJA	**19.8** ± 19.6	**35.7** ± 18.1	**10.0** ± 10.3	**24.6** ± 7.7	**10.3** ± 13.3	**22.4** ± 12.1

Table A3.7: Absolute difference between the long-term future (2071-2100) and historical (1976-2005) periods, considering the average values of potential and actual evapotranspiration, evaporation, flow, and other water balance components of the five climate models considered. Results are reported with the standard deviation for simulations considering the increase and stable CO2 values, RCPs 8.5 and annual, summer, and winter seasons, in terms of 5th and 95th percentiles and mean. The 5th and 95th percentiles and the mean are calculated considering the 28 years of the 5 climate models.

Variable (unit)	Period	*5th percentile*		*Mean*		*95th percentile*	
		Constant CO_2	**Increasing CO_2**	**Constant CO_2**	**Increasing CO_2**	**Constant CO_2**	**Increasing CO_2**
Potential evapotranspiration (mm)	*Annual*	**203.0** ± 37.6	**-192.4** ± 58.6	**225.4** ± 45.4	**-211.7** ± 52.6	**260.4** ± 75.9	**-227.7** ± 52.3
	DJF	**12.3** ± 4.3	**-19.6** ± 5.1	**13.1** ± 4.9	**-29.7** ± 5.9	**12.0** ± 6.7	**-42.0** ± 7.3
	JJA	**113.1** ± 35.6	**-45.2** ± 32.6	**116.7** ± 26.7	**-70.8** ± 30.3	**125.6** ± 40.0	**-93.4** ± 27.3
Actual evapotranspiration (mm)	*Annual*	**-18.7** ± 46.9	**-83.9** ± 23.8	**-10.9** ± 36.7	**-109.8** ± 22.4	**-0.4** ± 29.7	**-126.8** ± 33.6
	DJF	**-2.8** ± 8.0	**-17.0** ± 4.1	**-3.0** ± 2.6	**-25.3** ± 4.5	**-6.1** ± 2.5	**-35.9** ± 5.7
	JJA	**-8.9** ± 22.8	**-10.6** ± 5.4	**-2.6** ± 17.9	**-20.5** ± 11.4	**-6.0** ± 15.2	**-37.9** ± 14.7
Evaporation (mm)	*Annual*	**10.4** ± 10.8	**-18.9** ± 8.7	**16.9** ± 6.9	**-18.2** ± 7.1	**25.9** ± 5.7	**-15.5** ± 8.2
	DJF	**2.9** ± 3.7	**-3.8** ± 1.5	**4.9** ± 0.7	**-5.8** ± 1.5	**7.1** ± 1.0	**-7.7** ± 1.7
	JJA	**4.4** ± 3.1	**2.8** ± 2.3	**9.0** ± 3.2	**5.4** ± 3.2	**13.5** ± 4.9	**5.4** ± 3.7
Istia streamflow (m^3/s)	*Annual*	**1.2** ± 2.2	**4.4** ± 3.4	**3.8** ± 4.8	**10.1** ± 6.7	**7.3** ± 10.5	**16.1** ± 11.7
	DJF	**0.8** ± 2.6	**5.0** ± 4.7	**5.7** ± 7.0	**17.4** ± 10.5	**16.5** ± 19.4	**39.3** ± 23.1
	JJA	**-0.1** ± 0.1	**0.03** ± 0.1	**0.3** ± 1.9	**1.4** ± 2.2	**1.5** ± 7.5	**4.8** ± 7.1
Water yield (mm)	*Annual*	**6.8** ± 16.0	**22.5** ± 23.4	**27.8** ± 33.4	**63.2** ± 44.1	**35.7** ± 69.9	**94.4** ± 83.6
	DJF	**0.5** ± 1.6	**2.5** ± 2.6	**10.0** ± 11.6	**26.8** ± 16.3	**32.5** ± 34.8	**73.9** ± 44.6
	JJA	**-0.1** ± 0.2	**0.3** ± 0.2	**1.3** ± 3.9	**2.2** ± 4.0	**5.5** ± 19.6	**8.8** ± 18.1
Percolation (mm)	*Annual*	**12.0** ± 19.2	**50.2** ± 26.3	**17.2** ± 31.0	**67.8** ± 36.9	**26.8** ± 47.8	**86.1** ± 40.5
	DJF	**5.4** ± 8.5	**17.1** ± 12.2	**8.5** ± 13.2	**24.1** ± 14.3	**20.0** ± 31.6	**36.7** ± 28.2
	JJA	**-0.4** ± 0.7	**3.0** ± 1.9	**-0.9** ± 2.8	**6.9** ± 4.2	**-1.8** ± 8.0	**13.3** ± 10.2
Soil moisture (mm)	*Annual*	**-5.1** ± 29.0	**63.4** ± 19.0	**-7.6** ± 26.2	**52.1** ± 14.6	**-3.3** ± 20.8	**45.4** ± 10.1
	DJF	**3.7** ± 39.6	**74.4** ± 28.6	**-1.4** ± 32.6	**52.1** ± 17.8	**5.6** ± 43.1	**41.0** ± 23.0
	JJA	**-12.8** ± 18.0	**54.3** ± 17.5	**-15.2** ± 21.5	**46.7** ± 11.9	**-11.0** ± 22.3	**42.6** ± 12.3

A4: Supplementary materials chapter 4

Part 1: SWAT+ sensitivity analysis, calibration, validation

We performed a manual sensitivity analysis by calculating the relative sensitivity (S_r) of the whole set of crop parameters by individually perturbing them by +/- 20%, as in Brouziyne et al. (2018), with the equation:

$$S_r = \frac{[(O_{P+\Delta P} - O_{P-\Delta P}) / O_P]}{2\Delta P / P}$$

where OP is the model output with the input parameters set as base value, $O_{P+\Delta P}$ and $O_{P-\Delta P}$ are the model outputs with input parameters perturbed, ΔP is the absolute change in the value of the input parameter, and P is the base value of the input parameter.

The results of the sensitivity analysis are reported in Table A4.1. Table A4.2 shows the performance criteria used in this research from Jamieson et al. (1991) and Moriasi et al. (2007). The management applied in this study is reported in Table A4.3, while the performance of the model for monthly streamflow is reported in Table A4.4.

Differently from most of the studies found in the literature, with some exceptions, such as the study of Sun and Ren (2013), we used the whole set of crop parameters to perform calibration and validation. As in Sinnathamby et al. (2017), we also decided to include *esco* and *epco* in the calibration with crop yield, which are usually considered in the calibration for streamflow. In Sinnathamby et al. (2017), *epco* was reduced to 0.9 and *esco* to 0.6 for maize. The maximum leaf area index (*lai_pot*) for maize was frequently reduced to 5 (Hu et al., 2007; Palazzoli et al., 2015; Sinnathamby et al., 2017) while it was set to 3.5 in Nair et al. (2011) and to 4 in Wang et al. (2017). The harvest index (*harv_idx*) and the radiation use efficiency (*bm_e*) of maize were also mostly reduced, except for *harv_idx* in Musyoka et al. (2021) which was increased to 0.6 and *bm_e* in Hu et al. (2007) which was set to 46. For winter wheat, Brouziyne et al. (2018), Palazzoli et al. (2015) and Musyoka et al. (2021) increased *harv_idx* from the default up to 0.5, while Nair et al. (2011) decreased *harv_idx* to 0.35, *lai_pot* to 3 and *bm_e* to 25. Sun and Ren (2013) performed a multi-site calibration for wheat and maize and used the whole range of parameters reported in the previous studies. Additionally, they considered the light extinction coefficient (*ext_co*) and modified it in the range of 0.5-0.6. For sunflower, Brouziyne et al. (2018) increased *harv_idx* to 0.35 and *lai_pot* to 4 and decreased *bm_e* to 42 and *ext_co* to 0.7. The calibrated parameters in our study generally are within the ranges reported in the literature. To match some low yields, we drastically reduced *esco* and *epco* for sunflower in the Grosseto province to 0.35 and 0.6, respectively, and *harv_idx* and *lai_pot* for maize in the Siena province by 17.5% to 0.45 and 4.95, respectively.

Table A4.1: Rankings of the most sensitive parameters for durum wheat, maize and sunflower yield.

Durum wheat yield		Maize yield		Sunflower yield	
Sensitivity ranking	**Parameter**	**Sensitivity ranking**	**Parameter**	**Sensitivity ranking**	**Parameter**
1 (HS)	harv_idx	1 (HS)	harv_idx	1 (HS)	hu_lai_decl
2 (HS)	bm_e	2 (HS)	bm_e	2 (HS)	harv_idx
3 (HS)	days_mat	3 (HS)	days_mat	3 (HS)	bm_e
4 (MS)	lai_pot	4 (MS)	ext_co	4 (HS)	days_mat
5 (MS)	ext_co	5 (MS)	lai_pot	5 (HS)	lai_pot
6 (MS)	hu_lai_decl	6 (MS)	frac_hu1	6 (MS)	frac_hu2
7 (MS)	frac_hu2	7 (MS)	lai_max2	7 (MS)	lai_max2
8 (MS)	lai_max2	8 (MS)	lai_max1	8 (MS)	ext_co
9 (LS)	frac_hu1	9 (MS)	frac_hu2	9 (MS)	dlai_rate
10 (LS)	dlai_rate	10 (LS)	ru_vpd	10 (LS)	frac_hu1
11 (LS)	lai_max1	11 (LS)	rt_dp_max	11 (LS)	ru_vpd
12 (LS)	ru_vpd	12 (LS)	hu_lai_decl	12 (LS)	lai_max1
13 (LS)	rt_dp_max	13 (LS)	dlai_rate	13 (LS)	rt_dp_max
14 (NS)	can_ht_max	14 (NS)	can_ht_max	14 (NS)	can_ht_max
14 (NS)	harv_idx_ws	14 (NS)	harv_idx_ws	14 (NS)	harv_idx_ws
14 (NS)	stcon_max	14 (NS)	stcon_max	14 (NS)	stcon_max
14 (NS)	vpd	14 (NS)	vpd	14 (NS)	vpd
14 (NS)	frac_stcon	14 (NS)	frac_stcon	14 (NS)	frac_stcon

Table A4.2: Statistics used for model evaluation.

Statistic	**Variable**	**Time scale**	**Reference**	**Performance rating**			
				Excellent / Very good	*Good*	*Fair / Satisfactory*	*Poor / Unsatisfactory*
NRMSE	Crop yield	Annual	*Jamieson et al., 1991*	< 10%	10 – 20%	20 – 30%	> 30%
NSE	Flow	Monthly	*Moriasi et al., 2007*	> 0.75	0.65 – 0.75	0.5 – 0.65	< 0.5
Pbias	Flow, crop yield	Monthly, annual	*Moriasi et al., 2007*	< 10%	10 – 15 %	15 – 25%	> 25%

Table A4.3: The management schedule used for calibration and validation, in the historical simulation and the future simulations without adaptation strategies.

Crop	Operation	Date
Durum wheat	Mouldboard tillage	1st August
	Fertilization (18-46), 165 kg/ha	14th October
	Harrow tillage	15th October
	Sowing period	16th October – 1st November
	Fertilization (33-00), 200 kg/ha	10th February
	Fertilization (urea), 120 kg/ha	1st April
	Latest harvesting date	19th July
Sunflower	Mouldboard tillage	1st December
	Fertilization (18-46), 180 kg/ha	14th March
	Harrow tillage	15th March
	Sowing period	16th March – 1st April
	Fertilization (urea), 130 kg/ha	1st May
	Latest harvesting date	22nd October
Maize	Mouldboard tillage	1st December
	Fertilization (18-46), 220 kg/ha	14th March
	Harrow tillage	15th March
	Sowing period	16th March – 1st April
	Fertilization (33-00), 210 kg/ha	1st May
	Fertilization (urea), 200 kg/ha	1st June
	Latest harvesting date	22nd October
	Sprinkler irrigation	Automatic

Table A4.4: Calibration and validation statistics for monthly streamflow at the three gauging stations.

Monthly streamflow	Calibration		Validation	
Station	**NSE**	**Pbias**	**NSE**	**Pbias**
Buonconvento	0.77 [1]	17.38% [3]	-	-
Sasso d'Ombrone	0.79 [1]	3.96% [2]	0.72 [2]	18.25% [3]
Istia	0.53 [3]	25.27% [4]	0.72 [2]	18.8% [3]

[1] Very good; [2] Good; [3] Satisfactory; [4] Unsatisfactory.

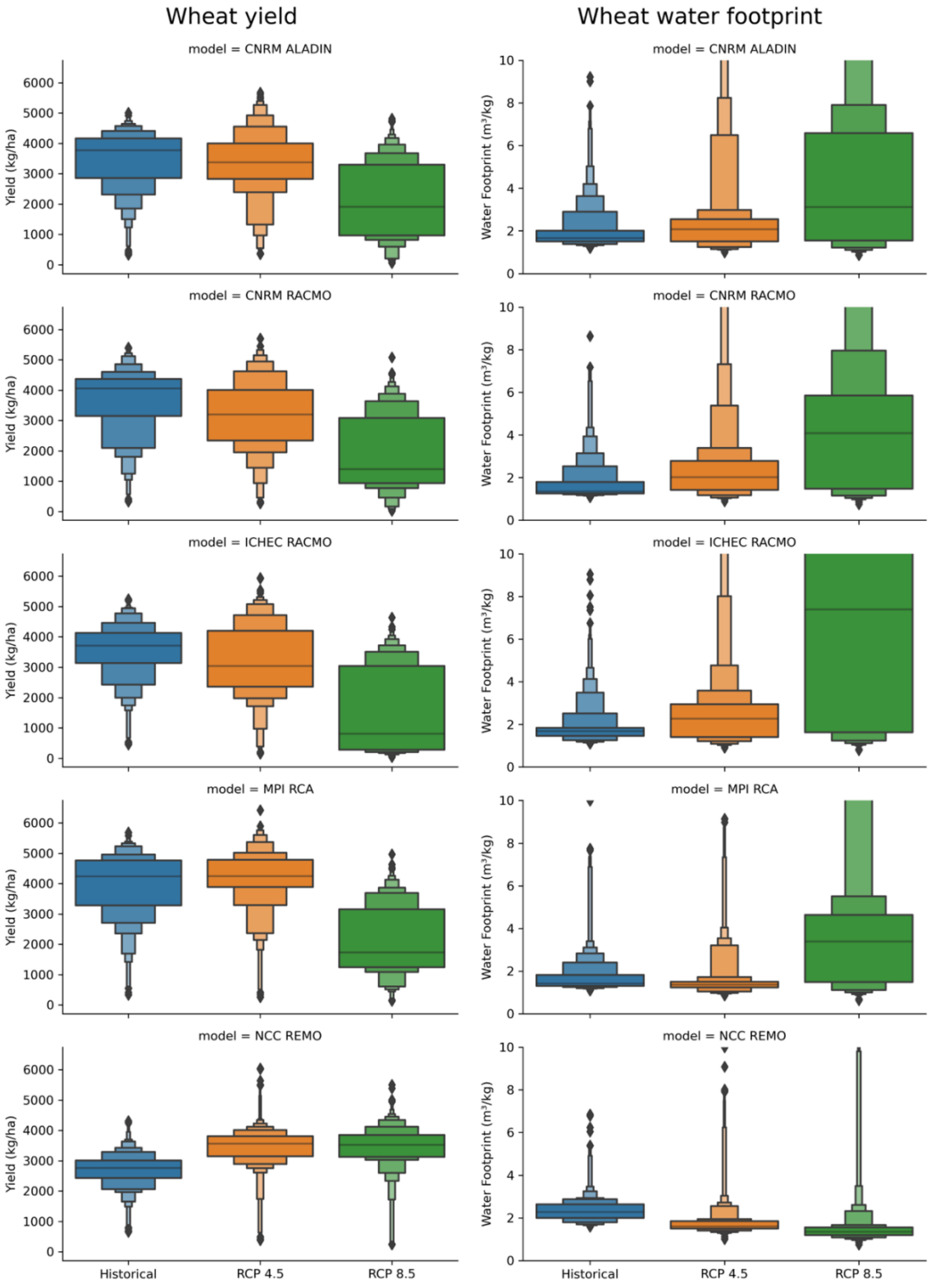

Figure A4.1: Boxen plots of the 28-years average wheat yield and water footprint for the five climate models and the historical, RCP 4.5 and 8.5 scenarios.

Part 2: Additional results

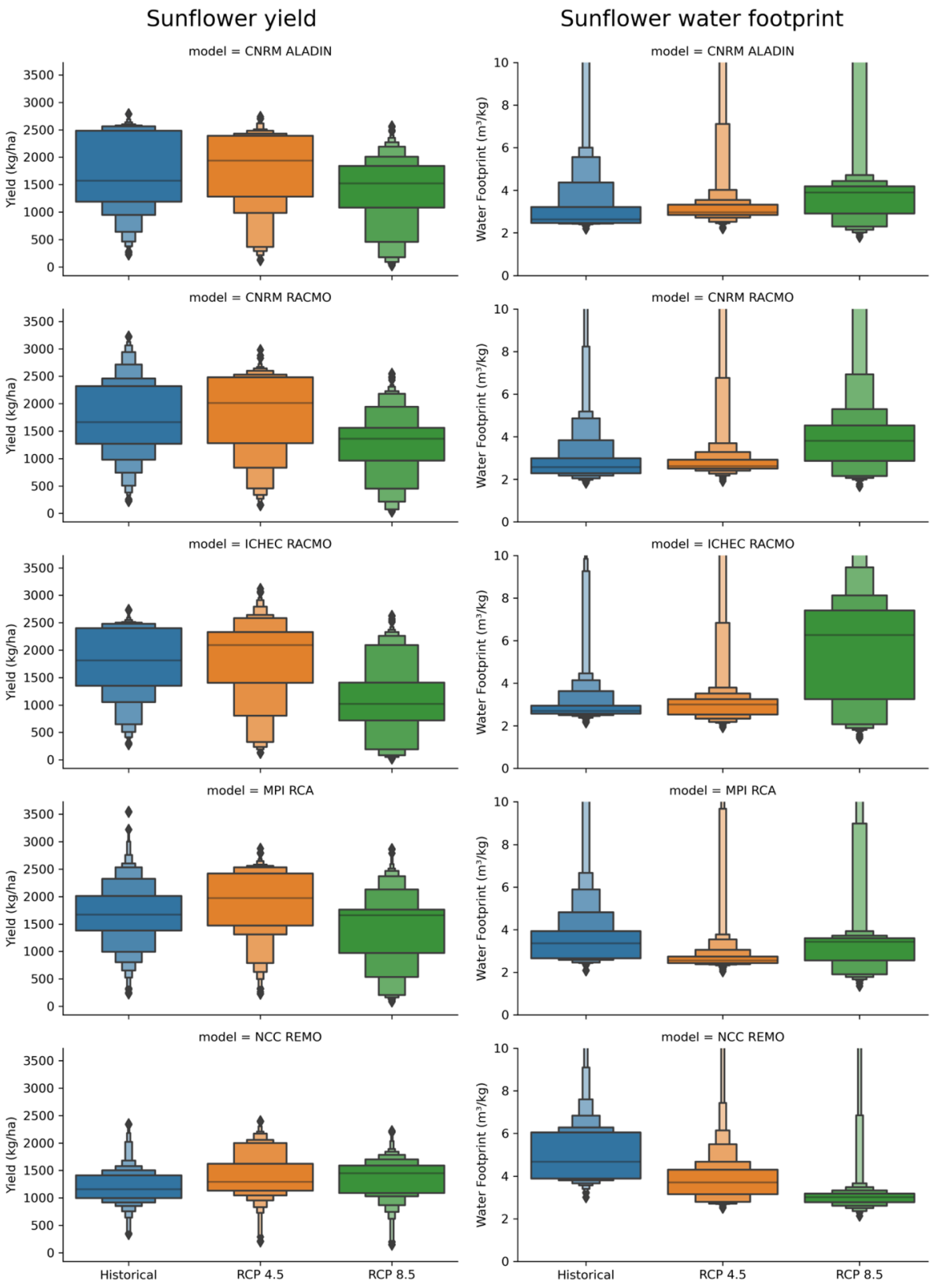

Figure A4.2: Boxen plots of the 28-years average sunflower yield and water footprint for the five climate models and the historical, RCP 4.5 and 8.5 scenarios.

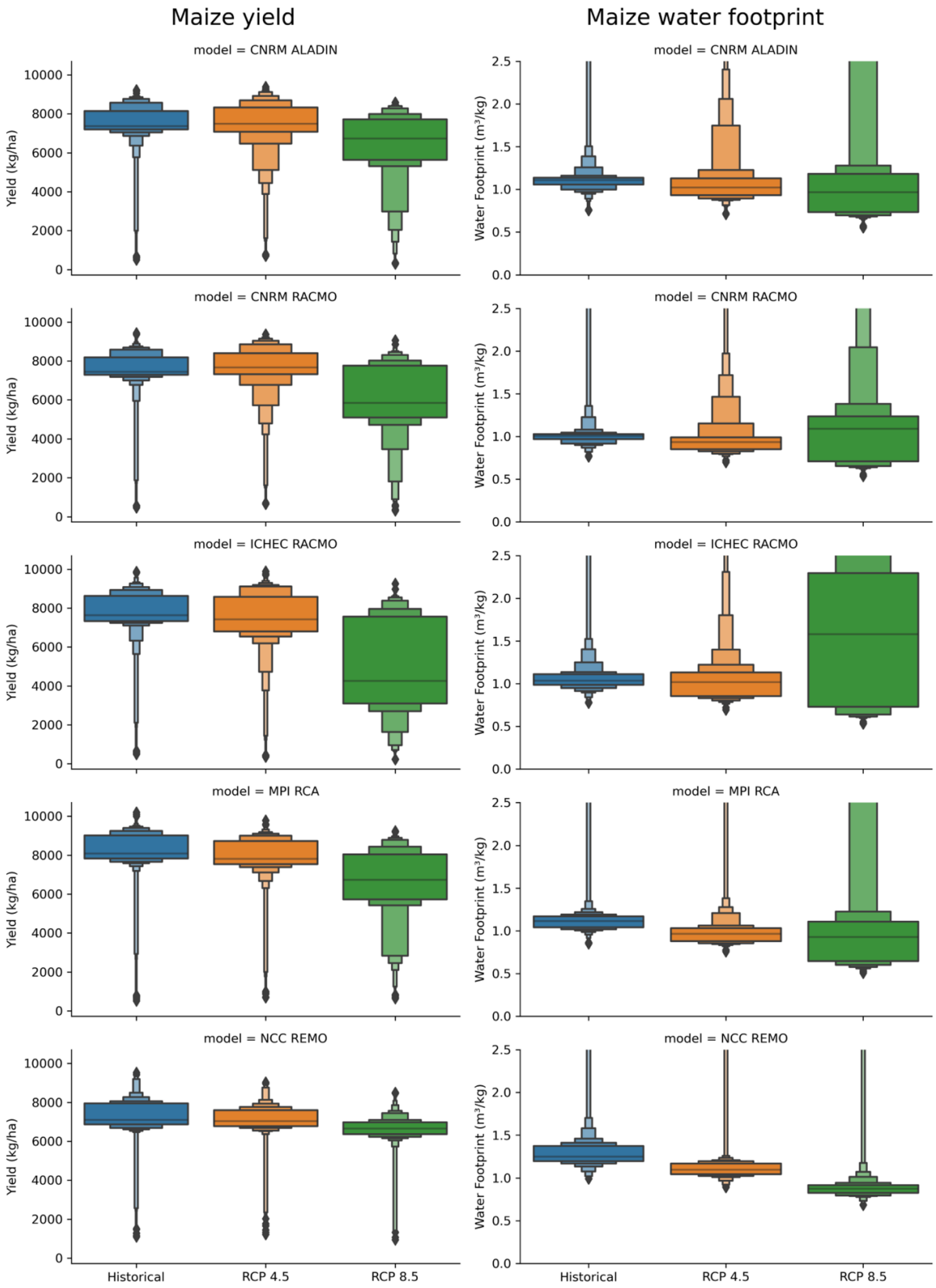

Figure A4.3: Boxen plots of the 28-years average maize yield and water footprint for the five climate models and the historical, RCP 4.5 and 8.5 scenarios.

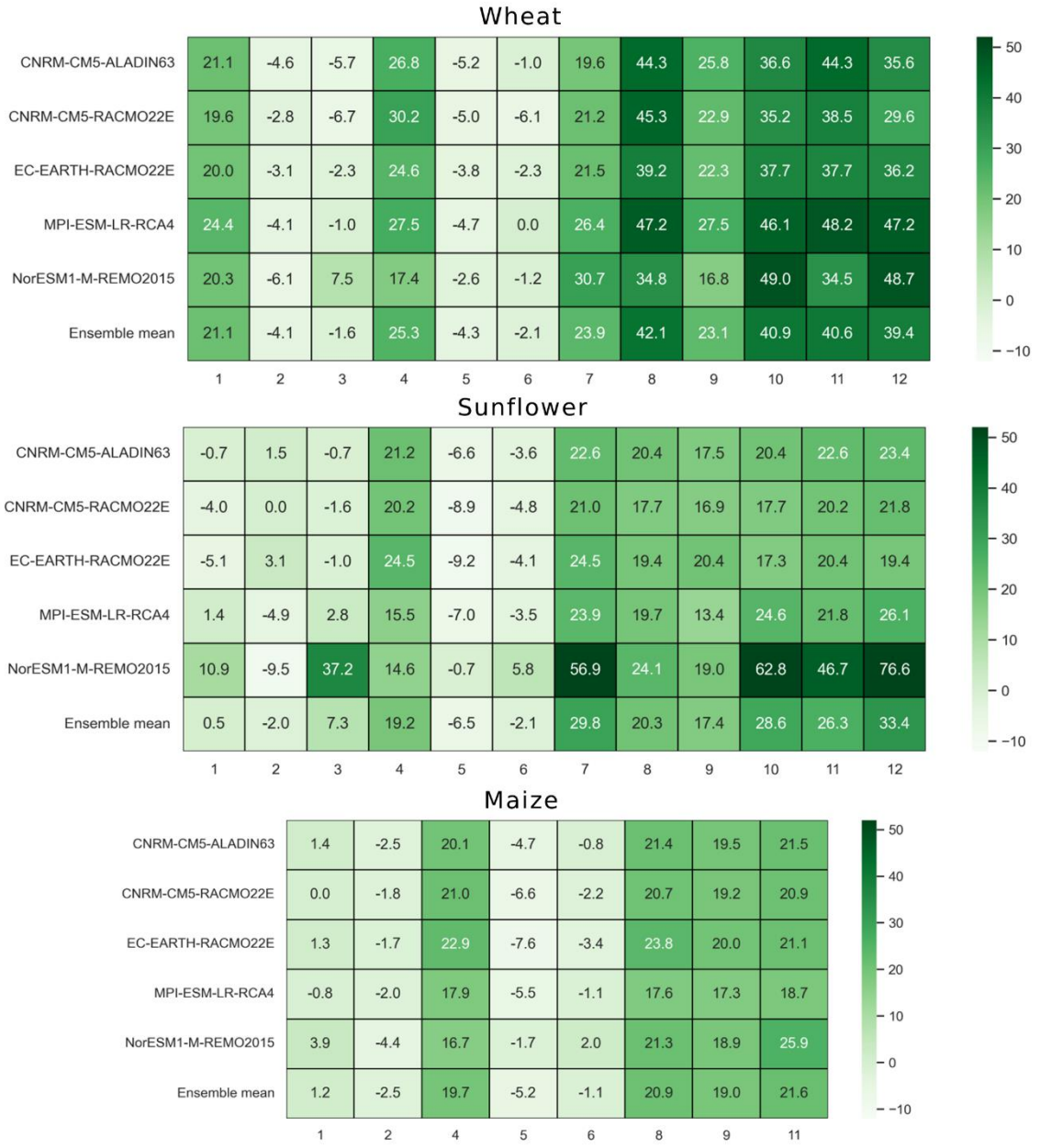

Figure A4.4: Effect of adaptation strategies on crop yield. Heatmaps created with the percentage changes for durum wheat, sunflower and maize yields, calculated considering the "no adaptation" and the different adaptation scenarios, for RCP 8.5.

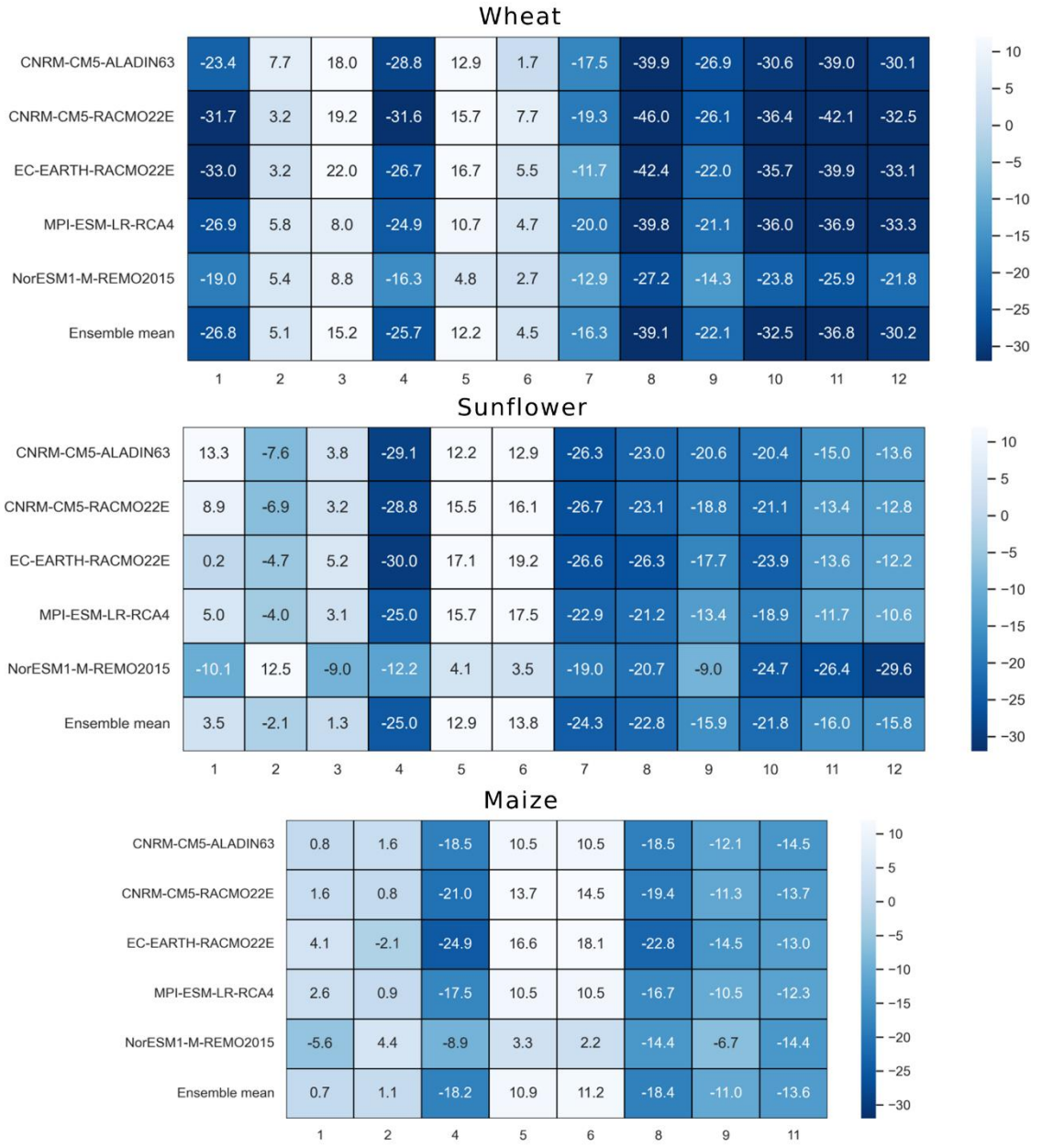

Figure A4.5: Effect of adaptation strategies on water footprint. Heatmaps created with the percentage changes for durum wheat, sunflower and maize water footprints, calculated considering the "no adaptation" and the different adaptation scenarios, for RCP 8.5.

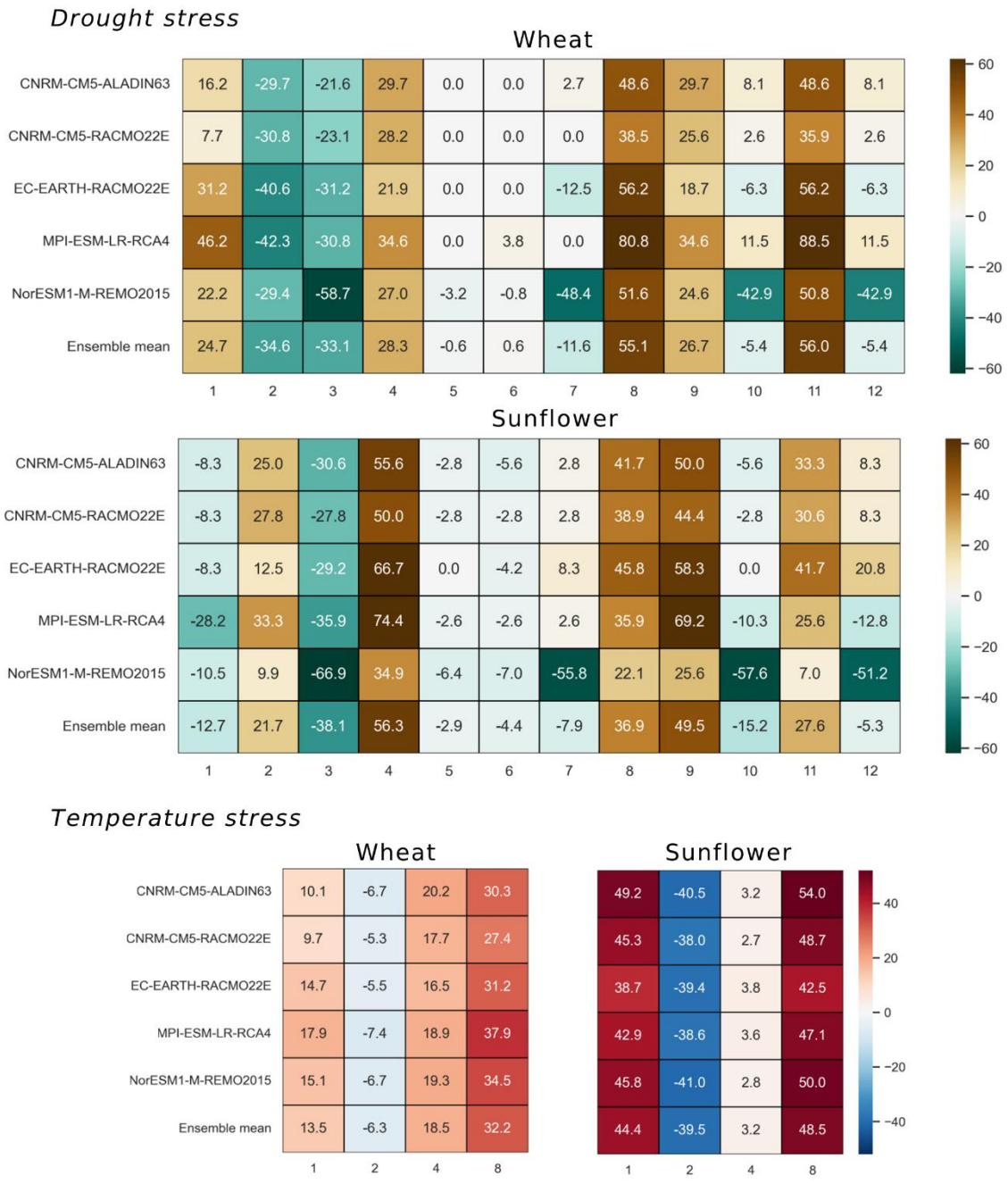

Figure A4.6: Effect of adaptation strategies on drought and temperature stresses. Heatmaps created with the percentage changes for durum wheat and sunflower drought and temperature stresses, calculated considering the "no adaptation" and the different adaptation scenarios, for RCP 8.5.

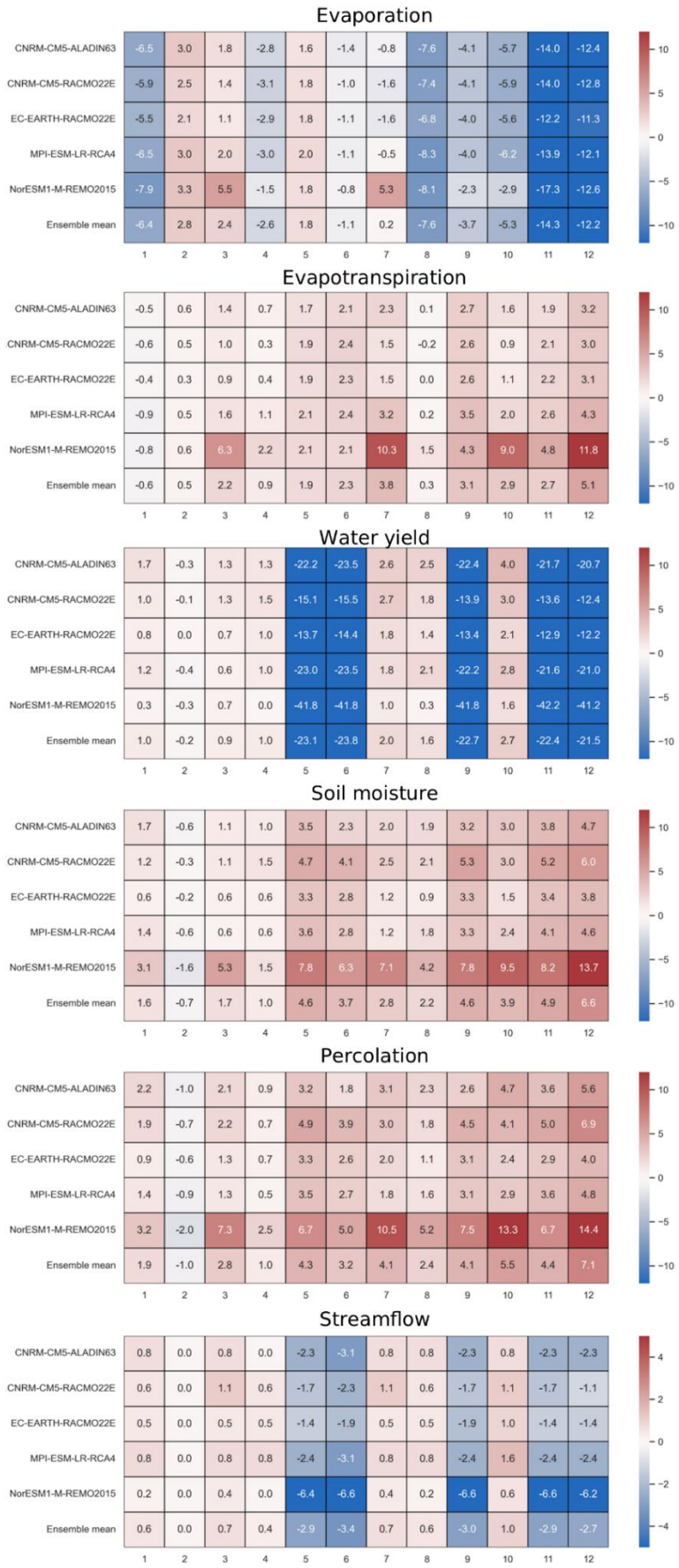

Figure A4.7: Effect of adaptation strategies on evaporation, evapotranspiration, water yield, soil moisture and percolation, considering only cropland, and streamflow at the outlet. Heatmaps created with the percentage changes, calculated considering the adaptation and no adaptation scenarios, for RCP 8.5.

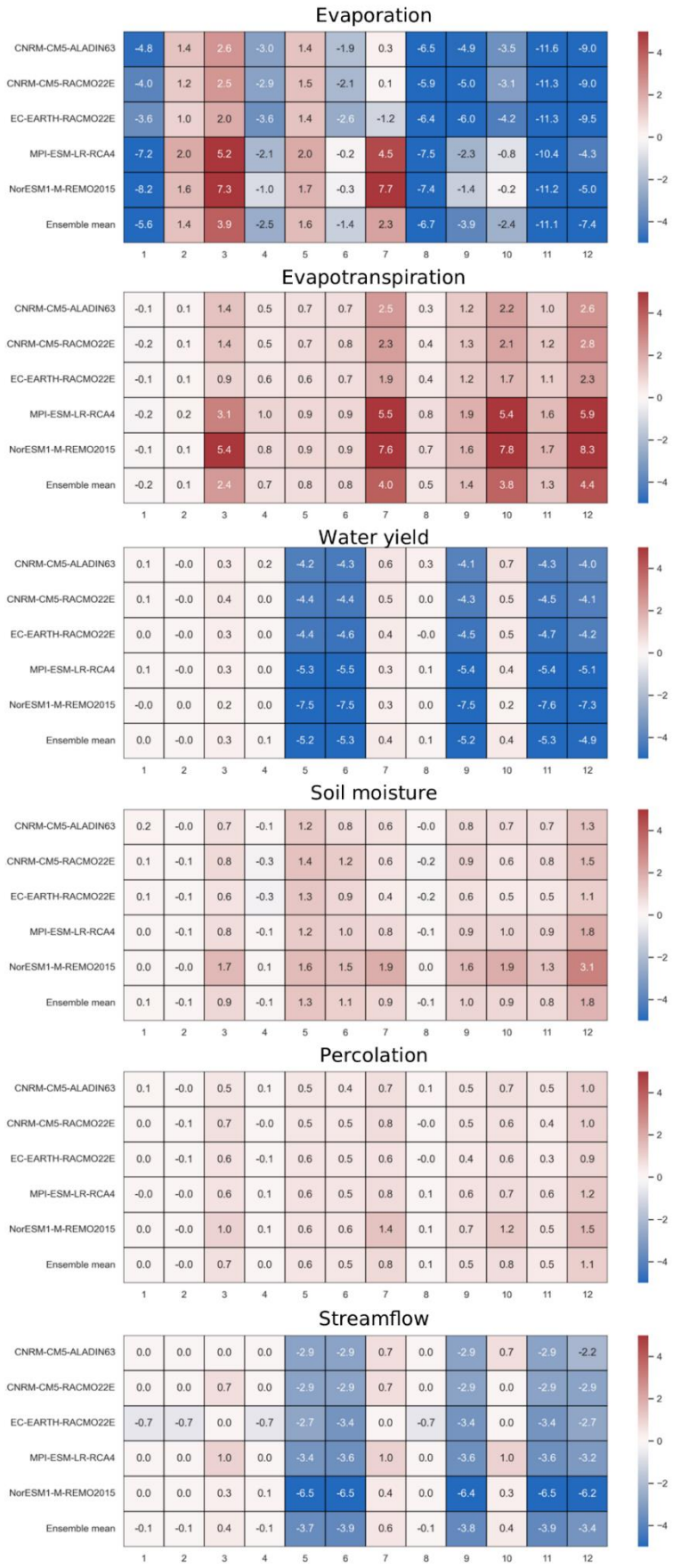

Figure A4.8: Effect of adaptation strategies on evaporation, evapotranspiration, water yield, soil moisture and percolation, considering the whole catchment, and streamflow at the outlet. Heatmaps created with the percentage changes, calculated considering the adaptation and no adaptation scenarios, for RCP 4.5.

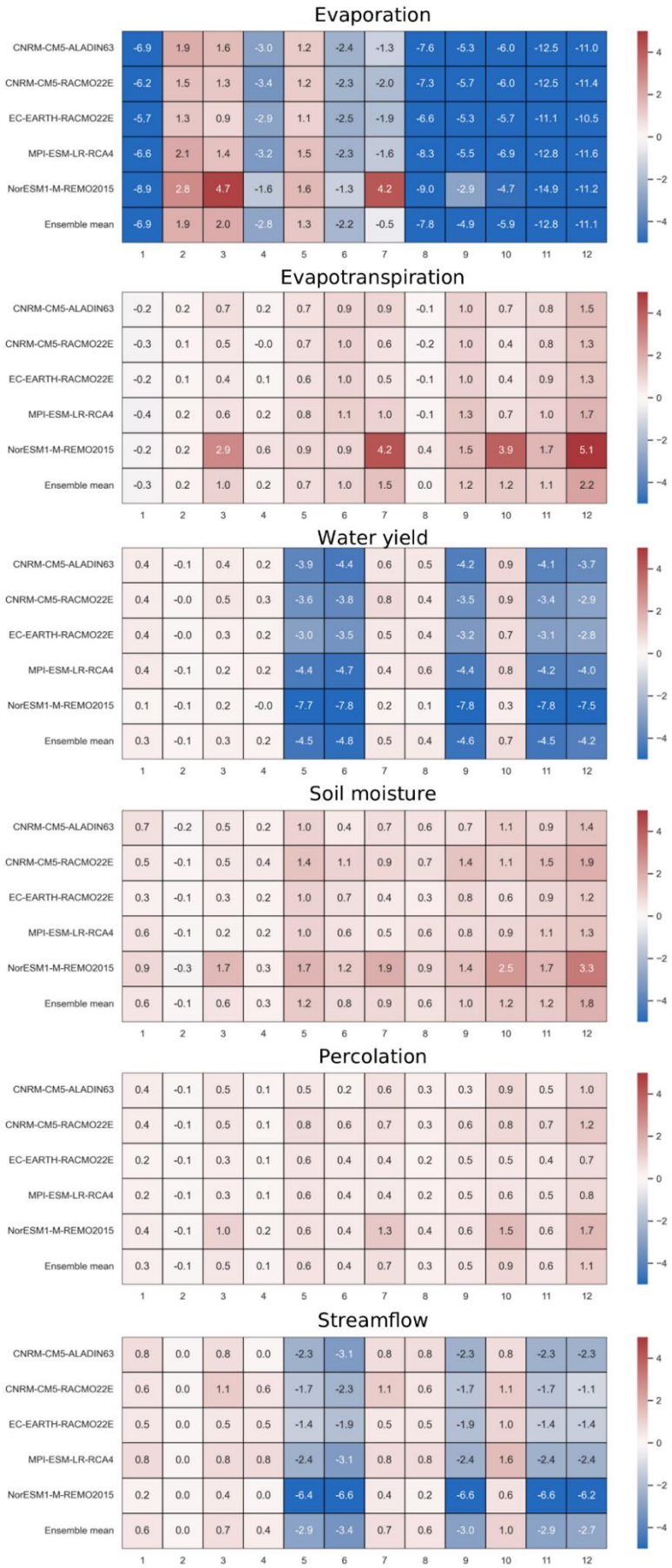

Figure A4.9: Effect of adaptation strategies on evaporation, evapotranspiration, water yield, soil moisture and percolation, considering the whole catchment, and streamflow at the outlet. Heatmaps created with the percentage changes, calculated considering the adaptation and no adaptation scenarios, for RCP 8.5.

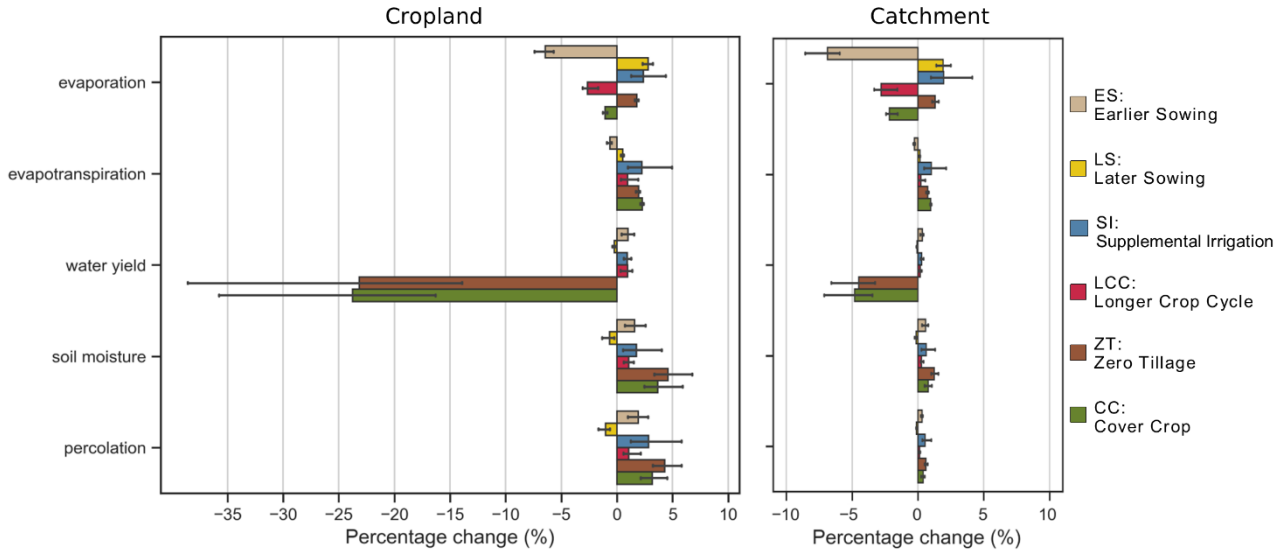

Figure A4.10: Comparison of the effects of adaptation strategies on water balance components for the whole catchment and only for cropland where the adaptation strategies are implemented. The barplots are created considering the percentage relative differences between adaptation and no adaptation scenarios. The graphs use outputs of RCP 8.5 simulations.

A5: Supplementary materials chapter 5

Part 1: Set up, calibration, validation and simulation of the SWAT+ model for the Juba and Shabelle catchments

0- Purpose of the model

This SWAT+ model setup is aimed at performing a climate risk assessment including model outputs to calculate indicators of climate hazards and adaptive capacity. The main focus is on water and agriculture, and therefore particular attention is given to crop yields.

1- Model setup

Data availability is a huge constraint especially in Somalia but also in Ethiopia. We had to rely on global datasets and reanalysis data. The list of inputs is reported in Table A5.1.

Table A5.1: List of inputs used to set up the model and for the simulations.

Data	Product	Resolution	Source
DEM	SRTM	Resampled 250 m	earthexplorer.usgs.gov/
Soil	FAO	Approximately 7.5 km	swat.tamu.edu/data/
Land use	Copernicus Global Land cover map	250 m	wapor.apps.fao.org/
pr, tasmax, tasmin, rsds (cal&val)	CHELSA-W5E5	Approximately 55 km	data.isimip.org/
hurs, sfcWind (cal&val)	EWEMBI	Approximately 55 km	data.isimip.org/
Climate variables (climate change)	ipsl-cm6a-lr_r1i1p1f1_w5e5 mri-esm2-0_r1i1p1f1_w5e5	Approximately 55 km	data.isimip.org/
Fertilizers	LUH2		luh.umd.edu/data.shtml
Crop calendar	FAO crop calendar	National	cropcalendar.apps.fao.org/#/home
Cropping pattern	Reports	Regional	Basnyat, 2007; FAO and WFP, 1997; EU, 2010

The model was set up for the period 1979-2016. To optimize crop simulation in the Somalian part of the basin maintaining a reduced simulation time, we did not set any slope threshold to create additional HRUs. Also, we reduced the number of subbasins in the upland Ethiopia. We based our representation of Somalian cropping patterns on reports from FAO and the European Union (Basnyat, 2007; FAO and WFP, 1997; EU, 2010). We split the rainfed agricultural land use into sorghum and maize, double-cropped in both rainy seasons. In the regions of Bay, Lower Shabelle and Lower Juba we set rainfed maize, while in the other regions rainfed sorghum. In the irrigated cropland we always set maize double-cropping, again cultivated only during the rainy seasons, for consistency.

The final basin delineation counted 32 subbasins, 1085 landscape units, and 6551 HRUs (Figure A5.1). The total area of the basin is 517740 km^2. Rangeland covers about 71%, followed by forests, slightly higher than 15%. Irrigated maize covers 1.06% of the whole basin, sorghum 0.15**%**, and rainfed corn 0.37%. We considered as irrigated cropland the WaPOR land use map class “Cropland, irrigated or under water management”, and it is worthwhile to note that the irrigated area is much higher compared for example to the Land Use Harmonization 2 (LUH2) dataset which we used as input in the following simulations of this study. Hence, we did not consider the total aggregated yield in the creation of our indicator, but we considered the yield/ha of rainfed maize and sorghum and irrigated maize. The cropland area is instead very similar to the land cover map used to set up the model and LUH2.

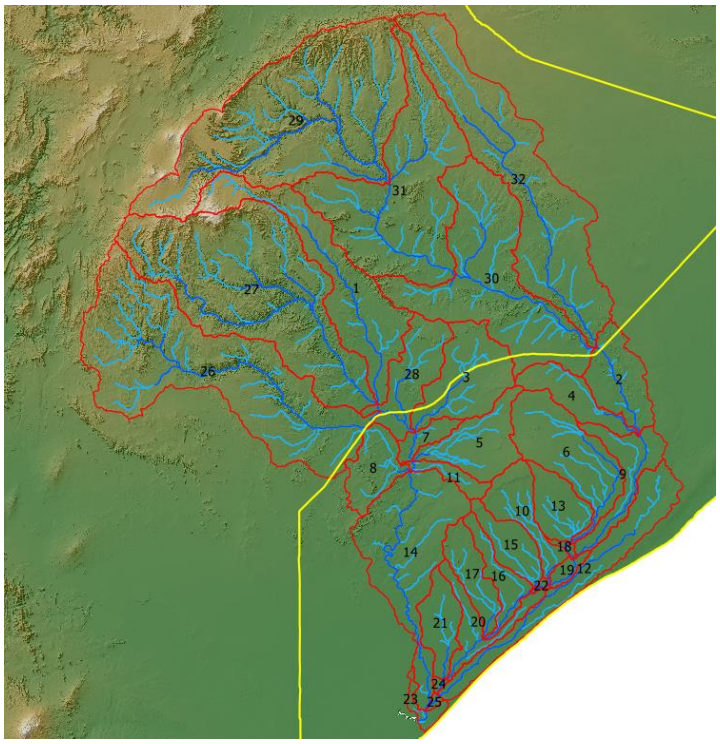

Figure A5.1: Elevation, subbasins, channels, and streams created in the delineation phase of the model, with the Somalian border.

The fertilization was set based on the LUH2 dataset, by calculating the average of the C4 crops, weighted considering the cropland area. We considered only C4 crops as they are the largest type of crop cultivated in Somalia and it is also reflected in LUH2 data. The dataset reports only nitrogen fertilization, and we assume the same amount of phosphorus applied. The annual amount was split between the two crops for each growing season, applied after sowing. The initial sowing and crop cycle length were retrieved from the FAO crop calendar data, even if these were then adjusted when calibrating with LAI and also considering other documents (Basnyat et al., 2007). More in detail, we created decision tables to better simulate the sowing strategy of farmers, which consists of sowing when the soil is wet enough in a given time window. Tillage was also scheduled before sowing. Automatic furrow irrigation was applied for irrigated maize, triggered by a water stress threshold of 0.1. Management operations are specified in Table A5.2.

Table A5.2: Management operations with date, description and crops used in the study.

Operation	**Date (dd/mm)**	**Description**	**Crops**
1st growing season (Gu)			
Tillage	15/03	Springplow	All
Sowing	21/03 – 10/04	Sowing time window	All
N fertilization	15/04	Elemental nitrogen, broadcast application	All
P fertilization	15/04	Elemental phosphorous, broadcast application	All
Harvest	<= 25/07	Later harvesting date allowed	All
Irrigation	Automatic	Furrow irrigation: 50 mm applied with 0.7 of efficiency, triggered by a 0.5 water stress threshold.	Irrigated maize
2nd growing season (Deyr)			
Tillage	05/09	Springplow	All
Sowing	11/09 -30/09	Sowing time window	All
N fertilization	05/10	Elemental nitrogen, broadcast application	All
P fertilization	05/10	Elemental phosphorous, broadcast application	All
Harvest	<= 15/01	Later harvesting date allowed	All
Irrigation	Automatic	Furrow irrigation: 30 mm applied with 0.5 of efficiency, triggered by a 0.1 water stress threshold.	Irrigated maize

2- Calibration and validation strategy

We applied a multi-step calibration process with multiple variables (Table A5.3) starting from Leaf Area Index (LAI) calibration to correctly match the two growing seasons and adjust the LAI parameters of crops, considering monthly average values. We then used the SWAT+Toolbox (v 1.0) to calibrate the model for discharge at Luuq and Belet Weyne gauging stations. Finally, we calibrate and validate the model for rainfed sorghum and rainfed and irrigated maize yield in representative HRUs. The parameters modified are reported together in Table 7.

Table 3: the data used with the period, time step, zones of application and the source.

Variable	Period	Time step	Zones	Source
LAI	2004-2014	Monthly average	Selected HRUs with cropland in Somalia	Copernicus, CGLOPS-1 (v. 2)
Streamflow	1984-1986 for calibration, 1987-1989 for validation	Monthly	Juba and Shabelle catchments	FAO-SWALIM
Crop yield	2004-2009 for validation, 2010-2014 for calibration	Gu and Deyr crop yields	Representative HRUs in Somalia	FEWS NET

A - Leaf area index

The selection of the HRUs considered in this calibration was based on an area threshold of 50 hectares and by visually checking the correspondence between LAI maps and land use, to be sure to include herbaceous crops and not perennial crops, characterized by high LAI throughout the year. We modified the parameters related to the LAI of sorghum and maize and we adapted the sowing date decision table and the days to maturity of the crops. The LAI remote sensing product has a low resolution and in the pixels there is mixed vegetation and also bare soil. For each HRU included in this part of the calibration, we considered the mean value of the remote sensing LAI. Considering these limitations, we did not completely rely on the values, but we focused on temporally matching the growing seasons. Results are shown in Fig. A5.2.

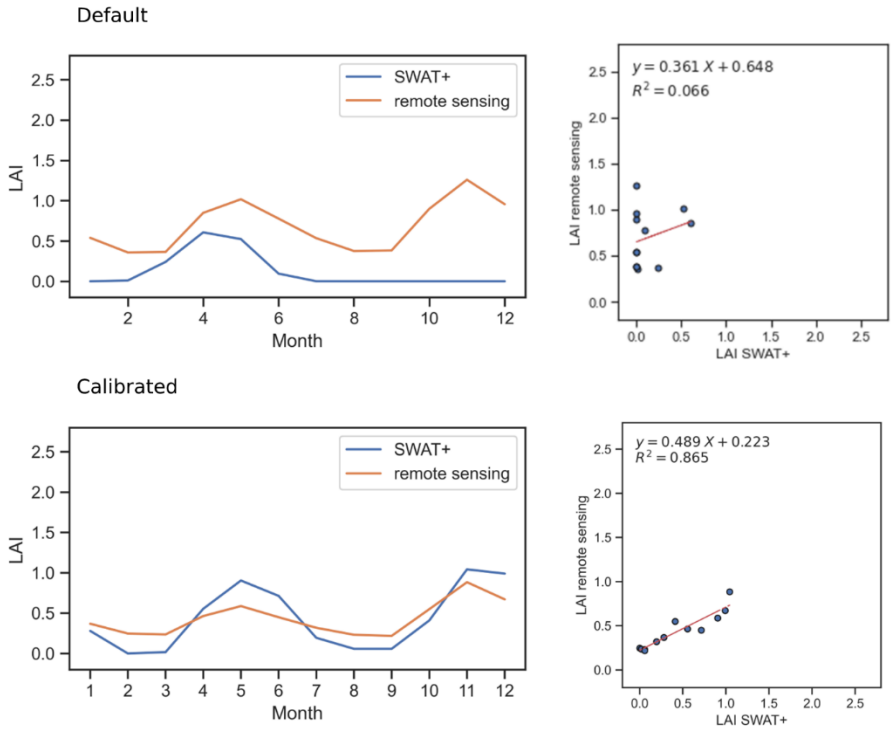

Figure A5.2: Monthly LAI for default and calibrated simulations.

B - Streamflow

We used the SWAT+ Toolbox to perform automatic calibration for the Luuq and Belet Weyne gauging stations. Satisfactory performances were obtained only for Luuq (Fig. A5.3, Table A5.4) and the Juba river, and therefore we only considered them in the calculation of the indicators to be used in the climate risk assessment. The calibrated values for Belet Weyne and the Shabelle river were kept to at least have a reasonable average representation of flow, which was highly overestimated by SWAT+. Performances at Luuq are satisfactory or better according to the criteria of Moriasi et al. (2007). Given the very low quality of the input data and the exploratory nature of the study, we consider the model validated for streamflow.

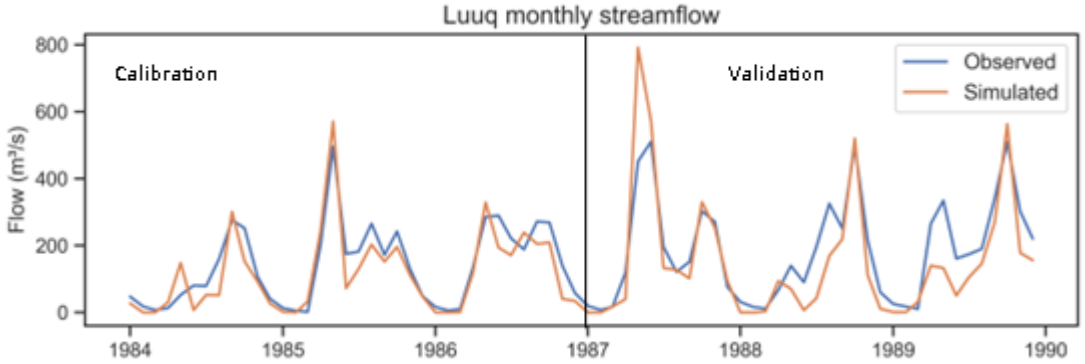

Figure A5.3: Hydrograph for Luuq with the monthly streamflow for calibration and validation.

Table A5.4: Performance statistics at the Luuq gauging station.

Streamflow	Calibration	Validation
NSE	0.79	0.65
Pbias	15.4%	18.1%
RSR	0.46	0.62
R^2	0.84	0.79

C- Crop yield

At the end of the process, we optimized the performance of the model in the simulation of maize (irrigated and rainfed) and sorghum (rainfed) yields. We selected the largest HRUs that are representative of cropping patterns in Somalia. The representative HRU for rainfed sorghum is in Bakool, in the Tiyeeglow and Xudur districts. The representative HRU for rainfed maize is in Bay, in the Baydhabo district. The representative HRU for irrigated maize is in Lower Shabelle, mainly in the Qoryooley district but also in Kuntuwaaray, Afgooye and Marka. Since Gu is the main growing season, we considered it for calibration and validation. We coupled a manual calibration to modify the plants.plt input file, to achieve similar magnitudes of values, with automatic calibration with the SWAT+ Toolbox, where we optimized RMSE by modifying parameters related to soil water.

SWAT+ model performances were satisfactory for irrigated maize (Fig. A5.4, Table A5.5) and rainfed sorghum (Fig. A5.5, Table A5.6), which we finally considered in the calculation of the indicators to be used in the climate risk assessment. Pbias and RMSE values were always satisfactory or better according to the criteria of Jamieson et al. (1991), while yield variability was captured only in the calibration period, with good values of R^2.

We had to strongly reduce yields, especially of maize, and we mostly did it by reducing the harvest index and LAI. We avoided modifying the radiation use efficiency parameter since it is also used in the equations to simulate the effect of CO_2 concentration. It is important to keep in mind that SWAT+ does not simulate yield reductions due to pests, diseases and extreme events such as floods, but only considers nutrients, temperature and water stresses. Despite the severe limitations in data availability and the simplified representation that we adopted, we could obtain satisfactory performances. Furthermore, it is known that the SWAT+ model is not optimal for estimating interannual crop yield variability, but it is reliable when estimating long-term average yields. For the purpose of this study, we considered the SWAT+ model validated for rainfed sorghum and irrigated maize crop yields.

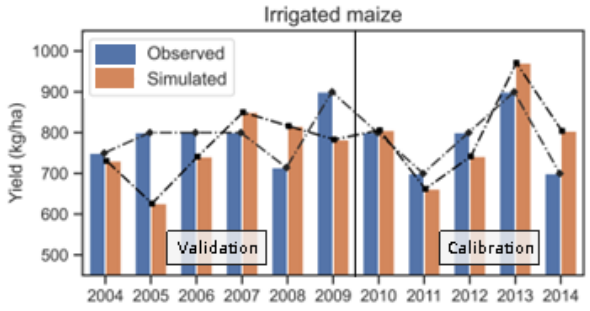

Figure A5.4: Calibration and validation for irrigated maize.

Table A5.5: Performance statistics for irrigated maize.

Maize	Calibration	Validation
Pbias	-2.2%	4.6%
RMSE	64.3 kg/ha	100.5 kg/ha
R^2	0.63	0.00

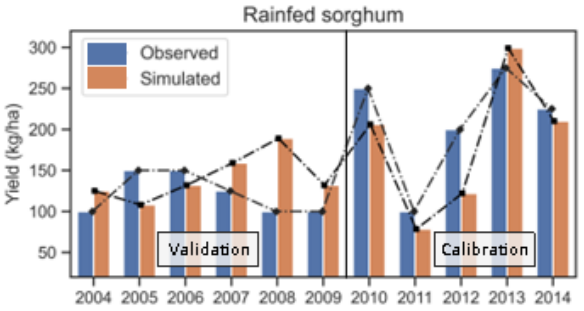

Figure A5.5: Calibration and validation for rainfed sorghum.

Table A5.6: Performance statistics for rainfed sorghum.

Sorghum	Calibration	Validation
Pbias	12.8%	-16.6%
RMSE	43.1 kg/ha	46.2 kg/ha
R^2	0.82	0.21

Table A5.7: Parameters and setting changed during the calibration process.

Parameters / setting	Zones/crops	File changed	Default value	Final value / %change
cn2	Juba	*calibration.cal*		-19.94%
cn2	Shabelle	*calibration.cal*		-18.76%
esco	Juba	*calibration.cal*		0.187
esco	Shabelle	*calibration.cal*		0.985
epco	Juba	*calibration.cal*		0.454
epco	Shabelle	*calibration.cal*		0.975
awc	Juba	*calibration.cal*		17.79%
awc	Shabelle	*calibration.cal*		19.44%
canmx	Juba	*calibration.cal*		-17.72%
canmx	Shabelle	*calibration.cal*		18.29%
k	Juba	*calibration.cal*		19.83%
k	Shabelle	*calibration.cal*		18.89%
perco	Juba	*calibration.cal*		19.78%
perco	Shabelle	*calibration.cal*		19.90%
surlag	Juba	*calibration.cal*		14.84
surlag	Shabelle	*calibration.cal*		7.25
esco	Rainfed sorghum (HRU 932)	*calibration.cal*		0.326
esco	Irrigated maize (HRU 1656)	*calibration.cal*		0.640
epco	Rainfed sorghum (HRU 932)	*calibration.cal*		0.028
epco	Irrigated maize (HRU 1656)	*calibration.cal*		0.119
awc	Rainfed sorghum (HRU 932)	*calibration.cal*		-19.39%
awc	Irrigated maize (HRU 1656)	*calibration.cal*		5.91%
z	Rainfed sorghum (HRU 932)	*calibration.cal*		-13.84%
z	Irrigated maize (HRU 1656)	*calibration.cal*		6.67%
k	Rainfed sorghum (HRU 932)	*calibration.cal*		16.85%
k	Irrigated maize (HRU 1656)	*calibration.cal*		-7.72%
perco	Rainfed sorghum (HRU 932)	*calibration.cal*		-14.43%
perco	Irrigated maize (HRU 1656)	*calibration.cal*		-10.57%
harv_idx	Maize	*plants.plt*	0.55	0.14
harv_idx	Sorghum	*plants.plt*	0.45	0.14
lai_pot	Maize	*plants.plt*	6	1.5
lai_pot	Sorghum	*plants.plt*	3	1.5
frac_hu1	Maize	*plants.plt*	0.15	0.1
frac_hu1	Sorghum	*plants.plt*	0.15	0.1
frac_hu2	Maize	*plants.plt*	0.5	0.45
frac_hu2	Sorghum	*plants.plt*	0.5	0.45
hu_lai_decl	Maize	*plants.plt*	0.8	0.75
hu_lai_decl	Sorghum	*plants.plt*	0.64	0.6
days_to_maturity	Maize	*plants.plt*		95
days_to_maturity	Sorghum	*plants.plt*		95
harv_idx_ws	Maize	*plants.plt*	0.3	0.1
harv_idx_ws	Sorghum	*plants.plt*	0.25	0.1
can_ht_max	Maize	*plants.plt*	2.5	1.5
rt_dp_max	Maize	*plants.plt*	2	1.5
rt_dp_max	Sorghum	*plants.plt*	2	1.5

3- Simulations

The historical simulations were set up for the period 1982-2014 while the future simulations were for the period 2068-2100, with three years of warm-up. We considered all the SSPs available in the CMIP6 simulations, and we retrieved bias-corrected climate input data from the ISIMIP data repository. While for SSPs 126, 245, 370 and 585 more General Circulation Models (GCMs) can be downloaded, for the SSP460 only the ipsl-cm6a-lr and the mri-esm2-0 are available. Hence, we considered only these two GCMs for all the SSPs (Table A5.1). All climate variables needed are available, except for relative humidity in SSPs 245 and 460. CO_2 values were retrieved from the ISIMIP repository (Büchner and Reyer, 2022), and we used the averaged 30 years as SWAT+ does not allow dynamical simulation of CO_2 concentrations (Table A5.6).

Table A5.6: CO_2 concentration values used in the simulations.

Simulation	CO_2 concentration (ppm)
base	366
historical	366
SSP126	461
SSP245	590
SSP370	757
SSP460	635
SSP585	940

The management was not changed in the main simulations to estimate the impacts of climate change on crop yields. Days to maturity are modified considering the increased temperatures due to climate warming (Table A5.8). The heat units are calculated for the calibration and validation simulation, considering the calibrated days to maturity for sorghum and maize. By subtracting the base temperature from the average temperature calculated by SWAT+ at HRU level, and averaged per month, we calculated the days to maturity required to reach the same amount of heat units, per scenario and GCM.

Table A5.7: Fertilization and irrigated areas used in the different scenarios considered.

Simulation	N fertilization (kg/ha/yr)	Irrigated area (%)
base	13	6
historical	13	6
SSP126	24.1	20
SSP245	100.1	1
SSP370	10	2
SSP460	14.9	2
SSP585	37.1	30

Adaptive capacity is simulated with SWAT+ simulating adaptation strategies, namely change in sowing dates and longer crop cycles. In these simulations, we also modified fertilizer application which was retrieved from LUH2 for the year 2100 (Table A5.7). Decision tables for sowing are modified moving the time window for sowing 20 days earlier and 20 days later. Days to maturity of the crops simulated are increased considering 224 more heat units required to reach maturity. We calculated the 224 heat units as the average increase in heat units with the increasing temperatures with constant days to maturity at 95 days, under all scenarios. We preferred to use this approach to remain consistent with the heat units' concept and not to favour the highest emission scenarios with the highest increases in temperature. As can be seen in Table A5.8, the maximum increase is 13 days and the minimum 9 days.

Table A5.8: Calculated heat units and days to maturity used in the simulations.

Scenario	GCM	Crop	Days to maturity	Heat units	New days to maturity	New heat units	Adapted heat units	Adapted days to maturity
base	\	sorghum	95	1723			1947	
base	\	irrigated corn	95	1986			2210	
base	\	rainfed corn	95	1950			2174	
historical	ipsl-cm6a-lr	sorghum	95	1718	\	\		
historical	ipsl-cm6a-lr	irrigated corn	95	1982	\	\		
historical	ipsl-cm6a-lr	rainfed corn	95	1944	\	\		
historical	mri-esm2-0	sorghum	95	1716	\	\		
historical	mri-esm2-0	irrigated corn	95	1980	\	\		
historical	mri-esm2-0	rainfed corn	95	1942	\	\		
ssp126	ipsl-cm6a-lr	sorghum	95	1825	89	1715	1954	102
ssp126	ipsl-cm6a-lr	irrigated corn	95	2089	90	1983	2216	101
ssp126	ipsl-cm6a-lr	rainfed corn	95	2050	90	1946	2175	101
ssp126	mri-esm2-0	sorghum	95	1793	91	1722	1954	104
ssp126	mri-esm2-0	irrigated corn	95	2052	92	1991	2218	103
ssp126	mri-esm2-0	rainfed corn	95	2011	92	1950	2173	103
ssp245	ipsl-cm6a-lr	sorghum	95	1944	84	1724	1944	95
ssp245	ipsl-cm6a-lr	irrigated corn	95	2206	85	1979	2206	95
ssp245	ipsl-cm6a-lr	rainfed corn	95	2166	85	1942	2166	95
ssp245	mri-esm2-0	sorghum	95	1861	88	1730	1954	100
ssp245	mri-esm2-0	irrigated corn	95	2122	89	1993	2207	99
ssp245	mri-esm2-0	rainfed corn	95	2082	89	1956	2166	99
ssp370	ipsl-cm6a-lr	sorghum	95	2047	80	1729	1942	90
ssp370	ipsl-cm6a-lr	irrigated corn	95	2309	82	1997	2213	91
ssp370	ipsl-cm6a-lr	rainfed corn	95	2268	82	1961	2175	91
ssp370	mri-esm2-0	sorghum	95	1973	82	1713	1953	94
ssp370	mri-esm2-0	irrigated corn	95	2233	84	1983	2211	94
ssp370	mri-esm2-0	rainfed corn	95	2193	84	1948	2171	94
ssp460	ipsl-cm6a-lr	sorghum	95	1988	82	1722	1947	93
ssp460	ipsl-cm6a-lr	irrigated corn	95	2250	84	1994	2203	93
ssp460	ipsl-cm6a-lr	rainfed corn	95	2209	84	1958	2164	93
ssp460	mri-esm2-0	sorghum	95	1917	85	1724	1955	97
ssp460	mri-esm2-0	irrigated corn	95	2177	86	1978	2221	97
ssp460	mri-esm2-0	rainfed corn	95	2136	86	1941	2179	97
ssp585	ipsl-cm6a-lr	sorghum	95	2135	76	1713	1958	86
ssp585	ipsl-cm6a-lr	irrigated corn	95	2394	79	1995	2220	88
ssp585	ipsl-cm6a-lr	rainfed corn	95	2353	79	1960	2182	88
ssp585	mri-esm2-0	sorghum	95	2020	80	1734	1940	91
ssp585	mri-esm2-0	irrigated corn	95	2278	82	1977	2210	92
ssp585	mri-esm2-0	rainfed corn	95	2235	82	1940	2168	92

4- Physical indicators

A set of outputs from SWAT+ and climate models are produced representing hazard, environmental susceptibility and, indirectly, resilience (Table A5.9), to be coupled with the socio-economic indicators which represent exposure and vulnerability. Even if we performed an analysis with agronomic adaptation and no adaptation measures to quantify the adaptive capacity, in the final composite indicator we consider only the yield outputs of the best-performing adaptation simulation. Additionally, we are using the dataset produced by Khan et al. (2023) to estimate historical and future water consumption, considering respectively the years 2015 and 2100. Five climate models were used in that study, but for consistency with the models available in ISIMIP, we only used the ipsl climate model.

Table A5.9: Indicators used derived from SWAT+ or from climate models.

Indicator	Component	Method	Description	Reference
Crop yield change (CYLavg)	Hazard, resilience	SWAT+	Average yield, to take into account climate change impacts	/
Crop yield change (CYL25)	Hazard, resilience	SWAT+	First quartile yield, to take into account yield variability	/
Meteorological drought (CDD)	Hazard	GCMs	Longest dry spell, the maximum number of consecutive dry days with P < 1 mm	RICCAR, Mysiak et al. 2018
Extreme precipitation (R20)	Hazard	GCMs	Annual number of days with P > 20 mm	RICCAR, ETCDDI
Extreme temperature (SU40)	Hazard	GCMs	Annual number of days with TMAX > 40 °C	RICCAR, ETCDDI
Water availability (WTRav)	Environmental susceptibility	SWAT+	Sum of annual average water yield and recharge weighted for the area	
Water consumption (WTRco)	Environmental susceptibility	Tethys	Total water consumption	Khan et al. 2023

Part 2: Exploratory analysis of the socio-economic indicators to be used in the climate risk assessment

Here, the variables evaluated to be included as indicators are analyzed (Table A5.10).

A- Total population

Population is expected to increase under all scenarios except for SSP585. Large differences in the magnitudes of the increase are observed, ranging from minor to very high increases for SSPs 126 and 370, respectively.

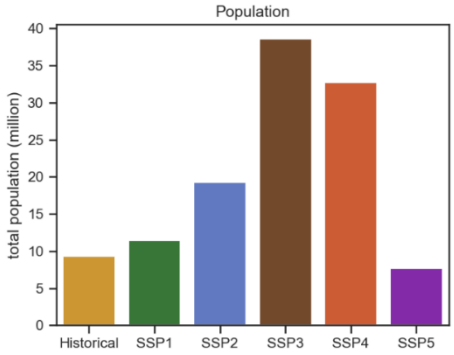

Figure A5.6: Total population in the scenarios considered.

B- Female population

The six scenarios considered are very similar, with values slightly higher than 50%.

Despite the importance of the gender issue, we are not including this indicator as it is not adding information to our composite indicator.

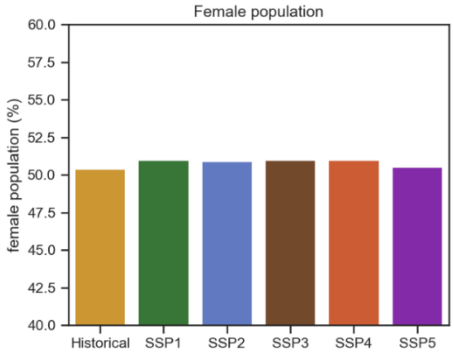

Figure A5.7: Female population in the scenarios considered.

C- Age

A huge change in the demography of the Somalian population is expected under all scenarios compared to 2010. Now, more than 40% of the population is under 15, and this percentage is expected to decrease especially under SSPs 126 and 585. On the other hand, the population over 65 is expected to increase, with the same scenarios that showed the highest increases. We consider young and old populations equally vulnerable, and therefore the impact of age is not as high as if we were to differentiate between different age groups. Operationally, we consider as an indicator the sum of the percentage of young and old age groups.

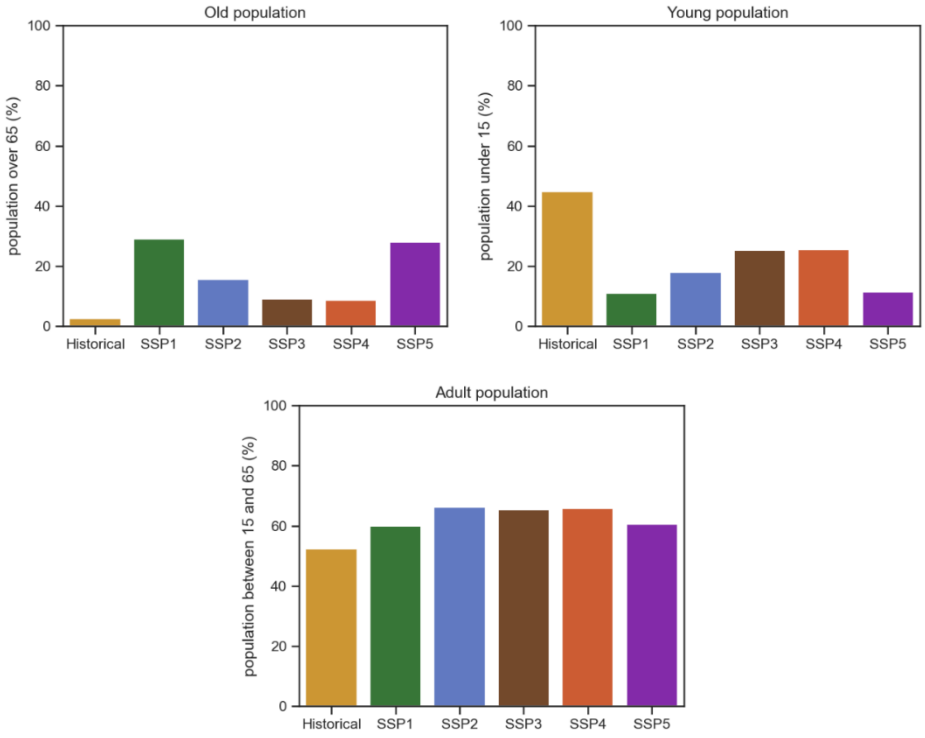

Figure A5.8: Age in the scenarios considered.

D- Urbanization

The share of urban population is expected to increase under all scenarios compared to 2010 (<40%). In particular, the share of people living in cities will be higher than 80% under SSPs 126, 460 and 585.

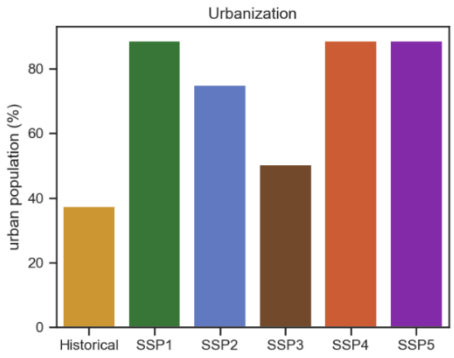

Figure A5.9: Urbanization in the scenarios considered.

E- Gross Domestic Products

The GDP is expected to increase by 2100 under all scenarios. The highest value is reached with SSP585, followed by SSPs 126 and 245. SSPs 370 and 460 show increases compared to the actual situation, but it is important to keep in mind that the figure shows the aggregated value and not per capita, and the population in these two scenarios is projected to drastically increase.

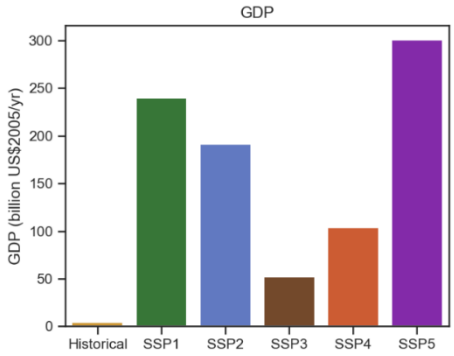

Figure A5.10: GDP in the scenarios considered.

F- Income Gini coefficient

Income inequality is projected to slightly increase for SSPs 370 and 460, while it significantly decreases for SSPs 126, 245, and 585. Despite the availability of projections for Somalia, the main model on which estimates are based did not include Somalia (Rao et al., 2019). Also, the two main explanatory variables are education and total factor productivity, which we also include directly or indirectly in our composite indicator. Hence, we are not considering the Income Gini coefficient as a vulnerability indicator. For the same reasons, we did not consider data about projected poverty headcounts, generated in the same study.

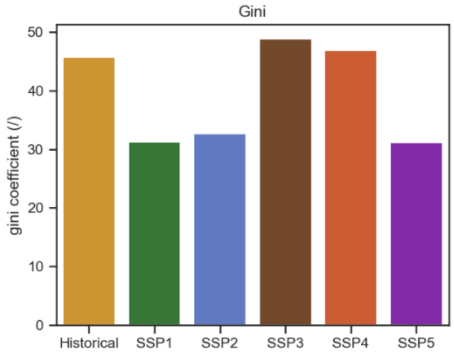

Figure A5.11: Gini coefficient in the scenarios considered.

G- Conflicts

Conflicts are very likely to occur in 2100 under SSPs 370 and 460, with probabilities higher than 50%, while for the other scenarios, the probability is lower than 10%.

The model used by Hegre et al. (2016) showed that conflict incidence declines as GDP and education increase while it increases with larger populations. The probabilities are available for the year 2100, but of course not for our baseline period since it is senseless to calculate probabilities for the past. As we included the GDP, population and education indicators in our analysis, and since our aim is also to compare with the present and historical situations, we are excluding conflict probability from our composite indicator.

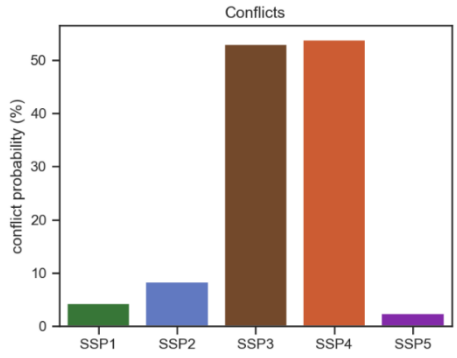

Figure A5.12: Conflicts in the scenarios considered.

H- Education

Future projections show an increase in literacy. The percentage of the population without education will decrease from more than 70% to 60% for SSPs 370 and 460 scenarios and below 20% for the other scenarios. Most of the people with education in SSPs 370 and 460 have only primary education. More than 50% have a secondary education level under SSP 245, the highest share. Under SSPs 126 and 585 slightly less than 40% of the population have tertiary education, a value slightly lower than secondary education.

To assign weights to the different levels of education, we consider no education the most vulnerable (weight value of 10) and tertiary education the least vulnerable (weight value of 0). The two intermediate primary and secondary education levels have weights of 3.33 and 6.66.

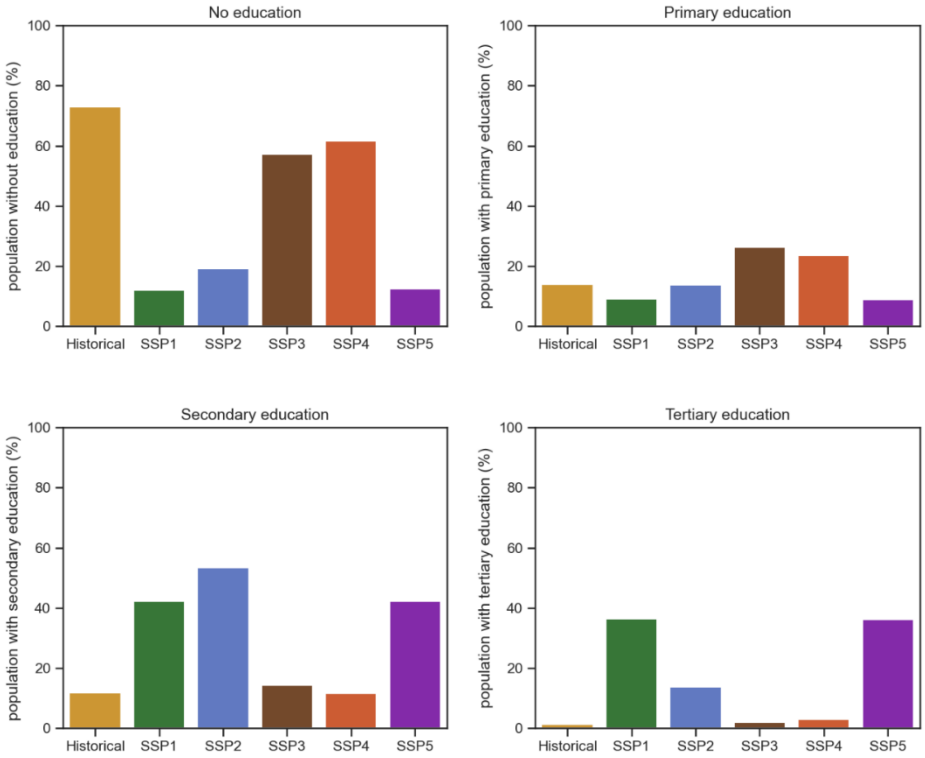

Figure A5.13: Education in the scenarios considered.

Table A5.10: The data considered, the unit, the categories, the motivation for considering them in the analysis, the sources and references are reported. Also, in the column "included" is specified if the data were used as indicator and how.

Data (unit)	Categories	Motivation	Included	Source	Reference
Total population (million)	/	Population is often used as the main exposure indicator	Yes, as exposure indicator	SSP Database - Version 2.0 (IIASA)	Samir KC, Wolfgang Lutz, The human core of the shared socioeconomic pathways: Population scenarios by age, sex and level of education for all countries to 2100, Global Environmental Change, Volume 42, 2017, 181-192, 3780, DOI:10.1016/j.gloenvcha.2014.06.004
Female population (%)	/	Female population is generally considered more vulnerable	No, value is always around 50%	SSP Database - Version 2.0 (IIASA)	Samir KC, Wolfgang Lutz, The human core of the shared socioeconomic pathways: Population scenarios by age, sex and level of education for all countries to 2100, Global Environmental Change, Volume 42, 2017, 181-192, 3780, DOI:10.1016/j.gloenvcha.2014.06.004
Age (% of population)	Young, adult, old population (<15 years, between 15 and 65 years, >65 years, respectively)	Young and old population is generally considered more vulnerable	Yes, considering young and old share of population	SSP Database - Version 2.0 (IIASA)	Samir KC, Wolfgang Lutz, The human core of the shared socioeconomic pathways: Population scenarios by age, sex and level of education for all countries to 2100, Global Environmental Change, Volume 42, 2017, 181-192, 3780, DOI:10.1016/j.gloenvcha.2014.06.004
Urbanization (%)	/	Rural population is generally considered more vulnerable	Yes	SSP Database - Version 2.0 (IIASA)	Leiwen Jiang, Brian C. O'Neill, Global urbanization projections for the Shared Socioeconomic Pathways, Global Environmental Change, Volume 42, 2017, 193-199, DOI:10.1016/j.gloenvcha.2015.03.008
GDP (billion US$2005/year)	/	Poor population is generally considered more vulnerable	Yes, considering the aggregate value	SSP Database - Version 2.0 (IIASA)	Jesús Crespo Cuaresma, Income projections for climate change research: A framework based on human capital dynamics, Global Environmental Change, Volume 42, 2017, 226-236,, DOI:10.1016/j.gloenvcha.2015.02.012
Income Gini coefficient (/)	/	The higher the inequality the higher the vulnerability	No, we already consider the explanatory variables and Somalia is not included in the original model used	SSP Database - Version 2.0 (IIASA)	Rao, N. D., Sauer, P., Gidden, M., & Riahi, K. (2019). Income inequality projections for the Shared Socioeconomic Pathways (SSPs). Futures, 105 (June 2018), 27–39. https://doi.org/10.1016/j.futures.2018.07.001
Conflict probability (%)	/	Conflicts can be considered to increase the vulnerability of the population, even if some studies consider conflicts as human hazards	No, we already consider the main explanatory variables and data for the present are not available.	Hegre et al., 2016	Hegre, H., Buhaug, H., Calvin, K. V, Nordkvelle, J., Waldhoff, S. T., & Gilmore, E. (2016). Forecasting civil conflict along the shared socioeconomic pathways. Environmental Research Letters, 11(5), 054002. https://doi.org/10.1088/1748-9326/11/5/054002
Education (% of population)	Population without education and with primary, secondary and tertiary education	A less educated population is generally considered more vulnerable	Yes, assigning weights to the different education levels	SSP Database - Version 2.0 (IIASA)	Samir KC, Wolfgang Lutz, The human core of the shared socioeconomic pathways: Population scenarios by age, sex and level of education for all countries to 2100, Global Environmental Change, Volume 42, 2017, 181-192, 3780, DOI:10.1016/j.gloenvcha.2014.06.004

Part 3: Future climate in the Juba and Shabelle catchments, Somalia

The two climate models used in this study partially disagreed on future precipitation (Fig. A5.14). ipsl-cm6a-lr predicted a strong increase in annual average precipitation, ranging from 21.7% for SSP126 to 73.5% for SSP585. The increases were consistent also for the individual rainy seasons, even if they were higher in the Deyr season (September-October-November-December) as compared to the Gu season (April-May-June-July). On the other hand, the annual increases predicted by mri-esm2-0 were much smaller, less than 10.6% for all the SSPs. In the Gu season, the precipitation will decrease according to this model, with the highest decrease under SSP585 of -14.7%. In the Deyr season, MRI predicted increased precipitation, with the highest increase again being observed for SSP585, amounting to 38.2%.

The models showed a clear increasing trend in future temperatures under all SSPs (Fig. A5.14). Overall, the increases predicted by ipsl-cm6a-lr were slightly higher as compared to mri-esm2-0. The minimum increases (<5%) were found for SSP126, while the maximum (up to 18%) for SSP585. No significant differences in patterns or trends were observed comparing annual, Gu and Deyr average temperatures.

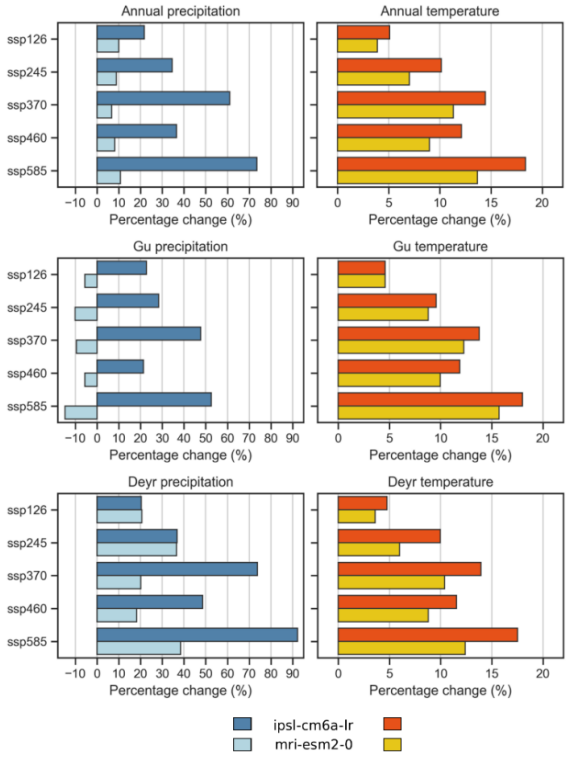

Figure A5.14: Percentage relative changes in precipitation and average temperature, considering the 30-years averages of the historical and future periods, and annual, Gu and Deyr seasons temporal scales.

Bibliography

1. Abbaspour, K. C., Rouholahnejad, E., Vaghefi, S., Srinivasan, R., Yang, H., & Kløve, B. (2015). A continental-scale hydrology and water quality model for Europe: Calibration and uncertainty of a high-resolution large-scale SWAT model. Journal of Hydrology, 524, 733–752. https://doi.org/10.1016/j.jhydrol.2015.03.027
2. Abbaspour, K. C., Vaghefi, S. A., Yang, H., & Srinivasan, R. (2019). Global soil, landuse, evapotranspiration, historical and future weather databases for SWAT Applications. Scientific Data, 6(1), 1–11. https://doi.org/10.1038/s41597-019-0282-4
3. Abdi-Soojeede, M. I. (2018). Crop Production Challenges Faced by Farmers in Somalia: A Case Study of Afgoye District Farmers. Agricultural Sciences, 09(08), 1032–1046. https://doi.org/10.4236/as.2018.98071
4. Abdullahi, O. A., Hassan, S. M. & Mohamed, M. J. (2022). Drought Effects in Somalia and Solution Proposals. African Journal of Climate Change and Resource Sustainability, 1(1), 13-25. https://doi.org/10.37284/ajccrs.1.1.807.
5. Adeux, G., Cordeau, S., Antichi, D., Carlesi, S., Mazzoncini, M., Munier-Jolain, N., & Bàrberi, P. (2021). Cover crops promote crop productivity but do not enhance weed management in tillage-based cropping systems. European Journal of Agronomy, 123, 126221. https://doi.org/10.1016/j.eja.2020.126221
6. AghaKouchak, A., Mirchi, A., Madani, K., Di Baldassarre, G., Nazemi, A., Alborzi, A., Anjileli, H., Azarderakhsh, M., Chiang, F., Hassanzadeh, E., Huning, L.S., Mallakpour, I., Martinez, A., Mazdiyasni, O., Moftakhari, H., Norouzi, H., Sadegh, M., Sadeqi, D., Van Loon, A.F., Wanders, N., 2021. Anthropogenic Drought: Definition, Challenges, and Opportunities. Rev. Geophys. 59, 1–23. https://doi.org/10.1029/2019RG000683
7. Ahmadalipour, A., & Moradkhani, H. (2018). Multi-dimensional assessment of drought vulnerability in Africa: 1960–2100. Science of the Total Environment, 644, 520–535. https://doi.org/10.1016/j.scitotenv.2018.07.023
8. Ahmadalipour, A., Moradkhani, H., Castelletti, A., & Magliocca, N. (2019). Future drought risk in Africa: Integrating vulnerability, climate change, and population growth. Science of the Total Environment, 662, 672–686. https://doi.org/10.1016/j.scitotenv.2019.01.278
9. Ahuja, L. R., Ma, L., & Anapalli, S. S. (2019). Biophysical system models advance agricultural research and technology: Some examples and further research needs. Bridging among disciplines by synthesizing soil and plant processes, 8, 1-32. https://doi.org/10.2134/advagricsystmodel8.2017.0008
10. Ainsworth, E. A., & Long, S. P. (2005). What have we learned from 15 years of free-air CO2 enrichment (FACE)? A meta-analytic review of the responses of photosynthesis, canopy properties and plant production to rising CO2. New phytologist, 165(2), 351-372. https://doi.org/10.1111/j.1469-8137.2004.01224.x
11. Aldinucci, M., Leonini, M., Marchetti, M. R., Nocchi, M., & Salleolini, M. (2012). Idrogeologia del sistema acquifero multifalda della pianura di Grosseto (Toscana meridionale). EngHydroEnv Geology 2012, 15, 61-81 - https://doi.org/10.1474/EHEGeology.2012-15.0-05.0295
12. Aloui, S., Mazzoni, A., Elomri, A., Aouissi, J., Boufekane, A., & Zghibi, A. (2023). A review of Soil and Water Assessment Tool (SWAT) studies of Mediterranean catchments: Applications, feasibility, and future directions. Journal of Environmental Management, 326(PB), 116799. https://doi.org/10.1016/j.jenvman.2022.116799
13. Andrijevic, M., Crespo Cuaresma, J., Muttarak, R., & Schleussner, C. F. (2020). Governance in socioeconomic pathways and its role for future adaptive capacity. Nature Sustainability, 3(1), 35–41. https://doi.org/10.1038/s41893-019-0405-0
14. Andrijevic, M., Schleussner, C. F., Crespo Cuaresma, J., Lissner, T., Muttarak, R., Riahi, K., ... & Byers, E. (2023). Towards scenario representation of adaptive capacity for global climate change assessments. *Nature Climate Change*, 1-10.
15. Antle, J., R. Valdivia, S. Gabriel, G. Hoogenboom, M. Madajewicz, C. Porter, C. Rosenzweig, A. Ruane and R. Sulser. (2021). INaRA: A Framework for Integrated National and Regional Assessments of Agricultural System Adaptation to Climate Change Version 1.0.
16. Arabi, M., Frankenberger, J. R., Engel, B. A., & Arnold, J. G. (2008). Representation of agricultural conservation practices with SWAT. Hydrological Processes, 22(16), 3042–3055. https://doi.org/10.1002/hyp.6890
17. Arias, P.A., et al. (2021). Technical Summary. In Climate Change 2021: The Physical Science Basis. Contribution of Working Group I to the Sixth Assessment Report of the Intergovernmental Panel on Climate Change. Cambridge University Press, Cambridge, United Kingdom and New York, NY, USA, pp. 33−144. doi:10.1017/9781009157896.002
18. Arnold, J. G., Bieger, K., White, M. J., Srinivasan, R., Dunbar, J. A., & Allen, P. M. (2018). Use of decision tables to simulate management in SWAT+. Water, 10(6), 713. https://doi.org/10.3390/w10060713
19. Arnold, J. G., Srinivasan, R., Muttiah, R. S., & Williams, J. R. (1998). Large area hydrologic modeling and assessment part I: model development 1. JAWRA Journal of the American Water Resources Association, 34(1), 73-89.
20. ARTEA Piani Colturali 2017, 2018. https://dati.toscana.it/dataset?res_format=SHP&organization=artea (last accessed 30th of July 2022).
21. Bachmair, S., Tanguy, M., Hannaford, J., & Stahl, K. (2018). How well do meteorological indicators represent agricultural and forest drought across Europe?. Environmental Research Letters, 13(3), 034042.

22. Bär, R., Rouholahnejad, E., Rahman, K., Abbaspour, K. C., & Lehmann, A. (2015). Climate change and agricultural water resources: A vulnerability assessment of the Black Sea catchment. *Environmental Science & Policy*, 46, 57–69.

23. Barazzuoli, P., Bouzelboudjen, M., Cucini, S., Kiraly, L., Menicori, P., Salleolini, M., 1999. Olocenic alluvial aquifer of the River Cornia coastal plain (southern Tuscany, Italy): database design for groundwater management. Environ. Geol. 39, 123–143. https://doi.org/10.1007/s002540050443

24. Barazzuoli, P., Nocchi, M., Rigati, R., Salleolini, M., 2008. A conceptual and numerical model for groundwater management: a case study on a coastal aquifer in southern Tuscany, Italy. Hydrogeol. J. 16, 1557–1576. https://doi.org/10.1007/s10040-008-0324-z

25. Barrett, C. B., & Constas, M. A. (2014). Toward a theory of resilience for international development applications. *Proceedings of the National Academy of Sciences of the United States of America*, *111*(40), 14625–14630. https://doi.org/10.1073/pnas.1320880111

26. Barron, J., Skyllerstedt, S., Giordano, M., & Adimassu, Z. (2021). Building Climate Resilience in Rainfed Landscapes Needs More Than Good Will. *Frontiers in Climate*, *3*(December), 1–13. https://doi.org/10.3389/fclim.2021.735880

27. Bartolini, G., Betti, G., Gozzini, B., Iannuccilli, M., Magno, R., Messeri, G., Spolverini, N., Torrigiani, T., Vallorani, R., & Grifoni, D. (2022). Spatial and temporal changes in dry spells in a Mediterranean area: Tuscany (central Italy), 1955–2017. International Journal of Climatology, 42(3), 1670–1691. https://doi.org/10.1002/joc.7327

28. Basnyat, D. B. (2007). Water Resources of Somalia. Technical Report. October, 236. FAO-SWALIM, Nairobi, Kenya.

29. Beck, H. E., Zimmermann, N. E., McVicar, T. R., Vergopolan, N., Berg, A., & Wood, E. F. (2018). Present and future köppen-geiger climate classification maps at 1-km resolution. Scientific Data, 5, 1–12. https://doi.org/10.1038/sdata.2018.214

30. Berg, A. (2022). Bridging the gap between simple metrics and model simulations of climate change impacts on land hydrology. *Earth's Future*, *10*(12), e2022EF003259.

31. Bianchi, D., Modina, D., Cavallaro, L., Spadaccini, R., Carnevali, P., Brancadoro, L., 2021. Vineyard water stress evaluation using a multispectral index: a case study in the Chianti area. Acta Hortic. 1314, 39–46. https://doi.org/10.17660/ActaHortic.2021.1314.6

32. Bianchi, S., Nocchi, M., Salleolini, M., 2011. Hydrogeological investigations in southern Tuscany (Italy) for coastal aquifer management. AQUA mundi 53–70. https://doi.org/10.4409/Am-028-11-0028

33. Biazin, B., Castelli, G., Bresci, E., & Keesstra, S. (2023). Advances in soil and water management for dryland areas. *Frontiers in Environmental Science*, *11*, 1266103.

34. Bieger, K., Arnold, J. G., Rathjens, H., White, M. J., Bosch, D. D., Allen, P. M., Volk, M., & Srinivasan, R. (2017). Introduction to SWAT+, A Completely Restructured Version of the Soil and Water Assessment Tool. *Journal of the American Water Resources Association*, *53*(1), 115–130. https://doi.org/10.1111/1752-1688.12482

35. Bindi, M., & Olesen, J. E. (2011). The responses of agriculture in Europe to climate change. Regional Environmental Change, 11(S1), 151–158. https://doi.org/10.1007/s10113

36. Bird, D. N., Benabdallah, S., Gouda, N., Hummel, F., Koeberl, J., La Jeunesse, I., Meyer, S., Prettenthaler, F., Soddu, A., & Woess-Gallasch, S. (2016). Modelling climate change impacts on and adaptation strategies for agriculture in Sardinia and Tunisia using AquaCrop and value-at-risk. Science of the Total Environment, 543, 1019–1027. https://doi.org/10.1016/j.scitotenv.2015.07.035

37. Birkmann, J., Cutter, S. L., Rothman, D. S., Welle, T., Garschagen, M., van Ruijven, B., O'Neill, B., Preston, B. L., Kienberger, S., Cardona, O. D., Siagian, T., Hidayati, D., Setiadi, N., Binder, C. R., Hughes, B., & Pulwarty, R. (2015). Scenarios for vulnerability: opportunities and constraints in the context of climate change and disaster risk. Climatic Change, 133(1), 53–68. https://doi.org/10.1007/s10584-013-0913-2

38. Birkmann, J., Sauter, H., Jamshed, A., Sorg, L., Fleischhauer, M., Sandholz, S., Wannewitz, M., Greiving, S., Bueter, B., Schneider, M., & Garschagen, M. (2020). Strengthening risk-informed decision-making: scenarios for human vulnerability and exposure to extreme events. Disaster Prevention and Management: An International Journal, 29(5), 663–679. https://doi.org/10.1108/DPM-05-2020-0147

39. Bocchiola, D., Nana, E., & Soncini, A. (2013). Impact of climate change scenarios on crop yield and water footprint of maize in the Po valley of Italy. Agricultural Water Management, 116, 50–61. https://doi.org/10.1016/j.agwat.2012.10.009

40. Boé, J. (2021). The physiological effect of CO2 on the hydrological cycle in summer over Europe and land-atmosphere interactions. Climatic Change, 167(1–2), 21. https://doi.org/10.1007/s10584-021-03173-2

41. Bonzanigo, L., Bojovic, D., Maziotis, A., & Giupponi, C. (2016). Agricultural policy informed by farmers' adaptation experience to climate change in Veneto, Italy. Regional Environmental Change, 16(1), 245–258. https://doi.org/10.1007/s10113-014-0750-5

42. Brooks, N., Neil Adger, W., Mick Kelly, P., 2005. The determinants of vulnerability and adaptive capacity at the national level and the implications for adaptation. Glob. Environ. Chang. 15, 151–163. https://doi.org/10.1016/j.gloenvcha.2004.12.006

43. Brouziyne, Y., Abouabdillah, A., Hirich, A., Bouabid, R., Zaaboul, R., & Benaabidate, L. (2018). Modeling sustainable adaptation strategies toward a climate-smart agriculture in a Mediterranean watershed under projected climate change scenarios. Agricultural Systems, 162, 154–163. https://doi.org/10.1016/j.agsy.2018.01.024

44. Büchner, M., & Reyer, C. (2022). ISIMIP3b atmospheric composition input data (v1.1). ISIMIP Repository. https://doi.org/10.48364/ISIMIP.482153.1

45. Bulut, A. P. (2023). Determining the water footprint of sunflower in Turkey and creating digital maps for sustainable agricultural water management. Environment, Development and Sustainability, 0123456789. https://doi.org/10.1007/s10668-022-02903-5

46. Butcher, J. B., Johnson, T. E., Nover, D., & Sarkar, S. (2014). Incorporating the effects of increased atmospheric CO2 in watershed model projections of climate change impacts. Journal of Hydrology, 513, 322–334. https://doi.org/10.1016/j.jhydrol.2014.03.073

47. Cammalleri C., Naumann G., Mentaschi L., Formetta G., Forzieri G., Gosling S., Bisselink B., De Roo A., Feyen L., 2020. Global warming and drought impacts in the EU. EUR 29956 EN, Publications Office of the European Union, Luxembourg. https://doi.org/10.2760/597045

48. Cantini, F., Castelli, G., Foderi, C., Salazar Garcia, A., López de Armentia, T., Bresci, E., Salbitano, F., 2019. Evidence-Based Integrated Analysis of Environmental Hazards in Southern Bolivia. Int. J. Environ. Res. Public Health 16, 2107. https://doi.org/10.3390/ijerph16122107

49. Caporali, E., Lompi, M., Pacetti, T., Chiarello, V., & Fatichi, S. (2021). A review of studies on observed precipitation trends in Italy. International Journal of Climatology, 41(S1), E1–E25. https://doi.org/10.1002/joc.6741

50. Cardona, O. D., van Aalst, M. K., Birkmann, J., Fordham, M., McGregor, G., Perez, R., Pulwarty, R. S., Schipper, E. L. F. & Sinh, B. T. (2012). Determinants of risk: exposure and vulnerability. In: Managing the Risks of Extreme Events and Disasters to Advance Climate Change Adaptation [Field, C.B., V. Barros, T.F. Stocker, D. Qin, D.J. Dokken, K.L. Ebi, M.D. Mastrandrea, K.J. Mach, G.-K. Plattner, S.K. Allen, M. Tignor, and P.M. Midgley (eds.)]. A Special Report of Working Groups I and II of the Intergovernmental Panel on Climate Change (IPCC). Cambridge University Press, Cambridge, UK, and New York, NY, USA, pp. 65-108.

51. Carrão, H., Naumann, G., & Barbosa, P. (2016). Mapping global patterns of drought risk: An empirical framework based on sub-national estimates of hazard, exposure and vulnerability. Global Environmental Change, 39, 108–124. https://doi.org/10.1016/j.gloenvcha.2016.04.012

52. Castellari, S., Venturini, S., Ballarin Denti, A., Bigano, A., Bindi, M., Bosello, F., Carrera, L., Chiriacò, M.V., Danovaro, R., Desiato, F., Filpa, A., Gatto, M., Gaudioso, D., Giovanardi, O., Giupponi, C., Gualdi, S., Guzzetti, F., Lapi, M., Luise, A., Marino, G., Mysiak, J., Montanari, A., Ricchiuti, A., Rudari, R., Sabbioni, C., Sciortino, M., Sinisi, L., Valentini, R., Viaroli, P., Vurro, M., Zavatarelli, M., 2014. Rapporto sullo stato delle conoscenze scientifiche su impatti, vulnerabilità ed adattamento ai cambiamenti climatici in Italia. Ministero dell'Ambiente e della Tutela del Territorio e del Mare, Roma.

53. Castelli, G., Foderi, C., Guzman, B. H., Ossoli, L., Kempff, Y., Bresci, E., & Salbitano, F. (2017). Planting waterscapes: Green infrastructures, landscape and hydrological modeling for the future of Santa Cruz de la Sierra, Bolivia. Forests, 8(11), 437. https://doi.org/10.3390/f8110437

54. Castelli, G., Piemontese, L., Quinn, R., Aerts, J., Elsner, P., Ertsen, M., Hussey, S., Filho, W. L., Limones, N., Mpofu, B., Neufeld, D. G., Ngugi, K., Ngwenya, N., Parker, A., Ryan, C., de Trincheria, J., Villani, L., Eisma, J., & Bresci, E. (2022). Sand dams for sustainable water management: Challenges and future opportunities. Science of The Total Environment, https://doi.org/10.1016/j.scitotenv.2022.156126.

55. Čerkasova, N., White, M., Arnold, J., Bieger, K., Allen, P., Gao, J., Gambone, M., Meki, M., Kiniry, J., & Gassman, P. W. (2023). Field scale SWAT+ modeling of corn and soybean yields for the contiguous United States: National Agroecosystem Model Development. Agricultural Systems, 210, 103695. https://doi.org/10.1016/j.agsy.2023.103695

56. Challinor, A. J., Simelton, E. S., Fraser, E. D. G., Hemming, D., & Collins, M. (2010). Increased crop failure due to climate change: Assessing adaptation options using models and socio-economic data for wheat in China. Environmental Research Letters, 5(3). https://doi.org/10.1088/1748-9326/5/3/034012

57. Chen, Y., Marek, G. W., Marek, T. H., Porter, D. O., Brauer, D. K., & Srinivasan, R. (2021). Simulating the effects of agricultural production practices on water conservation and crop yields using an improved SWAT model in the Texas High Plains, USA. Agricultural Water Management, 244, 106574. https://doi.org/10.1016/j.agwat.2020.106574

58. Chukalla, A. D., Reidsma, P., van Vliet, M. T., Silva, J. V., van Ittersum, M. K., Jomaa, S., ... & van Oel, P. R. (2020). Balancing indicators for sustainable intensification of crop production at field and river basin levels. *Science of The Total Environment*, *705*, 135925.

59. Ciscar, J. C., Ibarreta, D., Soria, A., Dosio, A., Toreti, A., Ceglar, A., ... & Feyen, L. (2018). Climate impacts in Europe: Final report of the JRC PESETA III project. Publications Office of the European Union), JRC Science for Policy Report EUR, 29427.

60. Clark, M., & Tilman, D. (2017). Comparative analysis of environmental impacts of agricultural production systems, agricultural input efficiency, and food choice. Environ. Res. Lett. 12. https://doi.org/10.1088/1748-9326/aa6cd5

61. Cline, W. R. (1996). The impact of global warming of agriculture: comment. The American Economic Review, 86(5), 1309-1311.

62. Cochrane, L., & Al-Hababi, R. (2023). Risk Categorization and Decision Prioritization for Climate Change Impacts: A Rapid Risk Assessment Methodology Applied in the State of Qatar. Environmental Advances, 100429.

63. Coppola, E., Nogherotto, R., Ciarlo', J. M., Giorgi, F., van Meijgaard, E., Kadygrov, N., Iles, C., Corre, L., Sandstad, M., Somot, S., Nabat, P., Vautard, R., Levavasseur, G., Schwingshackl, C., Sillmann, J., Kjellström, E., Nikulin, G., Aalbers, E., Lenderink, G., … Wulfmeyer, V. (2021). Assessment of the European Climate Projections as Simulated by the Large EURO-CORDEX Regional and Global Climate Model Ensemble. Journal of Geophysical Research: Atmospheres, 126(4), 1–20. https://doi.org/10.1029/2019JD032356

64. Cotti, D., Harb, M., Hadri, A., Aboufirass, M., Chaham, K. R., Libertino, A., Campo, L., Trasforini, E., Krätzschmar, E., Bellert, F., & Hagenlocher, M. (2022). An Integrated Multi-Risk Assessment for Floods and Drought in the Marrakech-Safi Region (Morocco). Frontiers in Water, 4(June). https://doi.org/10.3389/frwa.2022.886648

65. Crausbay, S.D., Ramirez, A.R., Carter, S.L., Cross, M.S., Hall, K.R., Bathke, D.J., Betancourt, J.L., Colt, S., Cravens, A.E., Dalton, M.S., Dunham, J.B., Hay, L.E., Hayes, M.J., McEvoy, J., McNutt, C.A., Moritz, M.A., Nislow, K.H., Raheem, N., Sanford, T., 2017. Defining Ecological Drought for the Twenty-First Century. Bull. Am. Meteorol. Soc. 98, 2543–2550. https://doi.org/10.1175/BAMS-D-16-0292.1

66. Cuaresma, J. C. (2017). Income projections for climate change research: A framework based on human capital dynamics. Global Environmental Change, 42, 226–236. https://doi.org/10.1016/j.gloenvcha.2015.02.012

67. Cuaresma, J. C., & Lutz, W. (2015). The demography of human development and climate change vulnerability: a projection exercise. Vienna Yearbook of Population Research, 241-261.

68. D'Ambrosio, E., Ricci, G. F., Gentile, F., & De Girolamo, A. M. (2020). Using water footprint concepts for water security assessment of a basin under anthropogenic pressures. Science of the Total Environment, 748, 141356. https://doi.org/10.1016/j.scitotenv.2020.141356

69. Dai, A., 2011. Drought under global warming: a review. WIREs Clim. Chang. 2, 45–65. https://doi.org/10.1002/wcc.81

70. Dakhlaoui, H., Seibert, J., & Hakala, K. (2020). Sensitivity of discharge projections to potential evapotranspiration estimation in Northern Tunisia. Regional Environmental Change, 20(2). https://doi.org/10.1007/s10113-020-01615-8

71. Dalla Marta, A., Eitzinger, J., Kersebaum, K. C., Todorovic, M., & Altobelli, F. (2018). Assessment and monitoring of crop water use and productivity in response to climate change. *The Journal of agricultural science*, *156*(5), 575-576.

72. Dalla Marta, A., Mancini, M., Ferrise, R., Bindi, M., & Orlandini, S. (2010). Energy crops for biofuel production: Analysis of the potential in Tuscany. Biomass and Bioenergy, 34(7), 1041–1052. https://doi.org/10.1016/j.biombioe.2010.02.012

73. Davis, K. F., Rulli, M. C., Seveso, A., & D'Odorico, P. (2017). Increased food production and reduced water use through optimized crop distribution. Nature Geoscience, 10(12), 919–924. https://doi.org/10.1038/s41561-017-0004-5

74. De Girolamo, A. M., Bouraoui, F., Buffagni, A., Pappagallo, G., & Lo Porto, A. (2017). Hydrology under climate change in a temporary river system: Potential impact on water balance and flow regime. River Research and Applications, 33(7), 1219–1232. https://doi.org/10.1002/rra.3165

75. De Groeve, T., Poljansek, K., & Vernaccini, L. (2015). Index for risk management-INFORM. JRC Science for Policy Reports (Brussels: European Commission).

76. Dechmi, F., & Skhiri, A. (2013). Evaluation of best management practices under intensive irrigation using SWAT model. Agricultural Water Management, 123(2013), 55–64. https://doi.org/10.1016/j.agwat.2013.03.016

77. Deryugina, T., Konar, M., 2017. Impacts of crop insurance on water withdrawals for irrigation. Adv. Water Resour. 110, 437–444. https://doi.org/10.1016/j.advwatres.2017.03.013

78. Dewulf, A., Karpouzoglou, T., Warner, J., Wesselink, A., Mao, F., Vos, J., Tamas, P., Groot, A. E., Heijmans, A., Ahmed, F., Hoang, L., Vij, S., & Buytaert, W. (2019). The power to define resilience in social–hydrological systems: Toward a power-sensitive resilience framework. *Wiley Interdisciplinary Reviews: Water*, *6*(6), 1–14. https://doi.org/10.1002/WAT2.1377

79. Di Baldassarre, G., Cloke, H., Lindersson, S., Mazzoleni, M., Mondino, E., Mård, J., Odongo, V., Raffetti, E., Ridolfi, E., Rusca, M., Savelli, E., Tootoonchi, F., 2021. Integrating Multiple Research Methods to Unravel the Complexity of Human-Water Systems. AGU Adv. 2, 1–6. https://doi.org/10.1029/2021AV000473

80. Di Baldassarre, G., Wanders, N., AghaKouchak, A., Kuil, L., Rangecroft, S., Veldkamp, T.I.E., Garcia, M., van Oel, P.R., Breinl, K., Van Loon, A.F., 2018. Water shortages worsened by reservoir effects. Nat. Sustain. 1, 617–622. https://doi.org/10.1038/s41893-018-0159-0

81. Di Lena, B., Vergni, L., Antenucci, F., Todisco, F., & Mannocchi, F. (2014). Analysis of drought in the region of Abruzzo (Central Italy) by the Standardized Precipitation Index. Theoretical and Applied Climatology, 115(1–2), 41–52. https://doi.org/10.1007/s00704-013-0876-2

82. Diodato, N., & Bellocchi, G. (2008). Drought stress patterns in Italy using agro-climatic indicators. Climate Research, 36(1), 53–63. https://doi.org/10.3354/cr00726

83. Diodato, N., Ljungqvist, F. C., Fiorillo, F., & Bellocchi, G. (2023). A framework for modelling emergent sediment loss in the Ombrone River Basin, central Italy. PLOS Water, 2(2), e0000072. https://doi.org/10.1371/journal.pwat.0000072

84. Doblas-Reyes, F.J., A.A. Sörensson, M. Almazroui, A. Dosio, W.J. Gutowski, R. Haarsma, R. Hamdi, B. Hewitson, W.-T. Kwon, B.L. Lamptey, D. Maraun, T.S. Stephenson, I. Takayabu, L. Terray, A. Turner, & Z. Zuo, (2021). Linking Global to Regional Climate Change. In Climate Change 2021: The Physical Science Basis. Contribution of Working Group I to the Sixth Assessment Report of the Intergovernmental Panel on Climate Change [Masson-Delmotte, V., P. Zhai, A. Pirani, S.L. Connors, C. Péan, S. Berger, N. Caud, Y. Chen, L. Goldfarb, M.I. Gomis, M. Huang, K. Leitzell, E. Lonnoy, J.B.R. Matthews, T.K. Maycock, T. Waterfield, O. Yelekçi, R. Yu, and B. Zhou (eds.)]. Cambridge University Press, Cambridge, United Kingdom and New York, NY, USA, pp. 1363–1512, doi:10.1017/9781009157896.012.

85. Dormann, C.F., Elith, J., Bacher, S., Buchmann, C., Carl, G., Carré, G., Marquéz, J.R.G., Gruber, B., Lafourcade, B., Leitão, P.J., Münkemüller, T., Mcclean, C., Osborne, P.E., Reineking, B., Schröder, B., Skidmore, A.K., Zurell, D., Lautenbach, S., 2013. Collinearity: A review of methods to deal with it and a simulation study evaluating their performance. Ecography (Cop.). 36, 27–46. https://doi.org/10.1111/j.1600-0587.2012.07348.x

86. Douville, H., et al. (2021). Water Cycle Changes. In Climate Change 2021: The Physical Science Basis. Contribution of Working Group I to the Sixth Assessment Report of the Intergovernmental Panel on Climate Change. Cambridge University Press, Cambridge, United Kingdom and New York, NY, USA, pp. 1055–1210. doi:10.1017/9781009157896.010.

87. Drobinski, P., Da Silva, N., Bastin, S., Mailler, S., Muller, C., Ahrens, B., Christensen, O. B., & Lionello, P. (2020). How warmer and drier will the Mediterranean region be at the end of the twenty-first century? Regional Environmental Change, 20(3). https://doi.org/10.1007/s10113-020-01659-w

88. Ducrocq, V., Drobinski, P., Gualdi, S., Raimbault, P., (2016). Sub-chapter 1.2.1. The water cycle in the Mediterranean. In: The Mediterranean Region under Climate Change: A Scientific Update [online]. IRD ´Editions, Marseille, pp. 73–81

89. Dumont, A., Mayor, B., López-Gunn, E., 2013. Is the Rebound Effect or Jevons Paradox a Useful Concept for better Management of Water Resources? Insights from the Irrigation Modernisation Process in Spain. Aquat. Procedia 1, 64–76. https://doi.org/10.1016/j.aqpro.2013.07.006

90. Easterling, W. E., Rosenberg, N. J., McKenney, M. S., Jones, C. A., Dyke, P. T., & Williams, J. R. (1992). Preparing the erosion productivity impact calculator (EPIC) model to simulate crop response to climate change and the direct effects of CO2. Agricultural and Forest Meteorology, 59(1-2), 17-34. https://doi.org/10.1016/0168-1923(92)90084-H

91. Eckhardt, K., & Ulbrich, U. (2003). Potential impacts of climate change on groundwater recharge and streamflow in a central European low mountain range. Journal of hydrology, 284(1-4), 244-252. https://doi.org/10.1016/j.jhydrol.2003.08.005

92. Eini, M. R., Salmani, H., & Piniewski, M. (2023). Comparison of process-based and statistical approaches for simulation and projections of rainfed crop yields. Agricultural Water Management, 277(November 2022). https://doi.org/10.1016/j.agwat.2022.108107

93. Eisenack, K., Villamayor-Tomas, S., Epstein, G., Kimmich, C., Magliocca, N., Manuel-Navarrete, D., Oberlack, C., Roggero, M., Sietz, D., 2019. Design and quality criteria for archetype analysis. Ecol. Soc. 24, art6. https://doi.org/10.5751/ES-10855-240306

94. El Afandi, G., Khalil, F. A., & Ouda, S. A. (2010). Using irrigation scheduling to increase water productivity of wheat-maize rotation under climate change conditions. Chilean Journal of Agricultural Research, 70(3), 474-484.

95. EM-DAT. https://www.emdat.be/ (last accessed 23 August 2023).

96. Enenkel, M., Brown, M. E., Vogt, J. V., McCarty, J. L., Reid Bell, A., Guha-Sapir, D., Dorigo, W., Vasilaky, K., Svoboda, M., Bonifacio, R., Anderson, M., Funk, C., Osgood, D., Hain, C., & Vinck, P. (2020). Why predict climate hazards if we need to understand impacts? Putting humans back into the drought equation. *Climatic Change*, *162*(3), 1161–1176. https://doi.org/10.1007/s10584-020-02878-0

97. ESCWA, ACSAD and GIZ (2017). Integrated Vulnerability Assessment: Arab Regional Application. RICCAR Technical Note, Beirut, E/ESCWA/SDPD/2017/RICCAR/TechnicalNote.2.

98. Estrela, T., Pérez-Martin, M. A., & Vargas, E. (2012). Impacts of climate change on water resources in Spain. *Hydrological Sciences Journal*, *57*(6), 1154-1167.

99. ETCCDI, http://etccdi.pacificclimate.org/list_27_indices.shtml

100. EU (2016). *Building Resilience: The EU's approach*. ECHO Factsheets

101. EU, 2010. Review and Identification of the Agriculture Programme for Somalia. Final Report – April 2010

102. Evin, G., Somot, S., & Hingray, B. (2021). Balanced estimate and uncertainty assessment of European climate change using the large EURO-CORDEX regional climate model ensemble. Earth System Dynamics, 12(4), 1543–1569. https://doi.org/10.5194/esd-12-1543-2021

103. Ewert, F., Rötter, R. P., Bindi, M., Webber, H., Trnka, M., Kersebaum, K. C., Olesen, J. E., van Ittersum, M. K., Janssen, S., Rivington, M., Semenov, M. A., Wallach, D., Porter, J. R., Stewart, D., Verhagen, J., Gaiser, T., Palosuo, T., Tao, F., Nendel,

C., … Asseng, S. (2015). Crop modelling for integrated assessment of risk to food production from climate change. Environmental Modelling and Software, 72, 287–303. https://doi.org/10.1016/j.envsoft.2014.12.003

104. FAO & WFP (1997). Special report: crop and food supply assessment mission to Somalia.

105. FAO (2016). The State of Food and Agriculture 2016. Climate change, agriculture and food security. Rome.

106. FAO (2020). The State of Food and Agriculture 2020. Overcoming water challenges in agriculture. Rome.

107. FAO (2021). The impact of disasters and crises on agriculture and food security: 2021. Rome. https://doi.org/10.4060/cb3673en

108. FAO, GIZ and ACSAD (2017). Climate Change and Adaptation Solutions for the Green Sectors in the Arab Region. RICCAR Technical Report, Beirut, E/ESCWA/SDPD/2017/RICCAR/TechnicalReport.2.

109. FAO, IFAD, UNICEF, WFP, WHO, 2019. The State of Food Security and Nutrition in the World 2019. Safeguarding against economic slowdowns and downturns. Rome, FAO.

110. Fatichi, S., Leuzinger, S., Paschalis, A., Langley, J. A., Donnellan Barraclough, A., & Hovenden, M. J. (2016). Partitioning direct and indirect effects reveals the response of water-limited ecosystems to elevated CO2. Proceedings of the National Academy of Sciences, 113(45), 12757-12762. https://doi.org/10.1073/pnas.1605036113

111. Fedele, G., Donatti, C. I., Harvey, C. A., Hannah, L., & Hole, D. G. (2019). Transformative adaptation to climate change for sustainable social-ecological systems. Environmental Science & Policy, 101, 116-125.

112. Feng, B., Zhuo, L., Xie, D., Mao, Y., Gao, J., Xie, P., & Wu, P. (2021). A quantitative review of water footprint accounting and simulation for crop production based on publications during 2002–2018. Ecological Indicators, 120(August 2019), 106962. https://doi.org/10.1016/j.ecolind.2020.106962

113. Ficklin, D. L., Luo, Y., Luedeling, E., & Zhang, M. (2009). Climate change sensitivity assessment of a highly agricultural watershed using SWAT. Journal of hydrology, 374(1-2), 16-29. https://doi.org/10.1016/j.jhydrol.2009.05.016

114. Fiseha, B. M., Setegn, S. G., Melesse, A. M., Volpi, E., & Fiori, A. (2014). Impact of Climate Change on the Hydrology of Upper Tiber River Basin Using Bias Corrected Regional Climate Model. Water Resources Management, 28(5), 1327–1343. https://doi.org/10.1007/s11269-014-0546-x

115. Foley J. A., Ramankutty N., Brauman K. A., Cassidy E. S., Gerber J. S., Johnston M., Mueller N. D., O'Connell C., Ray D. K., West P. C., Balzer C., Bennett E. B., Carpenter S. R., Hill J., Monfreda C., Polasky S., Rockstrom J., Sheehan J., Siebert S., Tilman D., Zaks D. P. M. (2011). Solutions for a cultivated planet. Nature

116. Folke, C. (2006). Resilience: The emergence of a perspective for social-ecological systems analyses. Global Environmental Change, 16(3), 253–267. https://doi.org/https://doi.org/10.1016/j.gloenvcha.2006.04.002

117. Folke, C., Carpenter, S. R., Walker, B., Scheffer, M., Chapin, T., & Rockström, J. (2010). Resilience thinking: Integrating resilience, adaptability and transformability. *Ecology and Society*, *15*(4). https://doi.org/10.5751/ES-03610-150420

118. Fontaine, M.M., Steinemann, A.C. (2009). Assessing Vulnerability to Natural Hazards: Impact-Based Method and Application to Drought in Washington State. Nat. Hazards Rev. 10, 11–18. https://doi.org/10.1061/(ASCE)1527-6988(2009)10:1(11)

119. Fung, F. (2018). How to Bias Correct, UKCP18 Guidance, Met Office

120. Funk, C., Peterson, P., Landsfeld, M., Pedreros, D., Verdin, J., Shukla, S., ... & Michaelsen, J. (2015). The climate hazards infrared precipitation with stations—a new environmental record for monitoring extremes. Scientific data, 2(1), 1-21.

121. Gabaldón-Leal, C., Lorite, I., Mínguez, M., Lizaso, J., Dosio, A., Sanchez, E., & Ruiz-Ramos, M. (2015). Strategies for adapting maize to climate change and extreme temperatures in Andalusia, Spain. Climate Research, 65, 159–173. https://doi.org/10.3354/cr01311

122. García-León, D., Standardi, G., Staccione, A. (2021). An integrated approach for the estimation of agricultural drought costs. Land use policy 100, 104923. https://doi.org/10.1016/j.landusepol.2020.104923

123. Garg, K. K., Bharati, L., Gaur, A., George, B., Acharya, S., Jella, K., & Narasimhan, B. (2012). Spatial mapping of agricultural water productivity using the swat model in Upper Bhima catchment, India. Irrigation and Drainage, 61(1), 60–79. https://doi.org/10.1002/ird.618

124. Garg, K. K., Singh, R., Anantha, K. H., Singh, A. K., Akuraju, V. R., Barron, J., … Dixit, S. (2020). Building climate resilience in degraded agricultural landscapes through water management: A case study of Bundelkhand region, Central India. *Journal of Hydrology*, 591, 125592.

125. Garofalo, P., Ventrella, D., Kersebaum, K. C., Gobin, A., Trnka, M., Giglio, L., Dubrovský, M., & Castellini, M. (2019). Water footprint of winter wheat under climate change: Trends and uncertainties associated to the ensemble of crop models. Science of the Total Environment, 658, 1186–1208. https://doi.org/10.1016/j.scitotenv.2018.12.279

126. Garrote, L., Iglesias, A., Granados, A., Mediero, L., & Martin-Carrasco, F. (2015). Quantitative assessment of climate change vulnerability of irrigation demands in Mediterranean Europe. *Water Resources Management*, *29*(2), 325-338.

127. Garschagen, M., Doshi, D., Reith, J., & Hagenlocher, M. (2021). Global patterns of disaster and climate risk—an analysis of the consistency of leading index-based assessments and their results. *Climatic Change*, *169*(1–2), 11. https://doi.org/10.1007/s10584-021-03209-7

128. GDO (2021). Risk of Drought Impacts for Agriculture (RDrI-Agri). http://edo.jrc.ec.europa.eu/gdo

129. Gebrechorkos, S. H., Taye, M. T., Birhanu, B., Solomon, D., & Demissie, T. (2023). Future Changes in Climate and Hydroclimate Extremes in East Africa. Earth's Future, 11(2). https://doi.org/10.1029/2022EF003011

130. Giannakopoulos, C., Le Sager, P., Bindi, M., Moriondo, M., Kostopoulou, E., & Goodess, C. M. (2009). Climatic changes and associated impacts in the Mediterranean resulting from a 2 °C global warming. Global and Planetary Change, 68(3), 209–224. https://doi.org/10.1016/j.gloplacha.2009.06.001

131. Giannini, A., & Bagnoni, V. (2000). Schede di tecnica irrigua per l'agricoltura toscana. Agenzia Regionale per lo Sviluppo e l'Innovazione nel Settore Agricolo-forestale (ARSIA), Firenze

132. Giannini, V., Mula, L., Carta, M., Patteri, G., & Roggero, P. P. (2022). Interplay of irrigation strategies and sowing dates on sunflower yield in semi-arid Mediterranean areas. Agricultural Water Management, 260(October 2021), 107287. https://doi.org/10.1016/j.agwat.2021.107287

133. Giordano M., Turral H., Scheierling S. M., Tréguer D. O., McCornick P. G., 2017. Beyond "More Crop per Drop": Evolving Thinking on Agricultural Water Productivity. IWMI Research Report 169

134. Giordano, R., Preziosi, E., Romano, E., 2013. Integration of local and scientific knowledge to support drought impact monitoring: some hints from an Italian case study. Nat. Hazards 69, 523–544. https://doi.org/10.1007/s11069-013-0724-9

135. Giorgi, F., & Gutowski Jr, W. J. (2015). Regional dynamical downscaling and the CORDEX initiative. Annual review of environment and resources, 40, 467-490.

136. Glavan, M., Ceglar, A., & Pintar, M. (2015). Assessing the impacts of climate change on water quantity and quality modelling in small Slovenian Mediterranean catchment - lesson for policy and decision makers. Hydrological Processes, 29(14), 3124–3144. https://doi.org/10.1002/hyp.10429

137. Gobin, A., Kersebaum, K., Eitzinger, J., Trnka, M., Hlavinka, P., Takáč, J., Kroes, J., Ventrella, D., Marta, A., Deelstra, J., Lalić, B., Nejedlik, P., Orlandini, S., Peltonen-Sainio, P., Rajala, A., Saue, T., Şaylan, L., Stričevic, R., Vučetić, V., & Zoumides, C. (2017). Variability in the Water Footprint of Arable Crop Production across European Regions. Water, 9(2), 93. https://doi.org/10.3390/w9020093

138. Gómez Gómez, C.M., Pérez Blanco, C.D., 2012. Do drought management plans reduce drought risk? A risk assessment model for a Mediterranean river basin. Ecol. Econ. 76, 42–48. https://doi.org/10.1016/j.ecolecon.2012.01.008

139. Gómez, J. A., Ben-Gal, A., Alarcón, J. J., De Lannoy, G., de Roos, S., Dostál, T., … Dodd, I. C. (2020). SHui, an EU-Chinese cooperative project to optimize soil and water management in agricultural areas in the XXI century. *International Soil and Water Conservation Research*, 8(1), 1–14.

140. Gormley-Gallagher, A. M., Sterl, S., Hirsch, A. L., Seneviratne, S. I., Davin, E. L., & Thiery, W. (2022). Agricultural management effects on mean and extreme temperature trends. *Earth system dynamics*, *13*(1), 419-438.

141. Grafton, R.Q., Williams, J., Perry, C.J., Molle, F., Ringler, C., Steduto, P., Udall, B., Wheeler, S.A., Wang, Y., Garrick, D., Allen, R.G., 2018. The paradox of irrigation efficiency. Science (80-.). 361, 748–750. https://doi.org/10.1126/science.aat9314

142. Grassi, S., Cortecci, G., Squarci, P., 2007. Groundwater resource degradation in coastal plains: The example of the Cecina area (Tuscany – Central Italy). Appl. Geochemistry 22, 2273–2289. https://doi.org/10.1016/j.apgeochem.2007.04.025

143. Greve, P., Roderick, M. L., Ukkola, A. M., & Wada, Y. (2019). The aridity Index under global warming. Environmental Research Letters, 14(12). https://doi.org/10.1088/1748-9326/ab5046

144. Gutiérrez, J.M., R.G. Jones, G.T. Narisma, L.M. Alves, M. Amjad, I.V. Gorodetskaya, M. Grose, N.A.B. Klutse, S. Krakovska, J. Li, D. Martínez-Castro, L.O. Mearns, S.H. Mernild, T. Ngo-Duc, B. van den Hurk, & J.-H. Yoon, (2021). Atlas. In Climate Change 2021: The Physical Science Basis. Contribution of Working Group I to the Sixth Assessment Report of the Intergovernmental Panel on Climate Change [Masson-Delmotte, V., P. Zhai, A. Pirani, S.L. Connors, C. Péan, S. Berger, N. Caud, Y. Chen, L. Goldfarb, M.I. Gomis, M. Huang, K. Leitzell, E. Lonnoy, J.B.R. Matthews, T.K. Maycock, T. Waterfield, O. Yelekçi, R. Yu, and B. Zhou (eds.)]. Cambridge University Press, Cambridge, United Kingdom and New York, NY, USA, pp. 1927–2058, doi:10.1017/9781009157896.021

145. Hagenlocher, M., Meza, I., Anderson, C. C., Min, A., Renaud, F. G., Walz, Y., Siebert, S., & Sebesvari, Z. (2019). Drought vulnerability and risk assessments: State of the art, persistent gaps, and research agenda. Environmental Research Letters, 14(8). https://doi.org/10.1088/1748-9326/ab225d

146. Hagenlocher, M., Renaud, F. G., Haas, S., & Sebesvari, Z. (2018). Vulnerability and risk of deltaic social-ecological systems exposed to multiple hazards. Science of the Total Environment, 631–632, 71–80. https://doi.org/10.1016/j.scitotenv.2018.03.013

147. Hall, J. W., & Leng, G. (2019). Can we calculate drought risk… and do we need to? *WIREs Water*, *6*(4), 2–5. https://doi.org/10.1002/wat2.1349

148. Haro-Monteagudo, D., Palazón, L., & Beguería, S. (2020). Long-term sustainability of large water resource systems under climate change: A cascade modeling approach. Journal of Hydrology, 582(December 2019), 124546. https://doi.org/10.1016/j.jhydrol.2020.124546

149. Hashi, A. O. (2017) "A Community Tragedy: The Unmanaged Water Commons in Southern Somalia," Bildhaan: An International Journal of Somali Studies, 17(9) Available at: https://digitalcommons.macalester.edu/bildhaan/vol17/iss1/9

150. Hawkins, E., & Sutton, R. (2011). The potential to narrow uncertainty in projections of regional precipitation change. Climate Dynamics, 37(1), 407–418. https://doi.org/10.1007/s00382-010-0810-6

151. Hayes, M.J., Wilhelmi, O. V., Knutson, C.L., 2004. Reducing Drought Risk: Bridging Theory and Practice. Nat. Hazards Rev. 5, 106–113. https://doi.org/10.1061/(asce)1527-6988(2004)5:2(106)

152. He, Q., Lu, H., Yang, K., Leung, L. R., Pan, M., He, J., & Yao, P. (2022). A simple framework to characterize land aridity based on surface energy partitioning regimes. Environmental Research Letters, 17(3), 34008. https://doi.org/10.1088/1748-9326/ac50d4

153. Hoekstra, A. Y. (2003). 'Virtual water trade between nations: A global mechanism affecting regional water systems. IGBP Global Change News Letter 54,2–4.

154. Hoekstra, A. Y., Chapagain, A. K., Aldaya, M. M., & Mekonnen, M. M. (2011). The water footprint assessment manual: Setting the global standard. Routledge.

155. Holling, C. S. (1973). Resilience and stability of ecological systems. Annual review of ecology and systematics, 4(1), 1-23.

156. Holzworth, D. P., Snow, V., Janssen, S., Athanasiadis, I. N., Donatelli, M., Hoogenboom, G., ... & Thorburn, P. (2015). Agricultural production systems modelling and software: current status and future prospects. *Environmental Modelling & Software*, *72*, 276-286.

157. Hoque, M.A.A., Pradhan, B., Ahmed, N., Sohel, M.S.I. (2021). Agricultural drought risk assessment of Northern New South Wales, Australia using geospatial techniques. Sci. Total Environ. 756, 143600. https://doi.org/10.1016/j.scitotenv.2020.143600

158. Houghton-Carr, H. A., Print, C. R., Fry, M. J., Gadain, H., & Muchiri, P. (2011). Evaluation des ressources en eau de surface des Rivières Juba et Shabelle dans le sud de la Somalie. Hydrological Sciences Journal, 56(5), 759–774. https://doi.org/10.1080/02626667.2011.585470

159. Hu, X., McIsaac, G. F., David, M. B., & Louwers, C. A. L. (2007). Modeling Riverine Nitrate Export from an East-Central Illinois Watershed Using SWAT. Journal of Environmental Quality, 36(4), 996–1005. https://doi.org/10.2134/jeq2006.0228

160. Huai, H., Chen, X., Huang, J., & Chen, F. (2020). Water-Scarcity Footprint Associated with Crop Expansion in Northeast China: A Case Study Based on AquaCrop Modeling. *Water*, *12*(1), 125.

161. Huang, J., Zhuo, W., Li, Y., Huang, R., Sedano, F., Su, W., Dong, J., Tian, L., Huang, Y., Zhu, D. & Zhang, X. (2018). Comparison of three remotely sensed drought indices for assessing the impact of drought on winter wheat yield. Int. J. Digit. Earth 13, 504–526. https://doi.org/10.1080/17538947.2018.1542040.

162. Hurtt, G. C., Chini, L., Sahajpal, R., Frolking, S., Bodirsky, B. L., Calvin, K., Doelman, J. C., Fisk, J., Fujimori, S., Goldewijk, K. K., Hasegawa, T., Havlik, P., Heinimann, A., Humpenöder, F., Jungclaus, J., Kaplan, J. O., Kennedy, J., Krisztin, T., Lawrence, D., … Zhang, X. (2020). Harmonization of global land use change and management for the period 850-2100 (LUH2) for CMIP6. In Geoscientific Model Development (Vol. 13, Issue 11). https://doi.org/10.5194/gmd-13-5425-2020

163. Iglesias, A., Mougou, R., Moneo, M., & Quiroga, S. (2011). Towards adaptation of agriculture to climate change in the Mediterranean. Regional Environmental Change, 11(SUPPL. 1), 159–166. https://doi.org/10.1007/s10113-010-0187-4

164. Iglesias, A., Quiroga, S., & Schlickenrieder, J. (2010). Climate change and agricultural adaptation: Assessing management uncertainty for four crop types in Spain. Climate Research, 44(1), 83–94. https://doi.org/10.3354/cr00921

165. Iocola, I., Bassu, S., Farina, R., Antichi, D., Basso, B., Bindi, M., Dalla Marta, A., Danuso, F., Doro, L., Ferrise, R., Giglio, L., Ginaldi, F., Mazzoncini, M., Mula, L., Orsini, R., Corti, G., Pasqui, M., Seddaiu, G., Tomozeiu, R., … Roggero, P. P. (2017). Can conservation tillage mitigate climate change impacts in Mediterranean cereal systems? A soil organic carbon assessment using long term experiments. European Journal of Agronomy, 90(July), 96–107. https://doi.org/10.1016/j.eja.2017.07.011

166. IPCC (2014). Climate Change 2014: Impacts, Adaptation and Vulnerability. Contribution of Working Group II to the Fifth Assessment Report of the Intergovernmental Panel on Climate Change. New York, NY: Cambridge University Press.

167. IPCC (2018). Special report on climate change and land. Summary for Policymakers

168. IPCC (2022). Climate Change 2022: Impacts, Adaptation, and Vulnerability. Contribution of Working Group II to the Sixth Assessment Report of the Intergovernmental Panel on Climate Change [H.-O. Pörtner, D.C. Roberts, M. Tignor, E.S. Poloczanska, K. Mintenbeck, A. Alegría, M. Craig, S. Langsdorf, S. Löschke, V. Möller, A. Okem, B. Rama (eds.)]. Cambridge University Press. Cambridge University Press, Cambridge, UK and New York, NY, USA, 3056 pp., doi:10.1017/9781009325844.

169. IPCC (2012). Glossary of terms. In: Managing the Risks of Extreme Events and Disasters to Advance Climate Change Adaptation [Field, C.B., V. Barros, T.F. Stocker, D. Qin, D.J. Dokken, K.L. Ebi, M.D. Mastrandrea, K.J. Mach, G.-K. Plattner,

S.K. Allen, M. Tignor, and P.M. Midgley (eds.)]. A Special Report of Working Groups I and II of the Intergovernmental Panel on Climate Change (IPCC). Cambridge University Press, Cambridge, UK, and New York, NY, USA, pp. 555-564.

170. Ismangil, D., Wiegant, D., Hagos, E., Steenbergen, F., Kool, M., Sambalino, F., Castelli, G., Bresci, E., & Hagos, F. (2016). *Managing the Microclimate. Flood-Based Livelihood Network - Practical Note 27. May 2017*. https://doi.org/10.13140/RG.2.2.15110.78409

171. ISTAT, Data Warehouse of Statistics Produced by ISTAT-Italian National Institute of Statistics. http://dati.istat.it/ (last accessed 30th of July 2022).

172. Jacob, D., Petersen, J., Eggert, B., Alias, A., Christensen, O. B., Bouwer, L. M., Braun, A., Colette, A., Déqué, M., Georgievski, G., Georgopoulou, E., Gobiet, A., Menut, L., Nikulin, G., Haensler, A., Hempelmann, N., Jones, C., Keuler, K., Kovats, S., Kröner, N., Kotlarski, S., Kriegsmann, A., Martin, E., van Meijgaard, E., Moseley, C., Pfeifer, S., Preuschmann, S., Radermacher, C., Radtke, K., Rechid, D., Rounsevell, M., Samuelsson, P., Somot, S., Soussana, J.-F., Teichmann, C., Valentini, R., Vautard, R., Weber, B. & Yiou, P. EURO-CORDEX (2014): new high-resolution climate change projections for European impact research Regional Environmental Changes. Vol. 14, Issue 2, pp. 563-578., https://doi.org/10.1007/s10113-013-0499-2

173. Jacob, D., Teichmann, C., Sobolowski, S., Katragkou, E., Anders, I., Belda, M., ... & Wulfmeyer, V. (2020). Regional climate downscaling over Europe: perspectives from the EURO-CORDEX community. Regional environmental change, 20(2), 1-20.

174. Jägermeyr, J., Gerten, D., Schaphoff, S., Heinke, J., Lucht, W., & Rockström, J. (2016). Integrated crop water management might sustainably halve the global food gap. *Environmental Research Letters*, *11*(2). https://doi.org/10.1088/1748-9326/11/2/025002

175. Jägermeyr, J., Müller, C., Ruane, A. C., Elliott, J., Balkovic, J., Castillo, O., Faye, B., Foster, I., Folberth, C., Franke, J. A., Fuchs, K., Guarin, J. R., Heinke, J., Hoogenboom, G., Iizumi, T., Jain, A. K., Kelly, D., Khabarov, N., Lange, S., … Schyns, J. F. (2021). Climate impacts on global agriculture emerge earlier in new generation of climate and crop models. 2(November). https://doi.org/10.1038/s43016-021-00400-y

176. Jamieson, P. D., Porter, J. R., & Wilson, D. R. (1991). A test of the computer simulation model ARCWHEAT1 on wheat crops grown in New Zealand. Field crops research, 27(4), 337-350.

177. Jeans, H., Castillo, G. E., & Thomas, S. (2017). The Future is a choice: absorb, adapt, transform: Resilience capacities. OXFAM

178. Jiang, L., & O'Neill, B. C. (2017). Global urbanization projections for the Shared Socioeconomic Pathways. Global Environmental Change, 42, 193–199. https://doi.org/10.1016/j.gloenvcha.2015.03.008

179. Jones, L. (2019). Resilience isn't the same for all: Comparing subjective and objective approaches to resilience measurement. In *Wiley Interdisciplinary Reviews: Climate Change* (Vol. 10, Issue 1, pp. 1–19). https://doi.org/10.1002/wcc.552

180. Jovanovic, N., Pereira, L. S., Paredes, P., Pôças, I., Cantore, V., & Todorovic, M. (2020). A review of strategies, methods and technologies to reduce non-beneficial consumptive water use on farms considering the FAO56 methods. Agricultural Water Management, 239(November 2019), 106267. https://doi.org/10.1016/j.agwat.2020.106267

181. Jurgilevich, A., Räsänen, A., Groundstroem, F., & Juhola, S. (2017). A systematic review of dynamics in climate risk and vulnerability assessments. Environmental Research Letters, 12(1). https://doi.org/10.1088/1748-9326/aa5508

182. Kalcic, M. M., Frankenberger, J., & Chaubey, I. (2015). Spatial Optimization of Six Conservation Practices Using Swat in Tile-Drained Agricultural Watersheds. Journal of the American Water Resources Association, 51(4), 956–972. https://doi.org/10.1111/1752-1688.12338

183. Kang, Y., Khan, S., & Ma, X. (2009). Climate change impacts on crop yield, crop water productivity and food security–A review. Progress in natural Science, 19(12), 1665-1674.

184. Kchouk, S., Melsen, L. A., Walker, D. W., and van Oel, P. R.: A geography of drought indices: mismatch between indicators of drought and its impacts on water and food securities, Nat. Hazards Earth Syst. Sci., 22, 323–344, https://doi.org/10.5194/nhess-22-323-2022, 2022.

185. Kersebaum, K., Kroes, J., Gobin, A., Takáč, J., Hlavinka, P., Trnka, M., Ventrella, D., Giglio, L., Ferrise, R., Moriondo, M., Dalla Marta, A., Luo, Q., Eitzinger, J., Mirschel, W., Weigel, H.-J., Manderscheid, R., Hoffmann, M., Nejedlik, P., Iqbal, M., & Hösch, J. (2016). Assessing Uncertainties of Water Footprints Using an Ensemble of Crop Growth Models on Winter Wheat. Water, 8(12), 571. https://doi.org/10.3390/w8120571

186. Khan, Z., Thompson, I., Vernon, C. R., Graham, N. T., Wild, T. B., & Chen, M. (2023). Global monthly sectoral water use for 2010–2100 at 0.5° resolution across alternative futures. Scientific Data, 10(1), 201. https://doi.org/10.1038/s41597-023-02086-2

187. Kishawi, Y., Mittelstet, A. R., Adane, Z., Shrestha, N., & Nasta, P. (2022). The combined impact of redcedar encroachment and climate change on water resources in the Nebraska Sand Hills. Frontiers in Water, 4, 208. https://doi.org/10.3389/frwa.2022.1044570

188. Kogan, F. N. (1995). Application of vegetation index and brightness temperature for drought detection. Adv. Sp. Res. 15, 91–100. https://doi.org/10.1016/0273-1177 (95)00079-T.

189. Kogan, F. N. (2001). Operational space technology for global vegetation assessment. Bull. Am. Meteorol. Soc. 82, 1949–1964. https://doi.org/10.1175/1520-0477(2001) 082<1949:OSTFGV>2.3.CO;2.

190. Lam, M. R., Matanó, A., Van Loon, A. F., Odongo, R. A., Teklesadik, A. D., Wamucii, C. N., van den Homberg, M. J. C., Waruru, S., and Teuling, A. J. (2023). Linking reported drought impacts with drought indices, water scarcity and aridity: the case of Kenya, Nat. Hazards Earth Syst. Sci., 23, 2915–2936, https://doi.org/10.5194/nhess-23-2915-2023, 2023.

191. Lange, S. & Büchner, M. (2021): ISIMIP3b bias-adjusted atmospheric climate input data (v1.1). ISIMIP Repository. https://doi.org/10.48364/ISIMIP.842396.1

192. Lange, S., & Büchner, M., (2020). ISIMIP2a atmospheric climate input data (v1.0). ISIMIP Repository. https://doi.org/10.48364/ISIMIP.886955

193. Lee, S., Yeo, I. Y., Sadeghi, A. M., McCarty, G. W., Hively, W. D., Lang, M. W., & Sharifi, A. (2018). Comparative analyses of hydrological responses of two adjacent watersheds to climate variability and change using the SWAT model. Hydrology and Earth System Sciences, 22(1), 689-708. https://doi.org/10.5194/hess-22-689-2018

194. Lemaitre-Basset, T., Oudin, L., & Thirel, G. (2022). Evapotranspiration in hydrological models under rising CO2: a jump into the unknown. Climatic Change, 172(3–4), 1–19. https://doi.org/10.1007/s10584-022-03384-1

195. Lemordant, L., Gentine, P., Swann, A. S., Cook, B. I., & Scheff, J. (2018). Critical impact of vegetation physiology on the continental hydrologic cycle in response to increasing CO 2. Proceedings of the National Academy of Sciences, 115(16), 4093–4098. https://doi.org/10.1073/pnas.1720712115

196. Liebhard, G., Klik, A., Neugschwandtner, R. W., & Nolz, R. (2022). Effects of tillage systems on soil water distribution, crop development, and evaporation and transpiration rates of soybean. Agricultural Water Management, 269(December 2021), 107719. https://doi.org/10.1016/j.agwat.2022.107719

197. Lionello, P., & Scarascia, L. (2018). The relation between climate change in the Mediterranean region and global warming. Regional Environmental Change, 18(5), 1481–1493. https://doi.org/10.1007/s10113-018-1290-1

198. Lobell, D. B. (2014). Climate change adaptation in crop production: Beware of illusions. Global Food Security, 3(2), 72-76.

199. Lorite I. J., Garcia-Vila M., Santos C., Ruiz-Ramos M., & Fereres E. (2013). AquaData and AquaGIS: Two computer utilities for temporal and spatial simulations of water-limited yield with AquaCrop

200. Ludwig, R., Roson, R., Zografos, C., & Kallis, G. (2011). Towards an inter-disciplinary research agenda on climate change, water and security in Southern Europe and neighboring countries. Environmental Science and Policy, 14(7), 794–803. https://doi.org/10.1016/j.envsci.2011.04.003

201. Ma, L., Ahuja, L. R., Saseendran, S. A., Malone, R. W., Green, T. R., Nolan, B. T., Bartling, P. N. S., Flerchinger, G. N., Boote, K. J., & Hoogenboom, G. (2015). A protocol for parameterization and calibration of RZWQM2 in field research. Methods of Introducing System Models into Agricultural Research, 2, 1–64. https://doi.org/10.2134/advagricsystmodel2.c1

202. Magno, R., De Filippis, T., Di Giuseppe, E., Pasqui, M., Rocchi, L., Gozzini, B., 2018. Semi-automatic operational service for drought monitoring and forecasting in the tuscany region. Geosci. 8, 1–24. https://doi.org/10.3390/geosciences8020049

203. Manrique, L. A., & Jones, C. A. (1991). Bulk density of soils in relation to soil physical and chemical properties. Soil Science Society of America Journal, 55(2), 476-481. https://doi.org/10.2136/sssaj1991.03615995005500020030x

204. Mantino, A., Marchina, C., Bonari, E., Fabbrizzi, A., Rossetto, R., 2017. Increase globe artichoke cropping sustainability using sub-surface drip-irrigation systems in a Mediterranean coastal area for reducing groundwater withdrawal. Geophys. Res. Abstr. 19, 18715.

205. Manyena, S. B. (2006). The concept of resilience revisited. Disasters, 30(4), 434-450.

206. Manzoni, S., Fatichi, S., Feng, X., Katul, G. G., Way, D., & Vico, G. (2022). Consistent responses of vegetation gas exchange to elevated atmospheric CO2 emerge from heuristic and optimization models. Biogeosciences, 19(17), 4387–4414. https://doi.org/10.5194/bg-19-4387-2022

207. Maraun, D., & Widmann, M. (2018). Statistical downscaling and bias correction for climate research. Cambridge University Press.

208. Marcinkowski, P., & Piniewski, M. (2018). Effect of climate change on sowing and harvest dates of spring barley and maize in Poland. International Agrophysics, 32(2), 265–271. https://doi.org/10.1515/intag-2017-0015

209. Marcinkowski, P., & Piniewski, M. (2024). Future changes in crop yield over Poland driven by climate change, increasing atmospheric CO2 and nitrogen stress. Agricultural Systems, 213, 103813.

210. Mariotti, A., Pan, Y., Zeng, N., & Alessandri, A. (2015). Long-term climate change in the Mediterranean region in the midst of decadal variability. Climate Dynamics, 44(5–6), 1437–1456. https://doi.org/10.1007/s00382-015-2487-3

211. Märker, M., Angeli, L., Bottai, L., Costantini, R., Ferrari, R., Innocenti, L., Siciliano, G., 2008. Assessment of land degradation susceptibility by scenario analysis: A case study in Southern Tuscany, Italy. Geomorphology 93, 120–129. https://doi.org/10.1016/j.geomorph.2006.12.020

212. Marzi, S., Mysiak, J., Essenfelder, A. H., Amadio, M., Giove, S., & Fekete, A. (2019). Constructing a comprehensive disaster resilience index: The case of Italy. PLoS ONE, 14(9), 1–23. https://doi.org/10.1371/journal.pone.0221585

213. Marzi, S., Mysiak, J., Essenfelder, A. H., Pal, J. S., Vernaccini, L., Mistry, M. N., Alfieri, L., Poljansek, K., Marin-Ferrer, M., & Vousdoukas, M. (2021). Assessing future vulnerability and risk of humanitarian crises using climate change and population projections within the INFORM framework. Global Environmental Change, 71(January). https://doi.org/10.1016/j.gloenvcha.2021.102393

214. Masia, S., Sušnik, J., Marras, S., Mereu, S., Spano, D., & Trabucco, A. (2018). Assessment of irrigated agriculture vulnerability under climate change in Southern Italy. *Water*, *10*(2), 209.

215. Massari, C., Avanzi, F., Bruno, G., Gabellani, S., Penna, D., & Camici, S. (2022). Evaporation enhancement drives the European water-budget deficit during multi-year droughts. 1527–1543. https://doi.org/10.5194/hess-26-1527-2022

216. Matese, A., Baraldi, R., Berton, A., Cesaraccio, C., Di Gennaro, S.F., Duce, P., Facini, O., Mameli, M.G., Piga, A., & Zaldei, A. (2018). Estimation of Water Stress in grapevines using proximal and remote sensing methods. Remote Sens. 10, 1–16. https://doi.org/10.3390/rs10010114

217. McKee, T. B., Doesken, N. J., & Kleist, J. (1993). The relationship of drought frequency and duration to time scales. In Proceedings of the 8th Conference on Applied Climatology (Vol. 17, No. 22, pp. 179-183).

218. MedECC, 2020. Climate and Environmental Change in the Mediterranean Basin – Current Situation and Risks for the Future. First Mediterranean Assessment Report [Cramer, W., Guiot, J., Marini, K. (eds.)] Union for the Mediterranean, Plan Bleu, UNEP/MAP, Marseille, France, 632pp. https://doi.org/10.5281/zenodo.4768833

219. Mekonnen, M. M., & Gerbens-Leenes, W. (2020). The water footprint of global food production. *Water*, *12*(10), 2696.

220. Mekonnen, M. M., & Hoekstra, A. Y. (2011). The green, blue and grey water footprint of crops and derived crop products. Hydrology and Earth System Sciences, 15(5), 1577-1600. https://doi.org/10.5194/hess-15-1577-2011

221. Mekonnen, M. M., & Hoekstra, A. Y. (2012). A global assessment of the water footprint of farm animal products. Ecosystems, 15(3), 401-415. https://doi.org/10.1007/s10021-011-9517-8

222. Merz, B., Aerts, J., Arnbjerg-Nielsen, K., Baldi, M., Becker, A., Bichet, A., Blöschl, G., Bouwer, L. M., Brauer, A., Cioffi, F., Delgado, J. M., Gocht, M., Guzzetti, F., Harrigan, S., Hirschboeck, K., Kilsby, C., Kron, W., Kwon, H.-H., Lall, U., … Nied, M. (2014). Floods and climate: emerging perspectives for flood risk assessment and management. Natural Hazards and Earth System Sciences, 14(7), 1921–1942. https://doi.org/10.5194/nhess-14-1921-2014

223. Meza, I., Hagenlocher, M., Naumann, G., Vogt, J., Frischen, J., 2019. Drought vulnerability indicators for global-scale drought risk assessments, EUR 29824 EN, Publications Office of the European Union, Luxembourg, ISBN 978-92-76-09210-0, doi:10.2760/73844, JRC117546.

224. Meza, I., Siebert, S., Döll, P., Kusche, J., Herbert, C., Rezaei, E. E., Nouri, H., Gerdener, H., Popat, E., Frischen, J., Naumann, G., Vogt, J. V., Walz, Y., Sebesvari, Z., & Hagenlocher, M. (2020). Global-scale drought risk assessment for agricultural systems. Natural Hazards and Earth System Sciences, 20(2), 695–712. https://doi.org/10.5194/nhess-20-695-2020

225. Michalscheck, M., Petersen, G., & Gadain, H. (2016). Impacts of rising water demands in the Juba and Shabelle river basins on water availability in south Somalia. Hydrological Sciences Journal, 61(10), 1877–1889. https://doi.org/10.1080/02626667.2015.1058944

226. Middleton, N., & Thomas, D. (1997). World atlas of desertification. ed. 2. Arnold, Hodder Headline, PLC.

227. Milly, P. C. D., & Dunne, K. A. (2017). A Hydrologic Drying Bias in Water-Resource Impact Analyses of Anthropogenic Climate Change. Journal of the American Water Resources Association, 53(4), 822–838. https://doi.org/10.1111/1752-1688.12538

228. Milly, P. C., & Dunne, K. A. (2016). Potential evapotranspiration and continental drying. Nature Climate Change, 6(10), 946-949.

229. Mishra, A. K., & Singh, V. P. (2010). A review of drought concepts. *Journal of Hydrology*, *391*(1–2), 202–216. https://doi.org/10.1016/j.jhydrol.2010.07.012

230. Mochizuki, J., Keating, A., Liu, W., Hochrainer-Stigler, S., & Mechler, R. (2018). An overdue alignment of risk and resilience? A conceptual contribution to community resilience. Disasters, 42(2), 361–391. https://doi.org/10.1111/disa.12239

231. Molden, D., Oweis, T., Steduto, P., Bindraban, P., Hanjra, M. A., & Kijne, J. (2010). Improving agricultural water productivity: Between optimism and caution. *Agricultural Water Management*, *97*(4), 528-535.

232. Monaco, E., Bonfante, A., Alfieri, S. M., Basile, A., Menenti, M., & De Lorenzi, F. (2014). Climate change, effective water use for irrigation and adaptability of maize: A case study in southern Italy. Biosystems Engineering, 128, 82–99. https://doi.org/10.1016/j.biosystemseng.2014.09.001

233. Monteleone, B., Borzí, I., Bonaccorso, B., & Martina, M. (2022). Developing stage-specific drought vulnerability curves for maize: The case study of the Po River basin. Agricultural Water Management, 269(February), 107713. https://doi.org/10.1016/j.agwat.2022.107713

234. Mori, S., Pacetti, T., Brandimarte, L., Santolini, R., & Caporali, E. (2021). A methodology for assessing spatio-temporal dynamics of flood regulating services. Ecological Indicators, 129, 107963. https://doi.org/10.1016/j.ecolind.2021.107963

235. Moriasi, D. N., Arnold, J. G., Van Liew, M. W., Bingner, R. L., Harmel, R. D. & Veith, T. L. (2007). Model Evaluation Guidelines for Systematic Quantification of Accuracy in Watershed Simulations. Transactions of the ASABE, 50(3), 885–900. https://doi.org/10.13031/2013.23153

236. Moriasi, D. N., Gitau, M. W., Pai, N., & Daggupati, P. (2015). Hydrologic and water quality models: Performance measures and evaluation criteria. Transactions of the ASABE, 58(6), 1763-1785.

237. Moriondo, M., Bindi, M., Kundzewicz, Z. W., Szwed, M., Chorynski, A., Matczak, P., Radziejewski, M., McEvoy, D., & Wreford, A. (2010). Impact and adaptation opportunities for European agriculture in response to climatic change and variability. Mitigation and Adaptation Strategies for Global Change, 15(7), 657–679. https://doi.org/10.1007/s11027-010-9219-0

238. Morison, J. I. L. (1987). Intercellular CO2 concentration and stomatal response to CO2. In: Zeiger E (ed) Stoma- tal function. G.D.Farquhar & I.R. Cowan. Stanford University Press, Stanford, pp 229–252

239. Moss, R. H., Edmonds, J. A., Hibbard, K. A., Manning, M. R., Rose, S. K., Van Vuuren, D. P., ... & Wilbanks, T. J. (2010). The next generation of scenarios for climate change research and assessment. Nature, 463(7282), 747-756.

240. Mourad, K. A. (2022). Post-conflict development, reviewing the water sector in Somalia. *Environment, Development and Sustainability*, *0123456789*. https://doi.org/10.1007/s10668-021-02096-3

241. Mueller N. D., Gerber J. S., Johnston M., Ray D. K., Ramankutty N., & Foley J. A. (2012). Closing yield gaps through nutrient and water management. Nature

242. Murken, L., Cartsburg, M., Chemura, A., Didovets, I., Gleixner, S., Koch, H., Lehmann, J., Liersch, S., Lüttringhaus, S., Rivas López, M. R., Noleppa, S., Roehrig, F., Schauberger, B., Shukla, R., Tomalka, J., Yalew, A. & Gornott, C., (2020). Climate risk analysis for identifying and weighing adaptation strategies in Ethiopia's agricultural sector. A report prepared by the Potsdam Institute for Climate Impact Research for the Deutsche Gesellschaft für Internationale Zusammenarbeit GmbH on behalf of the German Federal Ministry for Economic Cooperation and Development, 150 pp. DOI: 10.2312/pik.2020.003

243. Murthy, C.S., Laxman, B., Sesha Sai, M.V.R. (2015). Geospatial analysis of agricultural drought vulnerability using a composite index based on exposure, sensitivity and adaptive capacity. Int. J. Disaster Risk Reduct. 12, 163–171. https://doi.org/10.1016/j.ijdrr.2015.01.004

244. Musyoka, F. K., Strauss, P., Zhao, G., Srinivasan, R., & Klik, A. (2021). Multi-step calibration approach for SWAT model using soil moisture and crop yields in a small agricultural catchment. Water (Switzerland), 13(16). https://doi.org/10.3390/w13162238

245. Mysiak, J., Torresan, S., Bosello, F., Mistry, M., Amadio, M., Marzi, S., Furlan, E., & Sperotto, A. (2018). Climate risk index for Italy. Philosophical Transactions of the Royal Society A: Mathematical, Physical and Engineering Sciences, 376(2121). https://doi.org/10.1098/rsta.2017.0305

246. Nair, S. S., King, K. W., Witter, J. D., Sohngen, B. L., & Fausey, N. R. (2011). Importance of crop yield in calibrating watershed water quality simulation tools. Journal of the American Water Resources Association, 47(6), 1285–1297. https://doi.org/10.1111/j.1752-1688.2011.00570.x

247. Nana, E., Corbari, C., & Bocchiola, D. (2014). A model for crop yield and water footprint assessment: Study of maize in the Po valley. Agricultural Systems, 127, 139–149. https://doi.org/10.1016/j.agsy.2014.03.006

248. Napoli, M., & Orlandini, S. (2015). Evaluating the Arc-SWAT2009 in predicting runoff, sediment, and nutrient yields from a vineyard and an olive orchard in Central Italy. Agricultural Water Management, 153, 51–62. https://doi.org/10.1016/j.agwat.2015.02.006

249. Napoli, M., Cecchi, S., Orlandini, S., & Zanchi, C. A. (2014). Determining potential rainwater harvesting sites using a continuous runoff potential accounting procedure and GIS techniques in central Italy. Agricultural Water Management, 141, 55–65. https://doi.org/10.1016/j.agwat.2014.04.012

250. Napoli, M., Massetti, L., & Orlandini, S. (2017). Hydrological response to land use and climate changes in a rural hilly basin in Italy. Catena, 157(May), 1–11. https://doi.org/10.1016/j.catena.2017.05.002

251. Nauditt, A., Stahl, K., Rodríguez, E., Birkel, C., Formiga-Johnsson, R.M., Kallio, M., Ribbe, L., Baez-Villanueva, O.M., Thurner, J., Hann, H., 2022. Evaluating tropical drought risk by combining open access gridded vulnerability and hazard data products. Sci. Total Environ. 822, 153493. https://doi.org/10.1016/j.scitotenv.2022.153493

252. Naumann, G., Barbosa, P., Garrote, L., Iglesias, A., & Vogt, J. (2014). Exploring drought vulnerability in Africa: An indicator based analysis to be used in early warning systems. Hydrology and Earth System Sciences, 18(5), 1591–1604. https://doi.org/10.5194/hess-18-1591-2014

253. Neitsch, S., Arnold, J., Kiniry, J., & Williams, J. (2011). Soil & Water Assessment Tool Theoretical Documentation Version 2009. Texas Water Resources Institute, 1–647.

254. Nguyen, T.P.L., Seddaiu, G., Virdis, S.G.P., Tidore, C., Pasqui, M., Roggero, P.P., 2016. Perceiving to learn or learning to perceive? Understanding farmers' perceptions and adaptation to climate uncertainties. Agric. Syst. 143, 205–216. https://doi.org/10.1016/j.agsy.2016.01.001

255. Nkwasa, A., Chawanda, C. J., Jägermeyr, J., & van Griensven, A. (2022). Improved representation of agricultural land use and crop management for large-scale hydrological impact simulation in Africa using SWAT+. Hydrology and Earth System Sciences, 26(1), 71–89. https://doi.org/10.5194/hess-26-71-2022

256. Nkwasa, A., Waha, K., & van Griensven, A. (2023). Can the cropping systems of the Nile basin be adapted to climate change? Regional Environmental Change, 23(1), 1–14. https://doi.org/10.1007/s10113-022-02008-9

257. Noreika, N., Li, T., Winterova, J., Krasa, J., & Dostal, T. (2022). The Effects of Agricultural Conservation Practices on the Small Water Cycle: From the Farm- to the Management-Scale. Land, 11(5), 683. https://doi.org/10.3390/land11050683

258. Noreika, N., Li, T., Zumr, D., Krasa, J., Dostal, T., & Srinivasan, R. (2020). Farm-scale biofuel crop adoption and its effects on in-basin water balance. Sustainability (Switzerland), 12(24), 1–15. https://doi.org/10.3390/su122410596

259. Noreika, N., Winterová, J., Li, T., Krása, J., & Dostál, T. (2021). The small water cycle in the Czech landscape: How has it been affected by land management changes over time? Sustainability (Switzerland), 13(24). https://doi.org/10.3390/su132413757

260. Nouri, H., Stokvis, B., Galindo, A., Blatchford, M., & Hoekstra, A. Y. (2019). Water scarcity alleviation through water footprint reduction in agriculture: The effect of soil mulching and drip irrigation. Science of the Total Environment, 653, 241–252. https://doi.org/10.1016/j.scitotenv.2018.10.311

261. O'Neill, B. C., Carter, T. R., Ebi, K., Harrison, P. A., Kemp-Benedict, E., Kok, K., ... & Pichs-Madruga, R. (2020). Achievements and needs for the climate change scenario framework. Nature climate change, 10(12), 1074-1084.

262. O'Neill, B. C., Kriegler, E., Ebi, K. L., Kemp-Benedict, E., Riahi, K., Rothman, D. S., van Ruijven, B. J., van Vuuren, D. P., Birkmann, J., Kok, K., Levy, M., & Solecki, W. (2017). The roads ahead: Narratives for shared socioeconomic pathways describing world futures in the 21st century. *Global Environmental Change*, *42*, 169–180. https://doi.org/10.1016/j.gloenvcha.2015.01.004

263. O'Neill, B. C., Tebaldi, C., Van Vuuren, D. P., Eyring, V., Friedlingstein, P., Hurtt, G., Knutti, R., Kriegler, E., Lamarque, J. F., Lowe, J., Meehl, G. A., Moss, R., Riahi, K., & Sanderson, B. M. (2016). The Scenario Model Intercomparison Project (ScenarioMIP) for CMIP6. *Geoscientific Model Development*, *9*(9), 3461–3482. https://doi.org/10.5194/gmd-9-3461-2016

264. Oberlack, C., Sietz, D., Bonanomi, E. B., De Bremond, A., Dell' Angelo, J., Eisenack, K., Ellis, E. C., David, M., Giger, M., Heinimann, A., Kimmich, C., Kok, M. T., Navarrete, D. M., Messerli, P., Meyfroidt, P., Václavík, T., & Villamayor-Tomas, S. (2019). Archetype analysis in sustainability research: meanings, motivations, and evidence-based policy making. *Ecology and Society*, *24*(2). https://doi.org/10.5751/ES-10747-240226

265. OECD (2008). Handbook on Constructing Composite Indicators: Methodology and User Guide. OECD Publishing.

266. OECD (2021). Building the resilience of Italy's agricultural sector to drought. OECD food, agriculture and fisheries paper, 158. OECD publishing.

267. Ogallo, A. L., Omondi, P., Ouma, G. & Wayumba, G. (2018). Climate Change Projections and the Associated Potential Impacts for Somalia. American Journal of Climate Change, 07(02), 153–170. https://doi.org/10.4236/ajcc.2018.72011

268. Ogallo, A. L., Ouma, G. & Omondi, P. (2017). Changes in Rainfall and Surface Temperature Over Lower Jubba, Somalia. Journal of Climate Change and Sustainability, 1(2), 38–50. https://doi.org/10.20987/jccs.1.08.2017

269. Orlandini, S., Mancini, M., Orlando, F., & Marta, A.D. (2011). Integration of meteo-climatic and remote sensing information for the analysis of durum wheat quality in Val d'Orcia (Tuscany, Italy). Idojaras, Quarterly Journal of the Hungarian Meteorological Service. 115 (4), 233–245

270. Orlando, F., Dalla Marta, A., Mancini, M., Motha, R., Qu, J. J., & Orlandini, S. (2015). Integration of remote sensing and crop modeling for the early assessment of durum wheat harvest at the field scale. Crop Science, 55(3), 1280–1289. https://doi.org/10.2135/cropsci2014.07.0479

271. Ortega-Gaucin, D., Ceballos-Tavares, J.A., Ordoñez Sánchez, A., Castellano-Bahena, H. V. (2021). Agricultural Drought Risk Assessment: A Spatial Analysis of Hazard, Exposure, and Vulnerability in Zacatecas, Mexico. Water 13, 1431. https://doi.org/10.3390/w13101431

272. Oweis, T., & Hachum, A. (2006). Water harvesting and supplemental irrigation for improved water productivity of dry farming systems in West Asia and North Africa. *Agricultural water management*, *80*(1-3), 57-73.

273. Pacetti, T., Castelli, G., Schröder, B., Bresci, E., & Caporali, E. (2021). Water Ecosystem Services Footprint of agricultural production in Central Italy. Science of the Total Environment, 797, 149095. https://doi.org/10.1016/j.scitotenv.2021.149095

274. Padulano, R., Cesare Lama, G. F., Rianna, G., Santini, M., Mancini, M., & Stojiljkovic, M. (2020). Future rainfall scenarios for the assessment of water availability in Italy. 2020 IEEE International Workshop on Metrology for Agriculture and Forestry, MetroAgriFor 2020 - Proceedings, 241–246. https://doi.org/10.1109/MetroAgriFor50201.2020.9277599

275. Palazzoli, I., Maskey, S., Uhlenbrook, S., Nana, E., & Bocchiola, D. (2015). Impact of prospective climate change on water resources and crop yields in the Indrawati basin, Nepal. Agricultural Systems, 133, 143–157. https://doi.org/10.1016/j.agsy.2014.10.016

276. Panagopoulos, Y., Makropoulos, C., & Mimikou, M. (2012). Decision support for agricultural water management. Global Nest Journal, 14(3), 255–263. https://doi.org/10.30955/gnj.000887

277. Panagopoulos, Y., Makropoulos, C., Gkiokas, A., Kossida, M., Evangelou, L., Lourmas, G., Michas, S., Tsadilas, C., Papageorgiou, S., Perleros, V., Drakopoulou, S., & Mimikou, M. (2014). Assessing the cost-effectiveness of irrigation water management practices in water stressed agricultural catchments: The case of Pinios. Agricultural Water Management, 139, 31–42. https://doi.org/10.1016/j.agwat.2014.03.010

278. Parajuli, P. B., Jayakody, P., Sassenrath, G. F., Ouyang, Y., & Pote, J. W. (2013). Assessing the impacts of crop-rotation and tillage on crop yields and sediment yield using a modeling approach. Agricultural Water Management, 119, 32–42. https://doi.org/10.1016/j.agwat.2012.12.010

279. Pasqui, M., & Di Giuseppe, E. (2019). Climate change, future warming, and adaptation in Europe. Animal Frontiers, 9(1), 6–11. https://doi.org/10.1093/af/vfy036

280. Paumgarten, F., Locatelli, B., & Witkowski, E. T. (2020). Archetypes of climate-risk profiles among rural households in Limpopo, South Africa. *Weather, Climate, and Society*, *12*(3), 545-560.

281. Pellegrini, S., Vignozzi, N., Costantini, E. A. C., & L'Abate, G. (2007). A new pedotransfer function for estimating soil bulk density. Changing Soils In A Changing Wold: The Soils Of Tomorrow. Book of Abstracts. 5th International Congress Of European Society For Soil Conservation, Palermo, June 25-30 2007. Carmelo Dazzi Editor, 25–30.

282. Pesce, M., Critto, A., Torresan, S., Giubilato, E., Pizzol, L., & Marcomini, A. (2019). Assessing uncertainty of hydrological and ecological parameters originating from the application of an ensemble of ten global-regional climate model projections in a coastal ecosystem of the lagoon of Venice, Italy. Ecological Engineering, 133(April), 121–136. https://doi.org/10.1016/j.ecoleng.2019.04.011

283. Piano Nazionale di Adattamento ai Cambiamenti Climatici (PNACC), (2018). Allegato III, Impatti e Vulnerabilità Settoriali. Ministero dell'Ambiente e della Tutela del Territorio e del Mare. https://www.mite.gov.it/sites/default/files/archivio/allegati/clima/pnacc.pdf (last accessed 10th of January 2023)

284. Piemontese, L., Castelli, G., Fetzer, I., Barron, J., Liniger, H., Harari, N., ... & Jaramillo, F. (2020). Estimating the global potential of water harvesting from successful case studies. *Global environmental change*, *63*, 102121.

285. Piemontese, L., Kamugisha, R. N., Tukahirwa, J. M. B., Tengberg, A., Pedde, S., & Jaramillo, F. (2021). Barriers to scaling sustainable land and water management in Uganda: a cross-scale archetype approach. *Ecology and Society*, *26*(3). https://doi.org/10.5751/es-12531-260306

286. Pirttioja, N., Carter, T. R., Fronzek, S., Bindi, M., Hoffmann, H., Palosuo, T., Ruiz-Ramos, M., Tao, F., Trnka, M., Acutis, M., Asseng, S., Baranowski, P., Basso, B., Bodin, P., Buis, S., Cammarano, D., Deligios, P., Destain, M. F., Dumont, B., … Rötter, R. P. (2015). Temperature and precipitation effects on wheat yield across a European transect: A crop model ensemble analysis using impact response surfaces. Climate Research, 65, 87–105. https://doi.org/10.3354/cr01322

287. Prabnakorn, S., Maskey, S., Suryadi, F.X., de Fraiture, C., 2019. Assessment of drought hazard, exposure, vulnerability, and risk for rice cultivation in the Mun River Basin in Thailand. Nat. Hazards 97, 891–911. https://doi.org/10.1007/s11069-019-03681-6

288. Pulighe, G., Lupia, F., Chen, H., & Yin, H. (2021). Modeling climate change impacts on water balance of a mediterranean watershed using swat+. Hydrology, 8(4), 1–14. https://doi.org/10.3390/hydrology8040157

289. Rathjens, H., Bieger, K., Srinivasan, R., Chaubey, I., & Arnold, J. G. (2016). CMhyd user manual. Documentation for preparing simulated climate change data for hydrologic impact studies

290. Ray, D. K., Mueller, N. D., West, P. C., & Foley, J. A. (2013). Yield Trends Are Insufficient to Double Global Crop Production by 2050. PLoS ONE, 8(6), e66428. https://doi.org/10.1371/journal.pone.0066428

291. Reidsma, P., Wolf, J., Kanellopoulos, A., Schaap, B. F., Mandryk, M., Verhagen, J., & Van Ittersum, M. K. (2015). Climate change impact and adaptation research requires integrated assessment and farming systems analysis: A case study in the Netherlands. Environmental Research Letters, 10(4). https://doi.org/10.1088/1748-9326/10/4/045004

292. Renzi, N., Villani, L., Haddad, M., Strohmeier, S., el Din, M., Al Widyan, J., ... & Castelli, G. (2023). Modeling-based performance assessment of an indigenous macro-catchment water harvesting technique (Marab) in the Jordanian Badia. Land Degradation & Development.

293. Rey, D., Garrido, A., Mínguez, M. I., & Ruiz-Ramos, M. (2011). Impact of climate change on maize's water needs, yields and profitability under various water prices in Spain. Spanish Journal of Agricultural Research, 9(4), 1047. https://doi.org/10.5424/sjar/20110904-026-11

294. Riach, N., Glaser, R., Fila, D., Lorenz, S., & Fünfgeld, H. (2023). Climate risk archetypes. Identifying similarities and differences of municipal risks for the adaptation process based on municipalities in Baden-Wuerttemberg, Germany. *Climate Risk Management*, 100526.

295. Riahi, K., van Vuuren, D. P., Kriegler, E., Edmonds, J., O'Neill, B. C., Fujimori, S., Bauer, N., Calvin, K., Dellink, R., Fricko, O., Lutz, W., Popp, A., Cuaresma, J. C., KC, S., Leimbach, M., Jiang, L., Kram, T., Rao, S., Emmerling, J., … Tavoni, M. (2017). The Shared Socioeconomic Pathways and their energy, land use, and greenhouse gas emissions implications: An overview. Global Environmental Change, 42, 153–168. https://doi.org/10.1016/j.gloenvcha.2016.05.009

296. Richter, G. M., & Semenov, M. A. (2005). Modelling impacts of climate change on wheat yields in England and Wales: Assessing drought risks. Agricultural Systems, 84(1), 77–97. https://doi.org/10.1016/j.agsy.2004.06.011

297. Rivington, M., & Koo, J. (2010). Report on the meta-analysis of crop modelling for climate change and food security survey.

298. Rockström, J., & Falkenmark, M. (2015). Agriculture: increase water harvesting in Africa. Nature, 519(7543), 283-285.

299. Roderick, M. L., Greve, P., & Farquhar, G. D. (2015). On the assessment of aridity with changes in atmospheric CO 2. Water Resources Research, 51(7), 5450-5463.

300. Rodina, L. (2019). Defining "water resilience" : Debates , concepts , approaches , and gaps. May 2018, 1–18. https://doi.org/10.1002/wat2.1334

301. Rohat, G. (2018). Projecting drivers of human vulnerability under the shared socioeconomic pathways. International Journal of Environmental Research and Public Health, 15(3). https://doi.org/10.3390/ijerph15030554

302. Rojas, M., Lambert, F., Ramirez-Villegas, J., & Challinor, A. J. (2019). Emergence of robust precipitation changes across crop production areas in the 21st century. *Proceedings of the National Academy of Sciences*, *116*(14), 6673-6678.

303. Rosenzweig, C., Antle, J. M., Ruane, A. C., Jones, J. W., Hatfield, J., Boote, K.J., Thorburn, P., Valdivia, R.O., Descheemaeker, K., Porter, C.H., Janssen, S., Bartels, W.-L., Sulivan, A. & Mutter, C. Z. (2016). Protocols for AgMIP Regional Integrated Assessments Version 7.0.

304. Rossetto, R., De Filippis, G., Maria Piacentini, S., Matani, E., Sabbatini, T., Fabbrizzi, A., Ravenna, C., Benucci, C., Pacini, F., Masi, M., Menonna, V., Pei, A., Leoni, R., Lazzaroni, F., Guastaldi, E., Febo, S., Zirulia, A., Neri, S., 2018. Using flood water in Managed Aquifer Recharge schemes as a solution for groundwater management in the Cornia valley (Italy). Geophys. Res. Abstr. 20, 12861.

305. Rossetto, R., Debolini, M., Galli, M., Basile, P., Bonari, E., 2013. Is water a limiting factor for agricultural development in coastal Mediterranean plains? A case study in the Grosseto Province (Tuscany, Italy). Rend. Online Soc. Geol. Ital. 24, 279–281.

306. Rossi, L., Wens, M., De Moel, H., Cotti, D., Sabino Siemons, A.-S., Toreti, A., Maetens,W., Masante, D., Van Loon, A., Hagenlocher, M., Rudari, R., Meroni, M., Isabellon, M., Avanzi, F., Naumann, G., Barbosa P. (2023). European Drought Risk Atlas, Publications Office of the European Union, Luxembourg, doi:10.2760/608737, JRC135215.

307. Roudier, P., Sultan, B., Quirion, P., & Berg, A. (2011). The impact of future climate change on West African crop yields: What does the recent literature say?. Global environmental change, 21(3), 1073-1083.

308. Ruane, A. C., Rosenzweig, C., Asseng, S., Boote, K. J., Elliott, J., Ewert, F., Jones, J. W., Martre, P., McDermid, S. P., Müller, C., Snyder, A., & Thorburn, P. J. (2017). An AgMIP framework for improved agricultural representation in integrated assessment models. Environmental Research Letters, 12(12). https://doi.org/10.1088/1748-9326/aa8da6

309. Ruane, J. (2012). Coping with water scarcity: An action framework for agriculture and food security. FAO water reports 38

310. Ruiz-Ramos, M., Ferrise, R., Rodríguez, A., Lorite, I. J., Bindi, M., Carter, T. R., Fronzek, S., Palosuo, T., Pirttioja, N., Baranowski, P., Buis, S., Cammarano, D., Chen, Y., Dumont, B., Ewert, F., Gaiser, T., Hlavinka, P., Hoffmann, H., Höhn, J. G., … Rötter, R. P. (2018). Adaptation response surfaces for managing wheat under perturbed climate and CO2 in a Mediterranean environment. Agricultural Systems, 159, 260–274. https://doi.org/10.1016/j.agsy.2017.01.009

311. Rummukainen, M. (2016). Added value in regional climate modeling. Wiley Interdisciplinary Reviews: Climate Change, 7(1), 145-159.

312. Saadi, S., Todorovic, M., Tanasijevic, L., Pereira, L. S., Pizzigalli, C., & Lionello, P. (2015). Climate change and Mediterranean agriculture: Impacts on winter wheat and tomato crop evapotranspiration, irrigation requirements and yield. Agricultural Water Management, 147, 103–115. https://doi.org/10.1016/j.agwat.2014.05.008

313. Salmoral, G., Willaarts, B. A., Garrido, A., & Guse, B. (2017). Fostering integrated land and water management approaches: Evaluating the water footprint of a Mediterranean basin under different agricultural land use scenarios. Land Use Policy, 61, 24–39. https://doi.org/10.1016/j.landusepol.2016.09.027

314. Samir, K. C., & Lutz, W. (2017). The human core of the shared socioeconomic pathways: Population scenarios by age, sex and level of education for all countries to 2100. Global Environmental Change, 42, 181-192. https://doi.org/10.1016/j.gloenvcha.2014.06.004

315. Sapkota, T. B., Mazzoncini, M., Bàrberi, P., Antichi, D., & Silvestri, N. (2012). Fifteen years of no till increase soil organic matter, microbial biomass and arthropod diversity in cover crop-based arable cropping systems. Agronomy for Sustainable Development, 32(4), 853–863. https://doi.org/10.1007/s13593-011-0079-0

316. Satoh, Y., Shiogama, H., Hanasaki, N., Pokhrel, Y., Boulange, J. E. S., Burek, P., Gosling, S. N., Grillakis, M., Koutroulis, A., Müller Schmied, H., Thiery, W., & Yokohata, T. (2021). A quantitative evaluation of the issue of drought definition: A source of disagreement in future drought assessments. *Environmental Research Letters*, *16*(10). https://doi.org/10.1088/1748-9326/ac2348

317. Savelli, E., Rusca, M., Cloke, H., & Di Baldassarre, G. (2022). Drought and society: Scientific progress, blind spots, and future prospects. Wiley Interdisciplinary Reviews: Climate Change, 13(3), e761.

318. Saxton, K. E. & Rawls, W. J. (2006). Soil water characteristic estimates by texture and organic matter for hydrologic solutions. Soil Sci. Soc. Amer. J 70, 1569–1578. https://doi.org/10.2136/sssaj2005.0117

319. Scheff, J. (2018). Drought Indices, Drought Impacts, CO2, and Warming: a Historical and Geologic Perspective. Current Climate Change Reports, 4(2), 202–209. https://doi.org/10.1007/s40641-018-0094-1

320. Scheff, J., Coats, S., & Laguë, M. M. (2022). Why do the global warming responses of land-surface models and climatic dryness metrics disagree?. *Earth's Future*, *10*(8), e2022EF002814.

321. Schierhorn, F., Faramarzi, M., Prishchepov, A. V, Koch, F. J., & Müller, D. (2014). Quantifying yield gaps in wheat production in Russia. *Environmental Research Letters*, 9(8)

322. Schils R., Olesen J. E., Kersebaum K. C., Rijk B., Oberforster M., Kalyada V., Khitrykau M., Gobin A., Kirchev H., Manolova V., Manolov I., Trnka M., Hlavinka P., Paluoso T., Peltonen-Sainio P., Jauhiainen L., Lorgeou J., Marrou H., Danalatos N., Archontoulis S., Fodor N., Spink J., Roggero P. P., Bassu S., Pulina A., Seehusen T., Uhlen A. K., Żyłowska K., Nieróbca A., Kozyra J., Silva J. V., Maçãs B. M., Coutinho J., Ion V., Takáč J., Mínguez M. I., Eckersten H., Levy L., Herrera J. M., Hiltbrunner J., Kryvobok O., Kryvoshein O., Sylvester-Bradley R., Kindred D., Topp C. F. E., Boogaard H., de Groot H., Lesschen J. P., van Bussel L., Wolf J., Zijlstra M., van Loon M. P., van Ittersum M. K., 2018. Cereal yield gaps across Europe. European Journal of Agronomy. Vol. 101:109-120.

323. Schipanski, M. E., Barbercheck, M., Douglas, M. R., Finney, D. M., Haider, K., Kaye, J. P., ... & White, C. (2014). A framework for evaluating ecosystem services provided by cover crops in agroecosystems. Agricultural Systems, 125, 12-22. https://doi.org/10.1016/j.agsy.2013.11.004

324. Schulzweida, U., Kornblueh, L., & Quast, R. (2021). CDO user's guide. Climate data operators, Version 2.0.5.

325. Schwingshackl, C., Davin, E. L., Hirschi, M., Sørland, S. L., Wartenburger, R., & Seneviratne, S. I. (2019). Regional climate model projections underestimate future warming due to missing plant physiological CO2 response. Environmental Research Letters, 14(11), 114019. https://doi.org/10.1088/1748-9326/ab4949

326. Sebhat, M. (2015). Assessments of water demands for the Juba and Shabelle Rivers in Somalia. 109(2), 165–177. https://doi.org/10.12895/jaeid.20152.318

327. Sebhat, M., & Wenninger, J. (2014). Water balance of the Juba and Shabelle River basins the Horn of Africa. International Journal of Agricultural Policy and Research, 2(6), 238–255.

328. Seckler, D. (1996). The New Era of Water Resources Management: From "Dry" to "Wet" Water Savings. IIMI Research Report 1

329. Seneviratne, S.I., et al. (2021). Weather and Climate Extreme Events in a Changing Climate. In Climate Change 2021: The Physical Science Basis. Contribution of Working Group I to the Sixth Assessment Report of the Intergovernmental Panel on Climate Change. Cambridge University Press, Cambridge, United Kingdom and New York, NY, USA, pp. 1513–1766, doi:10.1017/9781009157896.013.

330. Setti, A., Castelli, G., Villani, L., Ferrise, R., Bresci, E. (2023). Modelling the impacts of water harvesting and climate change on rainfed maize yields in Senegal. Journal of Agricultural Engineering

331. Sharafi, L., Zarafshani, K., Keshavarz, M., Azadi, H., Van Passel, S., 2020. Drought risk assessment: Towards drought early warning system and sustainable environment in western Iran. Ecol. Indic. 114, 106276. https://doi.org/10.1016/j.ecolind.2020.106276

332. Siad, S. M., Iacobellis, V., Zdruli, P., Gioia, A., Stavi, I., & Hoogenboom, G. (2019). A review of coupled hydrologic and crop growth models. *Agricultural Water Management*, 224, 105746.

333. Sinnathamby, S., Douglas-Mankin, K. R., & Craige, C. (2017). Field-scale calibration of crop-yield parameters in the Soil and Water Assessment Tool (SWAT). Agricultural Water Management, 180, 61–69. https://doi.org/10.1016/j.agwat.2016.10.024

334. Skinner, C. B., Poulsen, C. J., & Mankin, J. S. (2018). Amplification of heat extremes by plant CO2 physiological forcing. Nature Communications, 9(1), 1094. https://doi.org/10.1038/s41467-018-03472-w

335. SMHI (2017). Regional Climate Modelling and Regional Hydrological Modelling Applications in the Arab Region. RICCAR Technical Note, Beirut, E/ESCWA/SDPD/2017/RICCAR/TechnicalNote.1

336. SMHI (2021). Product User Guide, Specification and Workflow. Dataset: Temperature and precipitation climate impact indicators from 1970 to 2100 derived from European climate projections. ECMWF Copermicus Report

337. Song, Y. I., & Lee, S. (2021). Climate change risk assessment for the Republic of Korea: developing a systematic assessment methodology. Landscape and Ecological Engineering, 1-12.

338. Sordo-Ward, A., Granados, A., Iglesias, A., Garrote, L., Bejarano, M., 2019. Adaptation Effort and Performance of Water Management Strategies to Face Climate Change Impacts in Six Representative Basins of Southern Europe. Water 11, 1078. https://doi.org/10.3390/w11051078

339. Spano D., Mereu V., Bacciu V., Marras S., Trabucco A., Adinolfi M., Barbato G., Bosello F., Breil M., Chiriacò M. V., Coppini G., Essenfelder A., Galluccio G., Lovato T., Marzi S., Masina S., Mercogliano P., Mysiak J., Noce S., Pal J., Reder A., Rianna G.,

Rizzo A., Santini M., Sini E., Staccione A., Villani V., & Zavatarelli M. (2020). “Analisi del rischio. I cambiamenti climatici in Italia”. DOI: 10.25424/CMCC/ANALISI_DEL_RISCHIO

340. Spinoni, J., Barbosa, P., Bucchignani, E., Cassano, J., Cavazos, T., Cescatti, A., Christensen, J. H., Christensen, O. B., Coppola, E., Evans, J. P., Forzieri, G., Geyer, B., Giorgi, F., Jacob, D., Katzfey, J., Koenigk, T., Laprise, R., Lennard, C. J., Kurnaz, M. L., … Dosio, A. (2021). Global exposure of population and land-use to meteorological droughts under different warming levels and SSPs: A CORDEX-based study. *International Journal of Climatology*, *41*(15), 6825–6853. https://doi.org/10.1002/joc.7302

341. Srinivasan, R., Zhang, X., & Arnold, J. (2010). SWAT ungauged: Hydrological budget and crop yield predictions in the upper Mississippi River basin. Transactions of the ASABE, 53(5), 1533–1546. https://doi.org/10.13031/2013.34903

342. Stagge, J.H., Kohn, I., Tallaksen, L.M. & Stahl, K. (2015). Modeling drought impact occurrence based on meteorological drought indices in Europe. J. Hydrol. 530, 37–50. https://doi.org/10.1016/j.jhydrol.2015.09.039.

343. Stewart, B. A., & Peterson, G. A. (2015). Managing green water in dryland agriculture. Agronomy Journal, 107(4), 1544–1553. https://doi.org/10.2134/agronj14.0038

344. Stockle, C. O., Williams, J. R., Rosenberg, N. J., & Jones, C. A. (1992). A method for estimating the direct and climatic effects of rising atmospheric carbon dioxide on growth and yield of crops: Part I—Modification of the EPIC model for climate change analysis. Agricultural systems, 38(3), 225-238. https://doi.org/10.1016/0308-521X(92)90067-X

345. Sugathan, N., Biju, V., & Renuka, G. (2014). Influence of soil moisture content on surface albedo and soil thermal parameters at a tropical station. Journal of earth system science, 123(5), 1115-1128. https://doi.org/10.1007/s12040-014-0452-x

346. Sun, C., & Ren, L. (2013). Assessment of surface water resources and evapotranspiration in the Haihe River basin of China using SWAT model. Hydrological Processes, 27(8), 1200–1222. https://doi.org/10.1002/hyp.9213

347. Sun, C., & Ren, L. (2014). Assessing crop yield and crop water productivity and optimizing irrigation scheduling of winter wheat and summer maize in the Haihe plain using SWAT model. Hydrological Processes, 28(4), 2478–2498. https://doi.org/10.1002/hyp.9759

348. Sun, L., Mitchell, S.W., & Davidson, A. (2012). Multiple drought indices for agricultural drought risk assessment on the Canadian prairies. Int. J. Climatol. 32, 1628–1639. https://doi.org/10.1002/joc.2385

349. Swann, A. L. S., Hoffman, F. M., Koven, C. D., & Randerson, J. T. (2016). Plant responses to increasing CO 2 reduce estimates of climate impacts on drought severity. Proceedings of the National Academy of Sciences, 113(36), 10019–10024. https://doi.org/10.1073/pnas.1604581113

350. Tabari, H., & Willems, P. (2023a). Global risk assessment of compound hot-dry events in the context of future climate change and socioeconomic factors. npj Climate and Atmospheric Science, 6(1), 74.

351. Tabari, H., & Willems, P. (2023b). Sustainable development substantially reduces the risk of future drought impacts. Communications Earth & Environment, 4(1), 180.

352. Tabari, H., Hosseinzadehtalaei, P., Thiery, W., & Willems, P. (2021). Amplified Drought and Flood Risk Under Future Socioeconomic and Climatic Change. Earth’s Future, 9(10), 1–24. https://doi.org/10.1029/2021EF002295

353. Taranu, I. S., Somot, S., Alias, A., Boé, J., & Delire, C. (2022). Mechanisms behind large-scale inconsistencies between regional and global climate model-based projections over Europe. Climate Dynamics, 0123456789. https://doi.org/10.1007/s00382-022-06540-6

354. Tarolli, P., Preti, F., & Romano, N. (2014). Terraced landscapes: From an old best practice to a potential hazard for soil degradation due to land abandonment. Anthropocene, 6, 10-25.

355. Taye, M. T., Ebrahim, G. Y., Nigussie, L., Hagos, F., Uhlenbrook, S., & Schmitter, P. (2022). Integrated water availability modelling to assess sustainable agricultural intensification options in the Meki catchment, Central Rift Valley, Ethiopia. Hydrological Sciences Journal, 67(15), 2271–2293. https://doi.org/10.1080/02626667.2022.2138403

356. Tenreiro, T. R., García-Vila, M., Gómez, J. A., Jimenez-Berni, J. A., & Fereres, E. (2020). Water modelling approaches and opportunities to simulate spatial water variations at crop field level. *Agricultural Water Management*, *240*, 106254.

357. Teutschbein, C., & Seibert, J. (2012). Bias correction of regional climate model simulations for hydrological climate-change impact studies: Review and evaluation of different methods. Journal of hydrology, 456, 12-29. https://doi.org/10.1016/j.jhydrol.2012.05.052

358. Themeßl, M., Gobiet, A., & Leuprecht, A. (2011). Empirical-statistical downscaling and error correction of daily precipitation from regional climate models. International Journal of Climatology, 31(10), 1530-1544.

359. Tittonell P., & Giller K. (2013). When yield gaps are poverty traps: The paradigm of ecological intensification in African smallholder agriculture. Field Crops Research Vol. 143: 76-90

360. Toreti, A., Deryng, D., Tubiello, F. N., Müller, C., Kimball, B. A., Moser, G., Boote, K., Asseng, S., Pugh, T. A. M., Vanuytrecht, E., Pleijel, H., Webber, H., Durand, J. L., Dentener, F., Ceglar, A., Wang, X., Badeck, F., Lecerf, R., Wall, G. W., … Rosenzweig, C. (2020). Narrowing uncertainties in the effects of elevated CO2 on crops. *Nature Food*, *1*(12), 775–782. https://doi.org/10.1038/s43016-020-00195-4

361. Torriani, D., Calanca, P., Lips, M., Ammann, H., Beniston, M., & Fuhrer, J. (2007). Regional assessment of climate change impacts on maize productivity and associated production risk in Switzerland. Regional Environmental Change, 7, 209-221.

362. Toscano, P., Ranieri, R., Matese, A., Vaccari, F. P., Gioli, B., Zaldei, A., Silvestri, M., Ronchi, C., La Cava, P., Porter, J. R., & Miglietta, F. (2012). Durum wheat modeling: The Delphi system, 11 years of observations in Italy. European Journal of Agronomy, 43, 108–118. https://doi.org/10.1016/j.eja.2012.06.003

363. Tramblay, Y., Llasat, M. C., Randin, C., & Coppola, E. (2020). Climate change impacts on water resources in the Mediterranean. Regional Environmental Change, 20(3), 4–6. https://doi.org/10.1007/s10113-020-01665-y

364. Trenberth, K. E. (2011). Changes in precipitation with climate change. *Climate Research*, *47*(1–2), 123–138. https://doi.org/10.3354/cr00953

365. Tubiello, F. N., Donatelli, M., Rosenzweig, C., & Stockle, C. O. (2000). Effects of climate change and elevated CO2 on cropping systems: model predictions at two Italian locations. European Journal of Agronomy, 13(2-3), 179-189.

366. Tuscany region (2010). Allegato 4 del Decreto n. 1340/08 e n.1696/04, https://www.regione.toscana.it/pan/manuali-di-riferimento (last accessed 30th of July 2022).

367. Udias, A., Pastori, M., Malago, A., Vigiak, O., Nikolaidis, N. P., & Bouraoui, F. (2018). Identifying efficient agricultural irrigation strategies in Crete. Science of the Total Environment, 633, 271–284. https://doi.org/10.1016/j.scitotenv.2018.03.152

368. Ullrich, A., & Volk, M. (2009). Application of the Soil and Water Assessment Tool (SWAT) to predict the impact of alternative management practices on water quality and quantity. Agricultural Water Management, 96(8), 1207–1217. https://doi.org/10.1016/j.agwat.2009.03.010

369. UN (2015). Transforming our world: the 2030 Agenda for Sustainable Development (A/RES/70/1). 35 pp. (available at https://www.un.org/ga/search/view_doc.asp?symbol=A/RES/70/1&Lang=E).

370. UN (2020). The United Nations World Water Development Report 2020: Water and Climate Change. UNESCO, Paris.

371. UN (2021). The United Nations World Water Development Report 2021: Valuing Water. UNESCO, Paris.

372. UNDRR (2015). Sendai Framework for Disaster Risk Reduction 2015–2030 (A/RES/70/1). 37 pp. (available at https:// www.preventionweb.net/files/43291_sendaiframeworkfordrren.pdf)

373. United Nations Economic and Social Commission for Western Asia (ESCWA), Arab Center for the Studies of Arid Zones and Dry Lands (ACSAD) and GIZ (Deutsche Gesellschaft für Internationale Zusammenarbeit). 2017. Integrated Vulnerability Assessment: Arab Regional Application. RICCAR Technical Note, Beirut, E/ESCWA/SDPD/2017/RICCAR/TechnicalNote.2.

374. Urquijo, J., De Stefano, L. (2016). Perception of Drought and Local Responses by Farmers: A Perspective from the Jucar River Basin, Spain. Water Resour. Manag. 30, 577–591. https://doi.org/10.1007/s11269-015-1178-5

375. Vaghefi, S. A., Abbaspour, K. C., Faramarzi, M., Srinivasan, R., & Arnold, J. G. (2017). Modeling crop water productivity using a coupled SWAT-MODSIM model. Water (Switzerland), 9(3), 1–15. https://doi.org/10.3390/w9030157

376. Valdivia R. O., Tui S. H., Antle J. M., Subash N., Singh H., Nedumaran S., Hathie I., Ashfaq M., Nasir J., Vellingiri G., Arunachalam L., Claessens L., MacCarthy D. S., Adiku S., Durand W., Dickson C., Mitter H. & Schönhart M. (2021). Representative Agricultural Pathways: A Multi-Scale Foresight Process to Support Transformation and Resilience of Farming Systems. Handbook of Climate Change and Agroecosystems, 47-102

377. Van Gaelen, H., Vanuytrecht, E., Willems, P., Diels, J., & Raes, D. (2017). Bridging rigorous assessment of water availability from field to catchment scale with a parsimonious agro-hydrological model. Environmental Modelling & Software, 94, 140–156. https://doi.org/10.1016/j.envsoft.2017.02.014

378. van Ittersum M. K., Cassman K. G., Grassini P., Wolf J., Tittonell P., & Hochman Z. (2013). Yield gap analysis with local to global relevance – A review. Field Crops Research. Vol. 143: 4-17

379. Van Liew, M. W., Feng, S., & Pathak, T. B. (2012). Climate change impacts on streamflow, water quality, and best management practices for the Shell and Logan Creek Watersheds in Nebraska, USA. International Journal of Agricultural and Biological Engineering, 5(1), 13-34. https://doi.org/10.3965/j.ijabe.20120501.003

380. Van Loon, A.F., Stahl, K., Di Baldassarre, G., Clark, J., Rangecroft, S., Wanders, N., Gleeson, T., Van Dijk, A.I.J.M., Tallaksen, L.M., Hannaford, J., Uijlenhoet, R., Teuling, A.J., Hannah, D.M., Sheffield, J., Svoboda, M., Verbeiren, B., Wagener, T., Van Lanen, H.A.J., 2016. Drought in a human-modified world: reframing drought definitions, understanding, and analysis approaches. Hydrol. Earth Syst. Sci. 20, 3631–3650. https://doi.org/10.5194/hess-20-3631-2016

381. van Noordwijk, M., van Oel, P., Muthuri, C., Satnarain, U., Sari, R. R., Rosero, P., Githinji, M., Tanika, L., Best, L., Comlan Assogba, G. G., Kimbowa, G., Andreotti, F., Lagneaux, E., Wamucii, C. N., Hakim, A. L., Miccolis, A., Abdurrahim, A. Y., Farida, A., Speelman, E., & Hofstede, G. J. (2022). Mimicking nature to reduce agricultural impact on water cycles: A set of mimetrics. Outlook on Agriculture, 51(1), 114–128. https://doi.org/10.1177/00307270211073813

382. Van Opstal, J., Droogers, P., Kaune, A., Steduto, P. and Perry, C. (2021). Guidance on realizing real water savings with crop water productivity interventions. Wageningen, FAO and FutureWater. https://doi.org/10.4060/cb3844en

383. van Ruijven, B. J., Levy, M. A., Agrawal, A., Biermann, F., Birkmann, J., Carter, T. R., Ebi, K. L., Garschagen, M., Jones, B., Jones, R., Kemp-Benedict, E., Kok, M., Kok, K., Lemos, M. C., Lucas, P. L., Orlove, B., Pachauri, S., Parris, T. M., Patwardhan, A., … Schweizer, V. J. (2014). Enhancing the relevance of shared socioeconomic pathways for climate change impacts, adaptation and vulnerability research. Climatic Change, 122(3), 481–494. https://doi.org/10.1007/s10584-013-0931-0

384. van Woesik, F., van Steenbergen, F., Sambalino, F., Jan de Boer, H., Ricci, J. M. P., Bastiaanssen, W. (2023). Managing the Local Climate: A third way to respond to climate change.

385. Varela-Ortega, C., Blanco-Gutiérrez, I., Esteve, P., Bharwani, S., Fronzek, S., & Downing, T. E. (2016). How can irrigated agriculture adapt to climate change? Insights from the Guadiana Basin in Spain. Regional Environmental Change, 16(1), 59–70. https://doi.org/10.1007/s10113-014-0720-y

386. Ventrella, D., Charfeddine, M., Giglio, L., & Castellini, M. (2012a). Application of DSSAT models for an agronomic adaptation strategy under climate change in Southern Italy: Optimum sowing and transplanting time for winter durum wheat and tomato. Italian Journal of Agronomy, 7(1), 109–115. https://doi.org/10.4081/ija.2012.e16

387. Ventrella, D., Charfeddine, M., Moriondo, M., Rinaldi, M., & Bindi, M. (2012b). Agronomic adaptation strategies under climate change for winter durum wheat and tomato in southern Italy: Irrigation and nitrogen fertilization. Regional Environmental Change, 12(3), 407–419. https://doi.org/10.1007/s10113-011-0256-3

388. Ventrella, D., Giglio, L., Charfeddine, M., & Dalla Marta, A. (2015). Consumptive use of green and blue water for winter durum wheat cultivated in Southern Italy. Italian Journal of Agrometeorology, 1, 33-44.

389. Ventrella, D., Giglio, L., Charfeddine, M., Lopez, R., Castellini, M., Sollitto, D., Castrignanò, A., & Fornaro, F. (2012c). Climate change impact on crop rotations of winter durum wheat and tomato in Southern Italy: Yield analysis and soil fertility. Italian Journal of Agronomy, 7(1), 100–107. https://doi.org/10.4081/ija.2012.e15

390. Vergni, L., & Todisco, F. (2011). Spatio-temporal variability of precipitation, temperature and agricultural drought indices in Central Italy. Agricultural and Forest Meteorology, 151(3), 301–313. https://doi.org/10.1016/j.agrformet.2010.11.005

391. Vermeulen, S. J., Dinesh, D., Howden, S. M., Cramer, L., & Thornton, P. K. (2018). Transformation in practice: a review of empirical cases of transformational adaptation in agriculture under climate change. Frontiers in Sustainable Food Systems, 2, 65.

392. Vicente-Serrano, S. M., Beguería, S., & López-Moreno, J. I. (2010). A multiscalar drought index sensitive to global warming: the standardized precipitation evapotranspiration index. *Journal of climate*, *23*(7), 1696-1718.

393. Vicente-Serrano, S. M., Miralles, D. G., McDowell, N., Brodribb, T., Domínguez-Castro, F., Leung, R., & Koppa, A. (2022b). The uncertain role of rising atmospheric CO2 on global plant transpiration. Earth-Science Reviews, 230(February), 104055. https://doi.org/10.1016/j.earscirev.2022.104055

394. Vicente-Serrano, S. M., Peña-Angulo, D., Beguería, S., Domínguez-Castro, F., Tomás-Burguera, M., Noguera, I., Gimeno-Sotelo, L., & El Kenawy, A. (2022a). Global drought trends and future projections. Philosophical Transactions. Series A, Mathematical, Physical, and Engineering Sciences, 380(2238), 20210285. https://doi.org/10.1098/rsta.2021.0285

395. Villani L., Castelli G., Hagos E. Y., Bresci E. (2018). Water productivity analysis of sand dams irrigation farming in northern Ethiopia. Journal of Agriculture and Environment for International Development. Vol. 112: 139-160

396. Villani, L., Castelli, G., Sambalino, F., Almeida Oliveira, L. A., & Bresci, E. (2021). Influence of trees on landscape temperature in semi-arid agro-ecosystems of East Africa. *Biosystems Engineering*, *212*, 185–199. https://doi.org/10.1016/j.biosystemseng.2021.10.007

397. Vogt, J. V., Naumann, G., Masante, D., Spinoni, J., Cammalleri, C., Erian, W., Pischke, F., Pulwarty, R., & Barbosa, P. (2018). Drought Risk Assessment and Management. A conceptual framework. In EUR 29464 EN, Publications Office of the European Union (Vol. 2018, Issue August). https://doi.org/10.2760/057223

398. Wang, Q., Huang, K., Liu, H., & Yu, Y. (2023). Factors affecting crop production water footprint: A review and meta-analysis. Sustainable Production and Consumption. https://doi.org/10.1016/j.spc.2023.01.008

399. Wang, R., Bowling, L. C., Cherkauer, K. A., Cibin, R., Her, Y., & Chaubey, I. (2017). Biophysical and hydrological effects of future climate change including trends in CO2, in the St. Joseph River watershed, Eastern Corn Belt. Agricultural Water Management, 180, 280–296. https://doi.org/10.1016/j.agwat.2016.09.017

400. Ward, J. H., 1963. Hierarchical Grouping to Optimize an Objective Function, Journal of the American Statistical Association, 58:301, 236-244, https://doi.org/10.1080/01621459.1963.10500845

401. Warsame, A. A., Sheik-Ali, I. A., Barre, G. M., & Ahmed, A. (2023). Examining the effects of climate change and political instability on maize production in Somalia. Environmental Science and Pollution Research, 30(2), 3293–3306. https://doi.org/10.1007/s11356-022-22227-1

402. Warsame, A. A., Sheik-Ali, I. A., Jama, O. M., Hassan, A. A., & Barre, G. M. (2022). Assessing the effects of climate change and political instability on sorghum production: Empirical evidence from Somalia. Journal of Cleaner Production, 360(August 2021), 131893. https://doi.org/10.1016/j.jclepro.2022.131893

403. Webber, H., Ewert, F., Olesen, J. E., Müller, C., Fronzek, S., Ruane, A. C., Bourgault, M., Martre, P., Ababaei, B., Bindi, M., Ferrise, R., Finger, R., Fodor, N., Gabaldón-Leal, C., Gaiser, T., Jabloun, M., Kersebaum, K.-C., Lizaso, J. I., Lorite, I. J., … Wallach, D. (2018). Diverging importance of drought stress for maize and winter wheat in Europe. Nature Communications, 9(1), 4249. https://doi.org/10.1038/s41467-018-06525-2

404. Whiting, L., Turral, H. & Droogers, P. (2023). Real water savings in agriculture. Next Generation Water Management Policy Briefs, Brief 1. Bangkok, FAO. https://doi.org/10.4060/cc1771en.

405. Williams, J. R. (1995). The EPIC Model in Computer Models of Watershed Hydrology Chapter 25 (Water Resources Publications. Highlands Ranch, CO. 1995).

406. World Bank (2019). Assessing Drought Hazard and Risk: Principles and Implementation Guidance. Washington, DC: World Bank.

407. World Health Organization (WHO) (2018). Climate and health country profile: Italy.

408. World Meteorological Organization (WMO) and Global Water Partnership (GWP) (2014). National Drought Management Policy Guidelines: A Template for Action (D.A. Wilhite). Integrated Drought Management Programme (IDMP) Tools and Guidelines Series 1. WMO, Geneva, Switzerland and GWP, Stockholm, Sweden.

409. World Meteorological Organization (WMO) and Global Water Partnership (GWP) (2017). Benefits of action and costs of inaction: Drought mitigation and preparedness – a literature review (N. Gerber and A. Mirzabaev). Integrated Drought Management Programme (IDMP) Working Paper 1. WMO, Geneva, Switzerland and GWP, Stockholm, Sweden.

410. Wu, Y., Liu, S., & Abdul-Aziz, O. I. (2012). Hydrological effects of the increased CO2 and climate change in the Upper Mississippi River Basin using a modified SWAT. Climatic Change, 110(3–4), 977–1003. https://doi.org/10.1007/s10584-011-0087-8

411. Yang, S., & Cui, X. (2019). Building regional sustainable development scenarios with the SSP framework. Sustainability (Switzerland), 11(20), 1–13. https://doi.org/10.3390/su11205712

412. Yang, Y., Roderick, M. L., Zhang, S., McVicar, T. R., & Donohue, R. J. (2019). Hydrologic implications of vegetation response to elevated CO2 in climate projections. Nature Climate Change, 9(1), 44–48. https://doi.org/10.1038/s41558-018-0361-0

413. Yimer, E. A., Riakhi, F. E., Bailey, R. T., Nossent, J., & van Griensven, A. (2023). The impact of extensive agricultural water drainage on the hydrology of the Kleine Nete watershed, Belgium. Science of The Total Environment, 885, 163903.

414. Yimer, E. A., Van Schaeybroeck, B., Van de Vyver, H., & Van Griensven, A. (2022). Evaluating probability distribution functions for the Standardized Precipitation Evapotranspiration Index over Ethiopia. Atmosphere, 13(3), 364.

415. Yin, Y., Zhang, X., Lin, D., Yu, H., Wang, J., & Shi, P. (2014). GEPIC-V-R model: A GIS-based tool for regional crop drought risk assessment. Agricultural Water Management, 144, 107–119. https://doi.org/10.1016/j.agwat.2014.05.017

416. Zabel, F., Müller, C., Elliott, J., Minoli, S., Jägermeyr, J., Schneider, J. M., ... & Asseng, S. (2021). Large potential for crop production adaptation depends on available future varieties. Global Change Biology, 27(16), 3870-3882.

417. Zargar, A., Sadiq, R., Naser, B., Khan, F.I., 2011. A review of drought indices. Environ. Rev. 19, 333–349. https://doi.org/10.1139/a11-013

418. Zhang, X., Zhang, Y., Tian, J., Ma, N., & Wang, Y.P. (2022). CO2 fertilization is spatially distinct from stomatal conductance reduction in controlling ecosystem water-use efficiency increase. Environmental Research Letters, 17(5), 054048. https://doi.org/10.1088/1748-9326/ac6c9c

419. Zhou, J., Jiang, S., Su, B., Huang, J., Wang, Y., Zhan, M., Jing, C., & Jiang, T. (2022). Why the Effect of CO2 on Potential Evapotranspiration Estimation Should Be Considered in Future Climate. Water (Switzerland), 14(6). https://doi.org/10.3390/w14060986

420. Zhu, Z., Piao, S., Myneni, R. B., Huang, M., Zeng, Z., Canadell, J. G., Ciais, P., Sitch, S., Friedlingstein, P., Arneth, A., Cao, C., Cheng, L., Kato, E., Koven, C., Li, Y., Lian, X., Liu, Y., Liu, R., Mao, J., … Zeng, N. (2016). Greening of the Earth and its drivers. Nature Climate Change, 6(8), 791–795. https://doi.org/10.1038/nclimate3004

421. Zollo, A.L., Rillo, V., Bucchignani, E., Montesarchio, M., Mercogliano, P., 2016. Extreme temperature and precipitation events over Italy: assessment of high-resolution simulations with COSMO-CLM and future scenarios. Int. J. Climatol. 36, 987–1004. https://doi.org/10.1002/joc.4401

422. Zucaro, R., & Tudini, L. (2008). Rapporto sullo stato dell'irrigazione in Toscana. INEA.

List of publications

Articles in scientific journals with an international referee system published during the PhD not included as Chapters in the thesis:

1. Lekarkar, K., Nkwasa, A., **Villani, L.,** & van Griensven, A. (2024). Localizing the agricultural impacts of 21st-century climate pathways in data-scarce catchments: A case study of the Nyando Catchment, Kenya. Agricultural Water Management
2. Yimer, E. A., De Trift, L., Lobkowicz, I., **Villani, L.,** Nossent, J., & van Griensven, A. (2024). The underexposed nature-based solutions: A critical state-of-art review on drought mitigation. Journal of Environmental Management
3. Yimer, E. A., Bailey, R. T., Van Schaeybroeck, B., Van De Vyver, H., **Villani, L.**, Nossent, J., & van Griensven, A. (2023). Regional evaluation of a new coupled geohydrological model (SWAT+gwflow) using a global aquifer dataset. Journal of Hydrology: Regional Studies
4. Renzi, N., **Villani, L**., Haddad, M., Strohmeier, S., el Din, M., Al Widyan, J., ... & Castelli, G. (2023). Modeling-based performance assessment of an indigenous macro-catchment water harvesting technique (Marab) in the Jordanian Badia. Land Degradation & Development.
5. Setti, A., Castelli, G., **Villani, L**., Ferrise, R., Bresci, E. (2023). Modelling the impacts of water harvesting and climate change on rainfed maize yields in Senegal. Journal of Agricultural Engineering
6. Castelli, G., Piemontese, L., Quinn, R., Aerts, J., Elsner, P., Ertsen, M., Hussey, S., Filho, W. L., Limones, N., Mpofu, B., Neufeld, D. G., Ngugi, K., Ngwenya, N., Parker, A., Ryan, C., de Trincheria, J., **Villani, L.,** Eisma, J., & Bresci, E. (2022). Sand dams for sustainable water management: Challenges and future opportunities. Science of The Total Environment
7. **Villani, L.**, Castelli, G., Sambalino, F., Oliveira, L. A. A., & Bresci, E. (2021). Influence of trees on landscape temperature in semi-arid agro-ecosystems of East Africa. Biosystems Engineering

International conference and symposium abstracts and/or posters presented during the PhD:

1. **Villani, L.,** Castelli, G., Piemontese, L., Penna, D., & Bresci, E., ”Integrating risk-related approaches towards greater policy impact”. International Workshop “Novel concepts for the mitigation of flood and drought risk, Bologna, Italy, September 2023 (oral presentation)
2. **Villani, L.,** Castelli, G., Yimer, E. A., Nkwasa, A., van Griensven, A., Penna, D., & Bresci, E., “Analysis of agronomic adaptation strategies within Mediterranean catchments: The case of Ombrone catchment, Tuscany”. AISSA under 40 conference, Salerno, Italy, July 2023. (poster)
3. **Villani, L.,** Castelli, G., Yimer, E. A., Nkwasa, A., van Griensven, A., Penna, D., & Bresci, E., “Hydrologic and agricultural impacts of climate change and management practices in a Mediterranean catchment”. Agricultural Model Intercomparison and Improvement Project workshop (AGMIP9), New York, USA, June 2023. (virtual oral presentation)
4. **Villani, L.,** Castelli, G., Yimer, E. A., Nkwasa, A., van Griensven, A., Penna, D., & Bresci, E., “Assessment of agronomic adaptation strategies to climate change in a Mediterranean watershed with SWAT+”. European Geosciences Union General Assembly. Vienna, Austria, April 2023. (oral presentation)
5. **Villani, L.,** Castelli, G., Yimer, E. A., Piemontese, L., van Griensven, A., Penna, D., & Bresci, E., “Evaluating agricultural risks in Central Italy by coupling drought risk assessment and agro-hydrological modelling”, 17th Plinius Conference on Mediterranean Risks, Frascati, Italy, October 2022. (oral presentation)

6. **Villani, L.,** Castelli, G., Piemontese, L., Penna, D., Bresci, E., "Drought risk assessment of five coastal agricultural watersheds in the Tuscany region" AIIA conference, Palermo, Italy, September 2022. (oral presentation)
7. **Villani, L.,** Castelli, G., Piemontese, L., Penna, D., Bresci, E., "Introducing robustness evaluation and archetype analysis in drought risk assessments" European Geosciences Union General Assembly. Vienna, Austria, May 2022. (oral presentation)
8. Castelli, G., Setti, A., **Villani, L.,** Ferrise, R., Bresci, E. "Modelling the impacts of water harvesting and climate change on rainfed maize yields in Senegal" European Geosciences Union General Assembly. Vienna, Austria, May 2022. (oral presentation)
9. **Villani, L.,** Castelli, G., Sambalino, F., Oliveira, L. A. A., Bresci, E. "Integrating UAV and satellite data to assess the effects of agroforestry on microclimate in Dodoma region, Tanzania", IEEE International Workshop on Metrology for Agriculture and Forestry (MetroAgriFor). Online, November 2020. (oral presentation)